Characterisation of *Listeria monocytogenes* using targeted proteomic analysis

Shurene Patrice Bishop Simon

A thesis submitted in partial fulfillment of the requirements of the Degree of Doctor of Philosophy

2012

THE UNIVERSITY OF LONDON

Barts & The London School of Medicine and Dentistry, Queen Mary, University of London

The programme of research was carried out at the Health Protection Agency (HPA), Microbiology Services, London

Abstract

Listeria monocytogenes is the causative agent of listeriosis, a severe foodborne infection that is increasing significantly in Europe and North America. A correlating factor contributing to the resurgence of listeriosis is the rise in consumption of cold-stored ready-to-eat (RTE) foods. The steady upsurge in disease requires more focused research to control the pathogen, *L. monocytogenes*. Currently, there is a plethora of diagnostic methods for the causative agent, however, each has limitations, one of which is the inability to correlate results across laboratories. This is a particular hindrance to an outbreak investigation in an age when food is transported widely across the globe. In this study, proteomic approaches were used to search for biomarkers that facilitate rapid characterisation of isolates against a background of differentially expressed proteins. A preamble to this investigation necessitated incorporation of an efficient lysis procedure to release maximum proteins. This was eventually achieved using a *Listeria* specific enzyme, endolysin, and a disruptive mechanical method. Liquid Chromatography-Mass Spectrometry/Mass Spectrometry (LC-MS/MS) data showed that bead beating and enzymatic lysis were the most efficient methods for analysis of the proteome. Dendrogram lineages, derived from MALD-TOF-MS spectra, strongly correlated with 16S rRNA analyses. Selective protein capture and analysis by MALD-TOF-MS (designated SELDI-TOF-MS) demonstrated considerable intraspecies diversity as revealed by dendrograms which were also visualised by 'Heat Maps'.

One-dimensional polyacrylamide gel electrophoresis and LC-MS/MS analysis of seven *L. monocytogenes* isolates, led to the successful identification of two proteins; a hypothetical protein, designated lwe06778 and a phosphoribosyl-AMP cyclohydrolase which were uniquely present at 4°C. This finding suggests that *L. monocytogenes* depends on the histidine biosynthesis pathway in order to survive at cold temperatures. It is hypothesised that the addition of inhibitors, specific to both proteins in RTE cold foods may be a useful means for controlling outbreaks of listeriosis in the future.

Table of Contents

List of Figures

List of Tables

Acknowledgement

"The stone which the builders refused is become the head stone of the corner." (Psalm 118:22 and Nesta Robert "Bob" Marley)

Rejected from conception and twice abandoned, death did not come to me nor did I succumb to life. Instead, I defied the odds, though they were stacked high against me. I therefore dedicated this thesis to myself for forging ahead against the tide.

First and foremost, I thank my Creator for instilling in me the strength and determination to turn life into a positive.

I would also like to thank my supervisor Professor Haroun Shah, for seeing my potential and deciding to take me on board. The process of doing a PhD is full of peaks and troughs, and he has seen me through, from start to end. For this I am truly grateful.

I thank my academic supervisor Professor Armine Sefton, for her administrative support and encouragement.

I thank everyone in DBHT for their valuable assistance especially; Renata Culak, the SELDI goddess, without her help this section would have been a tremendous struggle; Ming Fang, who never said no, and always found a gap in her heavy workload in which she would slot in my samples for Orbi-trap analysis; also Raju Misra and Tom Gaulton for helping me to make the most of Scaffold.

I thank everyone in FPRU for helping me to get to know *Listeria* and making it fun.

I thank my uncle Michael Alexander, simply for believing in me.

I thank my friends, who are also my second family for life, Kerry-Ann Smart-Clarke, Tsahai Buchanan, Toni Thomas-Bennett, and Sheree Mair, who have been a positive influence during the crucial growing up years.

Lastly, but by no means least, I would like to thank my husband Richard Simon. His unwavering, steadfast and loving support throughout the project helped to ease the pain. I thank him for being there to absorb the tears and his IT support, especially with figures. He is a metaphorical representation of IBM wet computer technology.

Declaration

I, Shurene Patrice Bishop Simon, hereby declare that the work in this thesis is my original work, except where stated otherwise:

The *Lactococcus lactis* FI10544 isolate containing the pUK vector and *L. lactis* FI1066 isolate containing the pUK vector with an endolysin gene insert was obtained from Nikki Horne (Institute of Food Research, Norwich).

L. monocytogenes F2365 peptides were processed using Liquid Chromatography/Mass Spectrometry/Mass Spectrometry (LC-MS/MS) by Min Fang (Department for Bioanalysis and Horizon Technologies (DBHT), HPA, Microbiology Services, London).

Peptides generated from *L. monocytogenes* protein extracts (which were expressed at 4°C and 37°C), were separated by Liquid Chromatograpy followed by the Q-Exactive MS/MS (Thermo Scientific) by Jenny Cho (Thermo Scientific, Hemel Hempstead).

Peptides generated from *L. monocytogenes* protein extracts (which were expressed at 4°C and 37°C), were separated using the deltaDOT PEREGRINE I system. Separated peptides were analysed using both deltaDOT's Equiphase Vertexing Alogrithm (EVA) and Generalised Separation Transform (GST) algorithm by Deepika Devanur (deltaDot, London).

_____

Shurene Patrice Bishop Simon

A b b r e v i a t i o n s

°C	**Degrees centigrade**
µg	**Microgram**
µl	**Microlitre**
%	**Percentage**
1-D	**One dimensional**
2-D	**Two dimensional**
ADP	**Adenoside diphosphate**
AICAR	**5-aminoimidazole-4-carboxamide 1-beta-D ribofuranosyl 5'- monophosphate**
AIDS	**Acquired immuno-deficiency disease syndrome**
AMP	**Adenoside monophosphate**
Arp2/3 complex	**Actin-related proteins 2 and 3**
ATP	**Adenosine triphosphate**
BHI	**Brain heart infusion**
BN	**Blood nutrient**
BTS	**Biological technical standard**
CAMP	**Christos, Atkins, Munch-Petersen**
CFU/g	**Colony forming units per gram**
CNS	**Central nervous system**
cm	**Centimetre**
CMBT	**5-chloro-2-mercaptobenzothiazole**
DBHT	**Department for Bioanalysis and Horizon Technologies**
DCs	**Dentritic cells**
DHB	**2, 5-dihydroxybenzoic acid**
DIGE	**Difference in-gel electrophoresis**
DNA	**Deoxyribonucleic acid**
DTT	**Dithiothreitol**
dsDNA	**Double stranded deoxyribonucleic acid**

DSMZ	**Deutsche sammlung von mikroorganismen und zellkulturen (German collection of microorganism and cell cultures)**
EIA	**Enzyme-based immunoassay**
ELISA	**Enzyme-linked immunosorbant assay**
EVA	**Equiphase vertexing alogrithm**
FISH	**Fluorescence *in situ* hybridisation**
FPRU	**Foodborne pathogen reference unit**
G	**Centripetal force**
GST	**Generalised separation transform**
GW	**Glycine/tryptophan**
HCCA	**Alpha - cyano - 4 hydroxycinnamic acid**
HisA	**Phospho-D-ribosyl formimino-5-amino-1-phosphoribosyl-4- imidazole carboxamide isomerase**
HisB	**Histidinol phosphatase**
HisC	**Histidinol phosphate amino transferase**
HisD	**Histidinol dehydrogenase**
HisE	**Phosphoribosyl-ATP pyrophosphohydrolase**
HisH	**Glutamine imidazole transferase**
HisI	**Phosphoribosyl-AMP cyclohydrolase**
HIV	**Human immuno-deficiency virus**
HPA	**Health protection agency**
HPr	**Histidine phosphocarrier**
iap	**Invasion associated protein**
IEF	**Isoelectric focussing**
IFR	**Institute of food research**
IGDP	**Imidazole glycerol phosphate dehydratase**
IGP	**Imidazole acetol phosphate**
IL	**Interleukin**
IMS	**Immunomagnetic separation**
INF	**Interferon**
inlA	**Internalin A gene**
InlA	**Internalin A protein**

InlB	**Internalin B protein**
inlB	**Internalin B gene**
L	**Litre**
LC-MS/MS	**Liquid chromatography - mass spectrometry/mass spectrometry**
LIPI-1	**Pathogenicity island 1**
LLO	**Listerolysin O**
LPXTG	**Leucine, proline, any amino acid, tyrosine and glycine**
LRR	**Leucine rich region**
mA	**Milliamp**
Mal	**MyD88 adaptor like**
MALDI-TOF-MS	**Matrix assisted laser desorption/ionisation - time of flight - mass spectrometry**
mg	**Milligram**
ml	**Millitre**
mM	**Millimolar**
Mpl	**Metalloprotease**
MRSA	**Methicillin resistant *Staphylococcus aureus***
MS	**Mass spectrometry**
MSSA	**Methicillin susceptible *Staphylococcus aureus***
MSP	**Main-spectrum**
MyD88	**Myeloid differentiating factor -88**
m/z	**Mass to charge**
NCTC	**National collection of typed cultures**
ng	**Nanogram**
NLRs	**Nucleotide-binding oligomerisation domain (NOD) - like receptors**
nm/s	**Nanometre per second**
NOD	**Nucleotide-binding oligomerisation domain**
NPF	**Nucleating promoting factor**
PAGE	**Polyacrylamide Gel Electrophoresis**

PAMPs	**Pathogen-associated molecular patterns**
PCR	**Polymerase chain reaction**
P_i	**Released phosphate**
PI	**Phosphatidylinositol**
PFGE	**Pulse field gel electrophoresis**
PFO	**Perfringolysin**
PLP	**Polyproline region**
PM	**Plasma membrane**
prfA	**Positive regulatory factor A**
PRPP	**5-phosphoribosyl 1-pyrophosphate**
PRRs	**Pattern recognition receptors**
PTS	**Phosphotransferase system**
RNA	**Ribonucleic acid**
RNI	**Reactive nitrogen intermediate**
ROS	**Reactive oxygen species**
SARAMIS	**Spectral ARchive and microbial identification system**
SDS	**Sodium dodecyl sulphate**
SELDI-TOF-MS	**Surface enhanced laser desorption - time of flight – mass spectrometry**
SPA	**Sinapinic acid**
TFA	**Trifluoroacetic acid**
Thymosine β4	**Tβ4**
TLRs	**Toll-like receptors**
TNF	**Tumour necrosis factor**
TRAM	**TRIF-related adapter molecule**
UK	**United Kingdom**
V	**Volts**
W	**Watt**
WASP	**Wiskott aldrich syndrome proteins**
Wave	**WASP verprolin**

Chapter 1: General Introduction

1.1 *Listeria*

1.1.1 *Listeria*: A brief history

The earliest record of the isolation of *Listeria* was in 1926 when Murray et al. isolated an organism from a diseased rabbit, which they named *Bacterium monocytogenes* (Gibbons 1972). The rabbit was observed to have large mononuclear leucocytosis (Gibbons 1972), and therefore the specific epithet *monocytogenes* was derived from the Greek word meaning, "generating monocytes" (Bergey et al. 1939). In 1927, Pirie described a similar organism which he named *Listerella hepatolytica*, but in an addendum to his report he acknowledged that the name assigned by Murray et al. (1926) was more appropriate. When the identity of the organism isolated by Murray et al. (1926) and Pirie (1927) were confirmed to be synonymous, the name *Listerella monocytogenes* took precedence (Gibbons 1972) and in 1934, *Listerella monocytogenes* first appeared in the 4th edition of the Manual of Determinative Bacteriology (Bergey 1934). It was later confirmed that the name *Listerella* was in honour of Joseph Lister, a British surgeon who pioneered antiseptic surgery (Breed, Murray, and Hitchens 1948; Gibbons 1972) (Bergey 1934).

The name *Listerella monocytogenes* continued into the 5th edition of the Bergey's Manual of Determinative Bacteriology, however, in the 6th edition of 1948, the genic *Listerella* was changed to *Listeria monocytogenes* (Breed, Murray, and Hitchens 1948). This change was possibly to avoid confusion as the same genus name was also used to describe Foraminfera and Mycetozoa (Gibbons 1972). The new name became accepted after two revisions by E.G.D. Murray in 1938 and 1945 (Breed, Murray, and Hitchens 1948), and was adopted in all future publications.

In 1961, 1966 and 1971, respectively; *Listeria denitrificans*, *Listeria grayi* and *Listeria murrayi*, were identified as new species, and in 1974 were included in the 8th edition of Bergey's Manual of Determinative Bacteriology (Buchanan and Gibbons 1974), while *L. monocytogenes* continued to be recognised as the type species. However, from 1966 onwards to 1984, morphological, biochemical, serological, chemical and nucleic acid evidence showed that *L. denitrificans* was in compatible with the genus description; and was shown to have a closer affinity with the genera *Oerskovia*, *Renibacterium*, and *Arthrobacter*. In each case; however, the data was tenuous and the organism therefore retained its status in the genus until further studies were carried out (Sneath 1986). Four new species were identified in the late

1970's to mid-1980's: *L. innocua* was identified by Seeliger and Schoofs in 1979, *L. welshimeri and L. seeligeri* by Rocourt and Grimont in 1983, and, *L. ivanovii* by Seeliger and Rocourt in 1984 (Sneath 1986). During this period, Wilkinson and Jones argued that *L. grayi* and *L. murrayi* were not sufficiently distinct and that they should be reduced to synonymy as *L. grayi*. Nevertheless they, remained separate while *L. dentrificans* was transferred to a separate genus; *Jonesia* (Holt et al. 1994). Finally, after much accumulative evidence *L. murrayi* was no longer retained as a separate species. Instead subspecies were defined and *L. grayi* was described as having two subspecies; *L. grayi* subsp. *grayi* and *L. grayi* subsp. *murrayi*. *L. ivanovii* was also subdivided and was categorised as *L. ivanovii* subsp. *ivanovii* and *L. ivanovii* subsp. *londoniensis* (De Vos et al. 2009).

In 2009, *L. marthii* and *L. rocourtiae* became the most recently discovered species: four *L. marthii* species were isolated from soil, standing water and flowing water systems in Finger Lakes National Forest, New York, USA (Graves et al. 2010) and one *L. rocourtiae* species was isolated from pre-cut lettuce in Austria (Leclercq et al. 2010). In total, the genus is currently comprised of 8 species.

1.1.2 Characteristics

All species are Gram positive bacilli, non-spore forming, facultatively anaerobic, motile with peritrichous flagella (if cultured below 30°C), and appear as short rods measuring 0.4-0.5 μm in width and 1-2 μm in length (De Vos et al. 2009). The growth and survival of most human pathogens are hindered at low temperatures, however, *Listeria* is capable of slow growth at 0°C, and can survive temperatures as low as -7°C (De Vos et al. 2009; Ramaswamy et al. 2007). Growth is optimal between 30°C and 37°C, limited at 45°C, and, *Listeria* does not survive heating above 60°C for 30 minutes (De Vos et al. 2009).

Some phenotypic characteristics which separate *Listeria* from other genera are: 1) its ability to metabolise aesculin and not urea , 2) its ability to catalyse the conversion of hydrogen peroxide to hydrogen and oxygen (catalase positive), and 3) its inability to use cytochrome c for the production of energy in the electron transport chain (oxidase negative) (De Vos et al. 2009).

1.1.3 Infection

Of the eight *Listeria* species, *L. monocytogenes* and *L ivanovii* are the most infectious. *L. monocytogenes* is pathogenic to a wide range of animals which include mammals and birds, while *L. ivanovii* primarily affects ruminants (Vazquez-Boland et al. 2001a). Infection by either organism may cause listeriosis. Though all other species are described as non-pathogenic, two exceptional cases of infection caused by *L. seeligeri* and *L. innocua* have been documented. In 1986, Rocourt and colleagues reported a case of acute purulent meningitis due to *L. seeligeri* infection in an immunocompetent adult male (Rocourt et al. 1986), while in 1994, Walker and colleagues reported a case of ovine meningoencephalitis, in which *L. innocua* was implicated (Walker et al. 1994). The above mentioned cases are indeed extremely rare; however, their occurrence gives support to the view that a small population of strains belonging to species described as non-pathogenic, may be capable of causing disease.

1.2 Listeria monocytogenes

1.2.1 Listeriosis

A small percentage of the general population (1-6%), are asymptomatic carriers of *L. monocytogenes* (Lamont et al. 2011; Olier et al. 2005; Ramaswamy et al. 2007). However, in the majority of other cases, infection by *L. monocytogenes* in healthy individuals may lead to; flu-like symptoms (for example; headache, chills, fatigue, muscular and joint pain (Liu 2006), nausea, vomiting, diarrhoea, fever and cramps (Bortollussi 2008). In such cases the infection may be self-limited as the immune system of healthy hosts is stimulated to combat and eradicate the infection: only few healthy individuals develop severe listeriosis (Bortollussi 2008). The more severe and life threatening form of listeriosis includes symptoms such as; bacteremia, meningitis and encephalitis; less common manifestations include inflammatory gastroenteritis, endocarditis and joint infections (Bortollussi 2008). In pregnant women, listeriosis may cause, spontaneous abortion, miscarriages, preterm delivery and still births (Lamont et al. 2011). Persons susceptible to the more severe cases of listeriosis (high risk individuals) include; the unborn, infants, pregnant mothers, persons over 60 and the immunocompromised. Immunocompromised individuals include persons; living with HIV/AIDS, cancer, kidney disease and persons receiving immuno-suppressant medication (Bortollussi 2008). The approximate *L. monocytogenes* infection dose sufficient to cause listeriosis in healthy and high risk individuals is 10-100 million and 0.1-10 million colony forming units respectively (Bortollussi 2008). High risk individuals with signs of listeriosis

are given an empiric therapy which includes ampicillin. Infants born to mothers with listeriosis are prescribed an antibiotic therapy which includes ampicillin and gentamicin (Bortollussi 2008).

Listeriosis, though rare, was in 2006 ranked amongst the fifth most common zoonotic infection in Europe after Salmonella, Campylobacter, Yersinia and VTEC diseases (Denny and McLauchlin 2008). Listeriosis has therefore become a very important disease and this is attributed to three main factors:

1) the mortality rate associated with listeriosis is 20 - 30%, and at times has been known to be 40% (Denny and McLauchlin 2008), this is relatively high in comparison to the mortality rate of other common zoonotic infections such as: *Salmonella enteriditis* 0.38% and *Campylobacter* species 0.02 - 0.1% (Liu 2006).

2) listeriosis carries one of the highest hospitalisation rates amongst known foodborne pathogens with 91% being reported in Europe (Denny and McLauchlin 2008), and 90% in the United States (Nightingale 2010).

3) recently, there has been a dramatic rise in the number of listeriosis cases. Trends in 2006 showed that the number of listeriosis cases have increased for European countries, namely; Germany, Netherlands, United Kingdom (UK), Ireland, Spain and Lithuania (Figure 1.1) (Allerberger and Wagner, 2010).

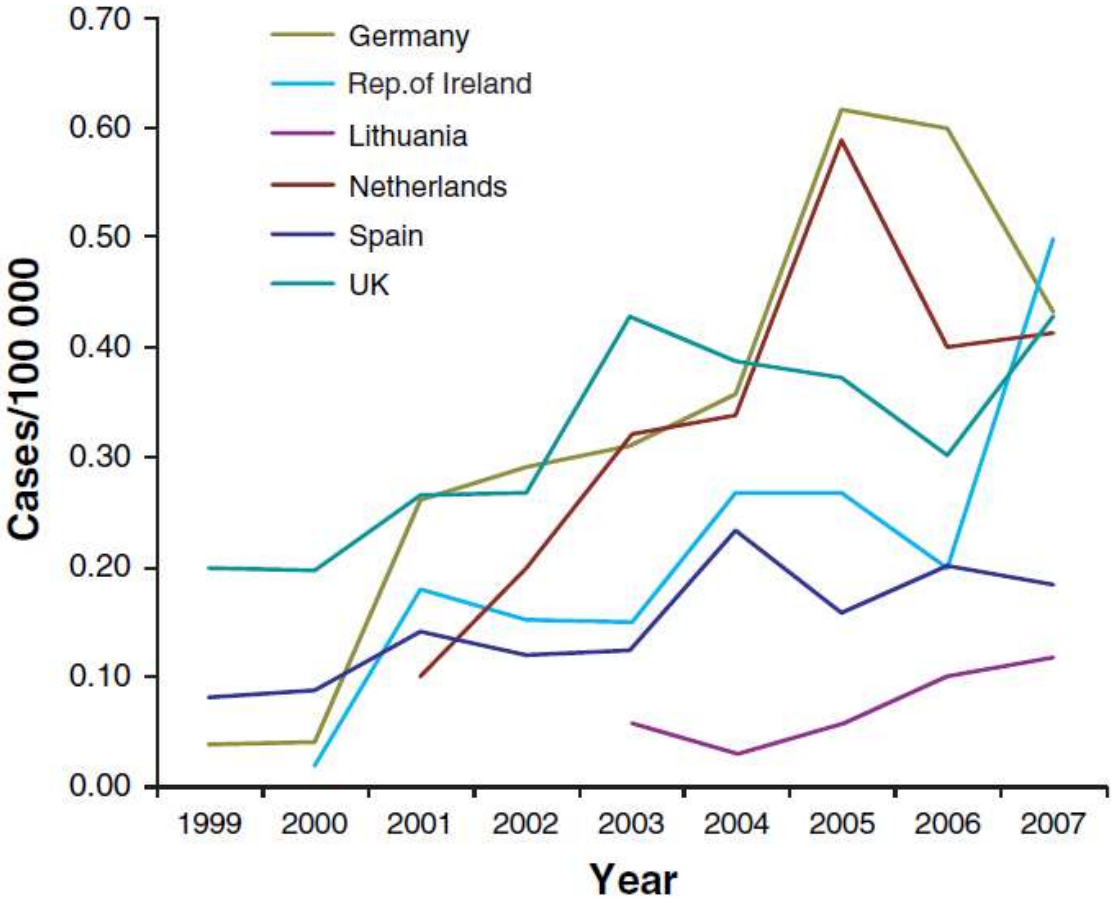

Figure 1.1. Incidence of listeriosis in Germany, Republic of Ireland, Lithuania, Netherlands, Spain and the UK from 1999 - 2007. The graph shows a plot of listeriosis cases/100 000 between 1999 and 2007. The trends indictate that overall the incidence of listeriosis continued to rise during this period (Allerberger and Wagner, 2010).

In 2006, the Health Protection Agency (HPA) reported a dramatic rise in sporadic nonpregnancy-associated listeriosis cases in England and Wales since 2001. Of the reported cases, 97% of patients' ages were available and the data showed that between 2001 and 2004, the risk of sporadic nonpregnancy-associated listeriosis among persons aged ≥60 increased by almost half, compared to 1990 - 2000. Also, a total of 44% of sporadic nonpregnancy-associated and 10% of sporadic pregnancy-associated cases of listeriosis resulted in mortality (Gillespie et al. 2006). Outside of Europe, listeriosis surveillance information seems to be lacking. Few countries worldwide collect data regarding the trends associated with foodborne pathogen diseases, with the collected data being limited to a few industrialised countries (Newell et al. 2010): this may explain the limited amount of surveillance data available outside of Europe. However, the data presented in this chapter shows that concerns regarding the rise of listeriosis cases are warranted especially among the elderly.

Gillespie and colleagues report that the incidence of listeriosis in England and Wales has almost doubled between 2001 and 2007 compared with 1990 and 1999, and that within this period, individuals affected were predominantly the elderly aged ≥ 60 (Gillespie et al. 2009). The same was also observed in other European countries. In Germany, the number of listeriosis case more than doubled between 2001 and 2005 with the increases being predominantly associated with persons aged ≥60 (Denny and McLauchlin 2008), while in France an upsurge was observed in 2006, predominantly among the same age group. In all cases, the rise in listeriosis cases was not associated with foodborne outbreaks and the reason for the observed rise particularly among the elderly remains unknown (Denny and McLauchlin 2008; Gillespie et al. 2006; Goulet et al. 2008). Therefore, in 2009, Gillespie and colleagues conducted a study with the aim of identifying factors that may explain the increase. They were able to conclude that the rise in listeriosis among the elderly may have occurred in patients with cancer or other conditions which require treatment with acid-suppressing medication. They therefore suggested that the potential role of proton pump inhibitors in human listeriosis be investigated (Gillespie et al. 2009).

1.2.2 Contamination of food

L. monocytogenes is ubiquitous: it is easily isolated from natural environments such as soil, water systems, vegetation and silage (Gray, Freitag, and Boor 2006) and is therefore the likely source of the organism in the food chain (Schuppler and Loessner 2010). Foods that are

typically contaminated with the organism include raw unwashed vegetables, soft cheeses (such as feta, brie and camembert (all made using unpasteurised milk)), paté, deli meats and hot dogs (Di et al. 2010; Lamont et al. 2011). In addition to the ability to grow at temperature limits mentioned in section 1.1.2, *L. monocytogenes* is able to tolerate high salt concentrations (up to 10%), and a broad pH range (pH 4.0 to 9.0) (Nightingale 2010). The organism may also be recovered from high temperature short time pasteurisation after exposure to 72°C if originally grown at 39°C and above (Rowan and Anderson 1998). Low storage temperatures and high salt are conditions often used to restrict the growth of foodborne pathogens in consumable products, while high cooking temperatures and pasteurisation are used to kill such organisms. However, the above mentioned features of *L. monocytogenes* facilitate its ability to survive in "ready to eat" (RTE) foods which have been properly refrigerated or frozen, foods with a high salt content, and, in foods where heating has not been thorough (that is, the product has not been uniformly heated for a substantial period, to a temperature which is lethal to the organism).

At present the European Commission's food safety criteria limit for *L. monocytogenes* is ≤ 100 colony forming units per gram (CFU/g) (Little et al. 2009), at the end of its shelf life. The presence of *L. monocytogenes* in food is constantly being surveyed in various European countries to deduce the amount of RTE foods which are beyond this limit, as a means of monitoring the food hygiene standards of manufacturers and retailers, for the safety of the general public. In 2009, Little and colleagues assessed the prevalence of *L. mono*cytogenes in selected retail RTE foods produced in the UK. They showed that the presence of *L. monocytogenes* in selected RTE foods was not exceeded in 99.7% cases. However, the limit was exceeded in 0.4% of prepacked sandwiches within their shelf life, and, in 0.7% of sliced meats within their shelf life (Little et al. 2009). In 2010, Pinto and colleagues surveyed the presence of *L. monocytogenes* in a selection of RTE foods produced in Southern Italy and found that the pathogen was present in 10% of the 1045 tested food items (Di et al. 2010). As a result of their findings, they expressed support for the view that *L. monocytogenes* is a priority for risk assessment (according to the Codex Committee on Food Hygiene) for the development of an international strategy for the reduction of illnesses that result from the consumption of contaminated foods. Generally, European surveillance data show that the majority of RTE food items are within the European Commission's food safety criteria limit, however, it is important that surveillance is continued so that food hygiene standards, as it

relates to *L. monocytogenes*, are improved. Persons more susceptible to listeriosis, may benefit from a lowering of the European Commission's food safety criteria limit to a zero tolerance on the presence of *L. monocytogenes* in RTE foods because their infection dose is lower than an invulnerable population.

1.2.3. Physiopathology

L. monocytogenes can enter the human body via routes such as;

a) the epidermis: this is particularly observed among ruminant raring farmers and veterinarians exposed to genital secretions following listerial miscarriages, and, is manifested as pyogranulomatous skin rashes (Kuhn, Scortti, and Vazquez-Boland 2008).

b) transplacental vertical transmission: from mother to foetus (Lamont et al. 2011).

c) the mouth, through the consumption of contaminated food (the main cause of sporadic and epidemic listeriosis) (Kuhn, Scortti, and Vazquez-Boland 2008).

Following ingestion of contaminated food, the organism is able to penetrate the body via the intestinal mucosa using two mechanisms: one of which involves the phagocytotic uptake by M cells of the Peyer's patches (Figure 1.2) (Kuhn, Scortti, and Vazquez-Boland 2008; Vazquez-Boland et al. 2001b). This is a less efficient method as opposed to translocation of the intestinal mucosa, whereby the organism directly invades enterocytes lining the absorptive epithelium of the microvilli (Kuhn, Scortti, and Vazquez-Boland 2008; Schuppler and Loessner 2010). Subsequent to invasion, the organism is able to replicate in the intestinal wall. Essential to these processes are a number of listerial virulence factors, (which will be discussed later in detail). The result is a local infection in the intestinal lymphoid structures (Vazquez-Boland et al. 2001b).

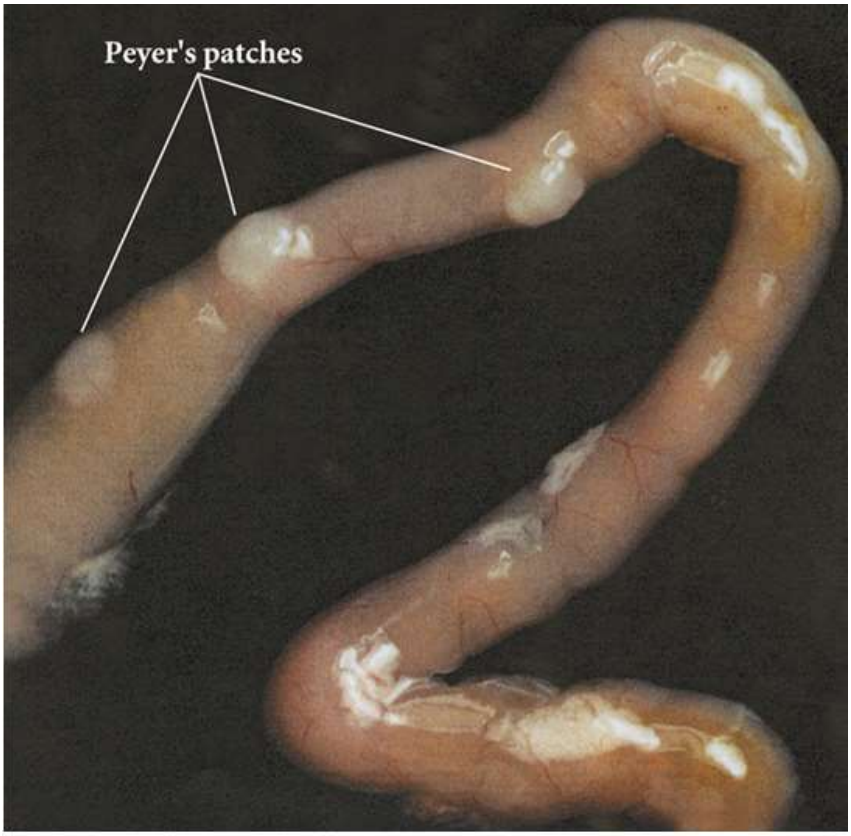

Figure 1.2. Peyers patches, visible as a small bulge on the small intestine. When *L. monocytogenes* is ingested, usually via consumption of contaminated food, the organism is able to penetrate the body via the intestinal mucosa using two mechanisms: one of which involves the phagocytotic uptake by M cells of the Peyer's patches (diagram taken from http://www.ppdictionary.com/bacteria/gnbac/enterocolitica.htm, 2011).

The infected site appears as a pyogranulomatous and the bacteria are present in mononuclear cells. This suggests that the antigen presentation occurs in the intestine and is a site of an immunological response to *L. monocytogenes* infection (Vazquez-Boland et al. 2001b). Following entry into the intestinal cells, *L. monocytogenes* is able to access the mesentric lymph nodes, liver, and spleen by blood or lymph (Vazquez-Boland et al. 2001b). This initial step of host colonisation is very rapid, and occurs within six hours in experimental mice (Kuhn, Scortti, and Vazquez-Boland 2008). The immune system is stimulated during the point of ileal gut infection and this is thought to play a major role in developing protective immunity against a second infection, as well as the prevention of spread to target organs such as; the central nervous system (CNS), where infection may cause meningioencephalitis; the blood stream, where it may cause septicaemia; and the uterus, where it may invade the placenta and subsequently infect the foetus. A physiopathological summary of *L. monocytogenes* infection is shown as a diagram below (Figure 1.3).

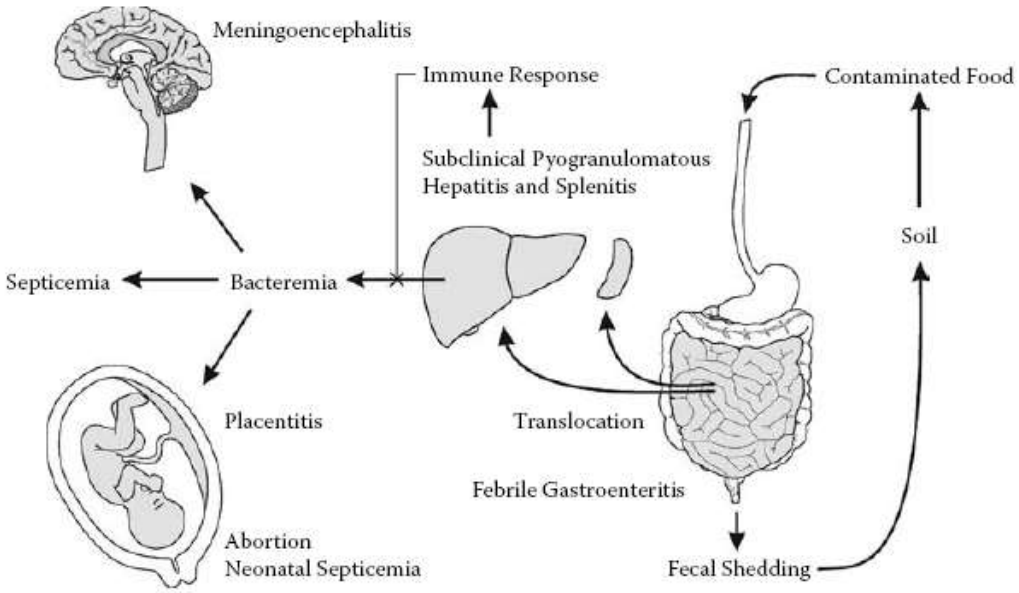

Figure 1.3. Physiopathological summary of *L. monocytogenes* infection. *L. monocytogenes* present in the environment, for example in soil, is a source of food contamination and enters the digestive system through the consumption of such products. Some of the bacteria are excreted ("fecal shedding") and may contaminate food crops which have been exposed to untreated or inadequately treated faeces, resulting in a contamination cycle. Non-excreted *L. monocytogenes* translocate into the ileac cells of the digestive system and subsequently into the mesenteric lymph nodes, liver and spleen (causing subclinical pyogranulomatous hepatitis and splenitis respectively). At this point, a sustained and efficient immune response may successfully clear the pathogen from the body. An unsuccessful or impaired immune response allows the pathogen to continue replication and spread to target areas such as; the CNS, the blood stream and the uterus (taken from Kuhn et al. 2008).

1.2.4. Immunity

1.2.4.1 Innate immunity

A means by which the body controls microbial infection is through the launch of an innate immune response, which is, a non-specific first line of defence against a broad range of pathogens. It is short term, yet very effective and important for the control of microbial multiplication and growth. Infection by *L. monocytogenes* through the consumption of contaminated food is the most natural and frequent route of infection. The bacteria first encounter bactericidal lysozymes secreted by intestinal mucosal cells, stomach gastric acid and antibacterial lectins in the intestine. Numerous other microbes symbiotically colonise the small intestine, *L. monocytogenes* is therefore forced to compete with these organisms for space and nutrients (Greginat and Grauling-Halama 2008). These conditions culminate to make survival of the organism extremely difficult, and few are able to survive in the intestine. Some are able to disseminate to other parts of the body via the circulatory system as blind passengers of macrophages and dendritic cells (DCs), subsequently decreasing the time spent interacting with mucosal environment.

Infected macrophages secrete various cytokines such as interleukin (IL)-1, IL-6, IL-12, IL-18 and the chemokine-monocyte chemoattractant protein-1 (MCP-1), which activates and recruits neutrophils, monocytes, T-cells, natural killer (NK) cells and DCs. IL-12 and IL-18 stimulates the production of gamma interferon (IFN-γ) and tumour necrosis factor (TNF) by T-cells and NK cells. IFN-γ and TNF by positive feedback enhances the bactericidal activity of macrophages. The outcome of the interactions amongst these immuno-components includes the onslaught of the bacteria by effector molecules such as; lysosyme, antimicrobial peptides (such as defensins - an antibacterial peptide), and reactive oxygen species (ROS) and reactive nitrogen intermediate (RNI). Only few cells such as Paneth cells (present in the intestinal microflora), and a specialised subpopulation of TNF and nitric oxide producing DCs have direct bactericidal activity (Greginat and Grauling-Halama 2008). Table 1.1 lists the effector molecules produced in *L. monocytogenes* target organs and the principal immune cells responsible for their production.

Table 1.1. Effector molecules produced in organs targeted by *L. monocytogenes* and the principal immune cells responsible for their production. When *L. monocytogenes* infects target organs the principal immune cells of the organ illicits an immune response by expressing specific effector molecules such as those listed in this table (adapted from Greginat and Grauling-Halama, 2008).

Abbreviations: ROS, Reactive oxygen species; RNI, Reactive nitrogen intermediate; TNF, Tumour necrosis factor; DCs, Dentritic cells; CNS, Central nervous system.

Target Organ	**Principal Immune Cell**	**Effector Molecule**
Stomach		Gastric acid
Intestine	Intestinal microflora Paneth cells	Antibacterial lectins, lysozyme, α-defensins
Liver	Kupffer cells	Defensins, lysozyme
Spleen	Macrophage	ROS, lysosyme, RNI
	TNF and inducible nitric oxide synthase producing DCs	TNF, RNI
CNS	Neutrophils	Defensins, lysozyme

The mechanisms involved in the production of effector molecules via cytokines and MCP-1 are not clearly understood, however, crucial to this overall process is the interaction between the invading organism's conserved pathogen-associated molecular patterns (PAMPs) and the host's pattern recognition receptors (PRRs) (Schuppler and Loessner 2010). Toll-like receptors (TLRs) and the nucleotide-binding oligomerisation domain (NOD) – like receptors (NLRs) are the two PRRs primarily involved in *L. monocytogenes* innate immunity (Schuppler and Loessner 2010).

TLRs are a family of glycoproteins present on the cell surface or within endosomes and are expressed on numerous cells, which include; macrophages, dendritic cells, B cells, T cells, mast cells and epithelial cells (Torres et al. 2004). To date, 10 human TLRs have been described. Their mode of action involves binding extracellular bacterial PAMPs such as lipopolysaccharides, lipoproteins, and flagellin, which leads to binding of four activating adaptors: myeloid differentiating factor -88 (MyD88), MyD88 adaptor like (Mal), Toll-interleukin-1 receptor (TIR) domain-containing adaptor inducing IFN-β (TRIF) and TRIF-related adapter molecule (TRAM) (Schuppler and Loessner 2010). Binding of activating adaptors leads to a cascade of signal transduction events which induces the expression of proinflammatory cytokines and interferons (INF) (Schuppler and Loessner 2010). TLR2 is one such PRR which interacts with listerial lipoproteins and lipoteichoic acids (Schuppler and Loessner 2010). The involvement of TLR2 in the control of *L. monocytogenes* infection has been described in detail by Torres et al. in 2004. Their results showed that TLR2 $^{-/-}$ knockout mice were more susceptible to *L. monocytogenes* systemic infection than wild type mice, and that TLR2 deficient mice had a reduced survival rate, increased bacterial burden in the liver and larger hepatic microabscesses. In addition, they observed that production of proinflammatory immune system components such as; TNF, IL-12 and nitric oxide, which are necessary for infection control, were also reduced in TLR2 deficient macrophages and dendritic cells that were challenged by *L. monocytogenes* (Torres et al. 2004).

While TLR2 has been described as the most relevant TLR for eliciting an innate immune response against *L. monocytogenes* (Torres et al. 2004), other TLR receptors play an active role in the inflammatory response. TLR5, for example, has been shown to bind flagellin - a structural protein component of *L. monocytogenes* flagella. The general observation is that *L. monocytogenes* does not produce flagella at 37°C, which is the human body temperature,

however ~ 20% of clinical isolates are able to produce flagella at this temperature (Way et al. 2004). There is evidence that TLR5 receptors are able to bind flagellin and mediate an immune response by inducing the expression of nuclear transcription factor-κB and TNF, albeit a lower response in comparison to the inflammatory response elicited by TLR2 and only in 20% of *L. monocytogenes* population (Way et al. 2004).

Nucleotide-binding oligermerisation domain (NOD) - like receptors (NLRs), are a family of receptors which have either a caspase recruiting N-terminal domain or a pyrin domain. Currently, 23 NLRs have been identified in humans, all of which are located in the cytosol of mammalian cells where they are responsible for eliciting an innate immune response against *L. monocytogenes* cells that have crossed the membrane barrier to inhabit the host cell (Schuppler and Loessner 2010). NLRs mediate a proinflammatory response through the activation of caspase I (Schuppler and Loessner 2010): an enzyme that cleaves immunogenic proteins such as IL-1β and IL-18 precursors, thus converting them into a mature and active form (Cervantes et al. 2008; Walsh et al. 2011). Of the 23 NLRs, the roles of NOD1 and NOD2 have been described in most detail. Lysozyme catalysis of *L. monocytogenes* peptidoglycan produces a diaminopimelic acid containing a di- or tri-peptide which aids in activation of NOD1. The function of activated NOD1 is to up-regulate transcription of proinflammatory genes and defensins. NOD 2 is also activated by another lysozyme catalytic product of *L. monocytogenes* peptidoglycan: muramyl dipeptide. Activated NOD2 leads to the expression of defensins as well as cryptidins (and α-defensin) which aid in disrupting the bacteria's membrane function (Schuppler and Loessner 2010).

Additional to the role of NLRs in destroying intracellular bacteria, another means by which intracellular bacteria are eliminated from the host cell is by autophagy: a term which in the context of this discussion, describes the enclosure of intracellular invading organisms in an autophagosome and subsequently its destruction while in the enclosure. A number of intracellular microorganisms are susceptible to destruction through autophagy; these include *Salmonella*, Group B *Streptococcus* and *Mycobacterium tuberculosis* (Schuppler and Loessner 2010). In contrast, it has been demonstrated that *L. monocytogenes* is able to evade autophagy due to the essential role of its ActA virulence protein (Yoshikawa et al. 2009). When *L. monocytogenes* invades the host cell, expression of the ActA transmembrane protein commences, and, is utilised to recruit host proteins VASP and Arp2/3 (actin-related proteins

2 and 3complex) in order for the pathogen to disguise itself as a host organelle. By doing so, *L. monocytogenes* avoids ubiquitination as well as LC3 and p62 accumulation which are essential for the occurrence of autophagy (Figure 1.4) (Schuppler and Loessner 2010; Yoshikawa et al. 2009).

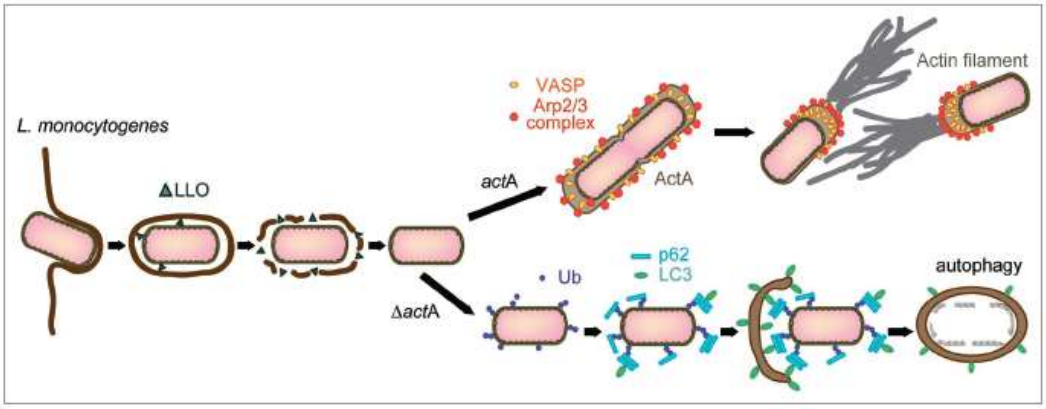

Figure 1.4. *L. monocytogenes* host cell entry and encapsulation in an autophagosome. The bacterium liberates itself from the membrane enclosure with the aid of its membrane-bound listerolysin O (LLO) virulence protein. Expression of membrane bound ActA protein facilitates the accumulation of host proteins VASP and Arp2/3 complex which camouflages the bacterium as a host organelle. The bacterium is therefore able to freely multiply and engage in actin-based motility for cell to cell spread. ActA deficient cells, however, are ubiquitinised and subsequently accumulate p62 and LC3 which are cues for entrapment by autophagosomes and ultimately cell degradation (taken from Yoshikawa et al. 2009).

1.2.4.2 Adaptive immunity

While the innate immune system is the initial response to *L. monocytogenes* infection and is a means of controlling the spread of the organism, the adaptive immune response, facilitates clearance of the organism and is responsible for a more vigorous response, should infection re-occur. Briefly, adaptive immunity is shaped by T-lymphocytes which when mature are subdivided into either CD8+ (otherwise called cytotoxic or killer cells) or CD4+ cells (otherwise called T-helper cells). Any cell infected with *L. monocytogenes* can present its antigens on their cell surface. Such cells are called antigen presenting cells (APC), and these antigens are presented via proteins called major histocompatibility complex (MHC). MHC is divided into class I and class II molecules. Class I MHC molecules presents cytosolic listerial proteins to $CD8^+$ T cells while MHC class II molecules present peptides to $CD4^+$ T cells (Mitsuyama 2008). The role of CD 4 T cells in controlling *L. monocytogenes* infection is unclear, however, the role of $CD8^+$ T cells is better understood. Upon antigen presentation $CD8^+$ T cells respond in two ways:

1) the cells release perforins which function to degrade the cell wall of *L. monocytogenes* and granzymes: a combination of serine proteases, digestive trypsin and chymotrypsin which degrade bacterial proteins, and,

2) the cells secrete IFN-γ and TNF which activate macrophages. IFN-γ plays an important role in resistance to *L. monocytogenes* as it activates resting macrophages which efficiently restricts proliferation of the organisms and is responsible for long term immunity (Schuppler and Loessner 2010).

$CD8^+$ T cells that persist in the body become stable and long lasting memory cells, which are vital to eliciting a more rapid response upon a second infection. Unlike $CD8^+$ T cells, $CD4^+$ T cells do not have a cytotoxic or phagocytic activity. Its roles are centred on facilitating the activity of other immune cells and as a result they are also known as T-helper cells. One means by which this is accomplished is by promoting the secretion of IFN-γ and TNF which maximise the killing efficiency of macrophages and proliferation of $CD8^+$ T cells (Mitsuyama 2008). Some $CD4^+$ T cells promote the production of IL-4, IL-5, IL-6, IL-10 and IL-13 which help to stimulate B- cells and increase antibody production (Mitsuyama 2008).

The basic review of the adaptive immune response, presented here provides an understanding of the fact that immuno-compromised persons and persons with an impaired cell-mediated

immunity are more susceptible to developing severe listeriosis, as such individuals have a diminished ability to produce T-lymphocytes and subsequently the cytokines vital to the adaptive immune system. They therefore lack the ability to fully clear the pathogen from host cells.

1.2.5 Intracellular life cycle and virulence proteins

There are a number of genes which are important and vital for the pathogenicity of *L. monocytogenes* and its intracellular life cycle. Some of these genes and protein products have been thoroughly characterised, yet, many remain unknown. However, as interest in *L. monocytogenes'* pathogenicity continues to grow, research is steadily uncovering other genes that contribute to virulence. Some of the well understood virulence genes are those located on pathogenicity island 1 (LIPI-1) and the internalins. The protein products of these genes function to grant *L. monocytogenes* its characteristic intracellular life cycle which is described as follows:

Contact with a potential host cell induces the formation of pseudopod- like structures. Progression of this stage results in the organism becoming entrapped in a primary phagosome (Kuhn, Scortti, and Vazquez-Boland 2008; Vazquez-Boland et al. 2001a). *L. monocytogenes* is then able to liberate itself from the compartment and into the cytosol where it concomitantly replicates and exhibits actin based motility. Propulsion of the bacteria occurs in random directions and those that reach the host cell membrane push against it resulting in the formation of pseudopod-like structures. As outward movement continues, the pseudo-like structure subsequently protrudes into the neighbouring cell where the organism becomes entrapped in a secondary phagosome (double membrane vacuole). This is followed by liberation of the bacteria from the secondary phagosome and the cycle is re-initiated (Vazquez-Boland et al. 2001a).

Pseudopod formation and uptake of the bacteria into a phagosome is as a result of *inlA* and *inlB* genes which encode internalin A and internalin B membrane bound extracellular proteins, respectively. Expression of a number of genes including; *inlA, inlB, hpt* and genes located on LIPI-1 1 are controlled by positive regulatory factor A (PrfA) protein, which is encoded by (*prfA)* (Figure 1.5). Genes downstream of the *prfA* transcription control site on LIPI-1 which facilitate the release of the bacteria from the phagosome are *hly, plcA* and *plcB*

which encodes listeriolysin O (LLO), phosphatidylinositol phospholipase C (PlcA) and phosphatidylcholine phospholipase C (PlcB) respectively. Also downstream are the *mpl* gene which encodes a metalloprotease (Mpl) that assists in the conversion of PlcB to a mature state, and, the *actA* gene which encodes the ActA protein that is vital for actin based motility (Gray, Freitag, and Boor 2006). The *hpt* gene product is a hexose phosphate transporter (Hpt) which is required for rapid growth in the host cytosol (Scortti et al. 2007). A schematic overview of the intracellular life cycle is depicted in Figure 1.6.

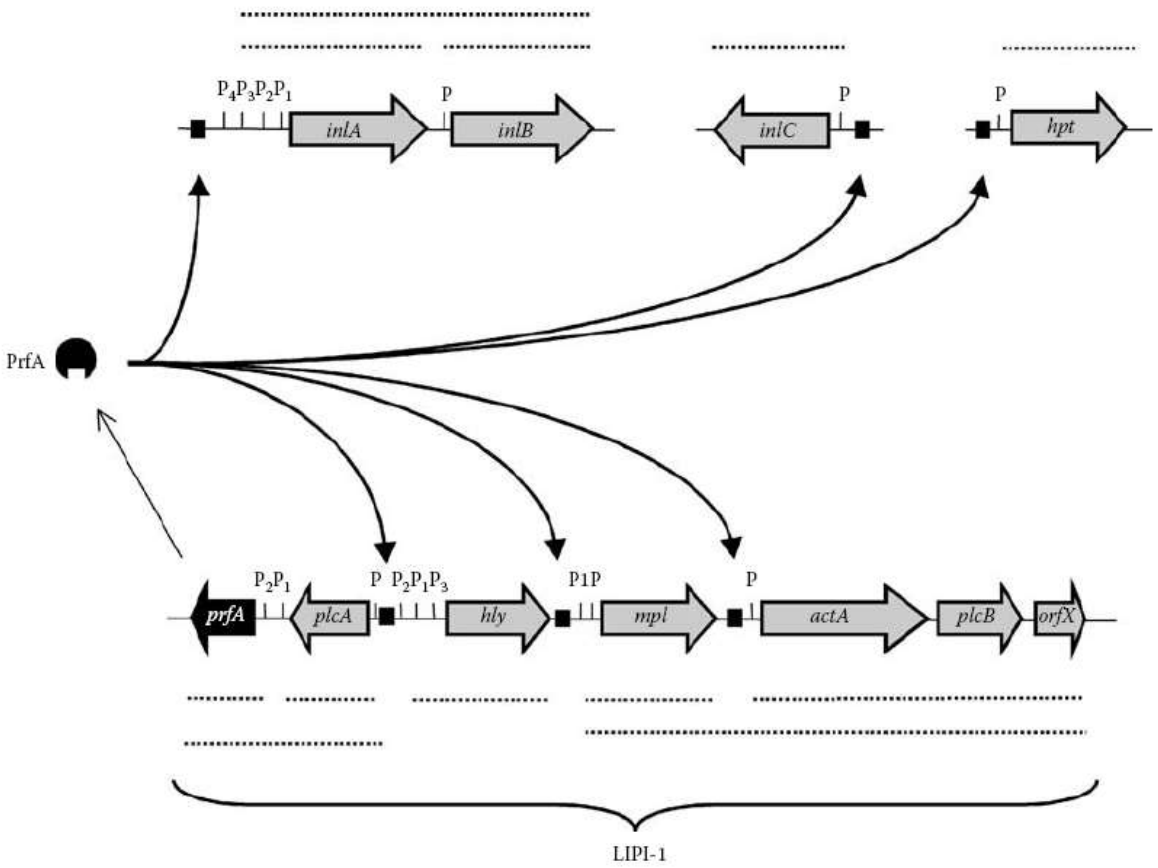

Figure 1.5. Transcriptional control of *L. monocytogenes* virulence genes by PrfA. The *prfA* gene product, PrfA, has a number of binding sites on LIPI-I and elsewhere within the genome (indicated by curved black arrows). Binding of PrfA switches on expression of downstream virulence genes; the transcripts of which may be monocistronic, bicistronic or polycistronic. (Virulence genes are depicted in solid grey arrows, except *prfA* which is depicted as a solid black arrow. Promoters are represented by "P" and transcripts by dotted lines) (Scortti et al. 2007) (taken from Scortti et al. 2007).

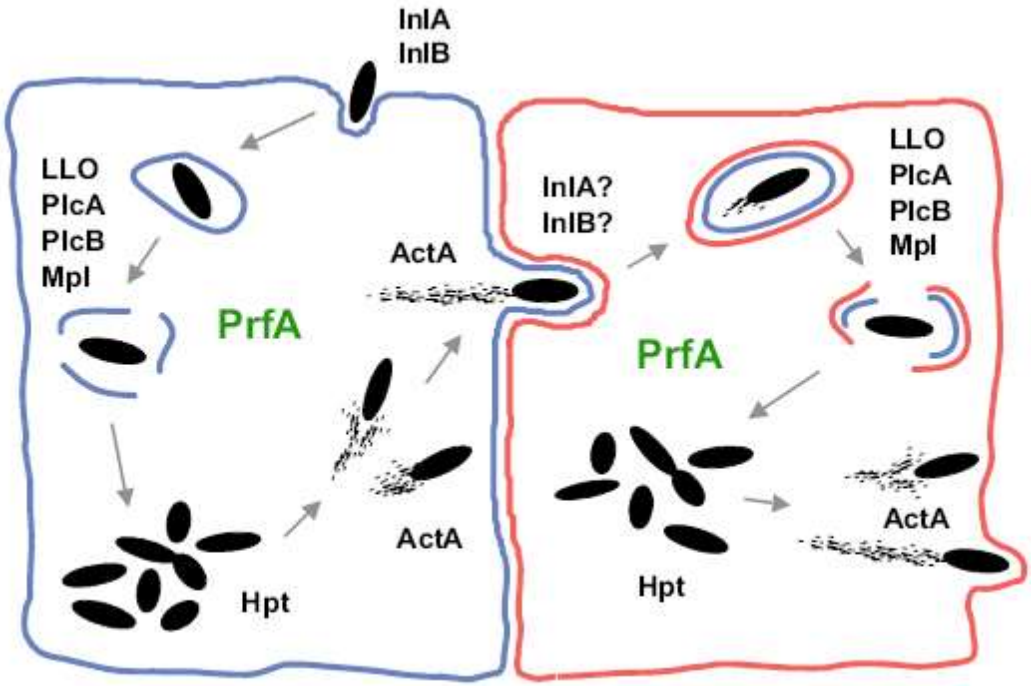

Figure 1.6. Schematic diagram of *L. monocytogenes* intracellular life cycle. The transcription regulator protein, PrfA, controls expression of the depicted bacterial proteins, (InlA, InlB, PlcA, PlcB, Mpl, ActA and Hpt), which are vital for the organism's intracellular lifecycle. InlA and InlB facilitate the organism's entry into the host cell where it is encapsulated in a primary phagosome. LLO, PlcA, PlcB and Mpl facilitate the disruption of the phagosome and release of the pathogen into the host cytoplasm. Hpt gene enables the pathogen to utilise the host cell's hexose phosphates as a carbon and energy source to fuel rapid multiplication (Chico-Calero et al. 2002). ActA is required for polymerisation of host cell actin which is vital for motility. The bacteria are able to propel itself in random directions throughout the cytoplasm. Those that move towards the host cell membrane begin to protrude into neighbouring cells where InlA and InlB again facilitate entry, and, the organism is encapsulated in a secondary phagosome and the life cycle is then re-initiated (taken from Scortti et al. 2007).

1.2.5.1 Positive regulatory factor A

PrfA expression is regulated by three promoter regions upstream of the *prfA* gene, namely; P*prfA*$_{P1}$ and P*prfA*$_{P2}$ which direct a 0.9 kb and 0.8 kb monocistronic *prfA* mRNA transcript respectively, and, the *plcA* promoter; P*plcA* which direct a 1.1 kb monocistronic *plcA* mRNA transcript and a 2.1 kb bicistronic *plcA-prfA* mRNA transcript (Figure 1.7) (Gray, Freitag, and Boor 2006). Research has shown that expression of PrfA is temperature dependent, and that this is due to the thermosensitive structure of the mRNA transcripts which undergoes conformational change at certain temperatures. The structure of the P*prfA*$_{P1}$ transcript at temperatures lower than 30°C inhibits translation, this however, melts at higher temperatures at which translation is unhindered. The bicistronic *plcA-prfA* transcript, which is dependent on PrfA activation, is only produced at high temperatures. In contrast to the P*prfA*$_{P1}$ transcript, the P*prfA*$_{P2}$ transcript contains a thermosensitive component and therefore transcription has been shown to occur at low temperatures (Gray, Freitag, and Boor 2006). A pool of untranslated *prfA* transcripts are therefore present at low temperatures; however, once the organism enters a human host (or other warm blooded hosts), PrfA may be rapidly synthesised (Gray, Freitag, and Boor 2006), which may be seen as a mechanism to increase survival while in a host system.

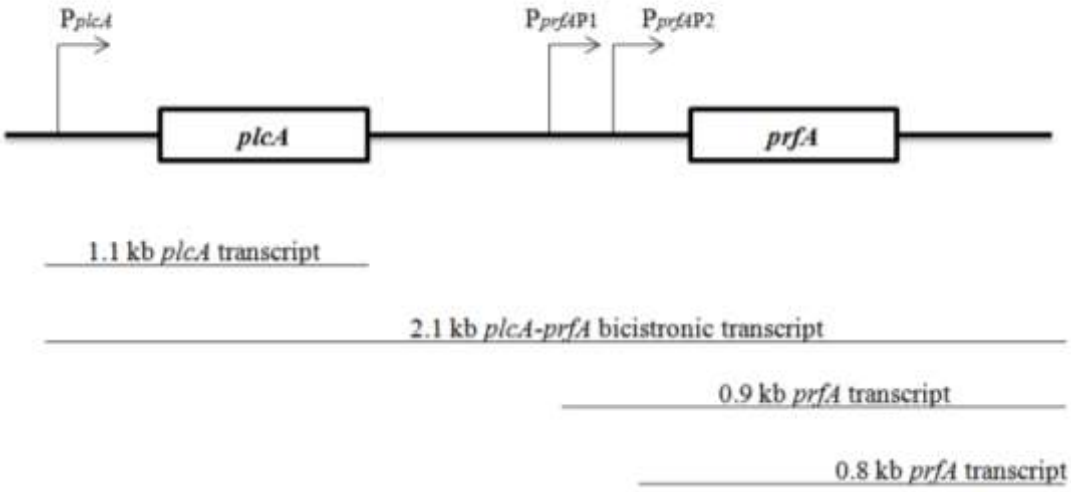

Figure 1.7. Promoter regions of the prfA gene and their gene transcripts. The bold line represents the nucleic acid sequence and boxed areas represent gene coding regions. Arrows indicate promoters and the transcription starting point. Lines below represent the mRNA transcripts which are labelled according to size (adapted from Gray, Freitag, & Boor 2006). PrfA expression is regulated by three promoter regions upstream of the *prfA* gene, namely; P*prfA*$_{P1}$ and P*prfA*$_{P2}$ which direct a 0.9 kb and 0.8 kb monocistronic *prfA* mRNA transcript respectively, and, the *plcA* promoter; P*plcA* which direct a 1.1 kb monocistronic *plcA* mRNA transcript and a 2.1 kb bicistronic *plcA-prfA* mRNA transcript.

1.2.5.2 Listerolysin O

LLO is described as a cholesterol-dependent pore forming toxin, which is structurally and functionally related to cytolysins, another group of pore forming toxins present in some gram positive pathogenic bacteria, such as; *Bacillus anthracis*, *Streptococcus pyogenes*, *Streptococcus pneumoniae* and *Streptococcus suis* (Gekara et al. 2010). Structural modeling and binding studies have given insight into the likely mechanisms that are involved in pore formation. In brief, LLO monomers have 4 domains and are able to bind the cholesterol lipid shaft of the primary and secondary phagosome via the tip of domain 4 (Figure 1.8). In order to form pores, it has been suggested that the monomers diffuse laterally to homo-oligermerise into a ring-like pre-pore complex. Subsequently, two α-helices located in domain 3, unfurl from domain 2 and become transmembrane hairpins (TMH) called TMH1 and TMH2. These hairpins are able to insert themselves into the membrane bilayer, where they form β-barrels which line the aqueous pore (Schnupf and Portnoy 2007).

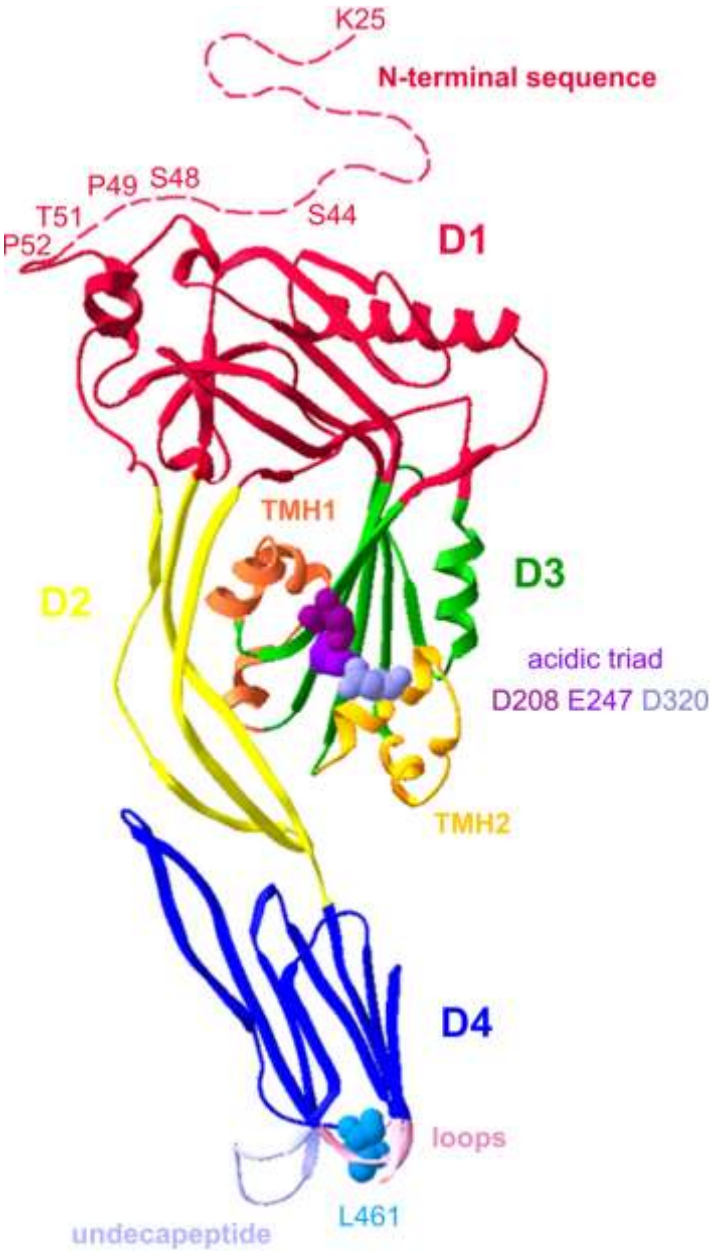

Figure 1.8. Predicted structure of LLO. The model depicts the 4 LLO domains (D1, D2, D3 and D4). Undecapeptide and loops are responsible for binding LLO to the phagosome membrane at cholesterol lipid shafts. Two sets of α-helices in domain 3 form transmembrane hairpins (TMH1 and TMH2), which form the β-barrel pore complex in the phagosome membrane bilayer. The acidic triad composed of amino acids D208, E247 and D320 plays a role in protein inactivation outside the phagosome and in the host cytoplasm (taken from Schnupf and Portnoy 2007).

The function of LLO is impaired outside the phagosome and this is due to the cytoplasmic pH of the host cell. The pH necessary for optimal activity of LLO is 5.5, while that of the phagosome ranges between pH 4.9 and 6.7, and has an average of pH 5.9 (Schnupf and Portnoy 2007). The cytoplasmic pH is > 6.0 and LLO therefore becomes denatured and functionally hindered within the cytosol. This functional impairment is vital to the pathogenic capability of the organism. *L. monocytogenes* expressing the cytolysin perfringolysin (PFO), a protein which is not pH dependent, escapes denaturation by the macrophage phagosomes. However, PFO was also active within the host cytoplasm and lysed the plasma membrane. This disrupted intracellular replication of the organism and as a result *L. monocytogenes* expressing PFO were avirulent. This provides a possible explanation of the need for a LLO pH inactivation mechanism (Schuerch, Wilson-Kubalek, and Tweten 2005). Mutation analysis has given insight into the regions vital for pH dependence. In 2005, Schuerch and colleagues clearly demonstrated that a $LLO^{E247M/D320K}$ mutant was stable at pH 7.4, while the wild type showed reduced haemolytic activity over time at the same pH. The LLO^{D208K} mutant had a lethal effect on the *E. coli* expression cells and therefore could not be studied, however the evidence was sufficient to support the hypothesis that the acid triad is responsible for LLO pH sensitivity (Schuerch, Wilson-Kubalek, and Tweten 2005). This clearly indicated that these juxtaposed amino acids play a role in pH dependence. It has been proposed that the three acidic amino acids in D3 become destabilised at cytosolic pH as a result of charge repulsion between the three carboxylic groups. However, the pH dependence of LLO is not sufficient to drive deprotonation of the carboxylic residues: denaturation is also temperature dependent. It has been suggested that > 30°C facilitates the further weakening of temperature sensitive interactions such as van der Waal forces, ionic bonds and hydrogen bonds (Schuerch, Wilson-Kubalek, and Tweten 2005). As both conditions (> pH 6.0 and > 30°C) exist in the host cytosol, LLO is readily inactivated outside of the phagosome and continues its intracellular cell cycle unhindered.

1.2.5.3 Phospholipases and metalloproteases

Release from the primary phagosome is also facilitated by the action of two phospholipase enzymes, (phosphatidylinositol phospholipase C (PI-PLC; PlcA) and phosphatidylcholine phospholipase C (PC-PLC; PlcB)), and a metalloprotease. Phospholipases are dispensable; however, they enhance the efficiency of escape from the phagosome. In the absence of PI-PLC and PC-PLC, the bacterium shows a significant decrease in its ability to escape the

primary vacuole and secondary vacuole respectively (Figure 1.9) (Yeung et al. 2007). Furthermore it was demonstrated that a mutant lacking both phospholipases was more than 500-fold less virulent than the wild type strain (Moser et al. 1997; Songer 1997).

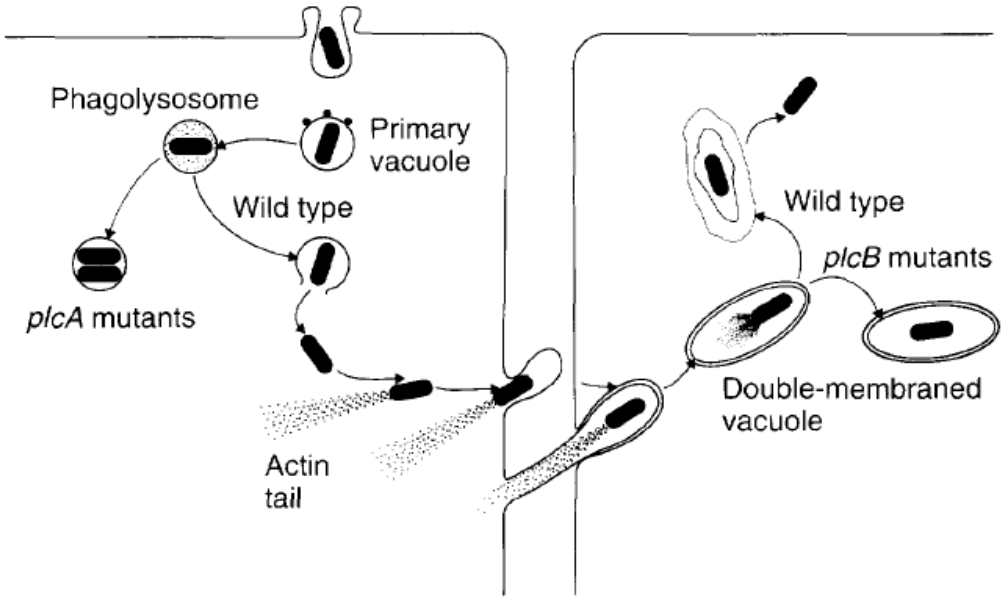

Figure 1.9. *L. monocytogenes* intracellular life cycle. plcA mutants are able to enter the cell by illiciting phagocytosis. However, unlike the wild type species, they are unable to escape the primary vacuole (phagosome) and progress to other stages in the life cycle. plcB mutants are unable to escape the secondary vacuole (phagosome) while the wild type is able to progress to other stages in the life cycle (taken from Songer 1997).

PI-PLC is a ubiquitous enzyme which catalyses the production of D-*myo*-inositol-1-phosphate and diacylglycerol from membrane-bound phosphatidylinositol (PI) by cleavage of its *sn*3-phosphodiester bond. The crystal structure of PI-PLC shows that the active site is located at the C-terminal and was located by crystallisation with myo-inositol (Moser et al. 1997). The enzyme is active between pH 5.5 and pH 7.0 and it is this ability to hydrolyse phagosomal PI in an acidic environment which supports evidence that it aids in phagosome lysis (Kuhn, Scortti, and Vazquez-Boland 2008). Unlike PI-PLC, PC-PLC is a broad range phospholipase (Yeung et al. 2007), which hydrolyses phosphatidylcholine, phosphatidylethanolamine, phosphatidylserine and spingomyelin (Kuhn, Scortti, and Vazquez-Boland 2008). PC-PLC is expressed as an inactive proenzyme, and activation is dependent on the cleavage of a 24 amino acid residue by Mpl. The enzyme is also active in the same pH range as PI-PLC and while *L. monocytogenes* is within the cytoplasm, the enzyme is maintained as an inactive pool at the membrane-cell wall interface. Once compartmentalised in a phagosome the pool of inactive enzyme is activated and translocated across the bacterial cell wall (Yeung et al. 2007).

Mpl is a member of the thermolysin family, a group of proteins capable of hydrolysing N-terminal bonds of hydrophobic amino acid residues in some proteins (Forster et al. 2011). This property accounts for its ability to cleave the PC-PLC proenzyme. It is also categorised as a zymogen, and is therefore expressed as an inactive enzyme. It has been suggested that Mpl is a 55 kDa protein composed of a 20 kDa propeptide domain and a 35 kDa catalytic domain. Activation of Mpl is an autocatalytic reaction and research carried out by Forester and colleagues in 2011 demonstrated that this is pH dependent. They demonstrated that the enzyme primarily remains associated with the bacterium at a cytosolic pH, and that upon a decrease in pH (a condition found in the phagosome), autocatalysis occurs resulting in release of the propeptide and catalytic domain across the bacterial cell wall (Forster et al. 2011).

Other processes involving the role of Mpl in *L. monocytogenes* intracellular life cycle has been hypothesised. This includes 1) Mpl targets secondary molecules whose degradation is required to efficiently transport PC-PLC across the bacterial cell wall, and 2) the protein may function as a chaperone by assisting with PC-PLC folding (Yeung, Zagorski, and Marquis 2005). Exploration of these hypothesises may reveal other roles of Mpl.

1.2.5.4 ActA

When released from the phagosome, the extracellular membrane-bound ActA, is free to interact with host cell cytosolic proteins which have an affinity to its protein motifs (Figure 1.10) (Lambrechts et al. 2008). This interaction is not only led by protein affinity, but also by the host mimicry features of ActA. The N-terminal site constitutes regions A (acidic region), AB (actin-binding region) and C (cofilin homology region), all of which mimic the binding activity of the Wiskott Aldrich Syndrome Proteins (WASP) and WASP verprolin (Wave) protein family. WASP and Wave are activators of actin related proteins 2 and 3 (Arp2/3 complex) which initiates the growth of a branching network of actin filaments (Bompard and Caron 2004). Region AB is a short actin monomer binding motif which putatively contains two WASP homology 2 domains. These are short actin binding motives, which, depending on the sequence variation are involved in monomer binding, nucleation, or filament elongation. In *L. monocytogenes*, this region binds G-actin, however, it has been reported that this region is not essential for *L. monocytogenes* motility (Lambrechts et al. 2008).

The central region of ActA is a polyproline region (PLP) containing FPPP or FPPIP motifs. The proline rich stretches mimic host cell cytoskeletal proteins such as zyxin, vinculin and palladin which are associated with focal adhesion and stress fibres. The proline rich region of these proteins and ActA bind host cell Ena-Vasp protein family. Actin-profilin complexes interact with Ena-Vasp and may increase the pool of actin monomers, as well as, bind to the N-terminal AB region and facilitates shuttling of the G-actin to the growing end of the actin filament.

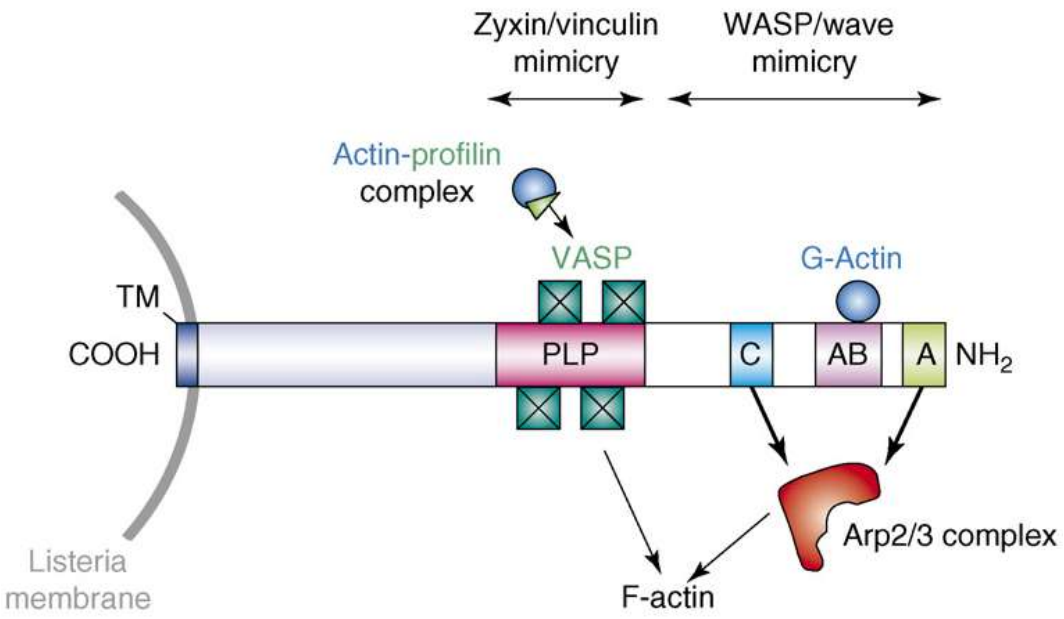

Figure 1.10. ActA protein motifs and interacting host proteins involved in actin tail formation. The N-terminal site (NH2), is comprised of regions; AB which binds G-actin, and, regions A and C which bind Arp2/3 complex. Together this section of ActA mimics the host cell's WASP/wave protein family, facilitating the recruitment of WASP proteins and subsequently more Arp2/3 complex binding. The central site mimics Zyxin/vinculim host proteins and is comprised of polyproline region (PLP) which binds Ena-Vasp. Actin-profilin protein complexes interact with Vasp proteins, and therefore increase the pool of actin polymers (taken from Lambrechts et al. 2008).

Other proteins essential to actin tail formation are; cofilin which is involved in filament-severing and depolymerising, and, capping proteins which regulate barbed end elongation of growing filaments. The barbed end is described as the growing end or the point at which the actin filament is elongated (Figure 1.11a). The growing actin filament potentially becomes branched, forming a network of cross-linked actin filaments (Figure 1.11b). The network of branched actin filaments are polarised into a filopodia (Figure 1.11c).

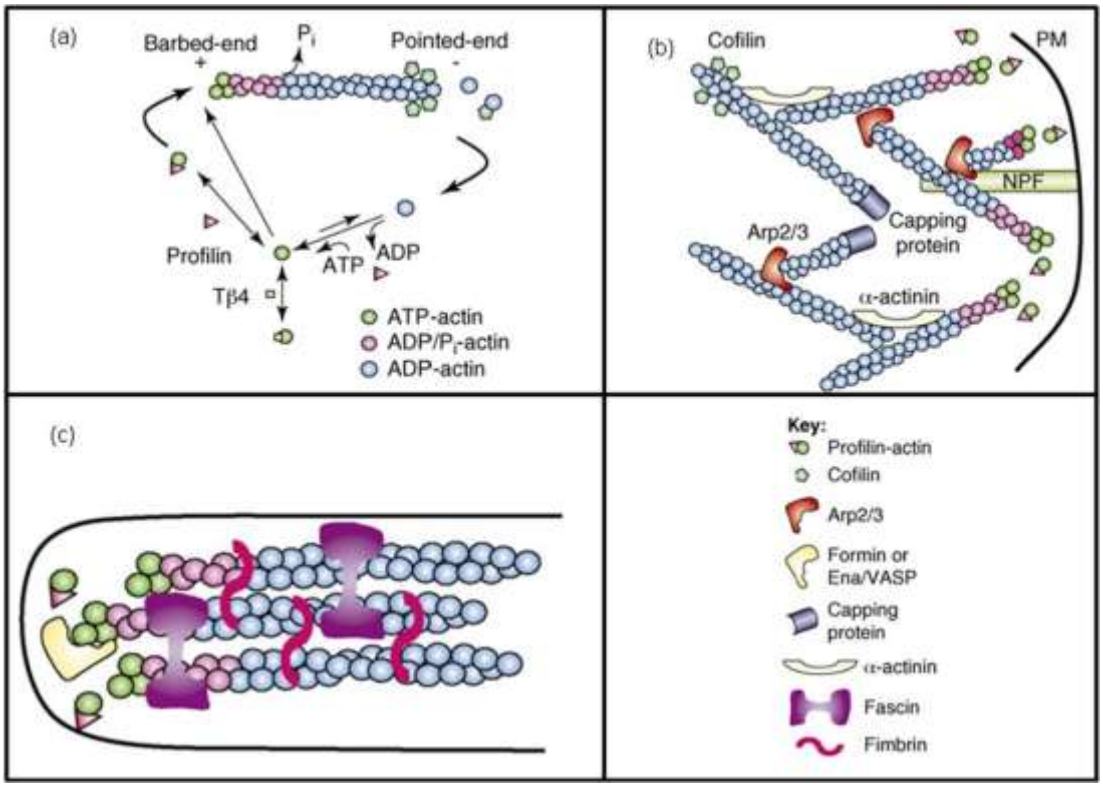

Figure 1.11. Components of *L. monocytogenes* flagella. (a) Formation of actin filament in equilibrium, and regulation by actin binding proteins. ATP-actin monomers are shuttled to the barbed end as profilin-actin, and, cofilin removes ADP-actin from the pointed end. ADP-actin are re-phosphorylated and are either stored in complex with thymosine β4 (Tβ4) or reused at the barbed end. (b) The network of actin filaments is comprised of branched and elongating filaments and is driven by a number of host cell actin binding proteins. Nucleating promoting factors (NPFs) such as WASP, recruit and activates Arp2/3 complex which initiates a new starting point for actin filament formation. Capping proteins terminate barbed end filament extension, cofilin re-introduces new actin monomers and α-actinin stabilises the network of filaments. (c) A simple representation of filament bundles in filapoda. Formin or Ena-VAsp facilitates continuous filament elongation which are bundled by fascin and fimbri (adapted from Lambrechts et al. 2008).

Initially the network of actin filaments are visible as actin clouds, however, this is eventually rearranged into a comet-shaped tail at one pole of the cell. The constant nucleation of actin at the barbed end provides the propulsive force which allows the organism to move in the host cytoplasm at a speed of up to 30nm/s. It has been proposed that this movement gives the added advantage of protection against host cell clearance (Lambrechts et al. 2008).

1.2.5.5 Internalins

The internalins are a multigene family exclusive to *Listeria*. This multigene family is present in *L. monocytogenes* and *L. ivanovii*, and has even been in the nonpathogenic species, *L. innocua* (Vazquez-Boland et al. 2001a). Of this group of proteins, internalin A and internalin B (InlA and InlB respectively) were the first to be discovered. Characteristic of the internalin protein family is a 20-22 leucine-rich repeat domain (LRR) at their N-terminal domain (Figure 1.12) (Seveau, Pizarro-Cerda, and Cossart 2007). Of the 24 proteins known in *L. monocytogenes*, 19 members including internalin A have an LPXTG motif, where X can be any amino acid. The motif facilitates adhesion of the protein to the peptidoglycan of the bacterial cell wall via covalent bonds (Seveau, Pizarro-Cerda, and Cossart 2007). InB is the sole member which has no LPXTG motif. Instead, the protein is bound to the bacterial cell wall by glycine/tryptophan-rich (GW) repeat modules which bind cell wall lipoteichoic acid by electrostatic force. Representation of this internalin family is shown in Figure 1.12. The remaining proteins are all secreted and therefore contain no LPXTG or GW motifs (Seveau, Pizarro-Cerda, and Cossart 2007). InlA and InlB have been demonstrated to be involved in uptake of the pathogen by non-phagocytic cells. InlA facilitates entry into epithelial cells while InlB facilitates invasion of a broader range of cells including; epithelial cells, endothelial cells, hepatocytes and fibroblasts (Seveau, Pizarro-Cerda, and Cossart 2007).

InlA is able to facilitate entry into cells via interaction with E-cadherin, an intercellular adhesion protein which ensures that cells within tissue are bound together. Interaction with E-cadherin is due to the specificity of InlA interaction with the proline amino acid at position 16 of the molecule.

InlB is able to interact with a number of receptor proteins in order to facilitate cell invasion. Of the numerous receptors, the c-Met receptor has been described as playing a key role. The c-Met receptor is a hepatocyte growth factor with cytoplasmic tyrosine kinase activity. Upon

binding of InlB to the receptor, phosphorylation of the cytoplasmic domain is induced and this leads to a cascade of signal transduction events which conclude with activation of the Arp2/3 complex, cortical actin cytoskeleton rearrangement and phagocytosis of the pathogen.

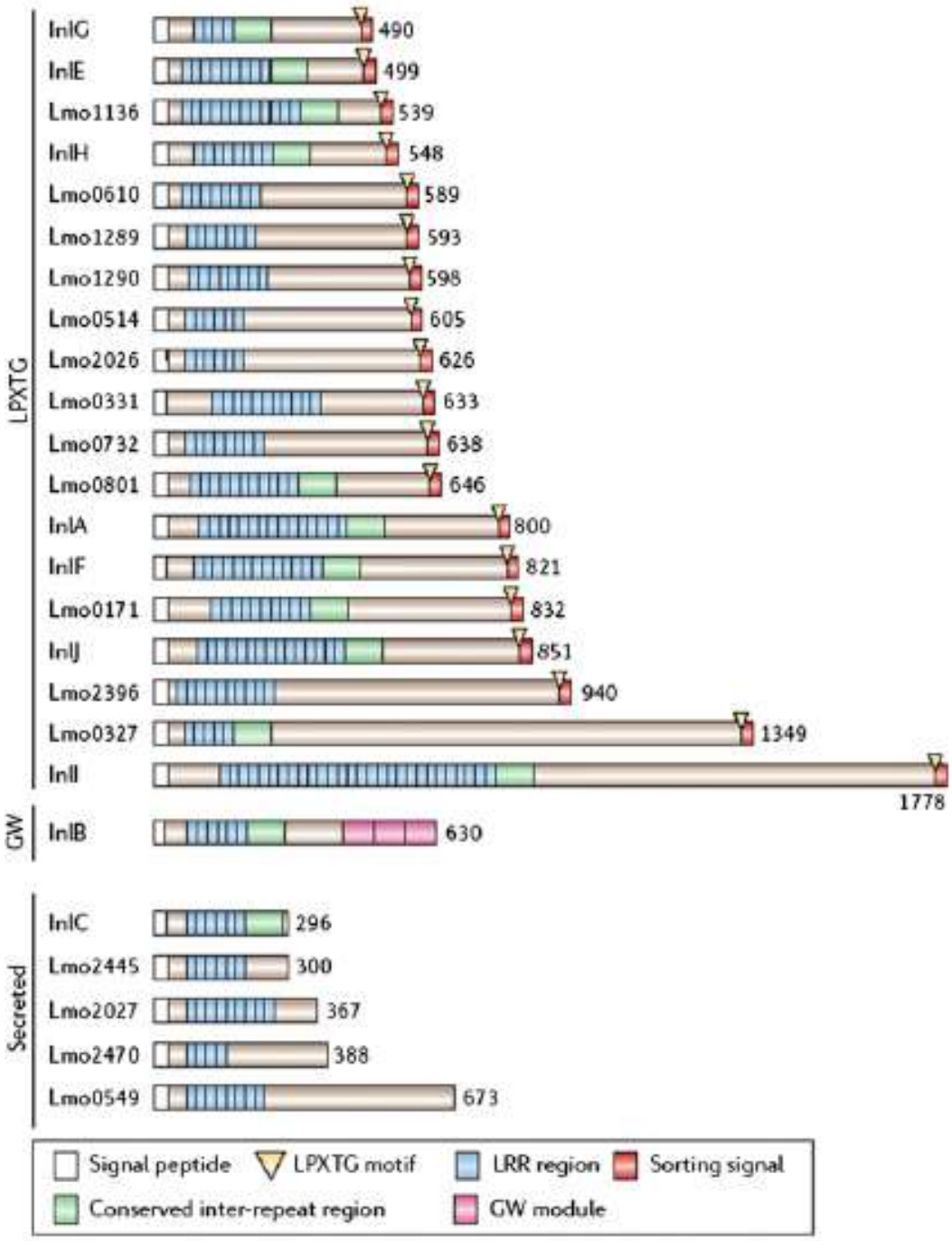

Figure 1.12. Internalin protein family. All the proteins have a signal peptide and the characteristic 20-22 leucine rich repeat. The LPXTG motif, where X can be any amino acid, anchors the protein in the bacterial cell wall. LPXTG is absent from InlB which uses its GW module to anchor itself in the bacterial cell wall. Secreted proteins have no LPXTG motif and lack a sorting signal (taken from Seveau et al. 2007).

1.2.5.6 Other virulence proteins

Although the genes located on LIPI-1 and the internalins tend to be the main focus of discussion when referring to virulence genes, it is important to note that there are other genes which play a key role in pathogenicity of the organism. One of the more frequently documented genes include: *bsh* which allows the organism to survive the acid condition in the small intestine caused by the release of bile. *Bsh* encodes bile salt hydrolases which hyrolyses the amide group adjacent to the steroid core, resulting in liberation of the glycine and taurine amino acid side chains thus rendering it less toxic to the pathogen (Begley, Hill, and Gahan 2006; Zhang et al. 2011). As research in this area increases, virulence-associated genes which play a role in the pathogenicity of *L. monocytogenes* are likely to be uncovered, which will ultimately provide clearer understanding of the numerous mechanisms involved in host infection.

1.2.6 Identification methods

Due to the severity of *L. monocytogenes* infection in high risk individuals, and the observed rise in the number of listeriosis cases, there has been an important need to improve techniques which offer rapid and discriminatory identification of the organism in order to help improve patient care. In the past, identification of the organism was based solely on certain phenotypic characteristics; such as motility, Gram stain, haemolysis and the Christie, Atkins, Munch-Petersen (CAMP) test; however, they are now being superseded by DNA-based methods. Although the latter have gained popularity, traditional methods remain valuable for the identification of *L. monocytogenes*, and as such, a brief description is given below, in addition to the more recent methods.

1.2.6.1 Phenotypic

1.2.6.1.1 Christos, Atkins, Munch-Petersen test

All *Listeria* species are Gram positive and motile with peritrichous flagella at < 30ºC and therefore these tests cannot be used to distinguish *L. monocytogenes* from other species of the same genus. However, the CAMP test, originally designed by Christie et al. in 1944 for the detection of group B streptococci, went through an evolutionary period over the years and was first described by Fraser in 1962, for the purpose of distinguishing *L. monocytogenes* from other hemolytic *Listeria* species (McKellar 1994). Briefly, the test is carried out by parallelly streaking *Staphylococcus aureus* and *Rhodococcus equi* on a rabbit or sheep blood

agar plate. The *Listeria* species to be identified is perpendicularly streaked on the same plate but not touching *S. aureus* and *R. equi*. Haemolysis by *L. monocytogenes* is enhanced in the vicinity of *S. aureus* while haemolysis by *L. ivanovii* is enhanced in the vicinity of *R. equi. L. seeligeri* also displays haemolysis in the vicinity of *S. aureus*, but to a lesser extent than *L. monocytogenes* (Figure 1.13) (Gasanov, Hughes, and Hansbro 2005). The remaining *Listeria spp.*: *L. grayi*, *L. innocua*, *L. marthii*, *L. rocourtiae* and *L. welshimeri*, are non-haemolytic and are therefore CAMP negative. It is worth noting that there are some *L. innocua* strains that are haemolytic (Liu 2008) as well as *L. monocytogenes* that are non-hemolytic (for example the type strain NCTC 10357 (Jones and Seeliger 1983). Such isolates would therefore not be correctly identified using the CAMP test.

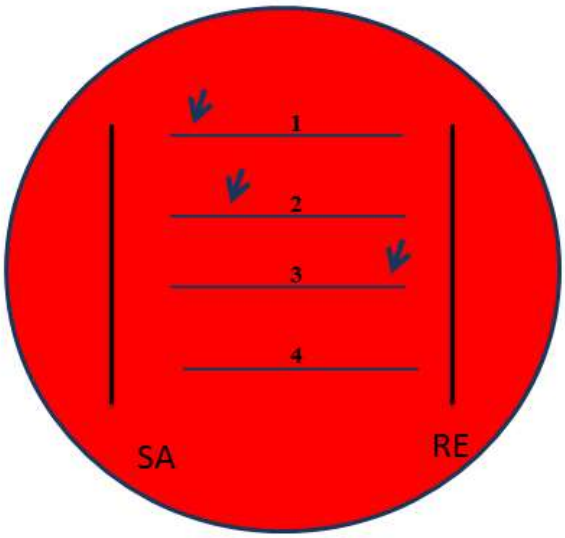

Figure 1.13. *Listeria spp.* CAMP Test. The diagram illustrates the type or result expected when performing a CAMP test to identify *L. monocytogenes*, *L. ivanovii* and *L. seeligeri*.
The red circled area is representative of a blood agar plate. Lines represent bacterial growth; SA = *S. aureus*, RE = *R. equi*, 1 = *L. monocytogenes*, 2 = *L. seeligeri*, 3 = *L. ivanovii* and 4 = *L. innocua*. Arrows indicate areas where β-haemolysis is heavily present. The *Listeria* species to be identified are perpendicularly streaked on the same plate but not touching *S. aureus* and *R. equi*. Haemolysis by *L. monocytogenes* is enhanced in the vicinity of *S. aureus* while haemolysis by *L. ivanovii* is enhanced in the vicinity of *R. equi*. *L. seeligeri* also displays haemolysis in the vicinity of *S. aureus*, but to a lesser extent than *L. monocytogenes.*

1.2.6.1.2 Immunological methods

Immunological methods used for identification are often available as commercial kits and are usually for the identification of *Listeria spp.* or *L. monocytogenes*. Immunological methods can be divided into four categories; visual immunoprecipitation, latex agglutination, immunomagnetic separation (IMS) and enzyme-based immunoassay (EIA). Identification is generally base on the simple but effective mechanism of using matrix bound *Listeria* antisera to bind *Listeria* antigens (Gorski 2008). Briefly, in visual immunoprecipitation, a lateral flow cassette is used. The enriched test sample is spotted onto a nitrocellulose membrane and it flows to a region of the membrane where gold or other visual detection chemistry is conjugated to *Listeria* antibodies. Depending on the kit, the appearance of a coloured line is indicative of a positive reaction (Gorski 2008). In latex agglutination procedures, a *Listeria* enrichment culture is added to *Listeria* antiserum bound to latex particles. The reaction is carried out on a dark coloured surface and agglutination is visible as white cloudy clumps. IMS involves the use of *Listeria* antibodies bound to magnetic beads. The beads are mixed with a contaminated microflora or enrichment culture, and incubated briefly (Gorski 2008). The organism is therefore sequestered and concentrated when the beads are washed and placed in a smaller volume (Mercanoglu et al. 2003). The beads are plated on a *Listeria* selective medium and identification is based on the appearance of *Listeria* colonies (or by further analysis such a colony immunoblotting (Gorski 2008). Finally, enzyme linked immunosorbent assay and enzyme linked immunosorbent fluorimetric assay are forms of EIA. Both are methods in which *Listeria* antisera is bound to a matrix such as a well of a microtitre plate. Briefly, an enrichment culture is added, followed by a brief incubation and washes. A solution containing another *Listeria* antiseria conjugated to an enzyme is added followed by an enzyme substrate. *Listeria* is confirmed by presence of colourimetric or fluorimetric change that is detected by visual inspection or a microplate reader. An advantage of using EIA is that detection is high throughput due to work being carried out in a multiwell plate (Gorski 2008).

The disadvantages associated with the use of most kits are: 1) they are often compromised by components of enrichment media such as high salt and (2) as they mostly identify *Listeria spp.*, further tests are necessary for identification to the species level. This method is therefore mostly suitable as a screening tool (Gorski 2008).

1.2.6.1.3 Biochemical and API *Listeria* tests

In the past, biochemical tests have been routinely used to differentiate *L. monocytogenes* from other *Listeria* species, based on differences in abilities to ferment certain sugars (Table 1.2). However, disadvantages associated with biochemical methods are monetary cost and time as confirmation of results can take up to 6 days (Liu 2006). The use of biochemical tests remain valuable today, though it has been modified and offered as a small and easy to use collection of tests known as API *Listeria* (BioMérieux) (McLauchlin 1997). The API *Listeria* is inexpensive and offers considerable reduction in identification time as results are available in 18- 24 hours. It is offered as 10 individual tests located on a single strip, and are as follows; DIM test (based on the presence or absence of arylamidase), aesculin hydrolysis, presence of α-mannosidase and acidification of: D-arabitol, D-xylose, L-rhamnose, α-methyl-D-glucoside, D-ribose, glucose-1-phosphate and D-tagatose (Table 1.3). The results are easily interpreted by colour changes as detailed by the manufacturer (Bille et al. 1992).

Previously a haemolysis test was required in order to distinguish *L. monocytogenes* from *L. innocua* as both could at times produce the same identification results (Table 1.2). However, the API *Listeria* negates the need for this as the incorporation of the DIM allows clear separation of both species (Table 1.3).

Table 1.2. Biochemical test outcomes used to differentiate *Listeria spp.*. The fermentation results of each sugar; L-rhamose, D-mannitol, D-xylose and A-methyl mannoside may be positive, negative or variable and the combination of results provides the basis of the identification(adapted from Gassanov et al. 2005).

Key: +, positive reaction; -, negative reaction; and V, variable reaction.

Test		***L. monocytogenes***	***L. innocua***	***L. ivanovii***	***L. seeligeri***	***L. welshimeri***	***L. grayi***
Fermentation of:	L-rhamnose	+	V	-	-	V	V
	D-mannitol	-	-	-	-	-	+
	D-xylose	-	-	+	+	+	-
	A-methyl mannoside	+	+	-	-	+	+

Table 1.3. API *Listeria* test outcomes used to differentiate *Listeria spp.*. The API is offered as 10 individual tests located on a single strip, and are as follows; DIM test (based on the presence or absence of arylamidase), aesculin hydrolysis, presence of α-mannosidase and acidification of: D-arabitol, D-xylose, L-rhamnose, α-methyl-D-glucoside, D-ribose, glucose-1-phosphate and D-tagatose (Table 1.3). The results are easily interpreted by colour changes as detailed by the manufacturer. The results may be positive, negative or variable and the combination of results provides the basis of the identification (adapted from Bille et al. 1992). Key: +, positive reaction; -, negative reaction; and V, variable reaction.

Test	***L. monocytogenes***	***L. innocua***	***L. ivanovii subsp ivanovii***	***L. ivanovii subsp londoniensis***	***L. seeligeri***	***L. welshimeri***	***L. grayi***
DIM	-	+	V	V	+	V	+
Aesculin hydrolysis	+	+	+	+	+	+	+
α-Mannosidase	+	+	-	-	-	+	V
D-Arabitol	+	+	+	+	+	+	+
D-Xylose	-	-	+	+	+	+	-
L-Rhamnose	+	V	-	-	-	V	-
α-Methyl-D-glucoside	+	+	+	+	+	+	V
D-ribose	-	-	+	-	-	-	+
Glucose-1-phosphate	-	-	+	V	-	-	-
D-Tagatose	-	-	-	-	-	+	-

As is often the case with most identification methods, API *Listeria* at times has to be used in conjunction with other tests in order to attain confident identification as in a very small number of cases it may result in no identification or misidentification. This was reported in 1992 by Bille et al. who tested a total of 646 *Listeria* strains (Table 1.4). They tested 258 strains of *L. monocytogenes*, 176 *L. innocua*, 75 *L. ivanovii*, 76 *L. seeligeri* and 47 *L. welshimeri* and found that 2.3%, 0.6%, 10.7%, 100% and 6.4% respectively, required additional tests for correct identification. A total of 1.3% and 4.3% of *L. ivanovii* and *L. welshimeri* were not identified while 2.1% of *L. welshimeri* were misidentified (Table 1.4).

Table 1.4. Identification results of 646 *Listeria* isolates using API *Listeria*. A total of 258 strains of *L. monocytogenes*, 176 *L. innocua*, 75 *L. ivanovii*, 76 *L. seeligeri* and 47 *L. welshimeri* were tested. Results showed that 2.3%, 0.6%, 10.7%, 100% and 6.4% respectively, required additional tests for correct identification. A total of 1.3% and 4.3% of *L. ivanovii* and *L. welshimeri* were not identified while 2.1% of *L. welshimeri* were misidentified. This data shows that API *Listeria* at times has to be used in conjunction with other tests in order to attain confident identification as in a very small number of cases it may result in no identification or misidentification (taken from Bille et al. 1992).

Species	No. of strains tested	No. (%) with the indicated overall result				
		Correct identification			No identification	Misidentification
		Without additional tests	With additional tests	Total		
L. monocytogenes	258	252 (97.7)	6 (2.3)	258 (100)	0 (0)	0 (0)
L. innocua	176	175 (99.4)	1 (0.6)	176 (100)	0 (0)	0 (0)
L. seeligeri	76	0 (0)	76 (100)	76 (100)	0 (0)	0 (0)
L. ivanovii	75	66 (88.0)	8 (10.7)	74 (98.7)	1 (1.3)	0 (0)
L. welshimeri	47	41 (87.2)	3 (6.4)	44 (93.6)	2 (4.3)	1 (2.1)
L. grayi	14	14 (100)	0 (0)	14 (100)	0 (0)	0 (0)
Total	646	548 (84.8)	94 (14.6)	642 (99.4)	3 (0.4)	1 (0.2)

1.2.6.2 Genotypic

Genotypic identification methods fall into two main categories; non amplification methods and amplification methods. Among the non-amplification methods are DNA-DNA hybridisation, gene probe hybridisation, southern blot and fluorescence *in situ* hybridisation (FISH). Amplification methods include traditional PCR, reverse transcription PCR, real time PCR and quantitative PCR.

1.2.6.2.1 DNA-DNA hybridisation

In DNA-DNA hybridisation, the DNA from the type strain is sheared and mixed with the radiolabelled DNA of the test isolate. The mixture is heated at 100°C for 3-4 minutes, and maintained at 60°C for 16 hours. The DNA is passed through a hypoxyapatite column which has the ability to retain double stranded DNA. The column is washed followed by elution of DNA. Radioactivity is measured and is commensurate to the amount of *Listeria* present (Liu et al. 2008). The use of radioactive labelling was later replaced with safer and equivalently sensitive options such as; biotin, enzymes and SYBR green which has a great affinity for dsDNA (Gasanov, Hughes, and Hansbro 2005).

1.2.6.2.2 Gene probe hybridisation, southern blot and fluorescent *in situ* hybridisation

DNA-DNA hybridisation was later replaced by various probe based detection methods which overall offered a reduction in identification time. A probe is a short stretch of single stranded nucleic acid sequence which is specific to a particular gene target and is labelled with an enzyme, biotin, fluorescence or a radio isotope. Probe-base detection methods include; gene probe hybridisation, southern blot and FISH. Briefly, for gene probe hybridisation, a number of targets are available for detection of *L. monocytogenes*. These mostly include virulence genes such as: *prfA*, *hly*, *inlA*, *inlB*, *inlC*, *inlD*, *plcA*, *plcB*, *mpl*, *actA*, flagellin (*fla*) and invasion-associated protein (*iap*) (Gasanov, Hughes, and Hansbro 2005). The overall principle involves hybridisation of the probe to test strain isolated DNA which is bound to a surface such as: nitrocellulose or nylon membrane or a microtitre plate. This method has been useful for the differentiation of *Listeria spp.* The disadvantage associated with this method is poor sensitivity, as a result of low copy number, (usually a minimum of 10^4 target copy

number is required for adequate detection) (Liu et al. 2008). For this reason PCR based methods have superseded gene probe hybridisation amplification.

Southern blot is similar to gene probe hybridisation in that a probe is used for detection. The method involves restriction enzyme digestion of test isolate DNA followed by separation of the resulting DNA fragments on an agarose gel. The gel is treated with alkali in order to produce single stranded fragments. This aids transfer and binding of the nucleic acid onto a nitrocellulose or nylon membrane and ultimately probe hybridisation. The membrane is baked or exposed to ultraviolet light (in the case of nitrocellulose and nylon, respectively), in order to affix the nucleic acid. This is followed by hybridisation of the nucleic acid with a fluorescent, chemogenic or radio labelled DNA or RNA probe. Unbound probe is subsequently removed by washing and hybridisation is visualised by colourimetric development (chemogenic probe), or auto radiography (fluorescent and radio labelled probe). This method has been used to differentiate *Listeria* species and also extends to differentiation of serotype 4b strains belonging to lineages I and II as well as further discrimination of IIIA, IIIB and IIIC subgroups (Liu et al. 2008). Serotyping will be discussed in more detail in section

FISH is another variant of probe gene probe hybridisation and is based on labelling a specific sequence in the chromosome so that it becomes visible under a microscope. It involves fixing test whole bacteria cells to a glass slide or to the well of a microtitre plate. The cells are permeabilised by incubation with proteinase K. This is followed by addition of a fluorescently labelled probe specific for 16S rRNA genes. The cells are then visualised under a microscope. All species of *Listeria* are identifiable using (Liu et al. 2008).

1.2.6.2.3 PCR amplification based methods

The polymerase chain reaction (PCR), a method developed by Kary Mullis in 1983, allows the exponential amplification of a gene target using key reaction components such as; primers which flank the nucleic acid target of interest and a heat stable polymerase necessary enzymatic amplification. It is widely applied for identification of *L. monocytogenes* and distinguishing the organism from other *Listeria* species. Targets genes commonly used for identification include, (but are not limited to), virulence genes. In its traditional and simple form, amplified gene target products are visualised by separation on an agarose gel, followed

by staining with a DNA chelating compound such as ethidium bromide. The presence of a DNA band of expected size is indicative of positive identification. This method has been employed over decades by numerous researchers: In 1991, Thomas et al. were able to distinguish *L. monocytogenes* from other *Listeria* species by the amplification of the listerolysin O genes regions unique to the organism (Thomas et al. 1991).

A number of PCR variants have also been implemented for identification, some of which include nested PCR, multiplex PCR, real time PCR and reverse transcriptase PCR. Briefly, nested PCR is used in instances where increased sensitivity is required, normally due to a low number of target organisms. It requires the use of two sets of primers, used in separate amplification rounds. In the first amplification, a larger target area is amplified. The PCR products are transferred to a second reaction tube where the second set of primers are used to amplify a region within the PCR products. Disadvantages associated with nested PCR are that it requires more time than conventional PCR and there is a chance of introducing contaminants in the process of transferring PCR products from the first PCR round to the second (Liu et al. 2008). Multiplex PCR permits simultaneous amplification of more than one gene. One of the first multiplex PCR assays designed for detection of *L. monocytogenes* was described by Furrer et al. in 1991, which based identification on the amplification of unique *hly* and *iap* gene regions (Furrer et al. 1991). Amplification of both genes is distinguishable by the visualisation of bands of different and expected sizes. A real time PCR assay involves the use of a fluorescent, DNA intercalating dye, such as SYBR green or EVA green, during the amplification process. The dye is introduced to the reaction mixture, and is less fluorescent in its unbound state. As the sequence is amplified, the dye binds to the double stranded DNA and fluoresces. The fluorescence is therefore at its highest when the number of amplicons is at its highest. This signal is detected by an optical sensor which monitors the process in real time. The advantage associated with this method is that it negates the need to separate the amplified fragments on an agarose gel. The results are therefore available shortly following the PCR. Additionally, multiplex real time PCR is possible provided that melt curve analysis is performed after PCR amplification is complete. This involves melting the dsDNA by a gradual increase in temperature. As the temperature is increased, the dsDNA is denatured and the dye is released, resulting in a decrease in fluorescence. The decrease in fluorescence is continuously detected in order to deduce the melting temperature (Tm). The Tm is defined as the point when 50% of the amplicons are double stranded and 50% are

single stranded and the resulting melt curve data are plotted as fluorescence versus time. This is known as melt curve analysis and is useful provided that the melting temperatures of each set of PCR products are sufficiently different (Liu et al. 2008). Unlike the methods previously described which requires DNA, reverse transcription PCR involves the use of mRNA from which complementary DNA is synthesised by a reverse transcriptase. This can be followed by the traditional PCR reaction and can be performed in the same reaction mixture. The advantage of this method is that it is highly sensitive, as it allows identification from a sample with a low copy number of mRNA molecules (Liu et al. 2008).

1.2.6.3 Outbreak investigation

Though useful, species level identification of *L. monocytogenes* is not sufficient for control of outbreaks in the human populations as it is not discriminatory. Discriminatory methods are valuable in efforts to control outbreaks as the information allows us to distinguish outbreak strains as well as provide a link to the source of contamination. Outbreak investigation methods therefore probe the organism even further than the phenotypic and genotypic identification methods previously discussed, providing a means of characterising the organism in greater detail.

1.2.6.3.1 Serological serotyping

Isolates that have been identified as *L .monocytogenes* can be further subdivided into subtypes by serotyping. Serotyping is a once widely used traditional phenotypic method which involves agglutination of the somatic (O) and flagella (H) proteins with corresponding antibodies. There are 15 *Listeria* somatic (O) antigens subtypes (I-XV) and 4 flagella (H) subtypes (A-D). Serotypes are determined by unique combinations of O and H antigens (Table 1.5), and based on the agglutination pattern *L. monocytogenes* is divided into at least 13 serotypes (Kerouanton et al. 2010; Liu 2006; Ragon et al. 2008).

Table 1.5. List of O and H antigens that agglutinate to form serotypes of *Listeria*. There are 15 *Listeria* somatic (O) antigens subtypes (I-XV) and 4 flagella (H) subtypes (A-D). Serotypes are determined by unique combinations of O and H antigens, and based on the agglutination pattern *L. monocytogenes* can be divided into at least 13 serotypes(taken from Liu 2006).

Serotype	O antigens	H antigens
1/2a	I, II	A, B
1/2b	I, II	A, B, C
1/2c	I, II	B, D
3a	II, IV	A, B
3b	II, IV	A, B, C
3c	II, IV	B, D
4a	(V), VII, IX	A, B, C
4b	V, VI	A, B, C
4c	V, VII	A, B, C
4d	(V), VI, VIII	A, B, C
4e	V, VI, (VIII), (IX)	A, B, C
7	XII, XIII	A, B, C
5	(V), VI, (VIII), X	A, B, C
6a	V, (VI), (VII), (IX), XV	A, B, C
6b	(V), (VI), (VII), IX, X, XI	A, B, C

There are a number of limitations associated with the use of this assay; (1) the high cost of obtaining antisera, (2) the inability to correlate serotype with species, a problem in the case of *L. monocytogenes* and *L. seeligeri* as both species contain serotypes 1/2a, 1/2b, 3b, 4a, 4b, 4c, and 6b, (3) the technical expertise required, (4) the difficulty in conclusively determining different serotypes and (5) discrepancies in results due to changes in the phenotypic characteristics of the bacteria. For these reasons, alternative methods have been explored which has seen serological serotyping being replaced by molecular serotyping.

1.2.6.3.2 Molecular serotyping

A number of molecular serotyping assays have been developed and includes methods designed by; Doumith and colleagues, 2004: Doumith and colleagues, 2005; Zhang and Knabel, 2005; and De Santis and colleagues, 2007 (Kerouanton et al. 2010). The technique involved in all methods revolve around the same principle, which is the use of a multiplex PCR assay for amplification of genus-specific, species-specific, and serotype-specific genes. Doumith and colleagues designed primers to amplify *L. monocytogenes* gene targets *lmo0737*, *lmo1118*, *ORF2819*, *ORF2819*, *ORF2110* and *prs*. These gene targets are present in specific serotypes of the organism and based on the presence or absence of certain bands, *L. monocytogenes* can be differentiated into sero-specific groups (Table 1.6) (Doumith et al. 2004).

Table 1.6. Gene targets which distinguish major *L. monocytogenes* serotypes. Doumith and colleagues designed primers to amplify *L. monocytogenes* gene targets *lmo0737*, *lmo1118*, *ORF2819*, *ORF2819*, *ORF2110* and *prs*. These gene targets are present in specific serotypes of the organism and based on the presence or absence of certain bands, *L. monocytogenes* can be differentiated into sero-specific groups (adapted from Doumith et al. 2004).

Gene target	Primer sequence (5'-3')[a]	Product size (bp)	Serovar specificity[b]	Protein encoded by the target gene
lmo0737	For: AGGGCTTCAAGGACTTACCC Rev: ACGATTTCTGCTTGCCATTC	691	*L. monocytogenes* serovars 1/2a, 1/2c, 3a, and 3c	Unknown, no similarity
lmo1118	For: AGGGGTCTTAAATCCTGGAA Rev: CGGCTTGTTCGGCATACTTA	906	*L. monocytogenes* serovars 1/2c and 3c	Unknown, no similarity
ORF2819	For: AGCAAAATGCCAAAACTCGT Rev: CATCACTAAAGCCTCCCATTG	471	*L. monocytogenes* serovars 1/2b, 3b, 4b, 4d, and 4e	Putative transcriptional regulator
ORF2110	For: AGTGGACAATTGATTGGTGAA Rev: CATCCATCCCTTACTTTGGAC	597	*L. monocytogenes* serovars 4b, 4d, and 4e	Putative secreted protein
prs	For: GCTGAAGAGATTGCGAAAGAAG Rev: CAAAGAAACCTTGGATTTGCGG	370	All *Listeria* species	Putative phosphoribosyl pyrophosphate synthetase

A limitation to this method is its inability to discriminate: serotype 1/2a from 3a, serotype 1/2b from 3b and 7, serotype 1/2c from 3c and serotype 4b from serotype 4d and 4e. However, serotypes 3a, 3b, 7, 4d and 4e are infrequently isolated from food and rarely implicated in disease (Doumith et al. 2004; Kerouanton et al. 2010), hence the method still remains valuable.

In a more recent study Kérouanton colleagues (2010) published an alternative multiplex PCR assay for *L. monocytogenes* serotyping. This simply incorporated all targets designed by Doumith and colleagues in 2004 and included a *prfA* gene target designed by D'Agostino and colleagues in 2004, for species-specific recognition (Kerouanton et al. 2010). Similar to the method described by Doumith and colleagues, this method fails to discriminate certain serotypes. Nevertheless, there are a number of merits associated with using both multiplex PCR assays, such as; (1) results are available quickly (within 1 day instead of 5 days as is the case with serological serotyping), (2) PCR patterns are easier to interpret than agglutination patterns (Kerouanton et al. 2010), (3) little expertise is required (relative to serological serotyping), (4) results are reproducible (as opposed to serological serotyping) and (5) the method is cheaper. It must however be mentioned that, serotyping is a first level of discrimination and that subtyping methods such as; pulse field gel electrophoresis (PFGE), amplified fragment length polymorphism (AFLP), (multilocus sequence typing) MLST and (variable number tandem repeats) VNTR, are required for epidemiological monitoring of food and human isolates in the event of an outbreak (Kerouanton et al. 2010).

1.2.6.3.3 Pulse field gel electrophoresis

Pulse field gel electrophoresis (PFGE), is widely known as the international gold standard for *L. monocytogenes* subtyping (Kerouanton et al. 2010). The method involves extraction and digestion of *L. monocytogenes* DNA with a rare cutting restriction enzyme, yielding 8-25 large fragments ranging in size from 20kb to over 20Mb (Nightingale 2010). Following restriction, the DNA is slowly separated on an agarose gel (for 30-50hrs) by applying alternating currents, which cause the DNA to move back and forth, resulting in higher resolution. This method has been used to divide *L. monocytogenes* into four lineages, and to discriminate isolates belonging to the same serotype, therefore allowing the differentiation of strains which are implicated in outbreaks. While PFGE is more discriminatory, there are limitations associated with its use, such, as; (1) it is time consuming - requiring up to

approximately 2 days for completion (Liu 2006), (2) it requires expertise and (3) the results at times do not translate across other laboratories, as different restriction enzymes are often used, therefore producing profiles that are not comparable. Due to these limitations PFGE is therefore not widely used (Liu 2006).

1.2.6.3.4 Amplified fragment length polymorphism

In 2002, an amplified fragment length polymorphism (AFLP) method was designed by Guerra and colleagues for *L. monocytogenes* subtyping. This proved to be quicker than PFGE (Guerra, Bernardo, and McLauchlin 2002) and was later, further developed and has been adopted as a molecular subtyping method by the Foodborne Pathogen Reference Unit (FBPRU), Heath Protection Agency (HPA), London, (Corcoran et al. 2006). This involved digestion of extracted DNA with a frequent cutting and a rare cutting restriction enzyme. Adaptors were ligated to complimentary ends of the restriction site and primers complementary to the adaptors were used to PCR amplify selected fragments (Parisi et al. 2010). The targets were separated by agarose gel electrophoresis and banding patterns recorded. Both AFLP and PFGE may vary between laboratories due to the use of different restriction enzymes.

1.2.6.3.5 Multilocus sequence typing

Multilocus sequence typing (MLST) relies on variation in nucleic acids sequence among seven chromosomal loci (usually 450 - 600 bp) (Nightingale 2010). A number of MSLT typing schemes have been designed for *L. monocytogenes* subtyping, which target housekeeping genes, virulence genes, or a combination of both (Nightingale 2010). The method involves PCR amplification of each sequence, followed by DNA sequencing. Using bioinformatics tools, the sequences of each loci are aligned and polymorphic sites identified. Allelic types are assigned based on polymorphisms and MLST types are assigned based on unique combinations of polymorphisms (Nightingale 2010; Parisi et al. 2010). MLST has become a robust tool for global epidemiological survey of microbial populations (Parisi et al. 2010), with a web-based database existing for *L. monocytogenes* (http://www.pasteur.fr/recherche/genopole/PF8/mlst/Lmono.html). Such a database enables inter-laboratory sequence data to be compared (Parisi et al. 2010). Other advantages include its potential to provide evolutionary information. For example, in 2008, Ragon and colleagues analysed MLST data and were able to suggest that serotype 4b and 1/2c diverged

from 1/2b and 1/2a respectively (Ragon et al. 2008). However, as the method is costlier and time consuming relative to AFLP (Parisi et al. 2010) and PFGE, it therefore has not superseded PFGE as the gold standard.

1.2.6.3.6 Multilocus variable number tandem repeat analysis

Multilocus variable number tandem repeat analysis (MLVA) is based on detection of a number of tandem repeat sequences (TRs) at specific loci in the chromosome. Mutations in TRs can occur during events such as DNA replication and recombination, leading to size changes and thus giving rise to the name variable number tandem repeats (VNTR) (Nightingale 2010). Recently, VNTR detection at multiple *L. monocytogenes* loci has been proven as a simple and reproducible subtyping method which is more discriminatory than PFGE (Chen et al. 2011). Briefly, in 2011 Chen and colleagues designed an MLVA method which involved amplification of the VNTR in a multiplex PCR. The products were resolved by capillary electrophoresis and fragment sizes determined using software analysis. The number of fragments was also determined and an allele numbering system assigned based on the number of TRs at each locus (Chen et al. 2011). In 2010, Nightingale speculated that, in future, a standardised MLVA protocol using well-characterised VNTR, may replace or complement PFGE, and subsequently, in 2011 Chen and colleagues have demonstrated the possibility of this occurrence.

1.3 Proteomics: A new approach to identification, diagnosis and characterisation

1.3.1 Matrix Assisted Laser Desorption/Ionisation - Time of Flight - Mass Spectrometry (MALDI-TOF-MS)

Matrix Assisted Laser Desorption/Ionisation - Time of Flight - Mass Spectrometry (MALDI-TOF-MS) is an analytical method used to measure the mass-to-charge (m/z) ratio of a range of macromolecular ions. It has a vast number of applications which include; the characterisation of synthetic polymers, the analysis of peptides and proteins, DNA and oligo nucleotide sequencing and the characterisation of recombinant proteins (Bucknall et al. 2002). The method typically involves applying the analyte to a target plate followed by mixing of the analyte with a matrix solution which is then allowed to air dry. The purpose of

the matrix is to co-crystalise with the sample and allow ionisation of the macromolecular ions upon exposer to laser energy in the proceeding step. Once the target plate is loaded into the MALDI-TOF Mass Spectrometer pulses of laser energy are fired onto the sample. This causes excitation of the molecules and their conversion into gaseous phase ions, which travel through a vacuum flight tube. Each ion travelling through the flight tube has a specific m/z ratio. The mass of each ion is determined by their time taken to reach a detector. Smaller ions will travel faster and reach the detector more quickly than larger ions. The masses detected are compiled to give a spectral fingerprint (mass spectrum) (Emonet et al. 2010). This spectral fingerprint provides a means of detecting molecules based on their size. Over the years this technology has been interfaced with software analysis so that the spectral fingerprints of numerous samples can be compared reliably. An initial step in this procedure is the generation of a superspectrum which is a composite mass spectrum of peaks shared by replicates of similar samples. The result of generating a number of superspectra is the generation of a database of various samples. The overall aim is to allow identification of an unknown sample by comparing its mass spectrum with known samples in the database. This is simply described as pattern matching.

This pattern matching principle can be applied to various areas of research. A survery of the literature shows that it is gradually being implemented in environmental, food and clinical microbiology research laboratories. Companies such as BioMérieux have developed the Shimadzu Launchpad software to compare the spectral profile to the superspectra in the Spectral ARchive And Microbial Identification System (SARAMIS) database. The MALDI BioTyper (software and database) is utilised by Brucker. The result of comparisons made by Brucker's MALDI Biotyper and Shimadzu Launchpad is the determination of the closet possible match and is the basis of identification (Emonet et al. 2010).

SARAMIS uses a linear confidence level score which is expressed as a percentage. This is equal to one-tenth of the accumulation points of matching with an upper cut-off of 999 points. On the other hand the MALDI Biotyper classifies results using a coefficient score which is the alogortihm of the points calculated by a different algorithm (Khöling et al. 2012).

As MALDI-TOF-MS is a sensitive method, it is currently being explored by other researchers as a method for the rapid identification of microorganisms directly from blood and urine samples without the need to isolate colonies. In 2010 Ferrieria et al. tested 238 urine samples and 68 blood culture samples using conventional methods and MALDI-TOF-MS (Ferrieria et al. 2010). Sample preparation involved two brief centrifugation steps in order to retrieve the bacteria. Results showed that, using MALDI-TOF-MS, 91.8% of urine isolates were identified at the species level and 92.7% were identified at the genus level, while 76% of blood culture isolates were identified to the species level and 96% were identified to the genus level. All results were confirmed using conventional biochemical tests.

Recently, in 2013 Leli et al. used MALDI-TOF MS to identify bacteria present in 109 blood cultures. They obtained correct identification for 57/62 (91.9%) aerobic/facultative anaerobic Gram-positive isolates, 53 (85.5%) at species level, and 4 (6.4%) at the genus level; 32/32 (100%) aerobic/facultative anaerobic Gram-negative isolates, 31 (96.9%) at species level, and 1 (3.1%) at the genus level; 7/7 (100%) obligate anaerobes, all at the genus level isolates. They found that the results were comparable to standard reference or automated methods. They also found that overall, the median identification time of MALDI-TOF MS vs reference standard methods was significantly shorter (Leli et al. 2013). Publications such as these continue to highlight the value of MALDI-TOF-MS.

1.3.2 Surface Enhanced Laser Desorption/Ionisation - Time of Flight - Mass Spectrometry (SELDI-TOF-MS)

Surface Enhanced Laser Desorption/Ionisation Time of Flight Mass Spectrometry (SELDI-TOF-MS) is a variation of MALDI-TOF-MS. The technology utilises ProteinChip arrays with a variety of surface chemistries that facilitate the capture and detection of a specific category of proteins prior to mass spectral analysis. SELDI-TOF-MS is a valuable tool for biomarker discovery and characterisation of microbes (Shah et al. 2005). A biomarker is molecule found in an organism and is a sign of a normal or an abnormal process. It can be a variety of molecules such as DNA, RNA, protein and other metabolites (Paul et. al. 2013). Chip arrays that are frequently used include Q10 (strong anion exchange) which captures negatively charged proteins, CM10 (weak cation exchange) which captures positively

charged proteins, IMAC30 (immobilized metal affinity capture) which captures proteins that bind polyvalent metal ions, as well as, H50 and H4 (hydrophobic) which captures large and small proteins respectively through hydrophobic interactions. Captured low molecular weight proteins which are not visible by sodium dodecyly (SDS)-polyacrylamide gel electrophoresis (PAGE) are usually resolved by SELDI-TOF-MS. This is evident upon converting the spectra into a gel view and comparing the images (Figure 1.14).

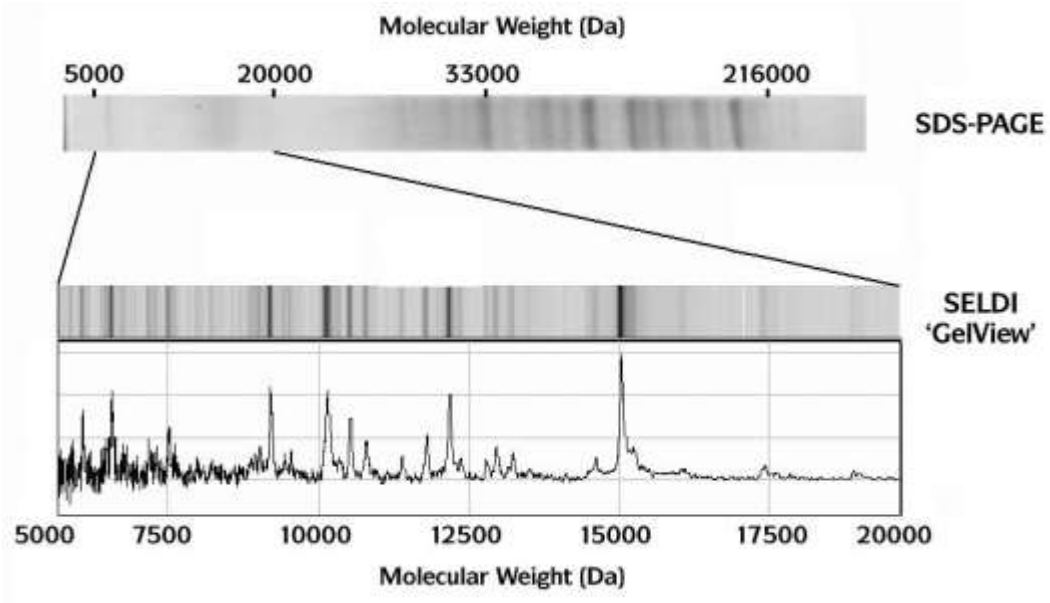

Figure 1.14. Comparison of a bacterial cell extract separated by SDS-PAGE and visualised using Coomassie Brilliant Blue (Top). Several peptides/proteins not seen by the SDS-PAGE, particularly the low molecular weight molecules are resolved by SELDI-TOF-MS (bottom spectrum). The intensities of the mass ions in the spectrum are represented as a 'Gel View' image (middle) for comparison (taken from Shah et al. 2005)

Since then, data emerging within the field of microbiology continue to highlight the value of SELDI-TOF-MS. In 2011 Shah and colleagues used the technology along with software analysis to trace the transition of methicillin resistance in sub-populations of *Staphylococcus aureus* (Shah et al. 2011). Also, in 2011 Kiehntopf and colleuages used SELDI-TOF-MS to differentiate *Campylobacter* species (Kiehntopf et al. 2011).

While the analysis of spectra generated by MALDI-TOF-MS has been standardised, the analysis of SELDI-TOF-MS data are not yet standardised and various alogarithms are utilised by different laboratories. Shah and colleagues used artificial neural network (Shah et al. 2011) while Kientopf and colleagues used ProteinChip Data Manager (Bio-rad) (Kiehntopf et al. 2011). However, analysis of SELDI-TOF-MS data using various logarithms makes it difficult to compare results across laboratories.

1.3.3 Diagnostic use of proteomic techniques

As mentioned in section 1.3.1 proteomic techniques such as MALDT-TOF-MS have been successfully introduced in microbiology diagnostic laboratories with results comparable to traditional biochemical tests. The added advantage of this approach is a drastic reduction in identification time. The technique also has diagnostic value in identifying biomarkers of human diseases and is being used to identify clinically diverse diseases such as cancer. In 2013, Paul and colleagues published a review which detailed the application of mass spectrometry based proteomics in molecular diagnostics, with particular reference to discovery of cancer biomarkers (Paul et. al. 2013). According to their review, almost all proteomic biomarker discovery platform use mass spectrometry as the central technique in asscociation with other proteomic approaches. These approaches can either be gel based (such as 2-dimensional (2-D) gel electrophoresis and 2-D Differential in gel electrophoresis) or gel free (such as Stable Isotope Labeling by Amino Acids in Cell Culture (SILAC) or Isobaric Tag for Relative and Absolute Quantitation (iTRAQ)).

A survey of the literature continues to show the diagnostic value of proteomic techniques across various diseases. In 2013, Di Domenico and colleagues used gel-based method, 2-D-PAGE coupled to mass spectrometry to identify high levels of several proteins indicative of Brugada Syndrome, a polygenic inherited cardiac disease characterised by life-threathening

arrhythmias and a high coincidence of sudden death. They hypothesised that the proteins which include apolipoprotein E, thrombin and vitamin D binding protein are potential markers for identification of the disease status (Di Domenico et al. 2013). In 2013, Kroksveen and colleagues, used iTRAQ and Orbitrap MS to discover cerebrospinal fluid proteins with significant difference between early multiple sclerosis patients and controls. They reported a significant abundance of alpha-1-antichymotrypsin, contactin-1, apolipoprotein D, clusterin, and kallikrein-6 and suggested that they may serve as diagnostic or prognostic biomarkers for multiple sclerosis. A survey of the literature also reveals that use of these mass spectrometry coupled techniques in diagnostic investigation is increasing across a vast number of diseases.

1.3.4 *Listeria monocytogenes* proteomics

As discussed previously proteomic approaches to diagnosis of diseases now frequently involves the use of mass spectrometry based approaches. The same appears to be true for *L. monocytogenes* proteomic investigations. As *L. monocytogenes* is capabable of surving adverse conditions such as freezing tempeartures, high salt and a broad pH range relative to other foodborne pathogens (see section 1.2.2), and since these factors contribute to its persistence in food and subsequently its ability to cause listeriosis, survival under these conditions continue to be the focus of proteomic studies. This is the case as proteins are the driving force of metabolic functions that enable the organism to survive these conditions, and in the case of virulence proteins (section 1.2.5) enables the organism to evade the host's physical and immune defence system. One metabolic ability which to date is not fully understood is the organism's ability to evade a valuable host defence measure, which is the high bile-salt condition throughout the gastro intestinal tract. In 2013, using multidimensional protein identification technology coupled with electrospray ionisation tandem mass spectrometry, Payne and colleagues were able to identify significant alterations in the presence of cell-wall-associated proteins, DNA repair proteins, protein folding chaperones and oxidative stress-response proteins. They report that using the type strain, 6 cell-envelop-associated proteins showed an increase in expression greater than 1-fold, 5 proteins associated with metabolic functions showed an increase in expression greater than 2-fold, whilst 11 proteins associated with information pathways, such as DNA repair, showed an increase in expression greater than 3-fold (Payne et al. 2013). This publication is one of many

highlighting that the fact that knowledge regarding *L. monocytoegenes* proteomics is expanding tremendously, with protein expression at various growth conditions and amongst various virulent and non-virulent strains being tested and compared. This view is further supported by the evidence provided in this study. The evidence presented in the results and discussion chapters expands our knowledge regarding *L. monocytogenes* proteomics by indicating a number of proteins differentially expressed at cold and ambient temperatures.

1.3.5 Lysis of cells

A preamble to proteomic analysis necessitates efficient extraction of proteins that are representative of the entire cell. However, complete lysis of *Listeria spp.* is very difficult. Isolated dry cell walls of *Listeria* strains are compose of about 30-40% peptidoglycan and the bulk of the wall is a carbohydrate of teichoic acids (Fielder 1988). The multilayered network of the peptidoglycan polymer and the extension of the cell wall by teichoic acids accounts for the robustness and difficulty in cell lysis. Lysostaphin, lysozyme and achromopeptidase are effective in lysing some Gram positive bacteria, however, *Listeria* in particular appears to be resistant (Fliss et al. 1991; Kämpfer et al. 1995. In 1991 Fliss and colleagues, and 1995 Kämpfer and colleagues reported successful lysis of the bacteria with enzymes such as mutanolysin (Fliss et al. 1991 and Kämpfer et al. 1995). This enzyme was originally purified from *Streptomyces globisporous*, and is recommended for lysis of a variety of Gram positive organisms (Fliss et al. 1991). However, recent developments show that endolysin, a *Listeria* specific enzyme, is more efficient in lysis of the organism. Endolysin is a term used to describe a broad range of bacteriophage lysins which are expressed by phages for the purpose of aiding their escape from their host cells (Loessner, M., et al., 2005; Courchesne, et al., 2009). These enzymes show extraordinary substrate specificity and high activity when added to *Listeria* cells, leading to the rapid degradation of the murein layers (Korndörfer et al. 2006). In 1995, Loessner and colleagues showed that 10 units of the enzyme was sufficient to clear a suspension of *L. monocytogenes* which was grown to the end of log phase, in a 10 ml volume of tryptose broth (Figure 1.15).

The enzyme is not commercially available. However, the use of the phage was recently approved by the United States Food and Drug Administration as an ingredient in Listex

P1000, a product for control of *Listeria sp.* in both raw and ready to eat products (Sonia et al 2010).

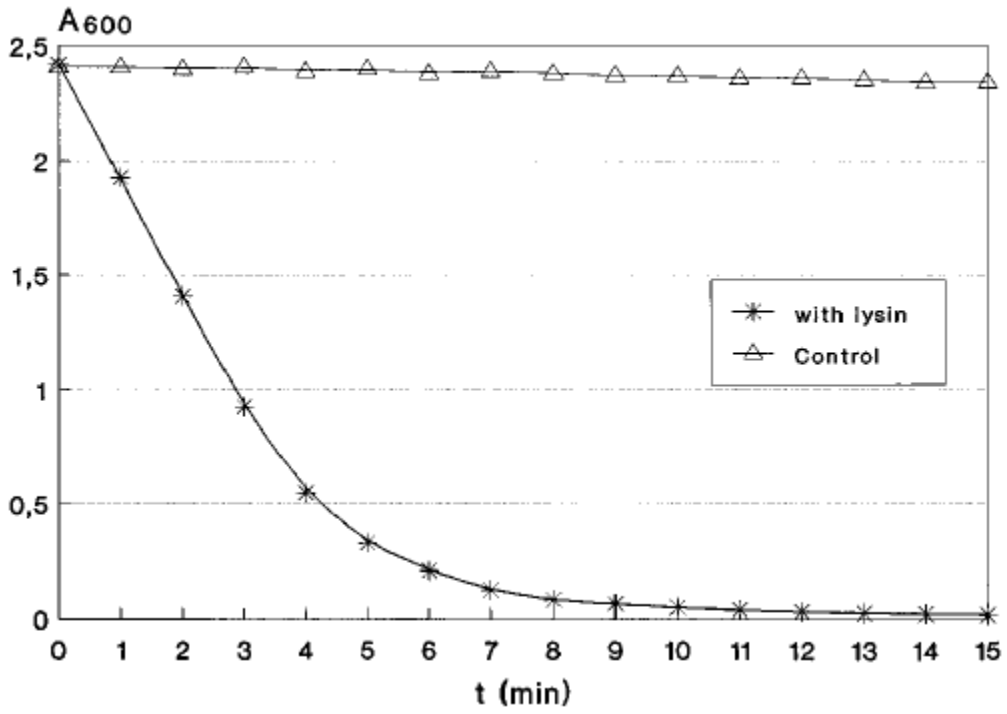

Figure 1.15. Lysis of *L. monocytogenes* WSLC1001 cells by bacteriophage endolysin. The plot of absorbance (y-axis) vs time (x-axis) shows that after 8 minutes the density of *L. monocytoegenes* present in the cell suspension decreased from 2.5 to ~0.1 A_{600} in 8 minutes. This data shows the efficiency of endolysin in lysing the species (taken from Loessner et al 1995).

The use of this enzyme may be valuable in *Listeria* proteomics research, facilitating greater amount of cytosolic protein for investigative studies. The conserved size of the *Listeria* genome is 2.8 - 3.2 Mb (den Bakker et al. 2010). Therefore theoretically the amount of protein that may be expected following efficient cell lysis would be 28 - 32 mg/ml. However, in reality, this figure is expected to decrease as a result of various factors such as the presence of introns, and changes in expression due to environmental conditions such as media and pH. Nevertheless, use of this enzyme may allow access to proteins which are not affected by these conditions.

1.4 Hypotheses

There is a large body of published data concerning the use of MALDI-TOF-MS for the rapid identification of bacterial species including *L. monocytogenes*, as detailed by Barbuddhe and

colleagues (Barbuddhe *et al.* 2008). By contrast, SELDI-TO-MS has received less attention, but has the potential to characterize microbial species at a higher resolution. The output of the data from these instruments are complex and represent mass ions derived mainly from proteins. Numerous mathematical approaches suach as dendrograms, heat maps, artificial neral networks are used to group isolates by similatity of their mass ion profiles into species, subspecies and types. It is envisaged that the generation of heat maps will be another approach to revealing the diversity to the *Listeria* species.

In common with other soil-derived human pathogens, *L. monocytogenes* has the capacity to grow over a wide temperature distribution. Consequently, there has been significant research into the molecular mechanisms that enable this organism to survive under these conditions. A review of the literature show that most of these investigations are carried out using the type strain which appears to be atypical of the species. It is envisaged that analysis of clinical and food isolates will show that that there are proteins which may be expressed in these isolates which are not present in the type strain. Should these proteins be present, they may serve as biomarkers of the *L. monocytogenes* presence at 4°C.

1.5 Aims and Objectives

The overall aim of this thesis was to use proteomic approaches to further characterise *L. monocytogenes* and subsequently assess the applicability of the information for tracing outbreak investigations.

The project had two specific aims:

1) to investigate the potential of proteomic-based platforms such as mass spectrometry to further characterise isolates of this *Listeria*.

2) to use proteomic tools to analyse proteins which may be differentially expressed at two selected temperatures, 4°C and 37°C.

Chapter 2: Materials and Methods

2.1. Selection of isolates for entire study

Clinical and food isolates were obtained from the FPRU, and the HPA identification number, serotype, source and AFLP profile of each isolate was recorded. Isolates were also obtained from DBHT which were originally obtained from NCTC and DSMZ (Table 2.1). Isolate were kept at - 80°C on storage beads (Pro-Lab Diagnostics), and when required, were cultured on a blood nutrient (BN) (HPA media department) agar plate and incubated overnight under aerobic conditions at 37°C. The exception was *Brochothrix spp.* which was cultured on APT (HPA media department) plates and incubated at 30°C. Purity was verified by visual inspection before use. To replenish stocks, each isolate was sub-cultured from a single colony and grown under the previously stated conditions. Purity was verified as before and isolates stored on - 80°C storage beads for later use in this study.

Table 2.1. List of isolates used in this study. If available information on strain number, serotype, source and AFLP pattern was also tabulated.

Organism	**Isolate Identification Number**	**Serotype**	**Source**	**AFLP**
L. monocytogenes	H10 162 0552	4b	Human	I
L. monocytogenes	H08 446 0286	4b	Food	I
L. monocytogenes	H09 012 0053	1/2b	Food	II
L. monocytogenes	H08 490 0250	1/2c	Food	VII+1
L. monocytogenes	H10 146 0091	1/2a	Food	IX
L. monocytogenes	H08 074 0271	1/2a	Human	IX
L. monocytogenes	F2365	4b	Human	-
L. monocytogenes	H08 162 0317	1/2a	Human	III
L. monocytogenes	H08 126 0107	4b	Human	XV
L. monocytogenes	H09 088 0603	4b	Human	V
L. monocytogenes	H08 180 0412	1/2a	Human	XI+1
L. monocytogenes	H08 520 0220	1/2b	Human	IIa
L. monocytogenes	H08 352 0191	1/2b	Human	IV-1
L. monocytogenes	H08 282 0003	1/2a	Food	VI
L. monocytogenes	H08 156 0404	1/2a	Food	XII
L. monocytogenes	H08 224 0145	1/2c	Food	VIIf
L. monocytogenes	H08 382 0048	4b	Food	V
L. monocytogenes	H08 454 0569	4b	Human	V+2
L. monocytogenes	H08 136 0109	1/2c	1/2c	VII
L. monocytogenes	H08 164 0195	1/2a	Food	XI-1
L. monocytogenes	H08 344 0402	1/2a	Human	VIIh
L. monocytogenes	H08 374 0182	4b	Human	IV-1
L. monocytogenes	H08 384 0314	1/2a	Human	XI+1
L. monocytogenes	H09 052 0645	1/2a	Food	XVI
L. monocytogenes	H09 112 0012	1/2a	Food	IV
L. monocytogenes	H09 224 0336	1/2a	Food	XIVd
L. monocytogenes	H09 224 0355	4b	Human	V
L. monocytogenes	H09 232 0063	4b	Human	I
L. monocytogenes	H09 094 0336	4b	Human	V
L. monocytogenes	H09 296 0322	1/2a	Human	IX
L. monocytogenes	H08 396 0517	1/2a	Human	IX
L. monocytogenes	H09 354 0308	4b	Human	I
L. monocytogenes	H09 404 0479	4b	Human	I

L. monocytogenes	H09 314 0192	1/2a	Human	IX
L. monocytogenes	H09 420 0585	4b	Human	I
L. monocytogenes	H09 066 0222	1/2a	Human	IX
L. monocytogenes	H09 400 0324	4b	Human	I
L. monocytogenes	H09 062 0066	1/2a	Human	IX
L. monocytogenes	H09 364 0232	4b	Human	I
L. monocytogenes	H08 360 0121	1/2a	Human	IX
L. monocytogenes	H09 392 0041	1/2c	Food	VII-1
L. monocytogenes	H10 172 0401	1/2a	Human	VII
L. monocytogenes	H10 170 0375	1/2a	Food	VII
L. monocytogenes	H10 126 0369	1/2a	Food	IX
L. monocytogenes	H10 074 0236	1/2b	Human	II
L. monocytogenes	H09 406 0833	1/2c	Human	VII
L. monocytogenes	H10 044 0420	1/2c	Food	IV
L. monocytogenes	H08 262 0274	1/2b	Human	IV
L. monocytogenes	H09 076 0244	1/2c	Food	VII
L. monocytogenes	H10 046 0271	1/2c	Food	VII
L. monocytogenes	H09 510 0595	1/2a	Human	IIIa
L. monocytogenes	H10 112 0014	4b	Food	IV
L. monocytogenes	H10 1780389	4b	Human	IV
L. monocytogenes	H09 348 0558	4b	Human	V
L. monocytogenes	H08 476 0100	4b	Food	V
L. monocytogenes	H10 202 0622	1/2c	Human	VII
L. seeligeri	H09 032 0787	-	Food	-
L. innocua	H09 304 0186	-	Human	-
L. ivanovii	H09 032 0783	-	Food	-
L. welshimeri	H09 032 0784	-	Food	-
L. grayi	H09 032 7077	-	Food	-
L. monocytogenes	NCTC 10357	1/2c	Rabbit	-
L. monocytogenes	NCTC 4883	4c	Bird	-
L. monocytogenes	NCTC 10888	4d	Sheep	-
L. monocytogenes	NCTC 5214	4a	Sheep	-
L. monocytogenes	NCTC 12426	4bX	-	-
L. monocytogenes	NCTC 4885	4b	Human	-
L. monocytogenes	NCTC 12480	4b	-	-
L. monocytogenes	NCTC 11994	4b	Food	-
L. monocytogenes	NCTC 5348	1/2c	Mammal	
L. monocytogenes	NCTC 7974	1a	Human	-
L. monocytogenes	NCTC 10890	7	Human	-

L. grayi subsp. grayi	NCTC 10815	-	Plant	-
L. grayi subsp. murrayi	NCTC 10812	-	Plant	
L. grayi subsp. murrayi	NCTC 10813	-	Plant	-
L. grayi subsp. murrayi	NCTC 10814	-	Plant	-
L. ivanovii subsp. londoniensis	NCTC 12701	-	-	-
L. innocua	NCTC 11288	6a	Cow	-
L. ivanovii subsp. ivanovii	NCTC 11846	-	Sheep	-
L. seeligeri	NCTC 11856	-	Soil	-
L. seeligeri	NCTC 10889		Human	-
L. seeligeri	NCTC 11289	-	Human	-
L. welshimeri	NCTC 11857	-	Compost	-
L. welshimeri	DSM 15452	-	-	-
B. thermosphacta	DSM 20171	-	-	-
B. thermosphacta	DSM 20599	-	-	-
B. campestris	DSM 4712	-	-	-

2.2. Purification of LM4 Endolysin

2.2.1 Culture growth conditions

Two strains of *Lactococcus lactis* were used;

1) FI 10544: which was transformed with a pUK200 vector and lacked the LM4 endolysin gene and His tag (negative control).

2) FI 1066: which was transformed with a pUK200 vector containing the endolysin gene (Figure 2.1).

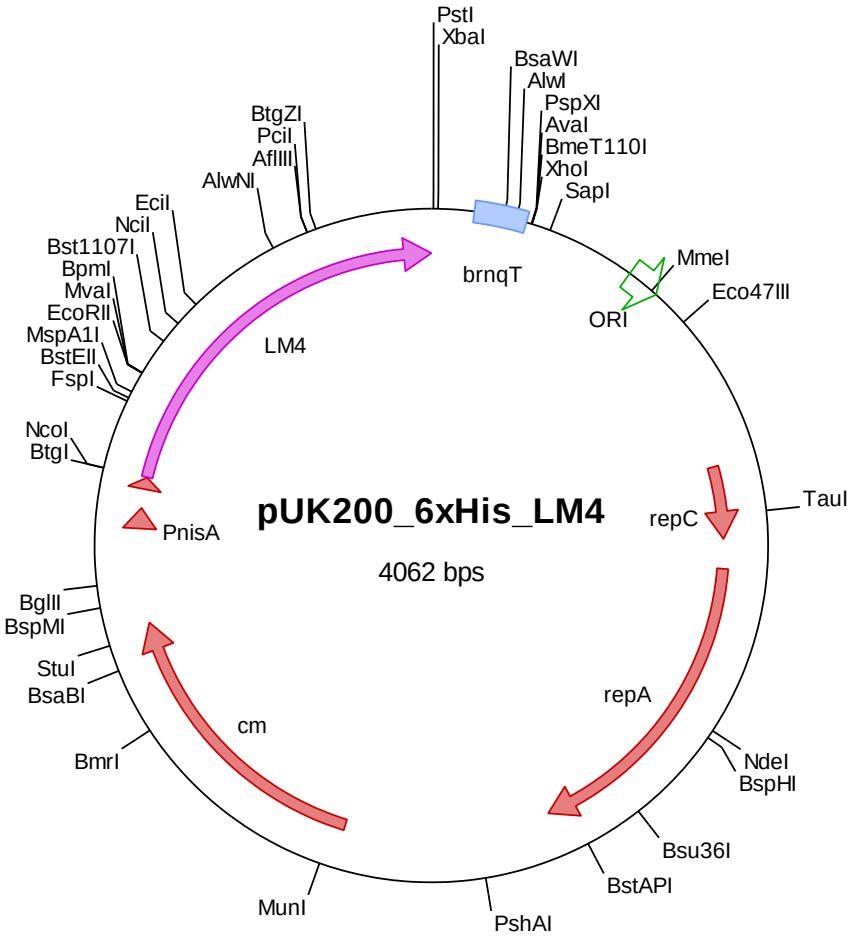

Figure 2.1. Vector map of pUK200_6His_LM4. The plasmid is 4062 bp in size with various restriction sites. The plasmid codes for the endolysin gene (LM4) which under the control of PnisA produces the *Listeria* specific lytic enzyme. (Diagram obtained from Nikki Horn, Institute of Food Research, 2010).

Separate starter cultures of *L. lactis* FI10544 and FI1066 were prepared by using 100 µl of 50% glycerol stock to inoculate 10 ml of GM17 media containing 5 µg/ml chloramphenicol, followed by overnight incubation at 30°C. A 2.5 ml volume of *L. lactis* FI10544 starter culture was used to inoculate 100 ml of GM17 (IFR media deparment) and 5 ml of *L. lactis* FI1066 starter culture was used to inoculate 200 ml of GM17. Chloramphenicol was added to both cultures to give a final concentration of 5 µg/ml followed by incubation at 30°C. The LM4 gene was induced at approximately 0.5 optical density 600 (OD_{600}) units by adding nisin to both cultures to a final concentration of 1ng/ml. The gene was induced for two hours.

2.2.2 *L. lactis* protein extraction

L. lactis FI10544 and FI1066 cultures were harvested by centrifugation at 6100*g* (J2 HS Beckman) for 5 minutes at 4°C. The supernatant was removed and each pellet was resuspended in 40 ml of PBS followed by centrifugation as before. This was repeated twice giving a total of three washes.

For each 100 mg of pelleted cells, 180 µl of lysis buffer (from QIA*express* Ni-NTA Fast Start kit) and 250 µl of glass beads were added. The samples were vortexed briefly and processed in a Fast Prep® (MP Biomedicals) (glass bead beating) at speed setting 6.0, for 30 seconds, followed by 10 minutes on ice. This was repeated 3 times. An extra 150 µl of lysis buffer was added per 100 mg of cell pellet. The samples were briefly vortexed, then centrifuged at maximal speed in a microcentrifuge for 5 minutes, to pellet glass beads and cell debris. A 5 µl sample of supernatant (soluble protein), was set aside for separation by one dimensional sodium dodecyl sulphate polyacrylamide gel electrophoresis (1-D SDS PAGE). The remaining supernatant was decanted by pipette, made up to 10 ml with lysis buffer and purified immediately.

2.2.3 His tag purification and 1-D SDS PAGE analysis of endolysin from *L. lactis* protein extracts

The protein was purified according to instructions in the QIA *express* Ni-NTA Fast Start handbook (procedures 1 and 2 were eliminated). A 5 µl sample of; flow through, first wash, second wash and eluent were set aside for analysis by 1-D SDS PAGE. The eluted protein was dialysed into a buffer containing: 50 mM phosphate pH 8.0 and 300 mM NaCl. The protein concentration was measured using a nanodrop 2000 (Thermo Scientific) and was stored in 50% sterile glycerol at - 20°C.

Loading buffer (Invitrogen) was added to each 5 µl sample that was set aside and proteins were separated on a Nupage® 10% Bis-Tris gel (Invitrogen), at 200V in MOPS buffer (Invitrogen) for 1 hour. The gel was washed three times in 50 ml sterile water for 5 minutes with shaking, then stained at room temperature with shaking using 20 ml of colloidal coomassie (Invitrogen) for 1 hour. After staining, the gel was left shaking in 50 ml sterile water overnight. The gel was imaged using Alpha imager (Genetic Research Instrumentation).

2.3 *L. monocytogenes* growth curve at 4°C and 37°C

NCTC 10357 and H101620552 were cultured separately on blood nutrient (BN) agar plates from beads stored at - 80°C. Each culture was incubated overnight under aerobic conditions at 37°C. Purity was verified by visual inspection before use. Each isolate was sub-cultured from a single colony and grown under the previous conditions. Purity was verified as before. A starter culture for each isolate was prepared by inoculating 5 ml of brain heart infusion (BHI) broth (HPA media department) with the growth from four colonies, followed by overnight incubation at 37°C.

Both isolates were grown in 50 ml BHI broth at 4°C and 37°C by inoculating 50 ml pre-chilled (4°C) and 50 ml pre-warmed (37°C) BHI broths with 1µl starter culture.
For each isolate a 50 ml 4°C pre-chilled BHI broth and a 50 ml pre-warmed (37°C) BHI broth was inoculated with 1 µl starter culture. Both were re-incubated at their corresponding temperatures. In order to obtain 4°C and 37°C growth curves, absorbance readings were recorded at OD_{600} (Biophotmeter, Eppendorf), daily and hourly respectively. Cultures incubated at 37°C and 4°C were recorded hourly and every 24 hours respectively. Both cultures were monitored until the readings were relatively constant. Growth curves at 4°C and 37°C were deduced by plotting absorbance at OD_{600} against time.

2.4 Growth and harvest of *Listeria spp.*

Isolates were cultured from - 80°C beads, starter cultures were prepared and used to prepare 50ml BHI broth cultures as previously detailed (section 2.3). Cultures were maintained until late exponential growth phase, that is, cultures incubated at 4°C and 37°C were harvested at OD_{600} of 0.65 - 0.75 and 0.8 - 1.0 respectively.

Cells were harvested by centrifugation (Z36HK, Hermle) at 6100 *g* for 5 minutes at 4°C. The supernatant was removed and each pellet was resuspended in 40 ml of PBS followed by centrifugation at 6100 *g* for 5 minutes at 4°C. This was repeated twice giving a total of three washes. Each pellet was resuspended in 1 ml of PBS and dispensed into a screw cap microfuge tube (eppendorf). The samples were centrifuged at maximal speed in a microcentrifuge (Heraeus Fresco 21 Centrifuge, Thermo Electron Corporation) for 10 minutes, the supernatants were decanted and the pellets weighed. The pellets were stored at -80°C until required.

2.5 Efficient lysis of *Listeria spp*

2.5.1 Determination of minimum amount of endolysin required for complete lysis of *Listeria spp.*

Using 37°C growth condition, a total of 12 pellets of a *L. monocytogenes* H10 162 0552 were prepared using starter culture conditions described in section 2.3 and growth and harvest conditions described in section 2.4. Each pellet was resuspended in 180 µl lysis buffer per 100 mg of pellet. (Lysis buffer: 2% Chaps, 50mM NaCl, 20mM Tris-HCl pH 8.0, 1mM EDTA, protease inhibitor cocktail (Roche) and 5mM DTT). Different amounts of endolysin were added to individual suspensions as follows; 0.0, 2.0, 2.2, 2.4, 2.6, 2.8, 3.0, 3.4, 3.8, 4.0, 4.5 and 5.0 µg per 100 mg pellet. Each suspension was vortexed briefly and incubated on ice of 30 minutes. Approximately 250 µl of blass beads (Sigma) was added per 100mg of cell pellet. The samples were then processed, in the Fast-Prep®-24 (MP Biomedicals) for 1 minute at speed setting 6.0 and incubated on ice for 10 minutes. This was repeated three times followed by the addition of a further 150 µl of lysis buffer per 100 mg pellet. The samples were vortexed briefly, then centrifuged at maximal speed in a microcentrifuge for 10 minutes to pellet the cell debris. The supernatant was removed, and the quality of the protein assessed using 1-D SDS PAGE. Briefly, a 1 µl volume of each sample supernatant was combined with 1 µl loading dye and 1 µl reducing agent (Invitrogen) followed by separation on Nupage® 4 - 12% Bis-Tris gel (Invitrogen), at 125V in MES buffer (Invitorgen) containing 500 ml antioxidant for 35 minutes. After electrophoresis, the proteins were fixed by incubating the gel in 50 ml 40% methanol and 10% acetic acid for 1 hour at room temperature. The proteins were stained overnight using 20 ml colloidal coomassie (Invitrogen) and the background destained by incubation in 25% methanol at room temperature. The gel was visualised using a Propic II instrument (Digilab).

The cell debris from each supernatant was visualised using a light microscope at x 1000 magnification (Nikon Labophot).

2.5.2 Lysis of a range of *Listeria spp.*

Cell pellets for each of the following isolates were prepared: *L. monocytogenes* F2365, NCTC 10888 - *L. monocytogenes*, NCTC 10357 - *L. monocytogenes*, NCTC 5348 - *L. monocytogenes*, NCTC 04883 - *L. monocytogenes*, NCTC 05124 - *L. monocytogenes*, NCTC 10815 - *L. grayi subsp grayi*, NCTC 10813 - *L. grayi* subsp *murrayi*, NCTC 11288 - *L.*

innocua, NCTC 11846 - *L. ivanovii* subsp. *ivanovii*, NCTC 12701 - *L. ivanovii* subsp. *londoniensis*, NCTC 11856 - *L. seeligeri*, and NCTC 11857 - *L. welshimeri*. This was achieved using 37°C growth condition, starter culture conditions described in section 2.4 and growth and harvest conditions described in section 2.5.

Pellets and protein extracts were processed as detailed in section 2.5.1. Modifications to the protocol include:
1) Duplicate pellets were prepared for each isolate one of which was lysed without endolysin and the other was lysed by adding 5.0 µg of endolysin per 100 mg of pellet.
2) The protein extract was quantified using Bradford assay and 5 µg of protein was analysed using 1-D SDS PAGE.
3) The cell debris of each sample was visualised using a light microscope (Nikon Eclipse Ti) and photographed Nikon Digital Sight camera unit.

2.5.3 Lysis of *L. monocytogenes* F2365 using endolysin, glass bead beating and pressure cycling

Three *L. monocytogenes* F2365 cell pellets were prepared. This was achieved using 37°C growth condition, starter culture conditions described in section 2.3 and growth and harvest conditions described in section 2.4.
Pellets and protein extracts were processed as detailed in section 2.5.1. Modifications to the protocol include:

1) The first pellet was lysed without endolysin and the second was lysed by adding 5.0 µg of endolysin per 100 mg of pellet, and the third pellet was lysed using the pressure cycler (Barocycler ® NEP2320, Pressure Biosciences Inc.) as follows. Briefly, the pellet was resuspended in 180 µl of buffer per 100 mg of pellet and cycled at 35 kpsi for 1 minute followed by atmospheric pressure for 1 minute for 30 cycles.

2) The protein extract was quantified using Bradford assay.

3) A volume containing 100 µg of protein was set aside for 2-D SDS PAGE analysis as detailed in section 2.6. A volume containing 5 µg of protein was set aside for 1-SDS PAGE analysis (as detailed in section 2.5.1), followed by Liquid Chromatography - Mass

Spectrometry/Mass Spectrometry (LC-MS/MS) analysis. The experiment was repeated twice equaling a total of three biological replicates.

4) The cell debris of each sample was not photographed.

2.6. 2-D SDS PAGE

2.6.1 Rehydration of Immobiline DryStrip gels and Isoelectric focussing (IEF)

Three lanes of an Immobiline DryStrip reswelling tray (GE Healthcare), were each filled with 340 µl of rehydration solution (7M urea, 2M thiourea, 2% CHAPS w/v, 2% IPG buffer (GE Helathcare) and 2µl of 1% w/v bromophenol blue) which contained; 2.8 mg DTT and 20 µl IPG buffer pH 4 -7 (GE Healthcare) per ml. An 18 cm, Immobiline DryStrip gel pH 4 - 7 (GE Healthcare), was placed gel side down in each lane containing rehydration solution. Care was taken to ensure air was not trapped under the strips. Each strip was covered with 2 ml of Immobiline DryStrip Cover Fluid (GE Healthcare). The strips were allowed to rehydrate overnight for 10 - 20 hours.

The protein extracts were spun in a microcentrifuge at 13,100*g* in order to pellet insoluble matter. A volume of supernatant containing 100 µg of protein was transferred to a microfuge tube. Rehydration solution containing 2.8 mg DTT and 20 µl IPG buffer pH 4 - 7 (GE Healthcare) per ml was added to the supernatant to give a total volume of 150 µl. The isoelectric focussing apparatus was set up according to instructions stated in the GE Healthcare 2-D Electrophoresis Principles and Methods handbook. The following Ettan IPGphor conditions were applied for protein focussing:

S1 Step-n-hold	300V	3:00 hours
S2 Gradient	100V	6:00 hours
S3 Step-n-hold	8000V	9:00 hours

After IEF, the gel strips were stored at - 80°C until ready for second dimension separation.

2.6.2 Preparation of 12.5% acrylamide gel cassettes

The gels were prepared by combining 31.21 ml of chromosolve water, 23.45 ml of 40% acrylamide, 18.75 ml of 1.5M Tris-HCl pH 8.8, 750 µl of 10% SDS, 833 µl of 10% APS and

20.83 µl of TEMED, and casting between glass plates according to instructions stated in the GE Healthcare 2-D Electrophoresis Principles and Methods handbook. An amendment to the instructions was the use of 80% isopropanol instead of 1-butanol to overlay the gels after casting.

2.6.3 Equilibration of gel strips and 2-D electrophoresis

Focused gel strips were removed from - 80°C storage and thawed at room temperature.
Each gel strip was placed in a separate well of an IPG DryStrip gel holding tray. A 4 ml volume of equilibration buffer (6M urea, 1.5M Tris-HCl pH 8.8, 28.6% v/v of 85% w/w glycerol, 29% w/v SDS and 2µl of 1% w/v bromophenol blue) containing 40 mg DTT was placed in each well and gel strips were equilibrated by gentle shaking for 15 minutes. The equilibration buffer was decanted by pipette and 4 ml of equilibration buffer containing 100 mg of idoacetamide was added to each well. The strips were equilibrated by gentle shaking for 15 minutes. Each strip was fixed on top of a 12.5% acrylamide gel using molten agarose sealing solution (0.5g agarose dissolved in 100 ml of 1X TGS buffer (Bio-Rad) and 2µl of 1% w/v bromophenol blue). Gel electrophoresis was carried out in an Ettan DALT six electrophoresis unit (GE Healthcare) as follows. The lower chamber was filled with 4.5 L of 1 X TGS buffer (Bio-Rad) and each gel cassette was slotted into a cassette carrier. Unoccupied gel cassettes were filled with blank cassettes. The upper buffer chamber was seated over the gels and the upper chamber was filled with 2 X TGS buffer. The unit was closed and electrophoresis was carried out at 10 mA/gel, 1W/gel and 80 V for 24 hours. Proteins were fixed by shaking in 200 ml 40% methanol for 1 hour and stained in sypro ruby protein gel stain (Invitrogen) overnight. The gels were destained in 200 ml 10% methanol for 1 hour and imaged with an Ettan™ DIGE Imager.

2.7 In-gel tryptic digestion of proteins for LC-MS/MS and data analysis

2.7.1 Destaining

Each lane of a 1-D SDS gel containing a protein sample was cut into 12 pieces, using a clean scalpel. Each gel piece was transferred into a well of a 96-well low-bind microtitre plate. Each gel piece was destained by incubation at room temperature with 500 µl of solution containing 25 mM ammonium bicarbonate and 50% methanol for 20 minutes. The solution was decanted by pipette and the process of destaining was repeated three times. A final 500

µl volume of solution was added and incubated with the gel pieces overnight to ensure complete removal of the colloidal coomassie stain.

2.7.2 Drying

The 25 mM ammonium bicarbonate/50% methanol solution was decanted by pipette and 500 µl of acetonitrile was added to each well. The microtitre plate was incubated at room temperature for 10 minutes. The acetonitrile was removed and this step was repeated. The gel pieces were allowed to air dry.

2.7.3 Reduction and alkylation

A 50 µl volume of 10 mM DTT in 25 mM ammonium bicarbonate was added to each gel piece and incubated at 60°C for 30 minutes. The excess was removed and 50 µl of 55 mM iodoacetamide in 25 mM ammonium bicarbonate was added to each piece and incubated for 45 minutes at room temperature in the dark. The excess was removed and the gel pieces were washed three times for 5 minute in 500 µl of 25 mM ammonium bicarbonate. The gel pieces were dehydrated as described in section 2.7.2.

2.7.4 Trypsinisation

Trypsin (Promega, mass spectrometry grade) was resuspended in 25 mM ammonium bicarbonate to a concentration of 10 ng/µl. A 40 µl volume was added to each gel piece. The plate was sealed and incubated at 37°C overnight for 16 hours.

2.7.5 Extraction

A 40 µl volume of 0.1% Trifluoroacetic acid (TFA) was added to each well and incubated for 60 minutes at room temperature. The plate was centrifuged at 3,000*g* for 5 minutes and the supernatants were transferred to a clean microtitre plate. The samples were stored at - 80°C until ready for analysis.

2.7.6 LC-MS/MS analysis

LC-MS/MS analysis relating to the efficient lysis of *Listeria spp.* (section 2.5) was carried out by Min Fang of Department of Bioanalysis and Horizon Technology (DBHT), HPA, using the Ultimate 3000 Dionex nano/capillary HPLC system coupled to a LTQ Orbitrap mass spectrometer (Thermo Scientific).

2.7.6 Database search

The MS data was generated as .RAW files. A database search alogarithm, Mascot (Matrix Science UK), was used to identify the peptides detected by LC-MS/MS. Parameters selected for peptide identification were: enzyme - trypsin, fixed modification - carbamidomethlylation of cysteine, variable modifications - oxidation of methionine, missed cleavage sites - 2 and peptide mass tolerance - +/- 10ppm. The results were imported into Scaffold 3 (Proteome Software, Inc). The analysis parameters selected in scaffold were; minimum protein = 20% and minimum number of peptides = 2.

2.8 Characterisation of *L. monocytogenes* using Matrix Laser Assisted Desorption/Ionisation - Time of Flight - Mass Spectrometry (MALDI-TOF-MS)

2.8.1 Target plate preparation using direct colony smears for the AXIMA CFR Plus MALDI-TOF-MS instrument (Shimadzu Corporation, UK) and data acquisition

A total of 23 isolates were analysed. Of these isolates, 17 were obtained from FPRU; 13 - *L. monocytogenes* and 1 isolate of each of the following species; *L. innocua, L. grayi, L. ivanovii, L. seeligeri and L. welshimeri*. The remaining 5 samples were NCTC isolates; *L. grayi subsp. grayi* - NCTC 10815, *L. innocua* - NCTC 11288, *L. ivanovii subsp. ivanovii* - NCTC 11846, *L. seeligeri* - NCTC 11856 and *L. welshimeri* - NCTC 11857.

Sub-cultures were prepared as detailed in section 2.1. and surface growth of one colony was evenly spread over a well of a 48 spot target plate (Shimadzu Corporation, UK) using a pipette tip. Wells G3 and G4 remained empty. Each isolate was applied in duplicate. One microlitre of 2, 5-dihydroxybenzoic acid (DHB) matrix was applied to each spot and mixed with the sample using a pipette tip. A second target plate was prepared using alpha-cyano-4-hydroxy cinnamic acid (HCCA) as an alternate matrix. The plates were air dried for approximately 10 minutes and sent to AnagnosTec, Germany, by courier. In order to minimise sample degradation, the plates were scheduled for arrival within 48 hours of preparation. The plate numbers and sample details were entered into a software template called Target Manager of the SARAMIS Satellite. The file was electronically transferred to AnagnosTec as a text file. *Escherichia coli* whole cell standards were applied to wells G3 and G4 of the target plates by an AnagnosTec staff. All reagents were supplied in the SARAMIS^{TM} Runit Box (AnagnosTec).

MS analysis was performed by AnagnosTec and results were updated remotely in the SARAMIS system available at the DBHT (Department of Bioanalysis and Horizons Technologies), HPA. The results appeared in the SARAMIS status bar where the each isolate present on the target plate was assigned a confidence coefficient. The results were copied and presented in table format. As mentioned earlier (section 1.31) the confidence coefficient is assigned during analysis by the Shimadzu Launchpad software. It is expressed as a percentage which is equal to one-tenth of the accumulation points of matching with an upper cut-off of 999 points.

2.8.2 Target plate preparation using direct colony smears for the Microflex LT MALDI-TOF-MS instrument (Bruker UK, Ltd)

A total of 89 *Listeria* isolates were analysed. Of these, 84 were obtained from FPRU; 78 - *L. monocytogenes,*1 - *L. grayi,* 2 - *L. innocua,* 1 - *L. ivanovii*, 1 - *L. seeligeri* and 1 - *L. welshimeri*. The remaining 5 samples were NCTC isolates; NCTC 10815 - *L. grayi subsp. grayi,* NCTC 11288 - *L. innocua,* NCTC 11846 - *L. ivanovii subsp. ivanovii,* NCTC 11856 - *L. seeligeri* and NCTC 11857 - *L. welshimeri*. Also, 1 - *Brochothrix campestris* and 1 - *Brochothrix thermosphacta* were analysed.

All sub-cultures were prepared as detailed in section 2.1 and the surface growth of a colony was evenly spread over a well of a 96 spot target plate. Each isolate was applied in duplicate. *Staphylococcus aureus* was used to smear two wells on the target plate and extracted and *E. coli* protein extracts called Biological Test Standard (BTS) (Bruker UK, Ltd.) was also spotted in duplicate on to the target plate. The spots were allowed to air dry. One microlitre of HCCA matrix was applied to each spot and allowed to air dry. The target plate was loaded into the Microflex LT MALDI-TOF-MS instrument and analysed as detailed in section 2.8.4.

2.8.3 Target plate preparation using formic acid extracted proteins for the Microflex LT MALDI-TOF-MS instrument (Bruker UK, Ltd)

Sub-cultures were prepared as detailed in section 2.1. Using a 1µl loop, single visibly pure colonies were scrapped from a plate until the loop was at full capacity. The cells were thoroughly resuspended into a 1.5 ml microfuge tube containing 300 µl of molecular grade water. A 900 µl volume of absolute ethanol was added and the cell suspensions were mixed

by inverting 6 times. The tubes were spun in a microcentrifuge at top speed for 2 minutes, supernatants were decanted completely and the pellets resuspended in 50 µl of 70% formic acid followed by addition of 50 µl acetonitrile. The suspensions were mixed by inverting 6 times, incubated at room temperature for 2 minutes, then spun in a microcentrifuge at top speed for 2 minutes.

A 2 µl volume of cell extract was applied to a spot on the target plate and allowed to air. One microlitre of HCCA matrix was applied to each spot and allowed to air dry. The target plate was loaded into the Microflex LT MALDI-TOF-MS instrument and analysed as detailed in section 2.8.4

2.8.4 Data acquisition from the Microflex LT MALDI-TOF-MS (Bruker) instrument

Briefly, the software used included MALDI Biotyper Real Time Client, Flex control and MALDI biotyper sample sheet. The name and position of each isolate on the target plate was entered into the MALDI biotyper sample sheet. The details entered were copied and pasted into the analyte placement window of the MALDI Biotyper Real Time Client. The "MALDI biotyper standard processing" option was selected for the data processing and identification method. The BDAL database was selected for spectral comparison with test isolate spectra. The instrument vacuum was allowed to reach $3e^{-6}$ and was verified by viewing the flex control software. Spectra generation was commenced by selecting "finish" in the MALDI Biotyper Real Time Client window. The real time window displayed the quality of the spectrum and classification of each sample. At the end of the run the results were made available in a new internet explorer window.

2.8.5 Construction of *Listeria spp.* main-spectrum (MSP) Dendrogram using MS profiles acquired by MALDIbiotyper

MS files for a total of 78 *Listeria* isolates were used for cluster analysis. Of the 78 isolates, 54 *L. monocytogenes* were obtained from the FPRU. The remaining isolates were NCTC and DSMZ isolates: NCTC 04885, 04883, 10888, 12426, 05214, 07973, 10890, 10357, 12480, 11994, 05348, 10887- *L. monocytogenes*; NCTC 10812 - *L.* grayi *subsp. murrayi*; NCTC 10813 and 10815 - *L. grayi subsp. grayi*, NCTC 10815 - *L. grayi subsp. grayi*, NCTC 11288

- *L. innocua,* NCTC 11846 - *L. ivanovii subsp. ivanovii*, NCTC 11856 - *L. seeligeri*, NCTC 11857 - *L. welshimeri*, NCTC 12701 - *L. ivanovii subsp. londoniensis*, NCTC 10889 - *L . seeligeri*, NCTC 11289 - *L. seeligeri*, and DSMZ 15452 - *L. welshimeri.* The isolates and target plate was prepared as detailed in section 2.8.3.

Table 2.2 List of 78 *Listeria* isolates used to generate the MSP Dendrogram shown in Figure 3.25. For simplicity, each isolate was assigned a number from 1-78 which can be used to identify its position on the dendrogram.

MSP Dendrogram number	**HPA Sample Number**	**Isolate**	**MSP Dendrogram number**	**HPA Sample Number**	**Isolate**
1	NCTC 10357	*L. monocytogenes*	40	NCTC 11856	*L. seeligeri*
2	H08 136 0109	*L. monocytogenes*	41	NCTC 11857	*L. welshimeri*
3	H08 156 0404	*L. monocytogenes*	42	H09 420 0585	*L. monocytogenes*
4	H08 162 0317	*L. monocytogenes*	43	H09 066 0222	*L. monocytogenes*
5	H08 164 0195	*L. monocytogenes*	44	H09 400 0324	*L. monocytogenes*
6	H08 224 0145	*L. monocytogenes*	45	H09 062 0066	*L. monocytogenes*
7	H08 180 0412	*L. monocytogenes*	46	H09 364 0232	*L. monocytogenes*
8	H08 282 0003	*L. monocytogenes*	47	H08 360 0121	*L. monocytogenes*
9	H08 344 0402	*L. monocytogenes*	48	NCTC 05214	*L. monocytogenes*
10	H08 352 0191	*L. monocytogenes*	49	NCTC 07973	*L. monocytogenes*
11	H08 374 0182	*L. monocytogenes*	50	NCTC 10890	*L. monocytogenes*
12	H08 382 0048	*L. monocytogenes*	51	NCTC 10357	*L. monocytogenes*
13	H08 348 0314	*L. monocytogenes*	52	NCTC 10814	*L. grayi*
14	H08 446 0286	*L. monocytogenes*	53	NCTC 12480	*L. monocytogenes*
15	H08 454 0569	*L. monocytogenes*	54	NCTC 12701	*L. ivanovii*
16	H08 520 0220	*L. monocytogenes*	55	NCTC 11994	*L. monocytogenes*
17	H09 052 0645	*L. monocytogenes*	56	NCTC 10889	*L. seeligeri*
18	H09 112 0012	*L. monocytogenes*	57	NCTC 11289	*L. seeligeri*
19	H09 126 0107	*L. monocytogenes*	58	NCTC 10812	*L. grayi*
20	H09 224 0336	*L. monocytogenes*	59	NCTC 05348	*L. monocytogenes*
21	H09 224 0355	*L. monocytogenes*	60	NCTC 10887	*L. monocytogenes*
22	H09 232 0063	*L. monocytogenes*	61	H09 392 0041	*L. monocytogenes*
23	H09 088 0603	*L. monocytogenes*	62	F2365	*L. monocytogenes*
24	H09 094 0336	*L. monocytogenes*	63	DSM 15452	*L.welshimeri*
25	H09 224 0145	*L. monocytogenes*	64	H08 490 0250	*L. monocytogenes*
26	H08 180 0412	*L. monocytogenes*	65	H10 172 0401	*L. monocytogenes*
27	H09 296 0322	*L. monocytogenes*	66	H10 170 0375	*L. monocytogenes*
28	H08 396 0517	*L. monocytogenes*	67	H10 162 0369	*L. monocytogenes*
29	H09 354 0308	*L. monocytogenes*	68	H10 162 0552	*L. monocytogenes*
30	H09 404 0479	*L. monocytogenes*	69	H10 074 0236	*L. monocytogenes*
31	H09 314 0192	*L. monocytogenes*	70	H08 074 0271	*L. monocytogenes*
32	NCTC 04885	*L. monocytogenes*	71	H09 012 0053	*L. monocytogenes*
33	NCTC 04883	*L. monocytogenes*	72	H09 406 0833	*L. monocytogenes*
34	NCTC 10888	*L. monocytogenes*	73	H10 146 0091	*L. monocytogenes*
35	NCTC 10813	*L. grayi*	74	H10 044 0420	*L. monocytogenes*
36	NCTC 12426	*L. monocytogenes*	75	H08 262 0274	*L. monocytogenes*
37	NCTC 10815	*L. grayi*	76	H09 076 0244	*L. monocytogenes*
38	NCTC 11288	*L. innocua*	77	H10 046 0271	*L. monocytogenes*
39	NCTC 11846	*L. ivanovii*	78	H09 510 0595	*L. monocytogenes*

MSP Dendrograms were constructed using the MALDI Biotyper 3 Bruker software.

2.9 Characterisation of *L. monocytogenes* using Surface Enhanced Laser Assisted Desorption/Ionisation - Time of Flight - Mass Spectrometry SELDI-TOF-MS

2.9.1 Bacterial culture and protein extraction

L. monocytogenes F2365 and *L. monocytogenes* NCTC 10357 cell pellets were prepared. This was achieved using 37°C growth condition, starter culture conditions described in section 2.3 and growth and harvest conditions described in section 2.4.

Pellets and protein extracts were processed as detailed in section 2.5.1. Modifications to the protocol include:

1) Pellets were lysed using the Fast Prep and endolysin was not used.
2) Protein was quantified using Bradford assay
3) Proteins were not separated on Nupage® 4 - 12% Bis-Tris gel (Invitrogen).
4) Cell debris was not visualised.

2.9.2 Preparation of ProteinChip CM10 Array

Two ProteinChip CM10 arrays (Bio-Rad) were placed in a bioprocessor. The arrays were washed by adding 250 µl of buffer: 50 mM Tris-HCl pH 8.4, to each well and shaking vigorously at approximately 200 rpm for 5 minutes. The buffer was decanted and the wash step was repeated.

L. monocytogenes F2365 and *L. monocytogenes* NCTC 10357 protein extracts were processed on separate arrays. A 150 µl volume of protein was added to each well, (wells A-G). The amount of protein in each 150 µl volume varied from 150 µg to 750 µg for *L. monocytogenes* F2365 and from 250 µg to 1200 µg for *L. monocytogenes* NCTC 10357. Wells H were loaded with 150 µl buffer. The arrays were incubated at room temperature for 30 minutes with shaking at approximately 200 rpm.

The protein extracts were decanted and each well was washed with buffer as before for a total of three washes. The buffer was decanted and 250 µl of distilled water was added to each well, followed by immediate decantation. The arrays were removed from the bioprocessor and allowed to air dry. Sinapinic acid (SPA) matrix (Bio-Rad) was resuspened in 400 µl of

solution containing 50% acetonitrile and 0.5% trifluoroacetic acid by vigorous vortexing. Undissolved particles were allowed to sediment and 0.5 µl of matrix solution was added to spots A-G of both arrays, and on spot H of the array used for processing *L. monocytogenes* NCTC 10357 protein extracts. The spots were allowed to air dry and another 0.5 µl of the matrix solution was added. A 0.5 µl volume of protein standard (Protein All-In-One Standard II (Bio-Rad)) was added to spot H of the array used for processing *L. monocytogenes* F2365 protein extracts. The spot was allowed to air dry and another 0.5 µl of the protein standard was added.

2.9.3 Preparation of ProteinChip H50 Array

Two ProteinChip H50 arrays were placed in a bioprocessor. The arrays were prewashed by adding 50 µl of buffer: 50% methanol, to each well and shaking vigorously at approximately 200 rpm for 5 minutes. The solution was decanted and the prewash step was repeated.

The arrays were washed by adding 50 µl of 50% methanol containing 0.1% TFA to each well and shaking vigorously for 5 minutes. The solution was decanted and the wash repeated.

L. monocytogenes F2365 and *L. monocytogenes* NCTC10357 protein extracts were processed on separate arrays. A 150 µl volume of protein was added to each well, (wells A - G). The amount of protein in each 150 µl volume varied from 200 µg to 546 µg for *L. monocytogenes* F2365 and from 150 µg to 984 µg for *L. monocytogenes* NCTC 10357. Wells H were occupied with 150 µl buffer. The arrays were incubated at room temperature for 30 minutes with shaking at approximately 200 rpm.

The protein extracts were decanted and each well was washed with 50% methanol containing 0.1% TFA for a total of three washes. The buffer was decanted and 250 µl of distilled water was added to each well, followed by immediate decantation.

SPA and protein standard were applied to spots as described in section 2.9.2.
This experiment was repeated on a separate occasion with the following modifications:

a) 50% methanol containing 1% TFA was substituted by 10% acetonitrile containing 0.1% TFA.

b) The amount of protein in each 150 µl volume varied from 200 µg to 450 µg for *L. monocytogenes* F2365 and from 150 µg to 984 µg for *L. monocytogenes* NCTC 10357.

2.9.4 Preparation of ProteinChip Q10 Array

Two ProteinChip Q10 arrays were placed in a bioprocessor. The arrays were washed by adding 250 µl of buffer: 20mM Tris-HCl, pH 7.4 containing 1% Triton, to each well and shaking vigorously at approximately 200 rpm for 5 minutes. The buffer was decanted and the wash step was repeated.

L. monocytogenes F2365 and *L. monocytogenes* NCTC10357 protein extracts were processed on separate arrays. A 150 µl volume of protein was added to each well, (wells A-G). The amount of protein in each 150 µl volume varied from 200 µg to 546 µg for *L. monocytogenes* F2365 and from 150 µg to 984 µg for *L. monocytogenes* NCTC 10357. Wells H were occupied with 150 µl buffer. The array was incubated at room temperature for 1 hour with shaking at 200 rpm.

The protein extracts were decanted and each well was washed as before for a total of three washes. The buffer was decanted and 250 µl of distilled water was added to each well, followed by immediate decantation.

SPA and protein standard were applied to spots as described in section 2.9.2.

2.9.5 SELDI-TOF-MS analysis of prepared ProteinChip Arrays

All ProteinChip array spots were completely dry before being analysed individually. Each array was loaded into a PBS II MALDI-TOF Mass Spectrophotometer (Ciphergen Biosystems). Spectral profiles were collected in the mass range 3000 - 50,000 kDa. The laser energy used was 220V. The resulting data was displayed in the programme window as a plot of abundance against mass/charger (m/z).

2.9.6 SELDI-TOF-MS analysis of a selection of isolates using ProteinChip H50 Arrays

A total of 30 isolates were analysed on ProteinChip H50 Arrays These included 21 *L. monocytogenes* isolates obtained from FPRU; 6 NCTC isolates; NCTC 10815 - *L. grayi*

subsp. grayi, NCTC 11288 - *L. innocua*, NCTC 11846 - *L. ivanovii subsp. ivanovii*, NCTC 11856 - *L. seeligeri*, NCTC 11857 - *L. welshimeri* and NCTC 10890 - *L. monocytogenes*; and 2 DSMZ isolates DSMZ 4712 - *Brochothrix campestris* and DSMZ 20171 - *Brochothrix thermosphacta*.

Cell pellets were prepared using 37°C growth condition, starter culture conditions described in section 2.3 and growth and harvest conditions described in section 2.4. *Brochothrix spp.* were cultured at 30°C on APT agar plates, in APT broths where appropriate, and harvested at approximately OD_{600} of 1.0.

Pellets and protein extracts were processed as detailed in section 2.5.1. Modifications to the protocol include:

1) Pellets were lysed using the Fast Prep and endolysin was not used.

2) Protein was quantified using Bradford assay and a volume containing 5 µg of protein separation on Nupage® 4 - 12% Bis-Tris gel (Invitrogen).

3) Cell debris was not visualised.

4) When lysates were obtained directly from sub-cultures 200 µl of lysis buffer was added to a microfuge tube and growth from 2 - 3 plates was removed using a 10 µl loop and resuspended in the lysis buffer by thoroughly swivelling the loop. Glass beads were added to occupy 1/3 of the tube contents volume.

2.9.7 SELDI-TOF-MS analysis of a selection of isolates using ProteinChip CM10 Arrays using (manual spotting protocol)

As an alternative to using the bioprocessor, samples were spotted manually. Briefly, 5 µl of buffer: 25 mM ammonium acetate/0.01% Triton, was added to each spot and incubated at room temperature for 5 minutes. The buffer was removed by pipetting and another 5 µl of buffer was added. This was removed following incubation at room temperature for 5 minutes. The protein extracts from section 2.10.6 were diluted to 2 mg/ml and 3 µl of extract (6 µg of protein) was added to individual spots. The arrays were incubated for 1 hour after which the samples were removed by pipette. The arrays were washed twice with 5 µl buffer as described earlier. The arrays were allowed to air dry. A 1 µl volume of standard was added to an empty spot and allowed to air dry before adding another 1 µl volume. A 0.75 µl volume of

SPA was added to each spot including an empty spot. The matrix was allowed to air dry and a further 0.75 µl SPA was added and allowed to air dry.

Each array was analysed as detailed in section 2.9.5. An amendment to the protocol included the increase of laser energy form 220V to 235V.

2.10 Differentially expressed *L. monocytogenes* proteins

2.10.1 Growth

Cell pellets for each of the following isolates were prepared: NCTC 10357, H101620552, H084460286, H090120053, H084900250, H101460091 and H080740271. One pellet was obtained from a 4°C culture and the other a 37°C culture. This was achieved using starter culture conditions described in section 2.3 and growth and harvest conditions detailed in section 2.4.

2.10.2 Protein extraction quantification and separation by 1-D SDS PAGE

Pellets were processed as detailed in section 2.5.1.

Modifications to the protocol include:

1) All pellets were lysed using the Fast Prep and endolysin was not used.

2) Protein was quantified using Bradford assay and a volume containing 5 µg of protein separation on Nupage® 4 - 12% Bis-Tris gel (Invitrogen).

3) Proteins were stained overnight using Simply Blue Safe Stain (Invitrogen) and background destained by incubation in 25% methanol at room temperature for 2 hours.

4) The gels were visualised using a Bio-Rad Gel Doc ^{TM} EZ Imager.

5) Cell debris was not visualised.

2.10.3 Proteins band intensity measurement

This was achieved using the Bio-Rad Image Lab 4.0 software.

2.10.4 deltaDOT analysis of differentially expressed proteins

Peptides generated from *L. monocytogenes* H101620552 protein extracts which were expressed at 4°C and 37°C were analysed by Deepika Devanur (deltaDOT). Briefly, the samples were de-salted using Pierce desalting columns prior to analysis.

Separation was carried using deltaDOT's proprietary capillary gel electrophoresis protocols using the PEREGRINE I system.

The data was analysed using both deltaDOT's Equiphase Vertexing Alogrithm (EVA) and Generalised Separartion Transform (GST) algorithm by Deepika Devanur (deltaDot).

2.10.5 Analysis of differentially expressed bands

Bands which appeared to have different intensities were excised and subject to in-gel tryptic digestion as detailed in section 2.7.1 - 2.7.5.

LC-MS/MS analysis was carried out by Jenny Cho of ThermoScientic in Hemel Hemstead, using the Easy nLC 1000 (Thermo Scientific) coupled on-line to a Q Exactive mass spectrometer (Thermo Scientific).

Chapter 3: Results

3.1 Efficient lysis of *Listeria spp.*

Efficient cell lysis is a necessity to proteomic investigations. Therefore in the early stage of this study, considerable time was spent to attain efficient lysis of *Listeria* species. This preliminary measure was important in order to ensure that the proteins being investigated were reproducible and representative of the entire cell, and subsequently allow a great level of confidence regarding experimental findings. Efficient lysis experiments commenced with the construction of *L. monoctogenes* growth curves in order to deduce the optimal point at which cells should be harvested for further study. Following this accomplishment characterisation studies were pursued using tool MS tool and these results are presented in sections 3.2 - 3.4.

3.1.1 Growth curve at 4°C and 37°C

It was decided that cells used in this study should be harevested at their exponential growth phase. This decision was taken as it is a widely helf view that cells are metabolically most active at this phase while the integrity of the cell is better retained. Growth curves were constructed in order to determine the exponential phase. The 4°C and 37°C growth curves for *L. monocytogenes* NCTC 10357 showed that when grown in BHI broth, cells harvested between OD_{600} 0.5 and 0.7 and between OD_{600} 0.8 and 1.0 respectively, are at their exponential phase (Figure 3.1 and Figure 3.2 respectively).

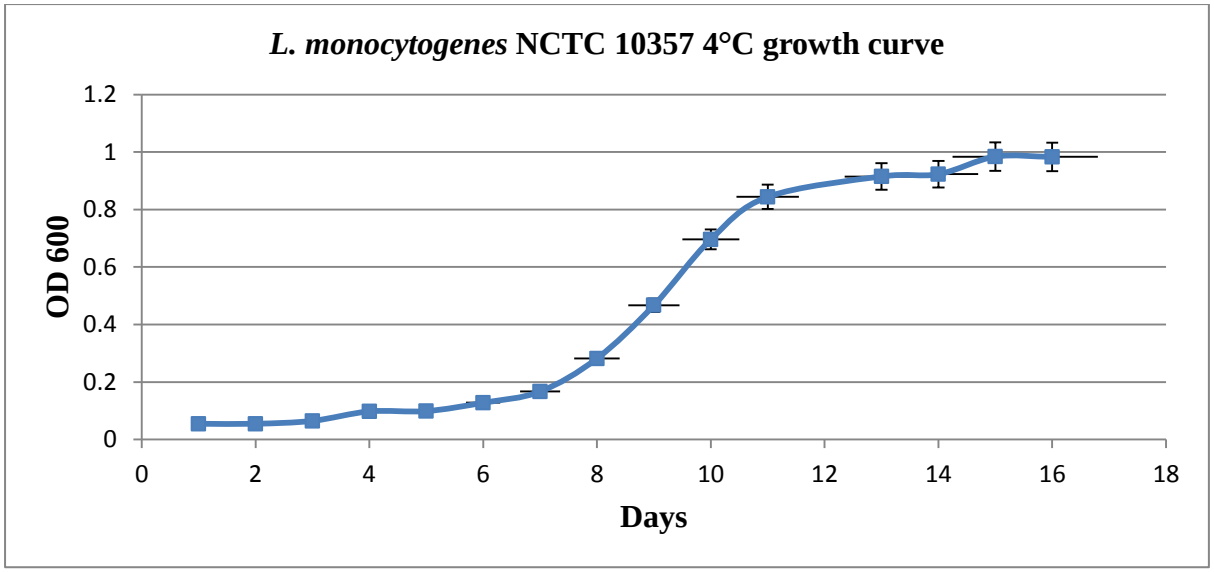

Figure 3.1. *L. monocytogenes* NCTC 10357 4°C growth curve. A plot of absorbance at OD_{600} (y-axis) versus days (x-axis). The curve shows that at an absorbance between OD_{600} 0.5 and 0.7 cells were in their exponential growth phase.

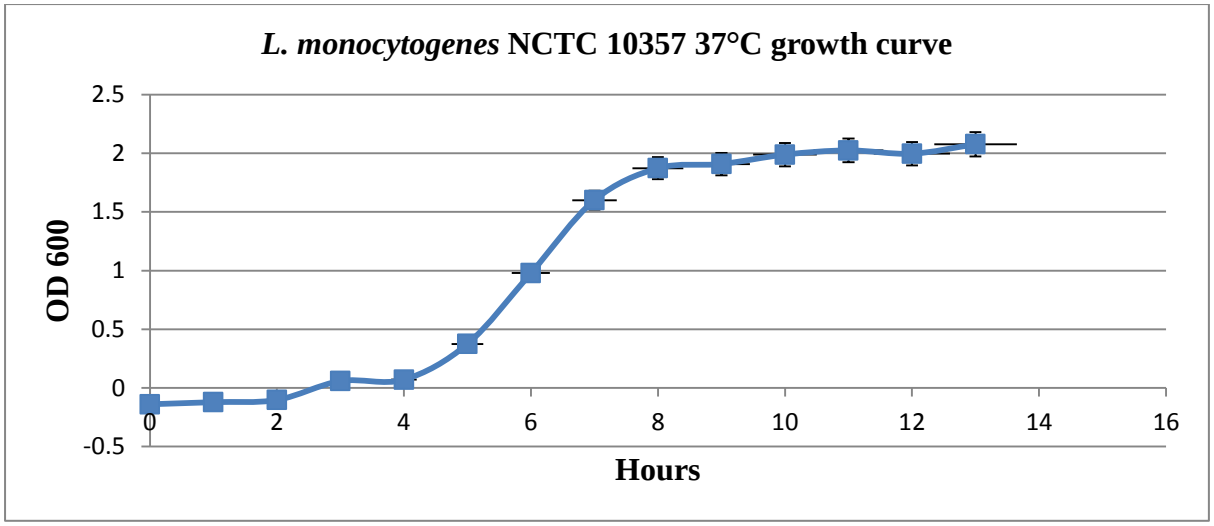

Figure 3.2. *L. monocytogenes* NCTC 10357 at 37°C growth curve. A plot of absorbance at OD_{600} (y-axis) versus days (x-axis). The curve shows that at an absorbance between OD_{600} 0.8 and 1.0 cells were in their exponential growth phase.

3.1.2 Purification of endolysin

A survey of the literature shows that endolysin is an efficient *Listeria* specific lytic enzyme. The enzyme is not commercially available hence it was necessary to undertake protein expression of the cloned endolysin gene and purification of the enzyme for subsequent use.

A stained image of the gel (on which *L. lactis* extracts reserved at every stage of the purification process) showed the presence of a number of bands (Figure 3.3). A comparison of the negative control soluble fraction (lane 1) and the induced expression strain (lane 2 and 3) showed the presence of a unique band in the induced expression strain. The predicted molecular weight of endolysin is 34044.3 Da, which is the approximate mass of the unique band, according to the protein marker (lane M). Addition of Ni-NTA (nickel nitrilotriacetic) facilitated in removal of the His-tagged endolysin proteins from the solution as Ni-NTA has an affinity for the 6x Histidine located at the N-terminal of the protein. The flow through shown in lanes 4 - 5 therefore lacked the unique band. Absence of the protein from the Ni-NTA wash buffer (lanes 6 and 7), showed that the protein remained bound to the beads. The protein was eluted from the Ni-NTA beads by washing with a high concentration of imidazole which has a greater affinity to Ni-NTA than 6x Histidine. The protein was successfully purified as the band in lane 8 represented the eluted protein.

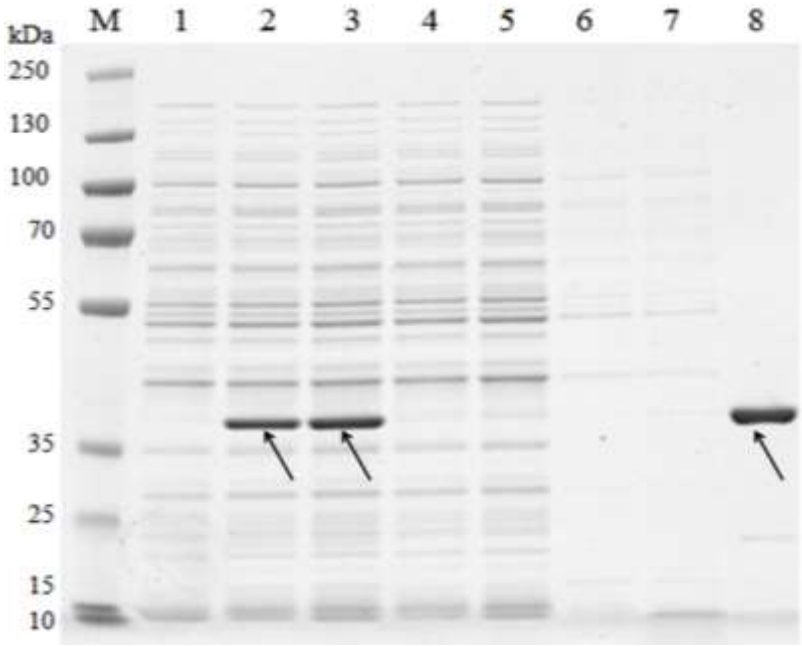

Figure 3.3. One-Dimensional SDS PAGE analysis of protein at each stage of endolysin purification. Lane; M- Marker, 1 - Soluble negative control, 2 and 3 - Soluble protein, 4 and 5 - Flow through, 6 and 7- First and second wash respectively, lane 8- Elution (endolysin). The gel shows the presence of a dense band in the 35 - 55 kDa marker region of lanes 2 and 3 (indicated by black arrow). This band is absent from negative control in lane 1 and was indicative of the presence the endolysin protein which is approximately 34 kDa. The same band was absent from the flow through and wash samples as a result of being bound to the Ni-NTA beads. Presense of the band in the eluate indicated that the endolysin was successfully removed from the Ni-NTA beads and that purification was successful (indicated by black arrow in lane 8).

3.1.3 Lysis of *Listeria spp*. using endolysin

A serotype 4b clinical isolate was lysed using various amounts (0.0, 2.0, 2.2, 2.4, 2.6, 2.8, 3.0, 3.4, 3.8, 4.0, 4.5, and 5.0 µg) of the purified endolyisn. Analysis on a 1-D protein gel showed that the enzyme did not cause protein degradation, which was indicated by the absence of smearing in each lane (Figure 3.4).

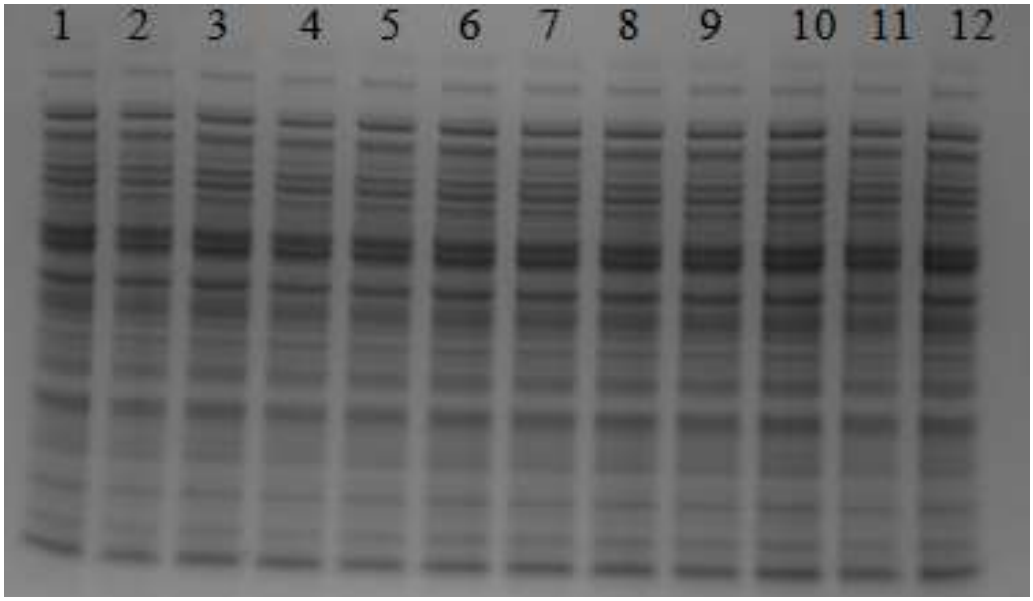

Figure 3.4. One-Dimensional SDS PAGE separation of protein extracted from *L. monocytogenes*, serotype 4b clinical isolate obtained from FPRU. Lanes 1- 12 are protein extracts obtained using 0.0 (negative control), 2.0, 2.2, 2.4, 2.6, 2.8, 3.0, 3.4, 3.8, 4.0, 4.5, and 5.0 µg of endolysin respectively. The image show that the use of endolysin in various amounts did not affect the integrity of the *L. monocytogenes* protein extracts as the protein profile of the negative control was similar to that of the other extracts.

Light microscopic examination of the cell debris was used to determine the minimum amount of enzyme required for complete lysis. In the negative control sample, consisting of unlysed *L. monocytogenes*, all cells appeared intact. Some intact cells were visible in samples to which 2.0 - 3.4 μg of endolysin was added. Observations showed that the amount of lysed cells increased as the amount of enzyme increased. More lysis was achieved when 3.8 - 4.5 μg of enzyme was used; however, a few cells appeared to be intact. There were no visibly intact cells when 5.0 μg of enzyme was used and lysis appeared to be complete. Based on these results, it was deduced that 5 μg of endolysin was sufficient to lyse a 100 mg pellet of this isolate, and was used to test lysis efficiency of other *L. monocytogenes* lineages and *Listeria* species. A total of 13 isolates were tested. These included, *L. monocytogenes* F2365, NCTC 10888, NCTC 10357, NCTC 5348, NCTC 04883, NCTC 05124, NCTC 10815, NCTC 10813, NCTC 11288, NCTC 11846, NCTC 12701, NCTC 11856 and NCTC 11857. Light microscopic examination showed that the enzyme efficiently and reproducibly lysed all other *Listeria* species (Figure 3.5) (two isolates shown). However, *L. grayi* subsp *grayi* (NCTC 10815) appeared to be less susceptible as some of the cells appeared to be intact. *L. rocourtiae* and *L. marthii* were not tested as the isolates were not part of the NCTC collection at the time of study.

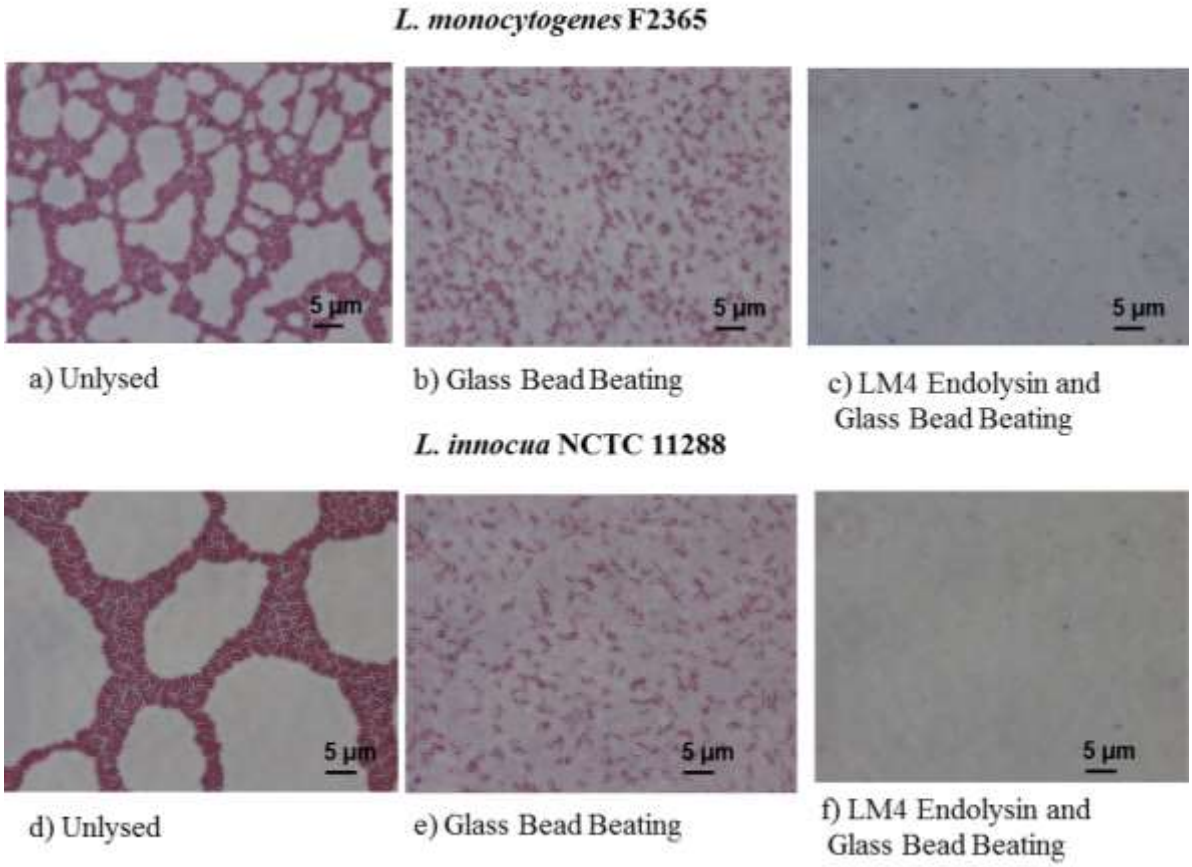

Figure 3.5. Gram stain images of *L. monocytogenes* F2365 and *L. innocua* cells (x 1000 magnification). Images (a) and (d) depicts *L. monocytogenes* F2365 and *L. innocua* respectively as unlysed small clustered rods. Images (b) and (e) show the cell debris post lysis by bead beating. The cells are no longer clustered, however, they appear to be intact, an indication that lysis is not complete. Images (c) and (f) show the cell debris post lysis with endolysin and bead beating. The absence of rod shaped cells indicated that complete cell lysis occured.

Separation of all 13 protein extracts on a 1-D gel also showed no evidence of smearing and this suggested that endolysin did not cause degradation of protein extracted from all *Listeria* species (Figure 3.6). The figure also revealed the similarities between the protein profiles of all the species. For example, protein bands at 160, 40 and 30 kDa (indicated by arrows) are consistenly seen across all profiles.

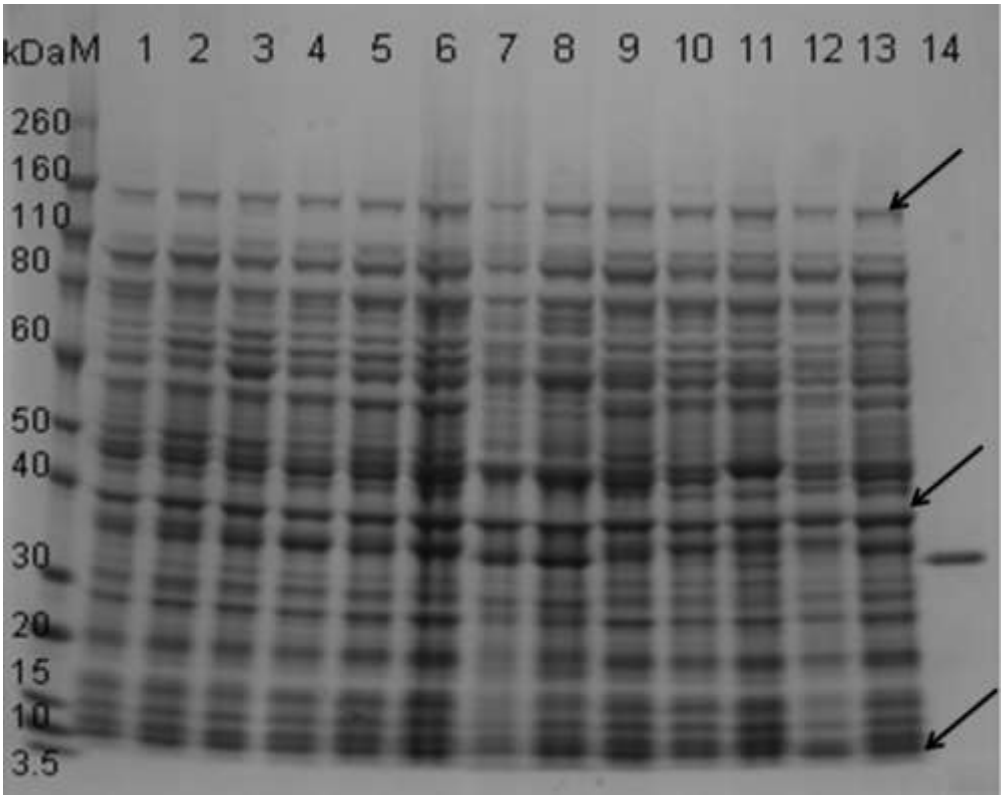

Figure 3.6. One-Dimensional SDS PAGE separation of *Listeria* protein extracts obtained from lysis with endolysin. M - Marker, 1- *L. monocytogenes* F2365, 2 - NCTC 10888, 3 - NCTC 10357, 4 - NCTC 5348, 5 - NCTC 04883, 6 - NCTC 05124, 7 - NCTC 10815, 8 - NCTC 10813, 9 - NCTC 11288, 10 - NCTC 11846, 11 - NCTC 12701, 12 - NCTC 11856, 13 - NCTC 11857, 14 - endolysin. The gel shows that endolysin did not affect the integrity of the various species of *Listeria* used in this experiment. It also emphasised the close similarity among *Listeria* by virtue of their similar protein profiles.

Protein concentrations were compared using a bar chart (Figure 3.7). The result also showed that overall, the use of endolysin facilitated in the release of more protein from *Listeria spp.* cells in comparison to lysing with glass beads or the barocycler. Furthermore, the data showed reproducibility across the methods as consistently, extraction with the barocycler yielded the least amount of protein, while extraction with endolysin liberated the highest amount of protein with the exception of *L. monocytogenes* F2365, NCTC 5348, NCTC 05214, and NCTC 11857 (4 of 13 isolates). A reason for this exception could be that errors occurred while simultaneously processing a large number of samples. In order to investigate whether this was the case, protein was extracted from *L. monocytogenes* F2365 (1 of the 4 samples in which an increase was not apparent), in three biological replicates. The results of all three experiments showed that the amount of protein extracted was highest when endolysin was used and least when the barocycler was used (Figure 3.8). This demonstrated that extraction of higher amounts of protein was reproducible when endolysin was used.

Analysis of these extracts on a 2-D gel showed that extracts obtained using endolysin contained more proteins (Figure 3.9), as assessed visually by 2-D gel electrophoresis. The experiment was carried out in three biological replicates (one replicate shown). The result was reproducible and the image showed that protein extraction using the barocycler leads to the least number of protein spots, whilst extraction with endolysin leads to the most number of protein spots evident on the gel.

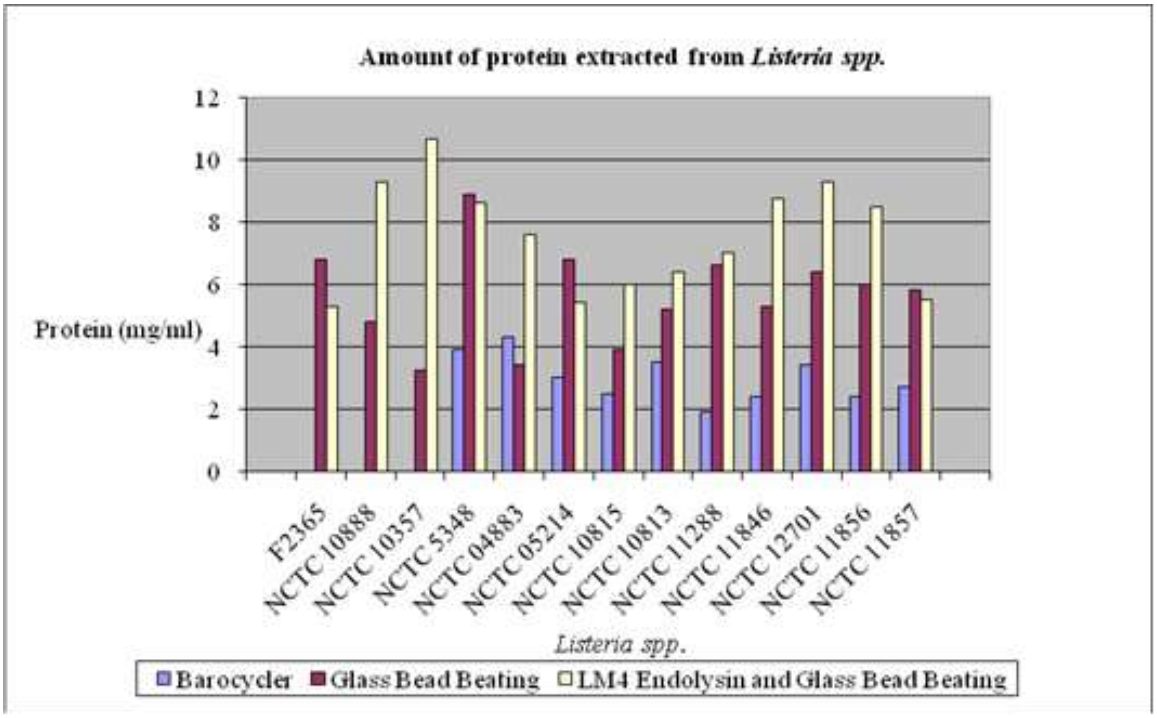

Figure 3.7. Amounts of protein (mg/ml) extracted from *Listeria spp* by lysis using barocycler, glass bead beating only and endolysin incubation followed by glass bead beating. Strains F2365, NCTC 10888 and NCTC 10357 were not tested. Overall, the data showed reproducibility across the methods as consistently, extraction with the barocycler yielded the least amount of protein, while extraction with endolysin liberates the highest amount of protein with the exception of F2365, NCTC 5348, NCTC 05214, and NCTC 11857.

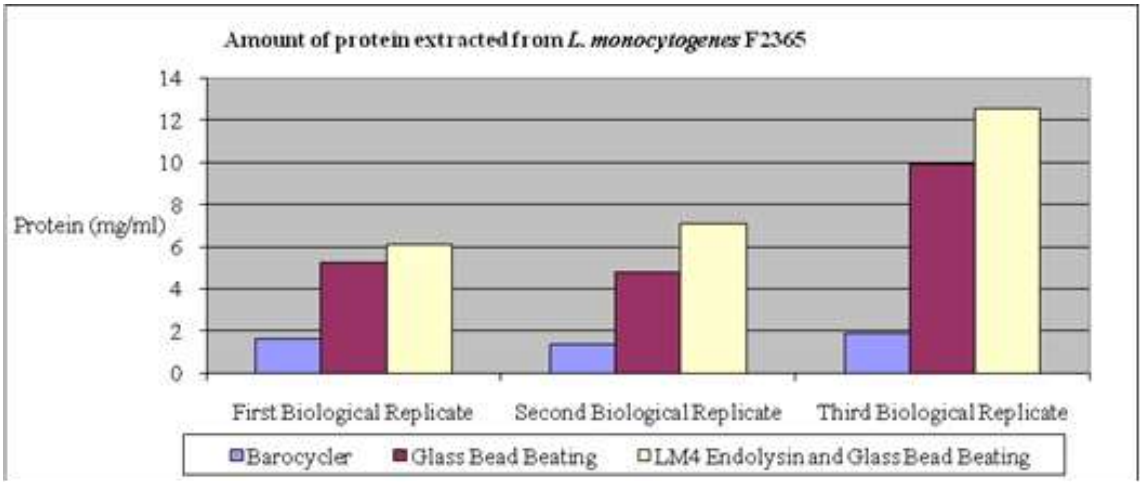

Figure 3.8. Amounts of protein (mg/ml), extracted from *Listeria monocytogenes* F2365 using barocycler, glass bead beating and endolysin incubation followed by glass bead beating. As above, data showed that lysis using the barocyler yields the least amount of protein across all biological replicates (< 2mg/ml) whereas lysis using endolysin liberates the highest amount of protein. Glass bead beating yielded 1mg/ml - 2.25mg/ml protein.

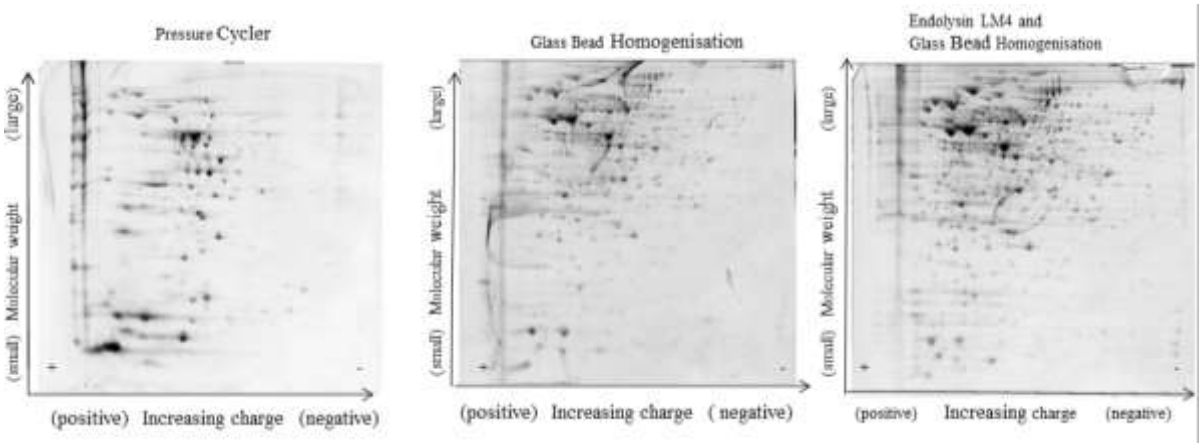

Figure 3.9. Two-dimensional SDS PAGE analysis of *L. monocytogenes* F2365 protein extracts obtained using a barocycler, glass bead beating and endolysin and glass bead beating. Protein molecular weights are indictated on the y-axis whilst charge is indicated on the x-axis. The "+" sign indicates the anodic side and the gel and the "-" sign indicates the cathodic side of the gel. The experiment was carried out in three biological replicates (one replicate shown). The result was reproducible and the image shows that protein extraction using the barocycler leads to the least number of protein spots, whilst extraction with endolysin leads to the most number of protein spots evident on the gel.

LC-MS/MS analysis of the extracts consistently showed that the number of proteins identified was higher when endolysin was used during extraction as opposed to glass bead beating only; this was verified by comparing each biological replicate (Figure 3.10), and by comparing both extraction methods (Figure 3.11). A comparison of each biological replicate showed that a difference of 14, 7 and 5 extra proteins were identified from extracts produced using endolysin, (Figures 3.10 a, b, and c respectively). A comparison of the extraction methods showed that 12 extra proteins were identified from extracts produced using endolysin (Figure 3.11). However, the lists of proteins identified showed that only 2 proteins (Table 3.1) were consistently present in extracts produced by incubation with endolysin, and which were absent from extracts produced using glass bead beating only. A list of all proteins identified can be found in Table A1 (see appendix).

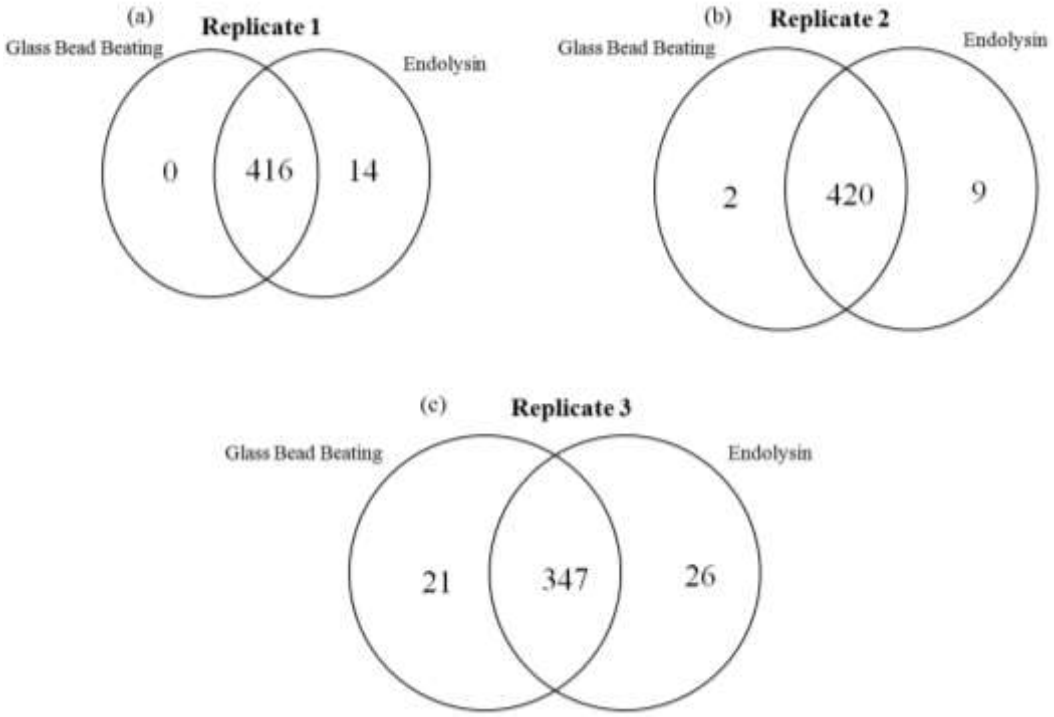

Figure 3.10. Venn diagram showing the number of proteins identified from *L. monocytogenes* F2365 cell extracts; a) first biological replicate shows that no unique proteins were produced using glass bead beating, 14 proteins were unique to extracts produced using endolysin and 416 proteins were found in both extracts; b) second biological replicate shows 2 proteins unique to extracts produced using glass bead beating, 9 proteins were unique to extracts produced using endolysin and 420 proteins were found in both extracts; c) third biological replicate shows that 21 proteins were unique to extracts produced using glass bead beating, 26 proteins were unique to extracts produced using endolysin and 347 proteins were found in both extracts.

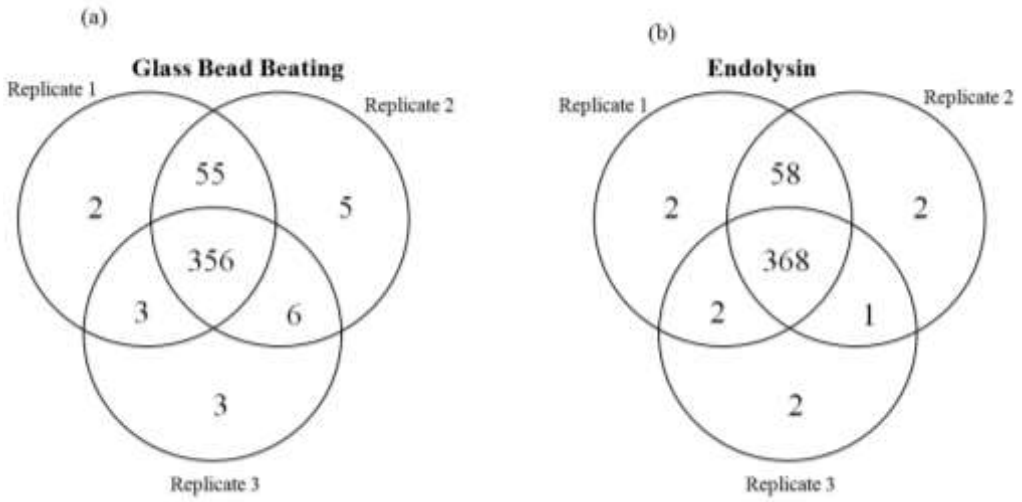

Figure 3.11. Venn diagram of number of proteins identified from *L. monocytogenes* F2365 cell extracts; a) a comparison of number of proteins identified in extracts produced using glass bead beating; b) a comparison of number of proteins identified in extracts produced using endolysin. Using the endolysin extraction method, a total of 368 proteins were consistenly identified across all 3 replicates. Using the glass beating method a total of 356 proteins were consistently identified across all 3 replicates.

Table 3.1. List of proteins uniquely and consistently present among all protein extracts produced using endolysin (replicates1, 2 and 3), the accession number and number of unique peptides found.

Protein name	Accession Number	Number of Unique Peptides		
		Replicate 1	Replicate 2	Replicate 3
ISPC	gi126143318	5	7	5
RNA Methyltransferase	gi 116871624	1	1	2

The accession number corresponding to ISPC was searched against the NCBI database and results showed that it is an immunogenic surface protein: a 86 kDa protein target of the humoral immune response to infection with *L. monocytogenes* serotype 4b. RNA Methyltransferase is a 51 kDa protein involved in the conversion of primary RNA transcript to mature RNA molecules. As the endolysin extraction method did not yield a great number of consistently identified proteins, the extraction method applied to all future experiments was glass bead beating only which proved to be sufficiently efficient.

3.2 Characterisation of *L. monocytogenes* using MALDI-TOF MS

Characterisation of *L. monocytogenes* using MALDI-TOF-MS was undertaken using direct smears of the organisms as well as by using formic acid protein extracts. Mass spectra analysis of *Listeria spp.* from direct smears using the AXIMA CFR Plus MALDI-TOF-MS instrument (Shimadzu Corporation, UK) and DHB matrix showed that protein mass ions of up to 16 kDa were detected; however, most peaks were up to 10 kDa (Figure 3.12). This data provided the first indication that in this study, MALDI-TOF-MS would be more effective for the characterisation of smaller molecular weight proteins, whereas SELDI-TOF-MS, is capable of detecting larger molecular weight proteins. Analysis using HCCA matrix showed a similar result (data not shown), therefore the focus was placed on inspecting ions up to 10 kDa.

Visual inspection of mass spectra profiles consistently showed that the major high intensity peaks detected were 4325 and 5301 kDa, while lower intensity peaks included 7591 and 9752 kDa (Figures 3.13). The occurrence of these peaks in multiple spectra of various *L. monocytogenes* species shows that these ions are consistently present within the species. It was therefore envisaged that in this study, the consistent detection of a number of protein ions amongst isolates would be the basis through which the species could be further characterised.

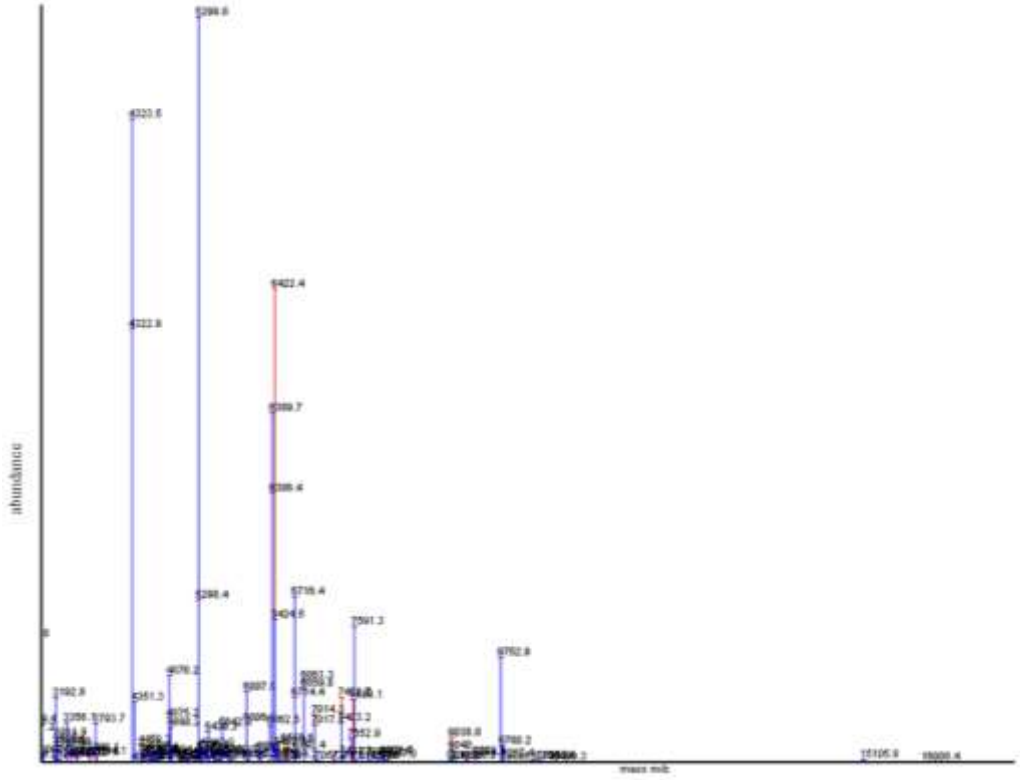

Figure 3.12. Mass spectrum of NCTC 10357 obtained using a direct colony smear. Ion abundance (y-axis) and ion mass (x) axis. Blue peaks represent ions detected in the isolate and red peaks represent ions in the SARAMIS *Listeria* superspectrum. The spectrum shows that using the AXIMA CFR Plus MALDI-TOF-MS instrument (Shimadzu Corporation, UK) and DHB matrix, protein mass ions of up to 16 kDa can be detected; however, most peaks are up to 10 kDa.

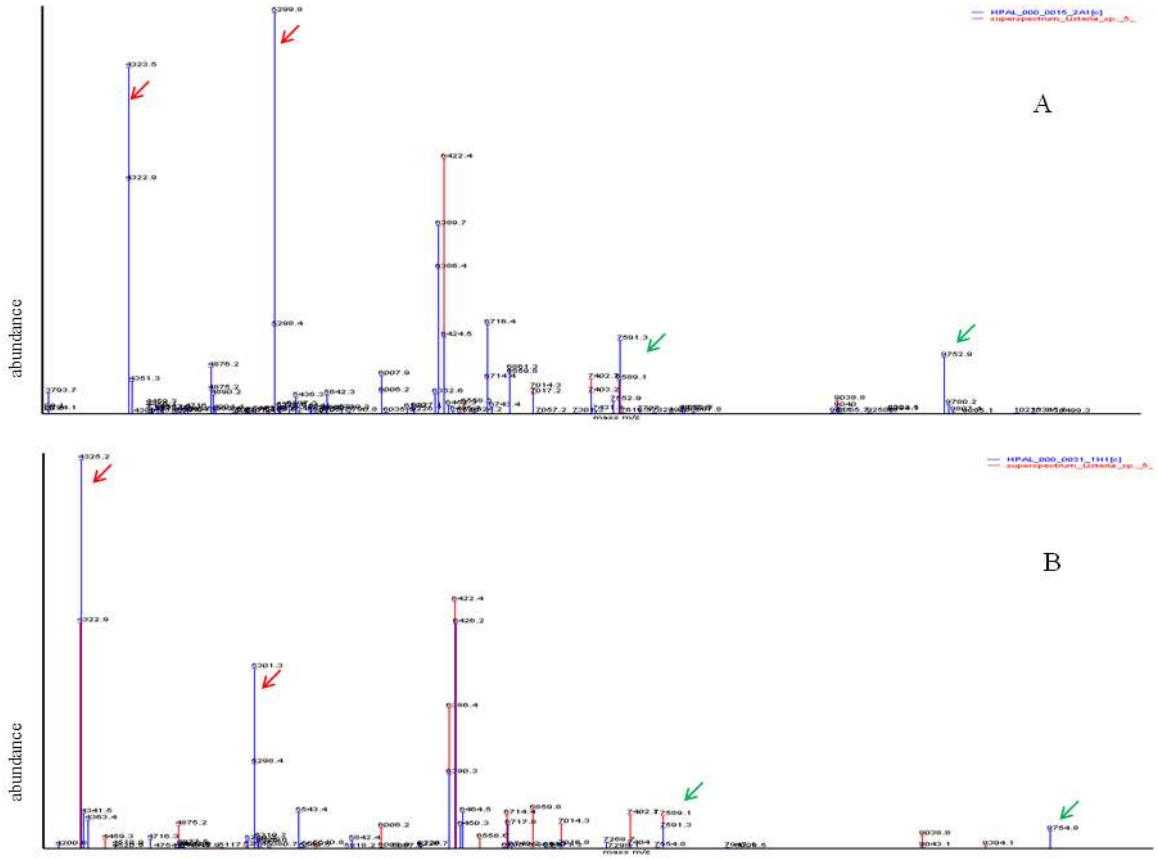

Figures 3.13. Mass spectra of (A) *L. monocytogenes* NCTC 10357 isolate and (B) *L. monocytogenes* NCTC 10890 isolate. Ion abundance (y-axis) and ion mass (x) axis. Blue peaks represent ions detected in the isolate and red peaks represent ions in the SARAMIS *Listeria* superspectrum. Visual inspection of the profiles consistently shows that the major high intensity peaks detected were 4325 and 5301 kDa (indicated by red arrows), while lower intensity peaks included 7591 and 9752 kDa (indicated by green arrows).

Though the quality of spectra obtained using SARAMIS MALDI-TOF-MS instrument was good (that is, ions detected were reproducible with consistent intensities), identification was predominantly genus level identification of all *Listeria* species. Of the 23 isolates analysed using DHB matrix 19 were positively identified as belonging to the genus *Listeria*, 1 was identified to the correct species level and the remaining 4 isolates yielded no identification results (Table 3.2). Analysis using HCCA yielded similar results and therefore did not appear to impact identification result. Of the 23 isolates tested, 18 were identified to genus level, 2 were identified to the species level and 4 were not identified (Table 3.3). This was an unexpected result as there are superspectra in the SARAMIS database representing each species of *Listeria*, which should have therefore facilitated species level identification.

Table 3.2. List of microorganisms smeared on the bioMérieux MALDI target plate, the HPA Sample Identification code, the identification confidence scores and the Taxnonmic Rank assigned by the SARAMIS analysis. The matrix used was DHB. Each isolate was tested in duplicates. The results showed that of the 23 isolates, 18 were identified to the genus level, 1 was identified to the species level and 4 were not identified.

HPA Sample Identification	**Isolate**	**Identification Confidence Score (%)**	**Results**
EGD-e	*L. monocytogenes*	99.9	*Listeria spp.*
EGD-e	*L. monocytogenes*	99.9	*Listeria spp.*
NCTC 10815	*L. grayi* subsp *grayi*	0	*no identification*
NCTC 10815	*L. grayi* subsp *grayi*	0	*no identification*
NCTC 11846	*L. ivanovii* subsp *ivanovii*	94.6	*Listeria spp.*
NCTC 11846	*L. ivanovii* subsp *ivanovii*	99.9	*Listeria spp.*
NCTC 11288	*L. innocua*	79.5	*Listeria spp.*
NCTC 11288	*L. innocua*	99.9	*Listeria spp.*
NCTC 11857	*L. welshimeri*	86.4	*Listeria spp.*
NCTC 11857	*L. welshimeri*	99.9	*Listeria spp.*
NCTC 11856	*L. seeligeri*	99.9	*Listeria spp.*
NCTC 11856	*L. seeligeri*	99.9	*Listeria spp.*
H09 032 787	*L. seeligeri*	99.9	*Listeria spp.*
H09 032 787	*L. seeligeri*	99.9	*Listeria spp.*
H09 304 0186	*L. innocua*	90.1	*Listeria spp.*
H09 304 0186	*L. innocua*	77.4	*Listeria spp.*
H09 032 0783	*L. ivanovii*	79.5	*Listeria spp.*
H09 032 0783	*L. ivanovii*	79.5	*Listeria spp.*
H09 032 0784	*L. welshimeri*	0	*no identification*
H09 032 0784	*L. welshimeri*	0	*no identification*
H09 0327 077	*L. grayi*	0	*no identification*
H09 0327 077	*L. grayi*	0	*no identification*

H08 162 0317	*L. monocytogenes*	90.3	*Listeria spp.*
H08 162 0317	*L. monocytogenes*	94.6	*Listeria spp.*
H09 126 0107	*L. monocytogenes*	99.9	*Listeria spp.*
H09 126 0107	*L. monocytogenes*	99.9	*Listeria spp.*
Control	*Escherichia coli*	99.9	*Escherichia coli*
Control	*Escherichia coli*	99.9	*Escherichia coli*
H09 088 0603	*L. monocytogenes*	90.3	*Listeria spp.*
H09 088 0603	*L. monocytogenes*	94.6	*Listeria spp.*
H08 180 0412	*L. monocytogenes*	99.9	*Listeria spp.*
H08 180 0412	*L. monocytogenes*	99.9	*Listeria spp.*
H08 520 0220	*L. monocytogenes*	81	*Listeria spp.*
H08 520 0220	*L. monocytogenes*	75.6	*Listeria spp.*
H08 352 0191	*L. monocytogenes*	99.9	*Listeria spp.*
H08 352 0191	*L. monocytogenes*	99.9	*Listeria spp.*
H08 446 0286	*L. monocytogenes*	99.9	*Listeria spp.*
H08 446 0286	*L. monocytogenes*	94.6	*Listeria spp.*
H08 382 0003	*L. monocytogenes*	91.8	*Listeria spp.*
H08 382 0003	*L. monocytogenes*	99.9	*Listeria spp.*
H08 156 0404	*L. monocytogenes*	91.8	*Listeria spp.*
H08 156 0404	*L. monocytogenes*	97.2	*Listeria spp.*
H08 224 0145	*L. monocytogenes*	97.2	*Listeria spp.*
H08 224 0145	*L. monocytogenes*	91.3	*Listeria monocytogenes*
H08 382 0048	*L. monocytogenes*	0	*no identification*
H08 382 0048	*L. monocytogenes*	86.4	*Listeria spp.*
H08 454 0569	*L. monocytogenes*	0	*no identification*
H08 454 0569	*L. monocytogenes*	0	*no identification*

Table 3.3. List of microorganisms smeared on the bioMérieux MALDI target plate, the HPA Sample Identification code, the identification confidence scores and the Taxnonmic Rank assigned by the SARAMIS analysis. The matrix used was HCCA. Each isolate was tested in duplicates. The results show that of the 23 isolates, 19 were identified to the genus level, 2 was identified to the species level and 3 were not identified.

HPA Sample Identification	**Isolate**	**Identification Confidence Score (%)**	**Results**
EGD-e	*L. monocytogenes*	87.6	*Listeria spp.*
EGD-e	*L. monocytogenes*	98.9	*Listeria spp.*
NCTC 10815	*L. grayi* subsp *grayi*	0	*no identification*
NCTC 10815	*L. grayi* subsp *grayi*	98.9	*no identification*
NCTC 11846	*L. ivanovii* subsp *ivanovii*	99.9	*Listeria spp.*
NCTC 11846	*L. ivanovii* subsp *ivanovii*	99.9	*Listeria spp.*
NCTC 11288	*L. innocua*	94.6	*Listeria spp.*
NCTC 11288	*L. innocua*	86	*Listeria spp.*
NCTC 11857	*L. welshimeri*	86.4	*Listeria spp.*
NCTC 11857	*L. welshimeri*	86.4	*Listeria spp.*
NCTC 11856	*L. seeligeri*	99.9	*Listeria spp.*
NCTC 11856	*L. seeligeri*	99.9	*Listeria spp.*
H09 032 787	*L. seeligeri*	91.8	*Listeria spp.*
H09 032 787	*L. seeligeri*	91.8	*Listeria spp.*
H09 304 0186	*L. innocua*	0	*no identification*
H09 304 0186	*L. innocua*	0	*no identification*
H09 032 0783	*L. ivanovii*	99.9	*Listeria spp.*
H09 032 0783	*L. ivanovii*	0	*no identification*
H09 032 0784	*L. welshimeri*	0	*no identification*
H09 032 0784	*L. welshimeri*	0	*no identification*
H09 0327 077	*L. grayi*	0	*no identification*

H09 0327 077	*L. grayi*	0	*no identification*
H08 162 0317	*L. monocytogenes*	99.9	*Listeria spp.*
H08 162 0317	*L. monocytogenes*	99.9	*Listeria spp.*
H09 126 0107	*L. monocytogenes*	98.9	*L. monocytogenes*
H09 126 0107	*L. monocytogenes*	84.8	*Listeria spp.*
Control	*Escherichia coli*	99.9	*Escherichia coli*
Control	*Escherichia coli*	99.9	*Escherichia coli*
H09 088 0603	*L. monocytogenes*	81.7	*Listeria spp.*
H09 088 0603	*L. monocytogenes*	0	*no identification*
H08 180 0412	*L. monocytogenes*	94.6	*Listeria spp.*
H08 180 0412	*L. monocytogenes*	94.6	*Listeria spp.*
H08 520 0220	*L. monocytogenes*	98.9	*Listeria spp.*
H08 520 0220	*L. monocytogenes*	81.7	*Listeria spp.*
H08 352 0191	*L. monocytogenes*	81.7	*Listeria spp.*
H08 352 0191	*L. monocytogenes*	98.9	*Listeria spp.*
H08 446 0286	*L. monocytogenes*	81.7	*Listeria spp.*
H08 446 0286	*L. monocytogenes*	98.6	*Listeria spp.*
H08 382 0003	*L. monocytogenes*	99.9	*Listeria spp.*
H08 382 0003	*L. monocytogenes*	99.9	*L. monocytogenes*
H08 156 0404	*L. monocytogenes*	97.2	*Listeria spp.*
H08 156 0404	*L. monocytogenes*	97.2	*Listeria spp.*
H08 224 0145	*L. monocytogenes*	98.9	*Listeria spp.*
H08 224 0145	*L. monocytogenes*	99.9	*L. monocytogenes*
H08 382 0048	*L. monocytogenes*	94.6	*no identification*
H08 382 0048	*L. monocytogenes*	90.3	*Listeria spp.*
H08 454 0569	*L. monocytogenes*	90.3	*Listeria spp.*
H08 454 0569	*L. monocytogenes*	0	*no identification*

As species level identification was not attainable, the Microflex LT MALDI-TOF-MS instrument (Bruker UK, Ltd) was investigated as an alternate approach. In the first instance this was investigating from direct smears. Good quality spectral profiles were obtained using HCCA matrix. The profiles were also similar to those obtained using the SARAMIS MALDI-TOF-MS instrument. Mass ions of similar sizes were detected (4322 and 5803 kDa), and the majority of peaks detected were up to ~10 kDA (Figure 3.14a and Figure 3.16a). These results provided confidence that the Micro LT MALDI-TOF-MS instrument could be used to accomplish the same goals which were set out earlier. Of the 89 *Listeria* isolates investigated, 57 (64%) were given secure genus identification, 31 isolates (35%) were high probable species and 1 isolate (1%) was probable genus (Figure 3.15). Of the 31 high probable species 2 isolates were assigned conflicting species identification: NCTC 10813 - *L. grayi subsp grayi* and NCTC 11289 - *L. seeligeri* were both identified as *L. monocytogenes*. All 57 isolates which were assigned secure genus score were correct and the isolate which was given a high probable genus score was also correct.

Species level identification was improved using the Microflex LT MALDI-TOF-MS instrument; however, there was a need to vastly improve the number of isolates identified to the species level prior to ascertaining its value for further discrimination. Barbuddhe et al. (2008) demonstrated that formic acid extraction improved *L. monocytogenes* identification results (Barbuddhe *et al.* 2008). Formic acid extraction was performed on 33 of the 89 *Listeria* isolates used in direct smear analysis, and visual inspection of mass spectral profiles showed that the number of mass ions detected had increase (Figures 3.14b and 3.16b). The spectra shows that relative to direct smears (Figure 3.14a and 3.16a), formic acid extraction resulted in the detection of a larger number of ions with ions such as 3702, 4325, 4698, 4878, 6364, 7402, 9340 and 9747 Da being consistently detected in other *L. monocytogenes* species. A total of 30 (94%) *Listeria* isolates were correctly identified to the species level while 3 isolates (6%) were assigned conflicting species identification (Figure 3.17). Discrepant identification included: NCTC 11289 - *L. seeligeri* which was identified as *L. monocytogenes,* NCTC 10813 - *L. grayi subsp grayi* which was identified as *L. innocua* and an isolate which was identified by the FPRU as *L. innocua* was identified as *L. grayi*.

A comparison of the pie charts in Figure 3.15 and Figure 3.17 shows that when the formic acid extraction method was used the percentage of isolated identified to the species level

increased by 69%. Also by, comparing the resulting score values it is evident that formic acid extraction facilitates better identification results. A sample of the compared score values are illustrated in Table 3.4. The data shows that the score values increased as a result of performing formic acid extraction. This subsequently let to a larger number of isolates being identified to species level.

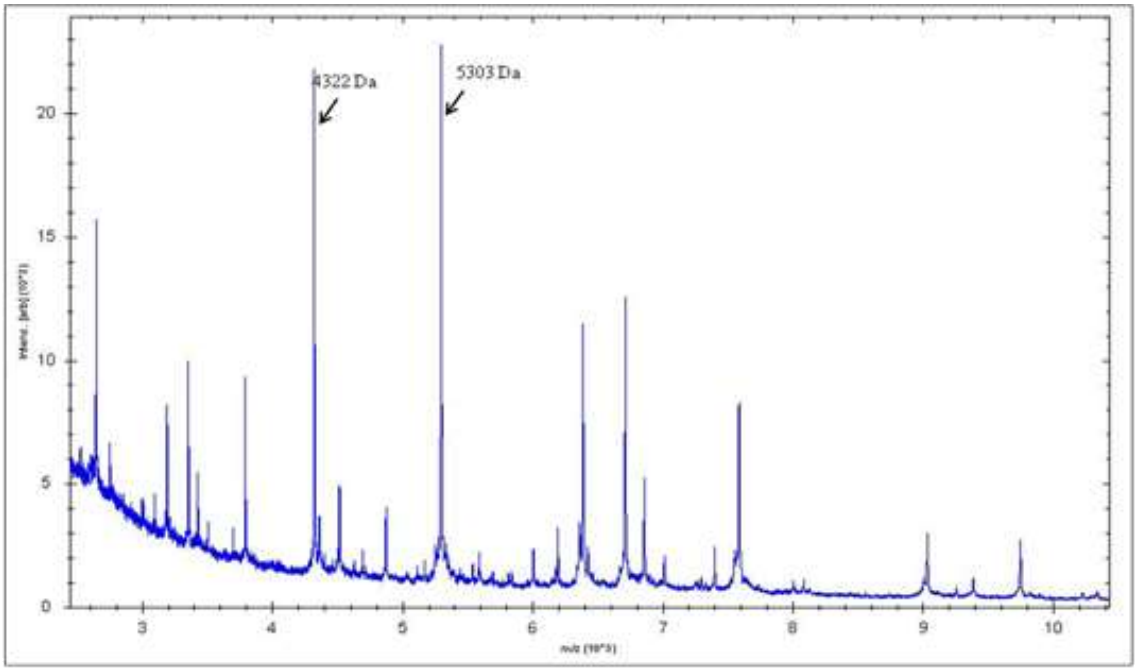

Figure 3.14a. Mass spectrum of *L. monocytogenes* NCTC 10357 derived directly from smeared cell preparations that were overlaid with HCCA matrix. Ion abundance (y-axis) and ion mass (x) axis. The spectrum was obtained using ths Microflex LT MALDI-TOF-MS instrument (Bruker UK, Ltd). The 4322 and 5303 Da ions which were detected using SARAMIS MALDI-TOF-MS instrument (Figure 3.13) were also detected here (indicated by arrows).

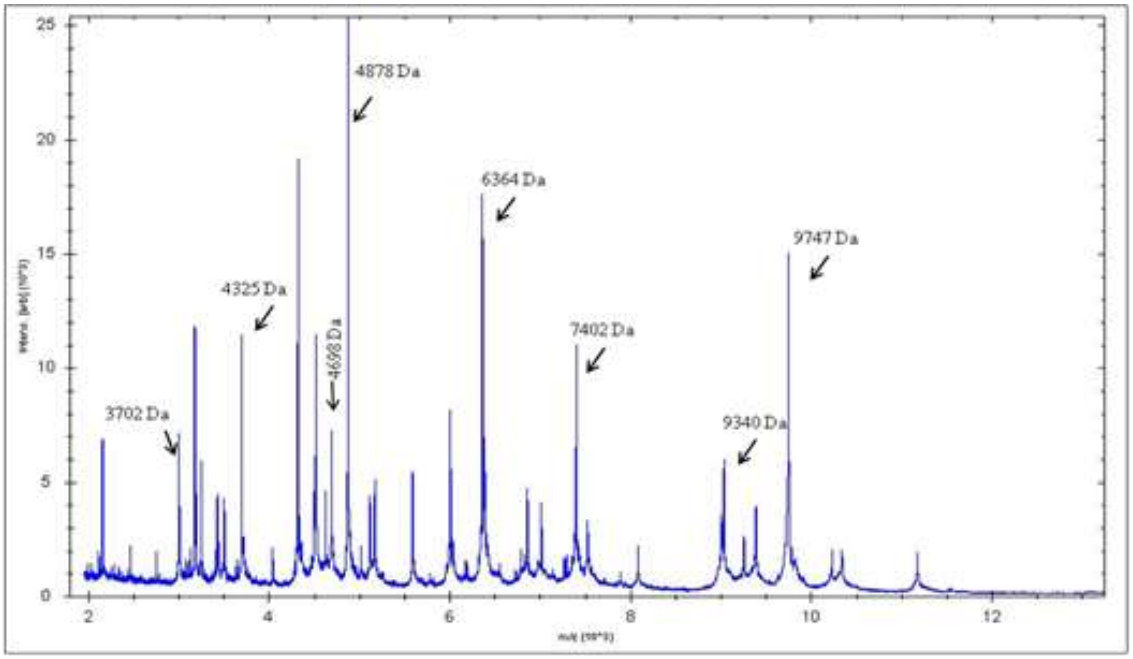

Figure 3.14b. Mass spectrum of *L. monocytogenes* NCTC10357 derived from formic acid extracts of cell that were overlaid with HCCA matrix. Ion abundance (y-axis) and ion mass (x) axis. The spectrum was obtained using ths Microflex LT MALDI-TOF-MS instrument (Bruker UK, Ltd). The spectrum shows that relative to direct smears (Figure 3.14a), formic acid extraction results in the detection of a larger number of ions. The arrows indicate some of the major peaks which are consistently detected in other *L. monocytogenes* species.

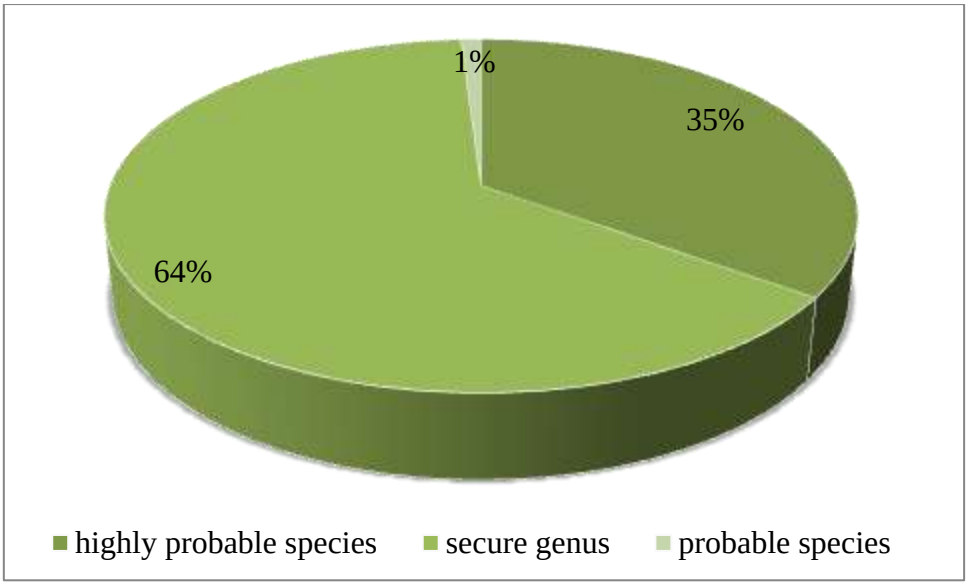

Figure 3.15. Pie chart showing the percentage of *Listeria* isolates identified using the MALDIbiotyper description; highly probable species, secure genus and probable genus. Of the 89 Listeria isolates investigated, 57 (64%) were given secure genus identification, 31 isolates (35%) were high probable species and 1 isolate (1%) was probable genus.

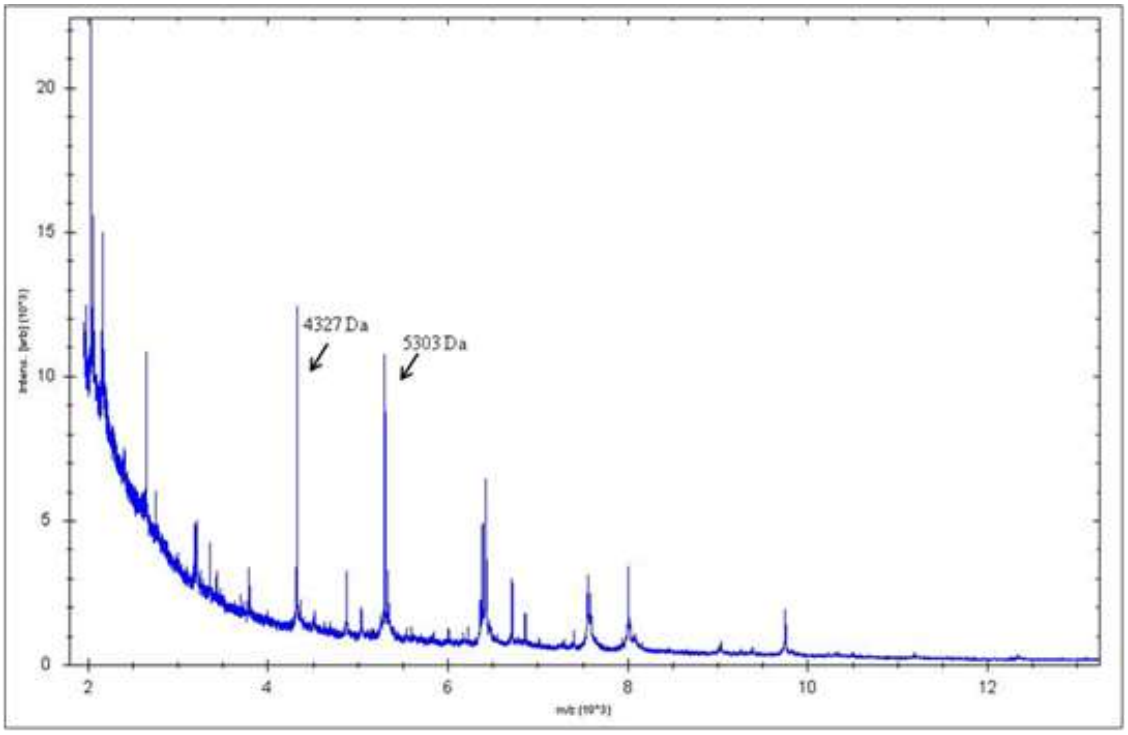

Figure 3.16a. Mass spectrum of *L. monocytogenes* NCTC 10890 derived directly from smeared cell preparations that were overlaid with HCCA matrix. Ion abundance (y-axis) and ion mass (x) axis. The spectrum was obtained using ths Microflex LT MALDI-TOF-MS instrument (Bruker UK, Ltd). The 4322 and 5303 Da ions which were detected using SARAMIS MALDI-TOF-MS instrument (Figure 3.13) were also detected here (indicated by arrows).

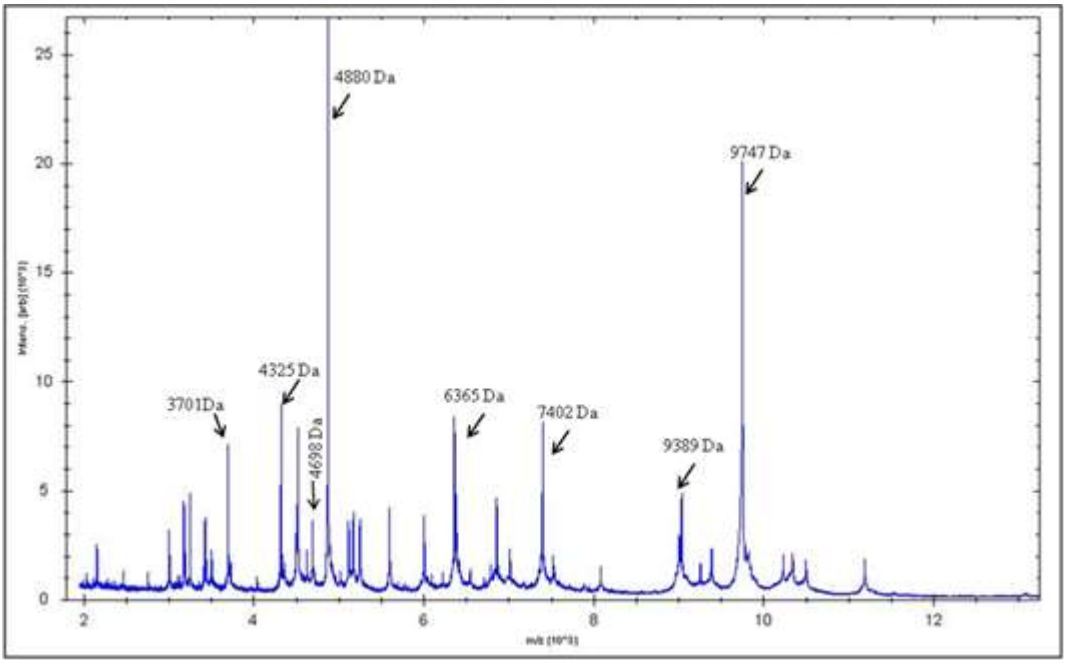

Figure 3.16b. Mass spectrum of *L. monocytogenes* NCTC 10890 derived from formic acid extracts of cell that were overlaid with HCCA matrix. Ion abundance (y-axis) and ion mass (x) axis. The spectrum was obtained using ths Microflex LT MALDI-TOF-MS instrument (Bruker UK, Ltd). The spectrum shows that relative to direct smears (Figure 3.16a), formic acid extraction results in the detection of a larger number of ions. The arrows indicate some of the major peaks which are consistently detected in other *L. monocytogenes* species.

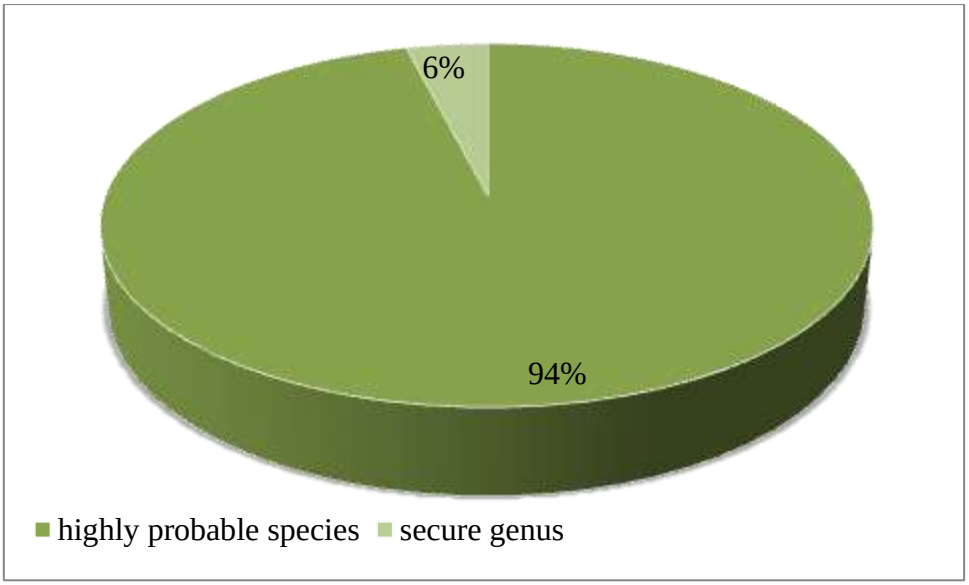

Figure 3.17. Pie chart showing the percentage of *Listeria* isolates identified in the MALDIbiotyper description; highly probable species and secure genus. A total of 30 (94%) *Listeria* isolates were correctly identified to the species level while 3 isolates (6%) were assigned conflicting species identification.

Table 3.4. Comparison of *Listeria spp.* score values whole cell smears and formic acid extracted proteins. The data shows that the score values increased as a result of performing formic acid extraction. This subsequently led to a a larger number of isolates being identified to species level.

Isolate	HP Sample Identification Code	Score (whole cell smears)	Score (formic acid extracted proteins)
L. monocytogenes	EGD-e	2.147	2.466
L. monocytogenes	NCTC 04885	2.174	2.337
L. monocytogenes	NCTC 04883	2.179	2.428
L. innocua	NCTC 11288	2.267	2.51
L. ivanovii subsp. ivanovii	NCTC 11846	2.167	2.336
L. grayi subsp murrayi	NCTC 10814	1.773	2.444
L. seeligeri	NCTC 11856	1.178	2.367
L. welshimeri	NCTC 11857	2.011	2.296

key:

high probable species identification	score 2.300-3000
secure identification	score 2.000-2.299
probable genus identification	1.700-1.999

As satisfactory species level identification was achieved, an attempt to further characterise *L. monocytogenes* strains was undertaken. An MSP dendrogram was generated using the MS profiles obtained from formic acid extractions. The result showed that *Listeria* isolates separated into two main clusters (Figure 3.18). The turquoise cluster contained *L. grayi* species only, while the red cluster contains all other species tested; *L. monocytogenes*, *L. innocua*, *L. grayi*, *L. ivanovii*, *L. seeliegeri* and *L. welshimeri* (a list of all isolates used to generate the MSP dendrogram can be found in section 2.8.5 of the Material and Methods section). The dendrogram in Figure 3.18 provided strong evidence to support the the use of MALDI-TOF-MS data for the further characterisation of *Listeria*. There was good congruence between the MSP dendrogram and the one generated using 16S rRNA data. Those species belonging to the red main cluster were further differentiated into 5 major clusters which will be further referred to as phena (Figure 3.19). Each phenon contained a mixture of isolates, that at this stage, did not cluster into separate phena. This suggests a large number of conserved ribosomal proteins amongst the species.

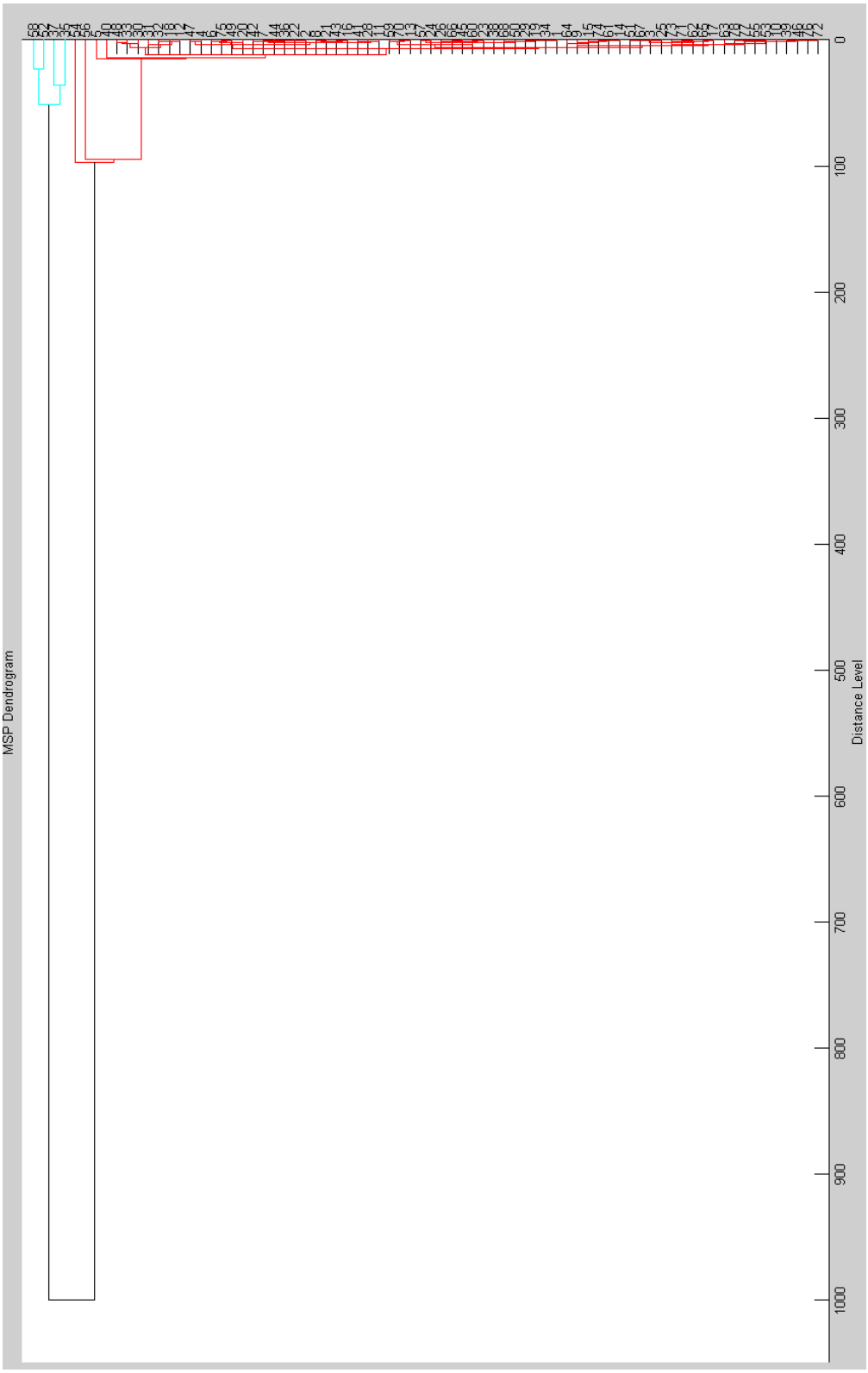

Figure 3.18. MSP Dendrogram of *Listeria spp.* obtained using MALDI-TOF-MS. The distance level is on the x-axis and isolates are on the y-axis. The dendrogram was generated by analysing the spectra of 78 isolates; *L. monocytogenes*, *L. ivanovii*, *L seeligeri*, *L.*

welshimeri, *L. innocua* and *L. grayi*. Each isolate is numbered for simplicity and the corresponding species name is recorded in Table 2.2. The turquoise cluster contained *L. grayi* species only, while the red cluster contains all other species. The dendrogram shows that whilst all species show correlation, *L. grayi* form a separate cluster at a distance level of 100.

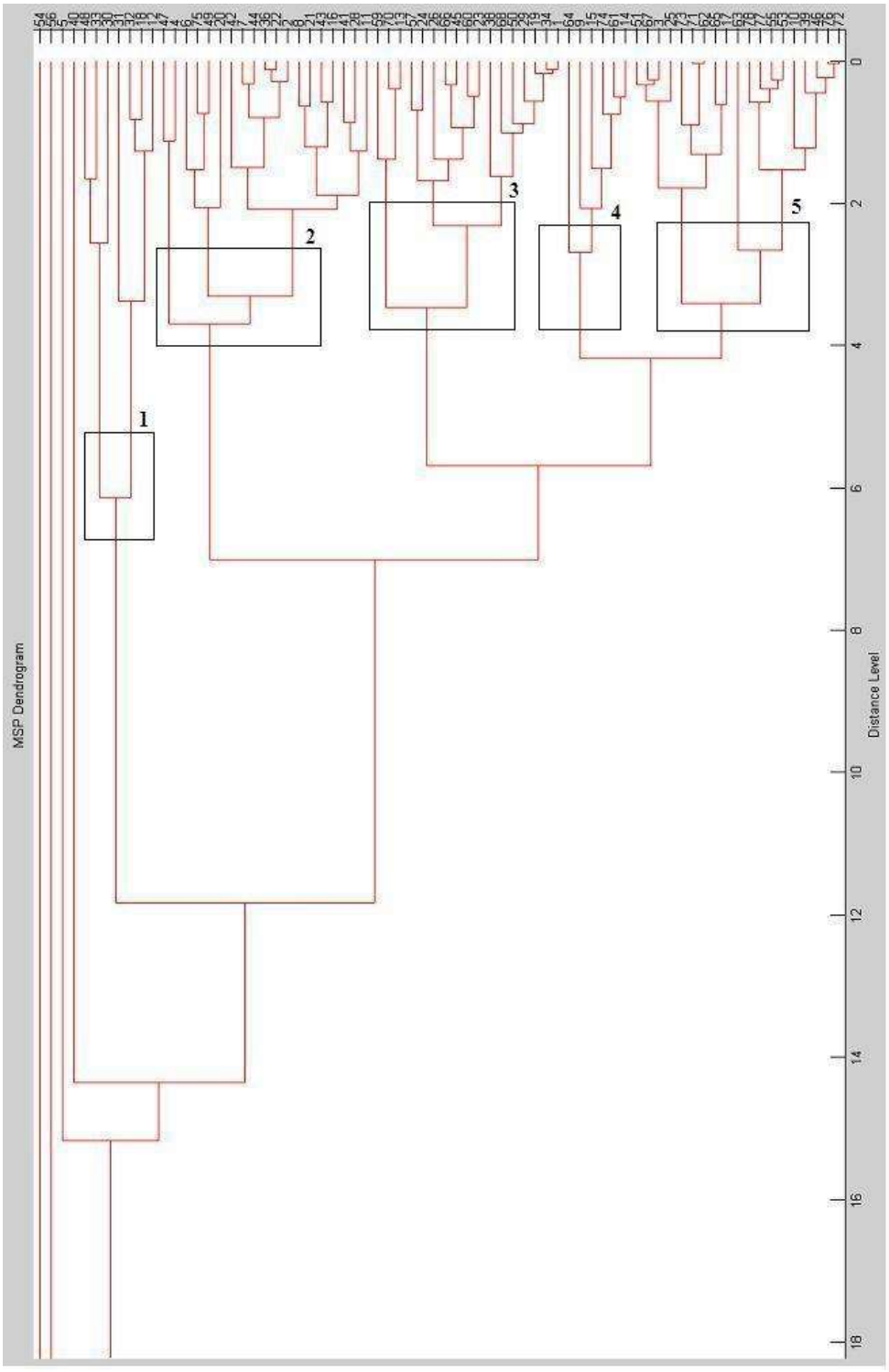

Figure 3.19. MSP Dendrogram of *Listeria spp.* obtained using MALDI-TOF-MS spectra (zoomed image of Figure 3.18), with distance level on the x-axis and isolates on the y-axis. The dendrogram was generated by analysing the spectra of 78 isolates; *L. monocytogenes*, *L. ivanovii*, *L seeligeri*, *L. welshimeri*, *L. innocua* and *L. grayi*. Each isolate is numbered for simplicity and the corresponding species name is recorded in Table 2.2. The 5 major identifiable phena are indicated by black boxes numbered 1-5. The dendrogram shows that

distance levels are relatively close, suggesting that a large number of conserved ribosomal proteins amongst the species.

3.3 Characterisation of *L. monocytogenes* using SELDI-TOF MS

SELDI-TOF-MS is an extension of MALDI-TOF-MS in which different classes of protein extracts are analysed. Ultimately profiles generated using SELDI-TOF-MS may also be used to generate MSP dendrograms and was executed in this study. SELDI-TOF-MS was explored in this study as an alternate method for the characterisation of *Listeria*. Whilst both MALDI-TOF-MS and SELDI-TOF-MS are able to detect proteins which may provide the basis for differentiation, in general former detects ribosomal proteins while the latter detects cytosolic proteins. As shown in the previous section, analysis of MSP dendrograms (derived from the analysis of MALDI-TOF-MS generated spectra) showed that results are comparable to dendrograms generated using 16S RNA data. Here comparability of SELDI-TOF-MS derived dendrograms is assessed.

Before characterisation, it was necessary to select the most appropriate ProteinChip Array. This was undertaken by testing *L. monocytogenes* F2365 and *L. monocytogenes* NCTC 10357 protein extracts, which were prepared from growth in BHI broth. The ProteinChips selected in this study were ProteinChip CM10, ProteinChip Q10 array and the ProteinChip H50 array, as they generally yield broader mass spectra. The chips were prepared using varing amounts of protein 150 - 1200 µg. This would enable the determination of the most suitable quantity of protein needed to obtain a larger number of peaks with high intensities. Initially 8 sets of stacked spectra were produced (Figure 3.20 - Figure 3.27). Using *L. monocytogenes* F2365 protein sample, the least number of peaks were dectected using the ProteinChip H50 array prepared with acetonitrile (Figure 3.22). The ProteinChip H50 array prepared with methanol, allowed detection of the largest number of peaks with the highest intensities (Figure 3.21). This is relative to Figures 3.20 and and Figure 3.23 which depicts proteins detected using ProteinChip CM10 and ProteinChip Q10 respectivley.

Visual inspection of results obtained using protein extracts from NCTC 10357, also showed that the least number of peaks were dectected using the ProteinChip H50 array prepared with acetonitrile (Figure 3.26). Further inspection showed that a large numbet of peaks were detected across all other chips: ProteinChip CM10 (Figure 3.24), ProteinChip H50, prepared using methanol (Figure 3.25) and ProteinChip Q10 (Figure 3.27). However, the results showed that in comparison to the ProteinChip CM10 and ProteinChip Q10 array, the ProteinChip H50 array prepared with methanol, led to the detection of the greatest number of

protein peaks. For ease of comparison a separate image was generated, see Figure 3.28. This image is a composite of results obtained as a result of applying 600 µg of NCTC 10357 protein extract to ProteinChip CM10 array (Figure 3.24), ProteinChip H50 array , prepared with methanol (Figure 3.25) and ProteinChip Q10 array (Figure 3.27).

According to the ProteinChip® instruction manuals the recommended maximum amount of protein that should be used is 350 µg, however, results show that for *Listeria spp.* this concentration needs to be greater and for ProteinChip H50 array in particular this is almost double (ca 600 µg). Also, at 600 µg the intensity of the peaks were greater, therefore using a higher amount of protein could offer a greater chance of detecting more peaks (Figure 3.28). The H50 ProteinChip array was therefore selected for further use in this study using 600 µg of protein extracts prepared from BHI broth and using 50% methanol as the binding buffer.

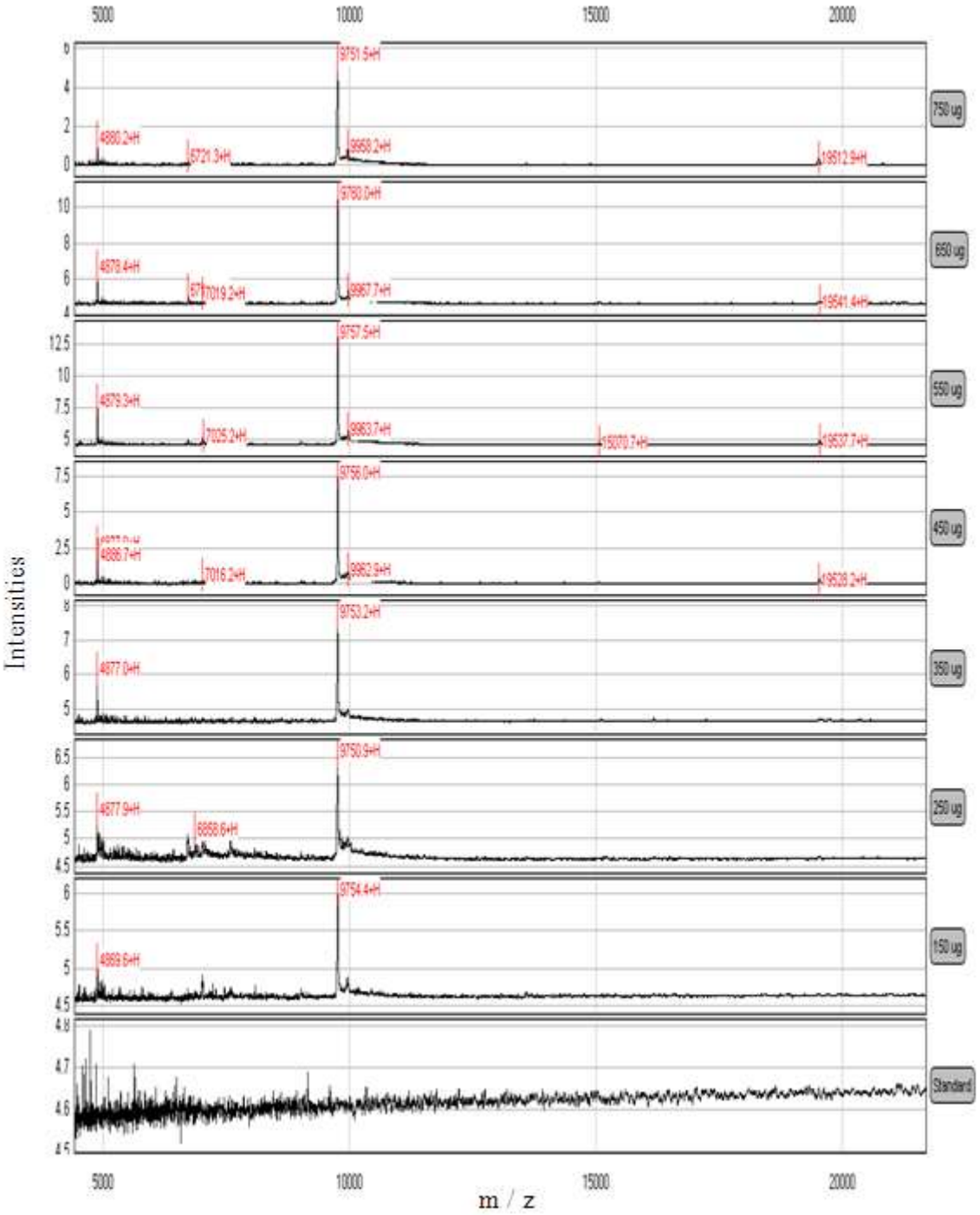

Figure 3.20. Ions detected on a ProteinChip CM10 array using *L. monocytogenes* F2365 protein extracts. The chip allows simultaneous processing of 8 samples and the data are therefore presented as 8 stacked spectra. The identity of each sample is noted at the end of each spectrum. From top to bottom they include 750 µg, 650 µg, 550 µg, 450 µg, 350 µg, 250 µg and 150 µg of protein and the Bio-Rad Standard was applied to the 8th spot. The image shows peak intensity (y-axis) versus m/z (x-axis).

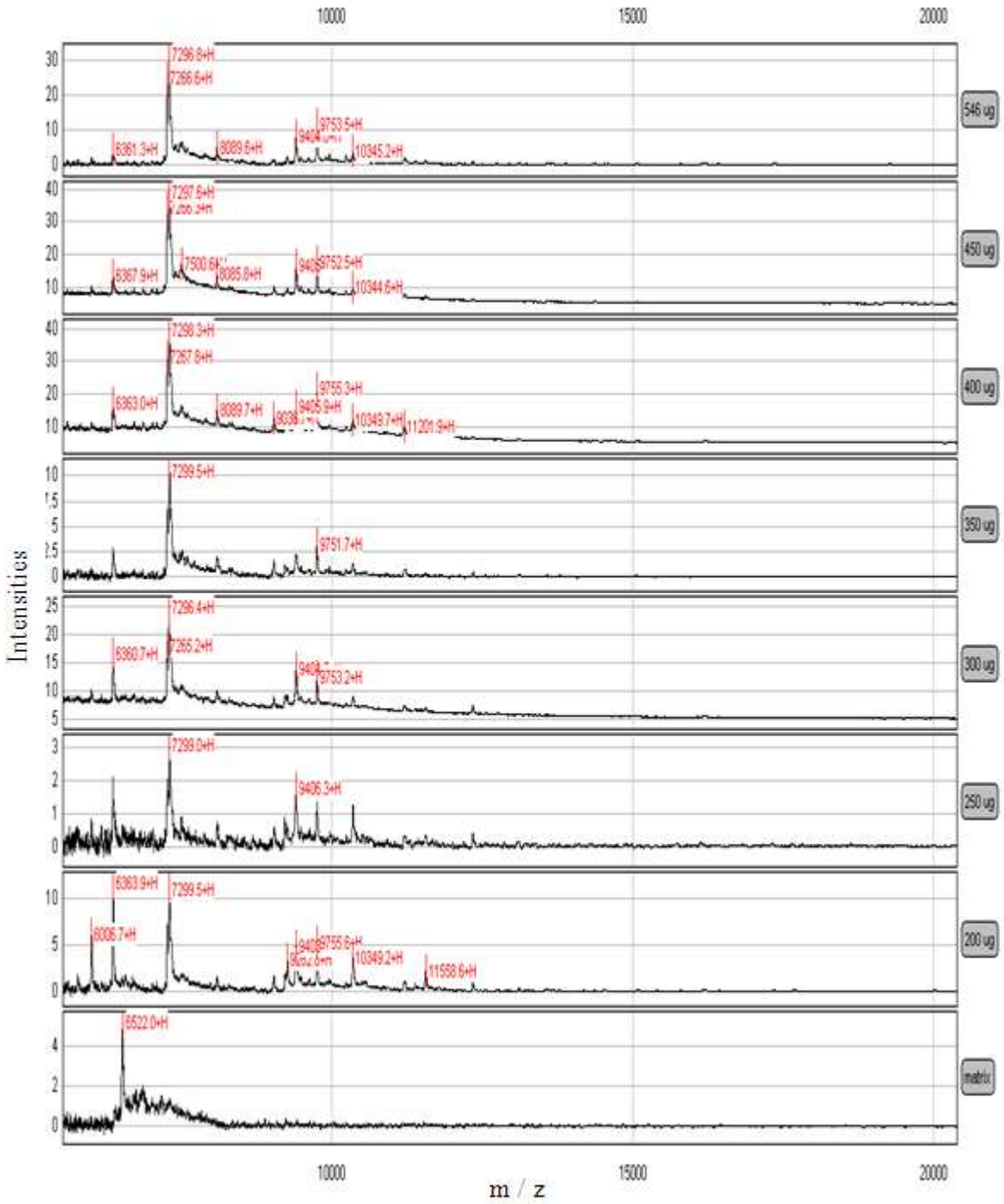

Figure 3.21. Ions detected on a ProteinChip H50 array which was prepared using methanol and *L. monocytogenes* F2365 protein extracts. The chip allows simultaneous processing of 8 samples and the data are therefore presented as 8 stacked spectra. The identity of each sample is noted at the end of each spectrum. From top to bottom they include 546 µg, 450 µg, 400 µg, 350 µg, 300 µg, 250 µg and 200 µg of protein was used to generate the spectra, and the Bio-Rad matrix solution was applied to the 8th spot. The image shows peak intensity (y-axis) versus m/z (x-axis).

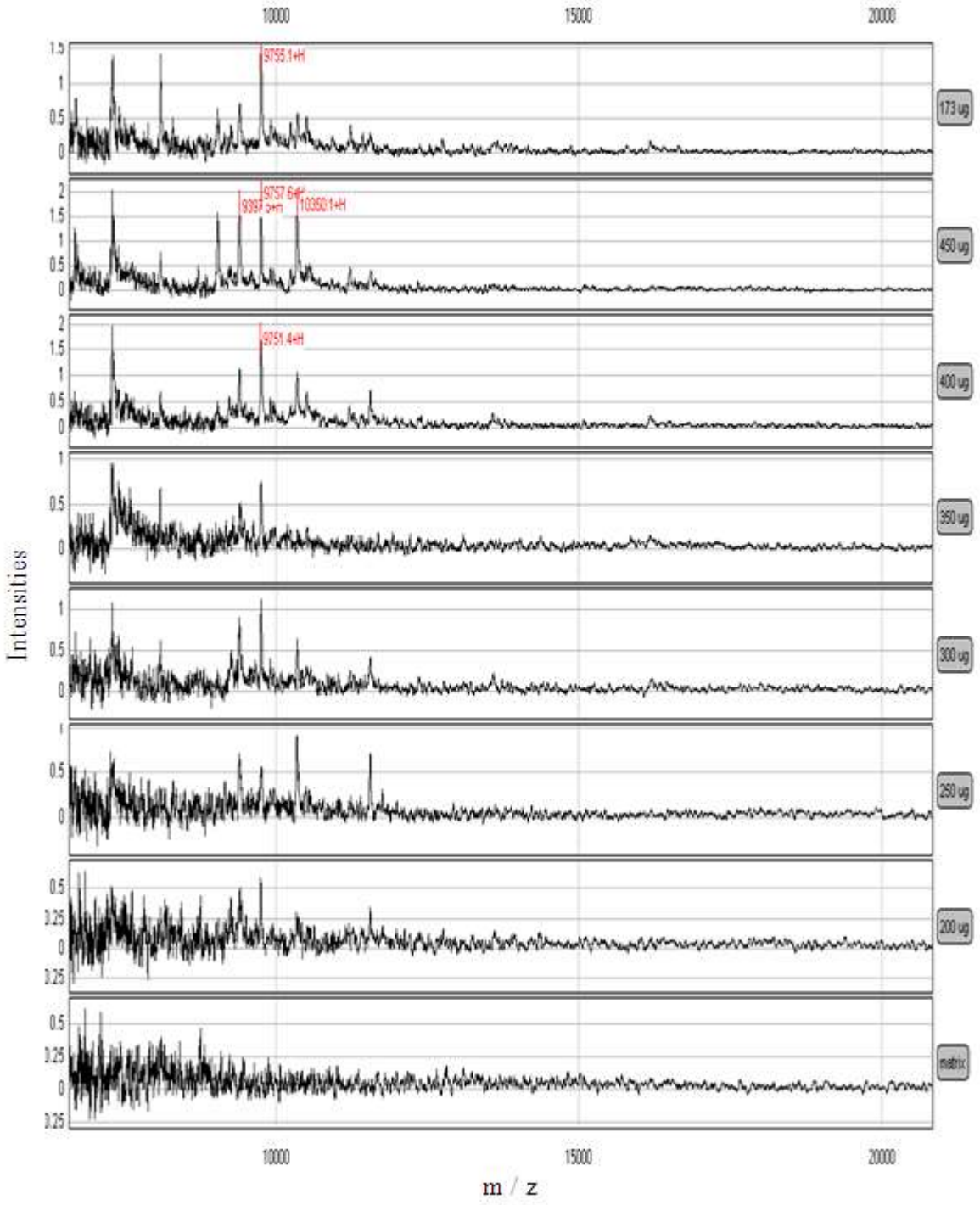

Figure 3.22. Ions detected on a ProteinChip H50 array which was prepared using acetonitrile and *L. monocytogenes* F2365 protein extracts. The chip allows simultaneous processing of 8 samples and the data are therefore presented as 8 stacked spectra. The identity of each sample is noted at the end of each spectrum. From top to bottom they include 173 µg, 450 µg, 400 µg, 350 µg, 300 µg, 250 µg and 200 µg of protein and the Bio-Rad matrix solution was applied to the 8th spot. The image shows peak intensity (y-axis) versus m/z (x-axis).

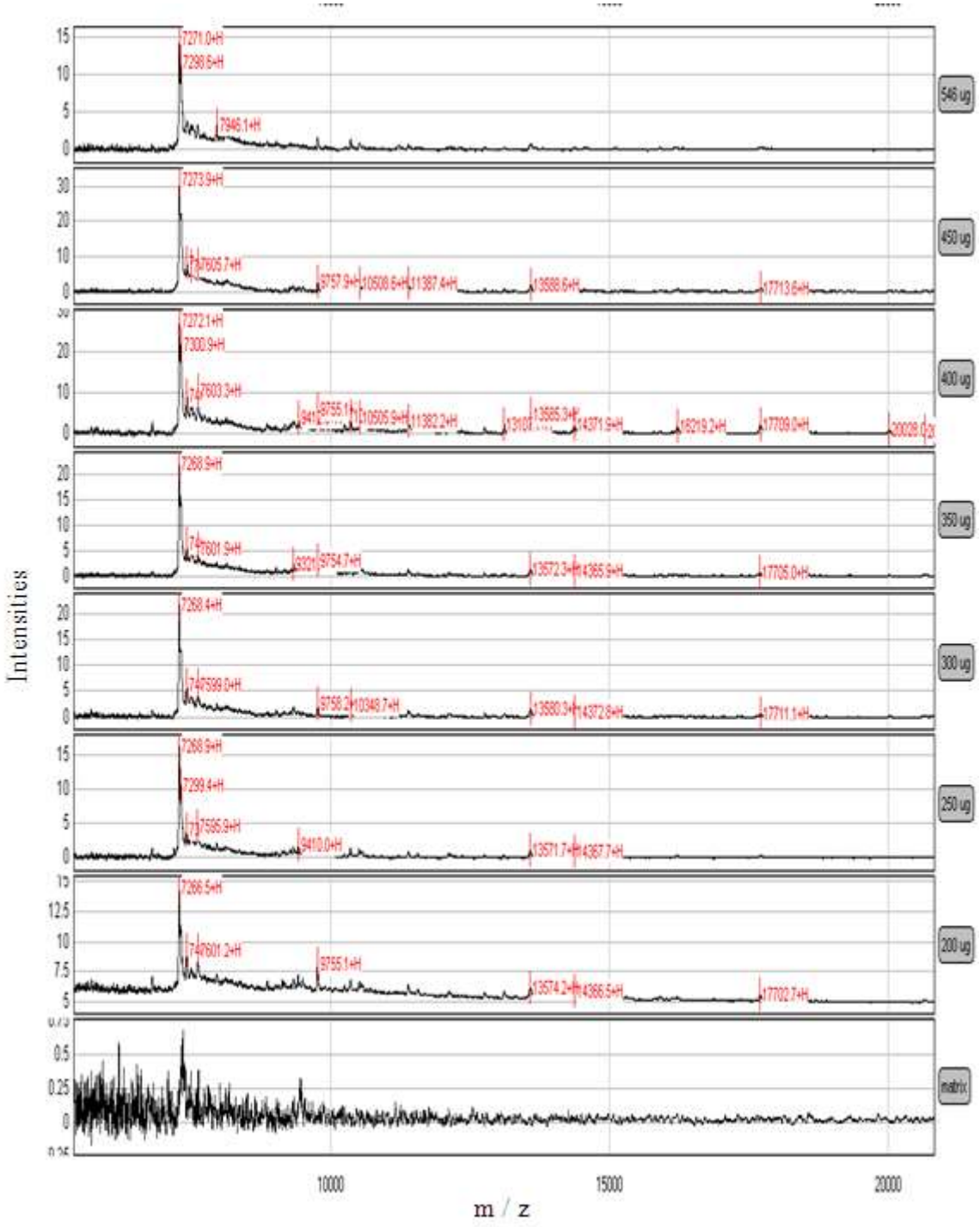

Figure 3.23. Ions detected on a ProteinChip Q10 array which was prepared using and *L. monocytogenes* F2365 protein extracts. The chip allows simultaneous processing of 8 samples and the data are therefore presented as 8 stacked spectra. The identity of each sample is noted at the end of each spectrum. From top to bottom they include 546 µg, 450 µg, 400 µg, 350 µg, 300 µg, 250 µg and 200 µg of protein and the Bio-Rad matrix solution was applied to the 8th spot. The image shows peak intensity (y-axis) versus m/z (x-axis).

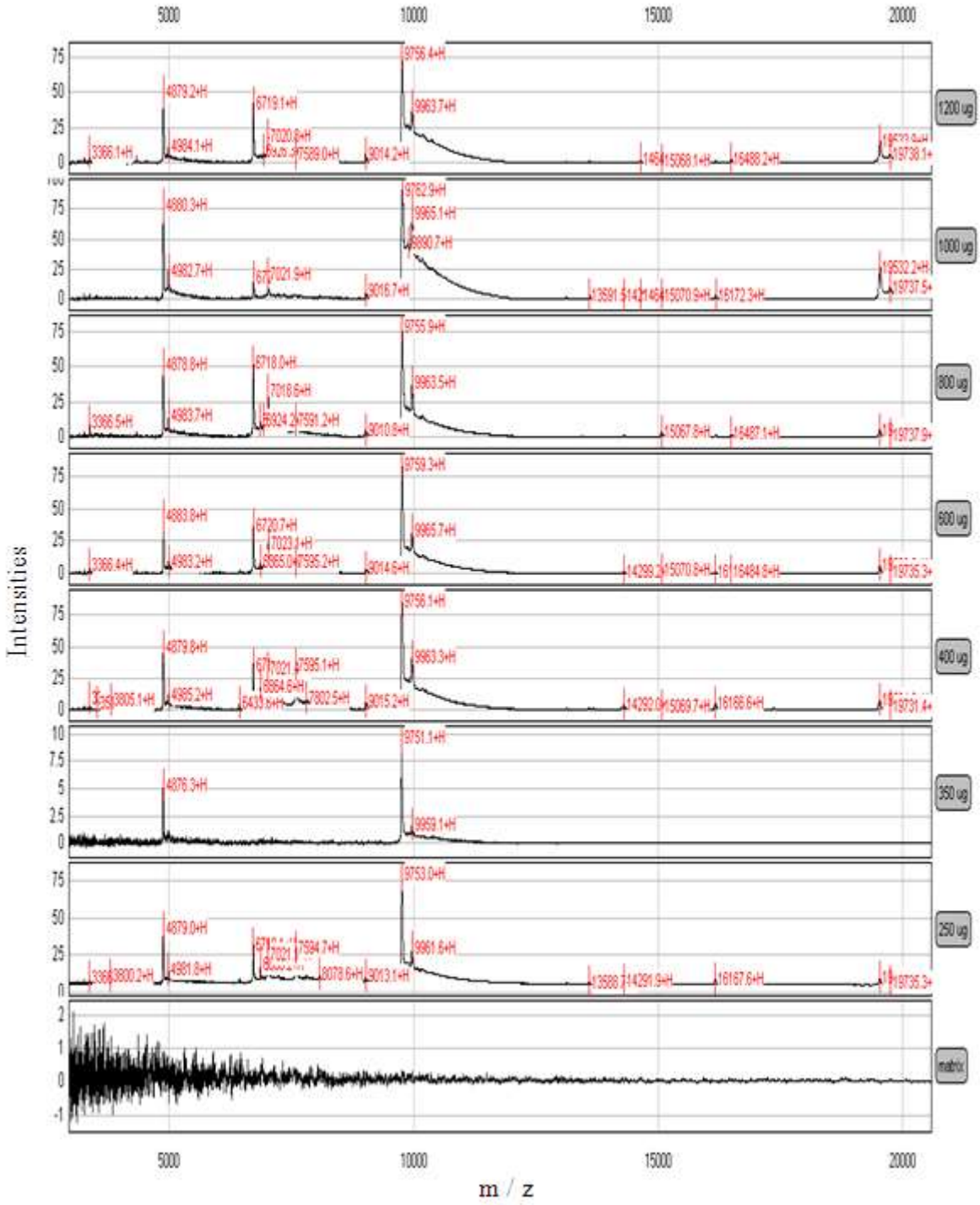

Figure 3.24. Ions detected on a ProteinChip CM10 array which was prepared using and *L. monocytogenes* NCTC 10357 protein extracts. The chip allows simultaneous processing of 8 samples and the data are therefore presented as 8 stacked spectra. The identity of each sample is noted at the end of each spectrum. From top to bottom they include 1200 µg, 1000 µg, 800 µg, 600 µg, 400 µg, 350 µg and 250 µg of protein and the Bio-Rad matrix solution was applied to the 8th spot. The image shows peak intensity (y-axis) versus m/z (x-axis).

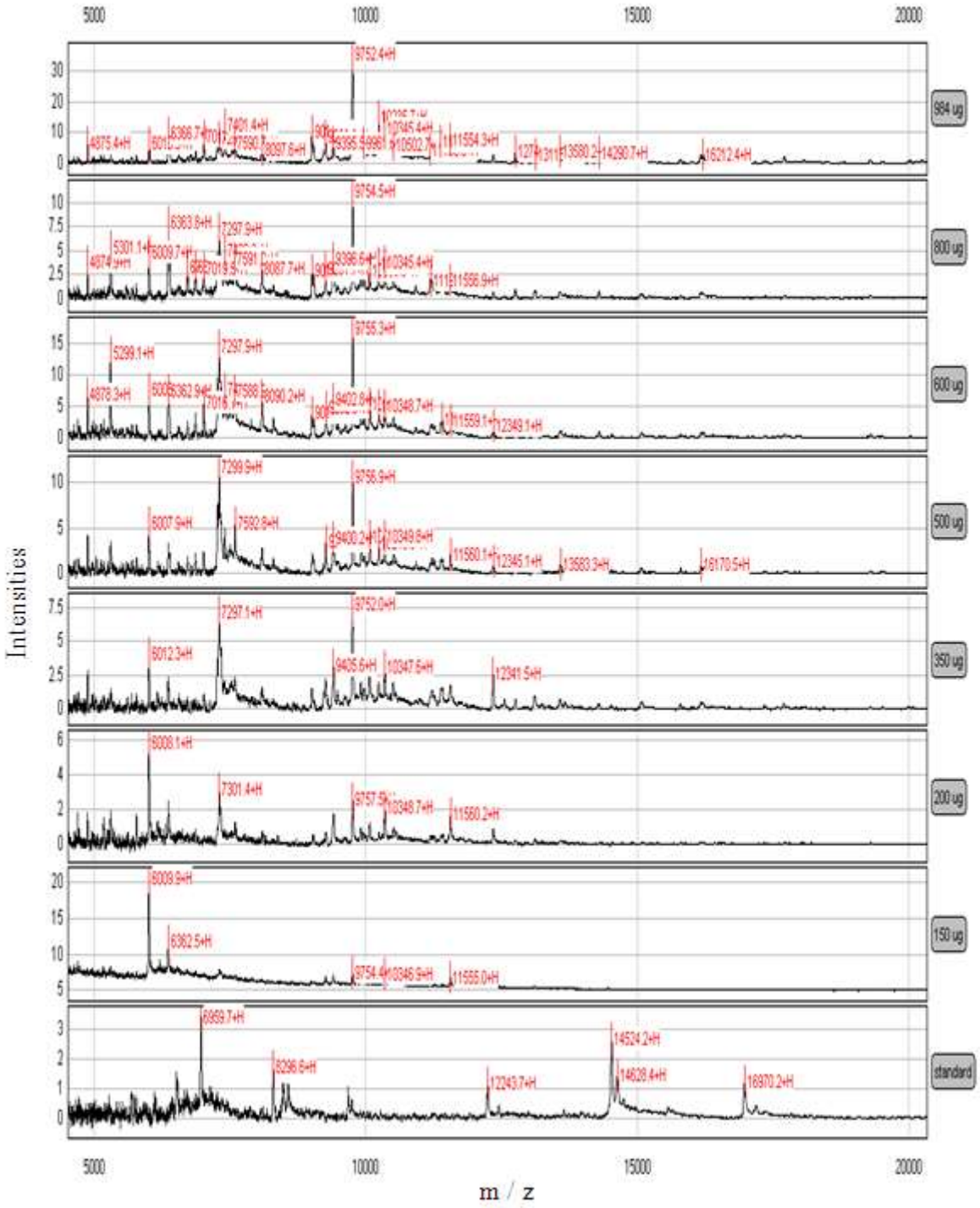

Figure 3.25. Ions detected on a ProteinChip H50 array which was prepared using methanol and *L. monocytogenes* NCTC 10357 protein extracts. The chip allows simultaneous processing of 8 samples and the data are therefore presented as 8 stacked spectra. The identity of each sample is noted at the end of each spectrum. From top to bottom they include 984 µg, 800 µg, 600 µg, 500 µg, 350 µg, 200 µg and 150 µg of protein and the Bio-Rad standard solution was applied to the 8th spot. The image shows peak intensity (y-axis) versus m/z (x-axis).

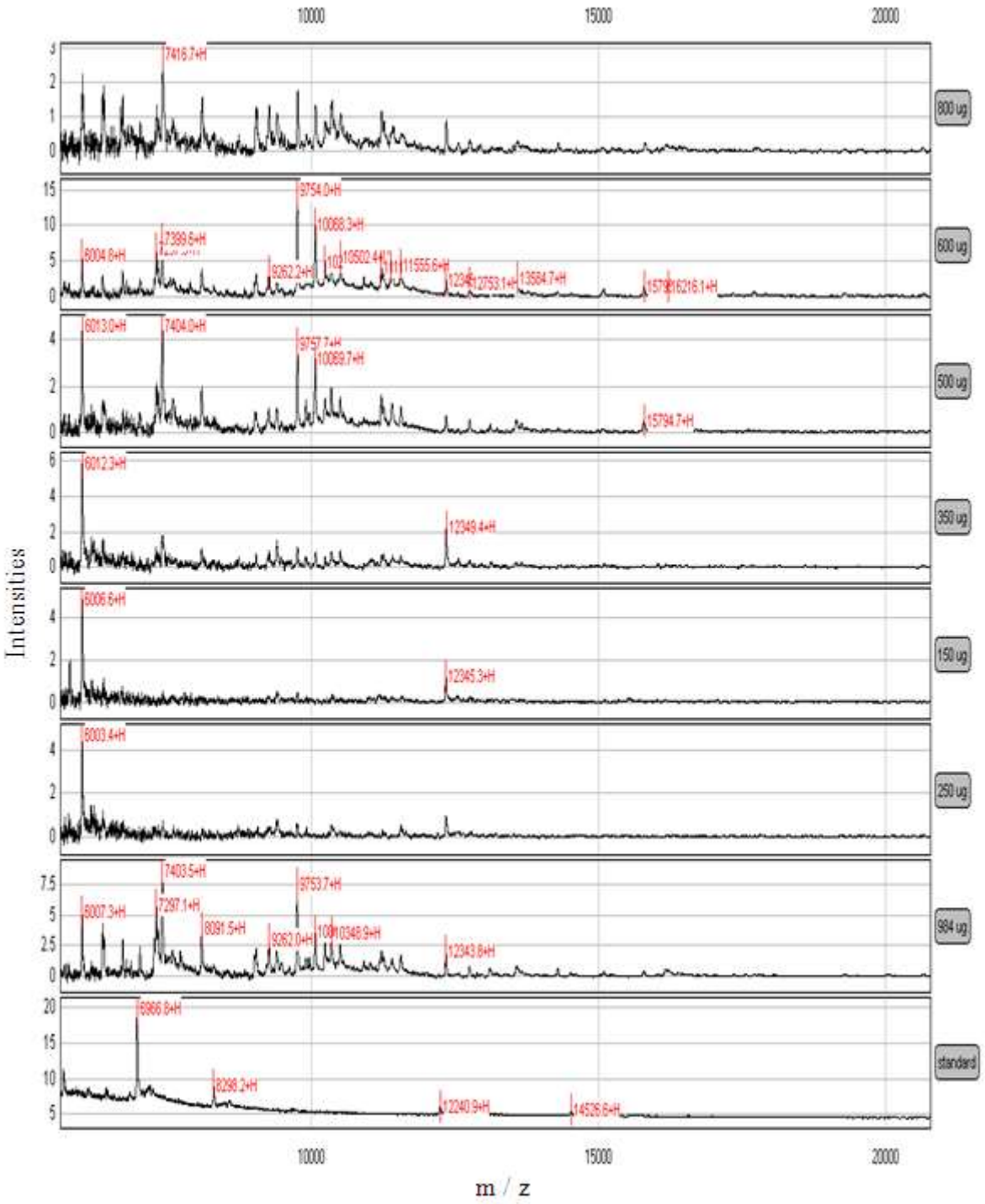

Figure 3.26. Ions detected on a ProteinChip H50 array which was prepared using acetonirile and *L. monocytogenes* NCTC 10357 protein extracts. The chip allows simultaneous processing of 8 samples and the data are therefore presented as 8 stacked spectra. The identity of each sample is noted at the end of each spectrum. From top to bottom they include 800 µg, 600 µg, 500 µg, 350 µg, 150 µg, 250 µg and 984 µg of protein and the Bio-Rad standard solution was applied to the 8th spot. The image shows peak intensity (y-axis) versus m/z (x-axis)

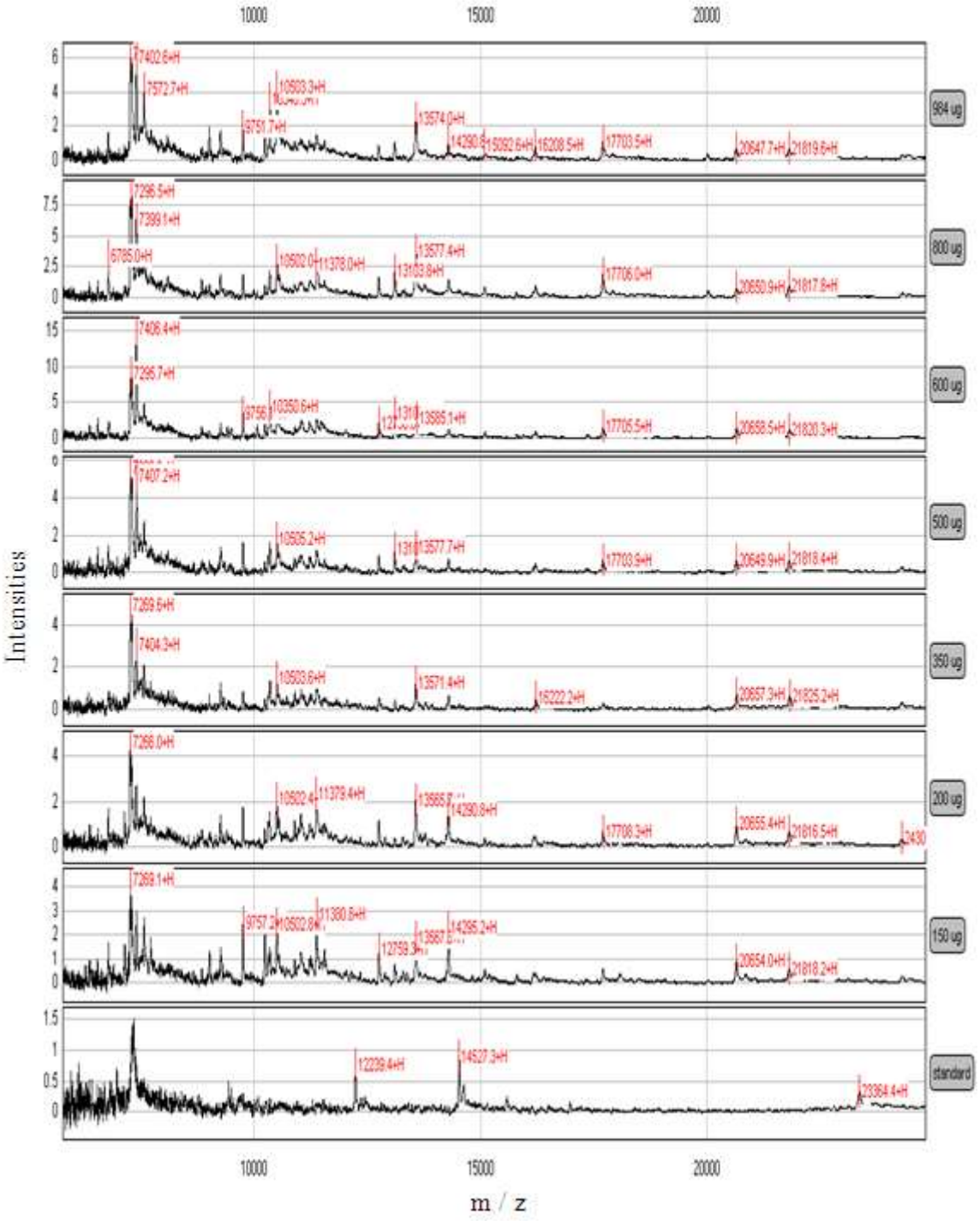

Figure 3.27. Ions detected on a ProteinChip Q10 array which was prepared using acetonirile and *L. monocytogenes* NCTC 10357 protein extracts. The chip allows simultaneous processing of 8 samples and the data are therefore presented as 8 stacked spectra. The identity of each sample is noted at the end of each spectrum. From top to bottom they include 984 µg, 800 µg, 600 µg, 500 µg, 350 µg, 200 µg and 150 µg of protein and the Bio-Rad standard solution was applied to the 8th spot. The image shows peak intensity (y-axis) versus m/z (x-axis).

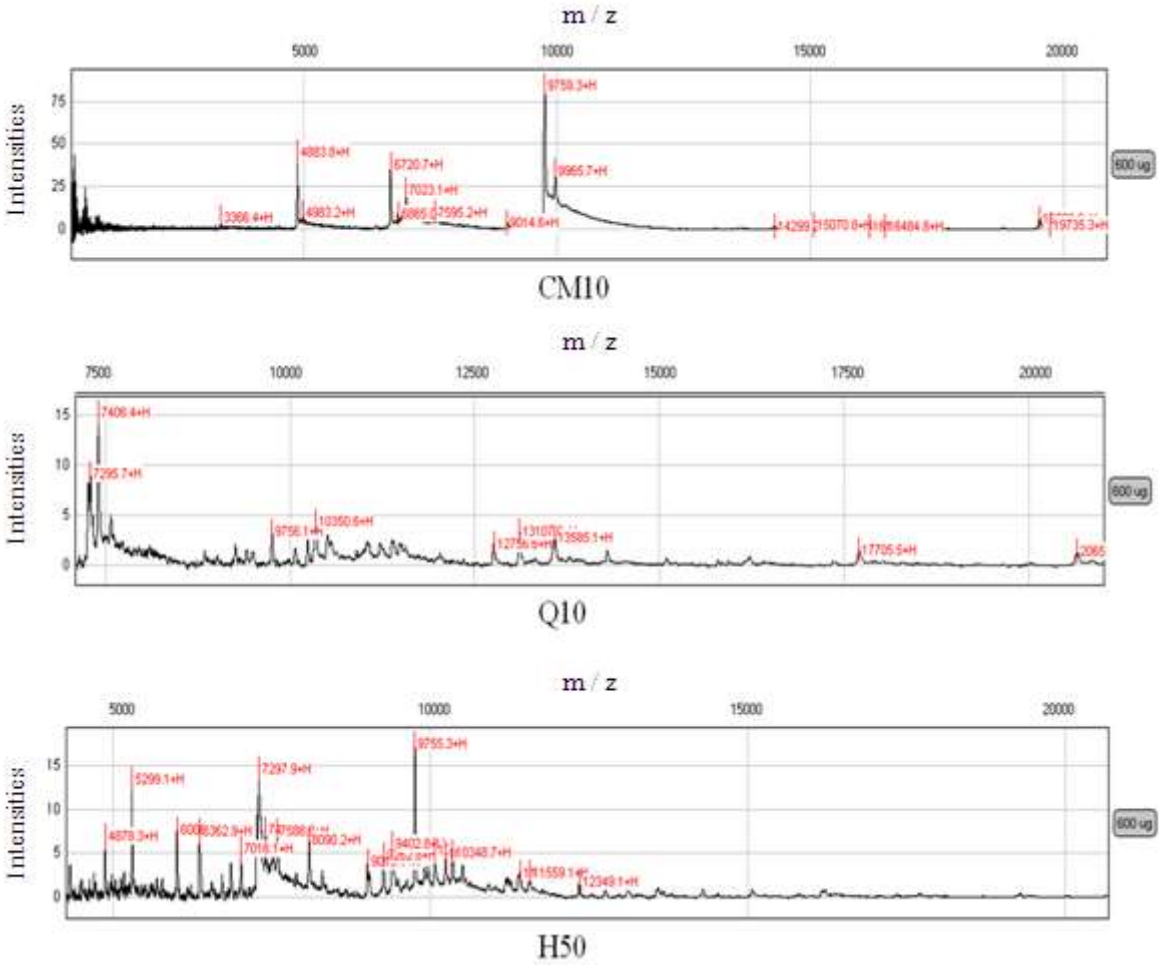

Figure 3.28. A comparison of *L. monocytogenes* NCTC 10357 proteins bound to a spot on a ProteinChip CM10 array (top spectra), ProteinChip Q10 array (middle spectra) and a ProteinChip H50 arrays. The data was pulled from Figure 3.24, Figure 3.25 and Figure 3.27 respectivley and shows peak intensity (y-axis) versus m/z ratio (x-axis). The amount of protein used was 600 µg. Visual inspection shows that a larger number of peaks were detected using the ProteinChip H50 array, whilst the ProteinChip CM10 array detected peaks at higher intensities.

A total of 30 isolates were selected for analysis on the ProteinChip H50 array. The results obtained were poor, in that, either insufficient peaks as seen in Figure 3.29 or no peaks were detected as in seen in Figure 3.30. This observation is relative to Figure 3.28 in which inspection of the ProteinChip H50 array shows a large numbe of peaks. This was an unexpected result and an investigation was carried out to access the quality of the protein extracts. The quality was assessed by separating all 30 of the protein samples on a 1-D SDS gel. The results showed that the protein extracts were not degraded as degradation would have appeared as smearing in the lanes (Figure 3.31 illustrates 8 of the 30 protein extracts). This therefore eliminated sample quality as the cause of poor MS spectra. In addition to demonstrating protein quality the gel also demonstrated the diversity among the species as there were several bands which were present in some isolates and absent in others. This result was a preliminary and positive indication of the diversity that may be detected in much greater detail. The SELDI-TOF-MS data was visualized using heat maps to enable comparative expression between strains (Figure 3.31).

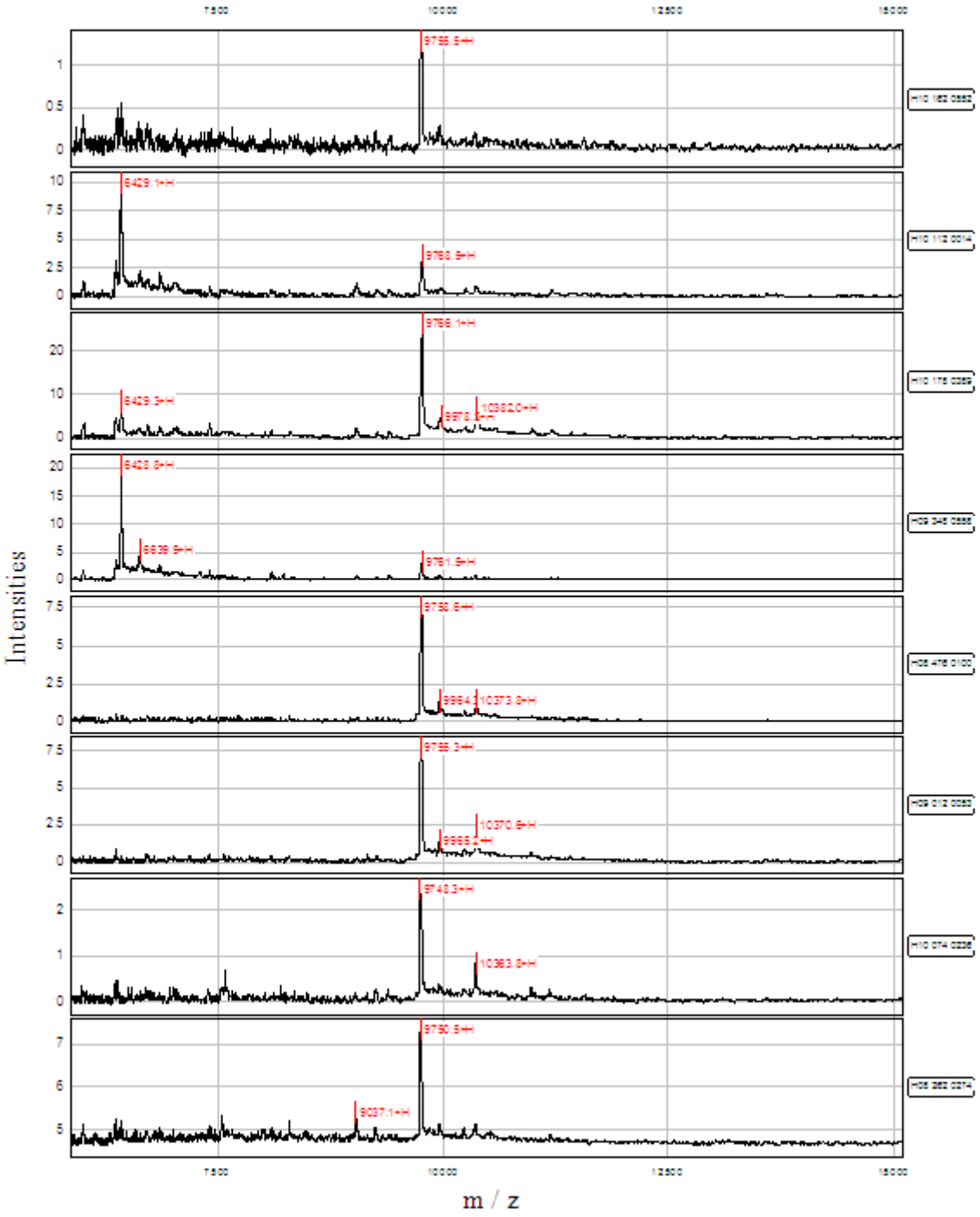

Figure 3.29. Ions detected on a ProteinChip H50 array which was prepared using methanol and 600 µg of various *L. monocytogenes* protein extracts. The chip allows simultaneous processing of 8 samples and the data are therefore presented as 8 stacked spectra. The identity of each sample is noted at the end of each spectrum. From top to bottom they include isolates H10 162 0552, H10 112 0014, H10 178 0389, H09 348 0558, H08 476 0100, H09 012 0053, H10 074 0236 and H08 262 0274. The image shows peak intensity (y-axis) versus m/z (x-axis).

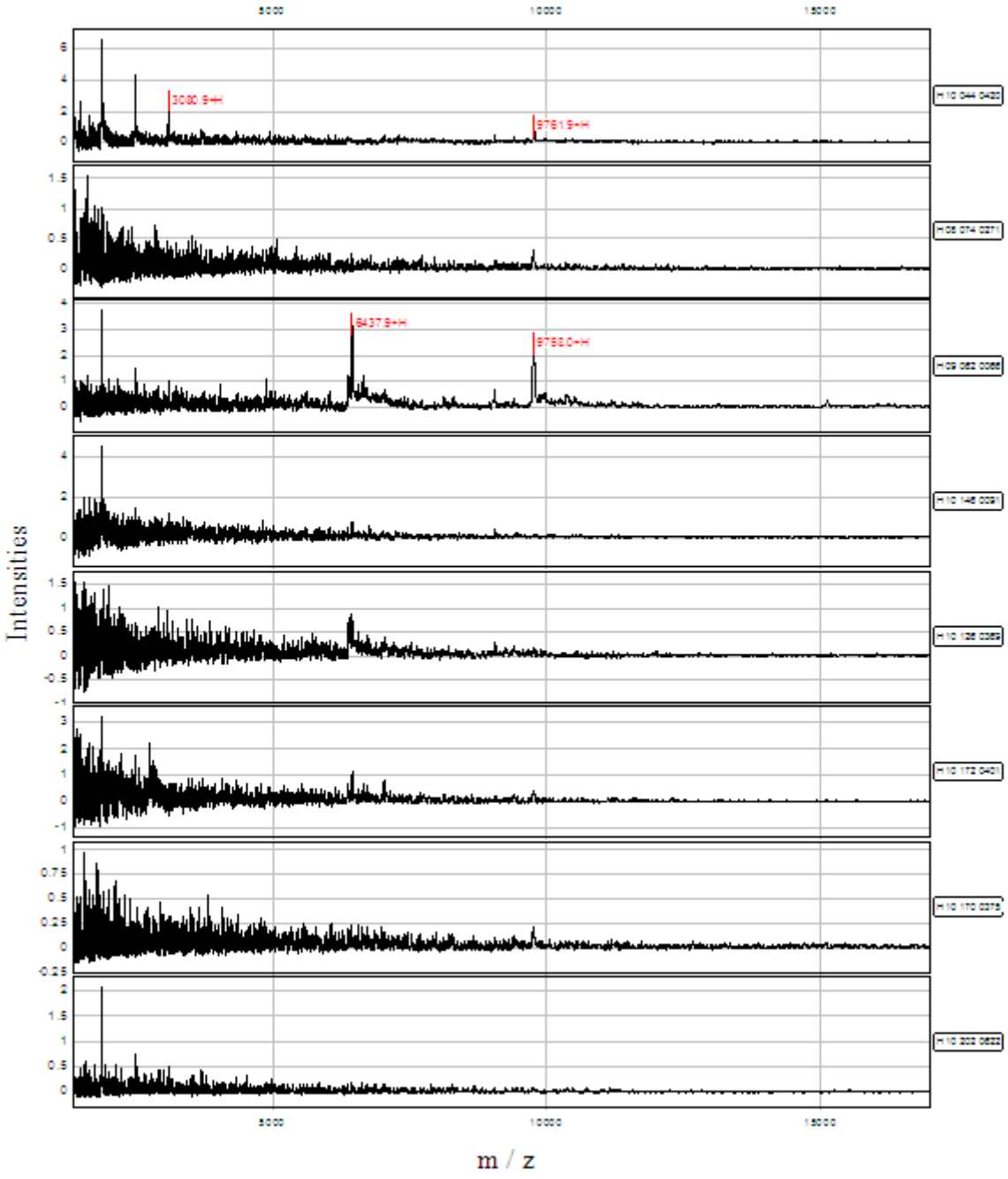

Figure 3.30. Ions detected on a ProteinChip H50 array which was prepared using methanol and 600 µg of various *L. monocytogenes* protein extracts. The chip allows simultaneous processing of 8 samples and the data are therefore presented as 8 stacked spectra. The identity of each sample is noted at the end of each spectrum. From top to bottom they include isolates H10 044 0420, H10 074 0271, H09 062 0066, H10 146 0091, H10 126 0369, H10 172 0401, H09 170 0375 and H10 202 0622. The image shows peak intensity (y-axis) versus m/z (x-axis).

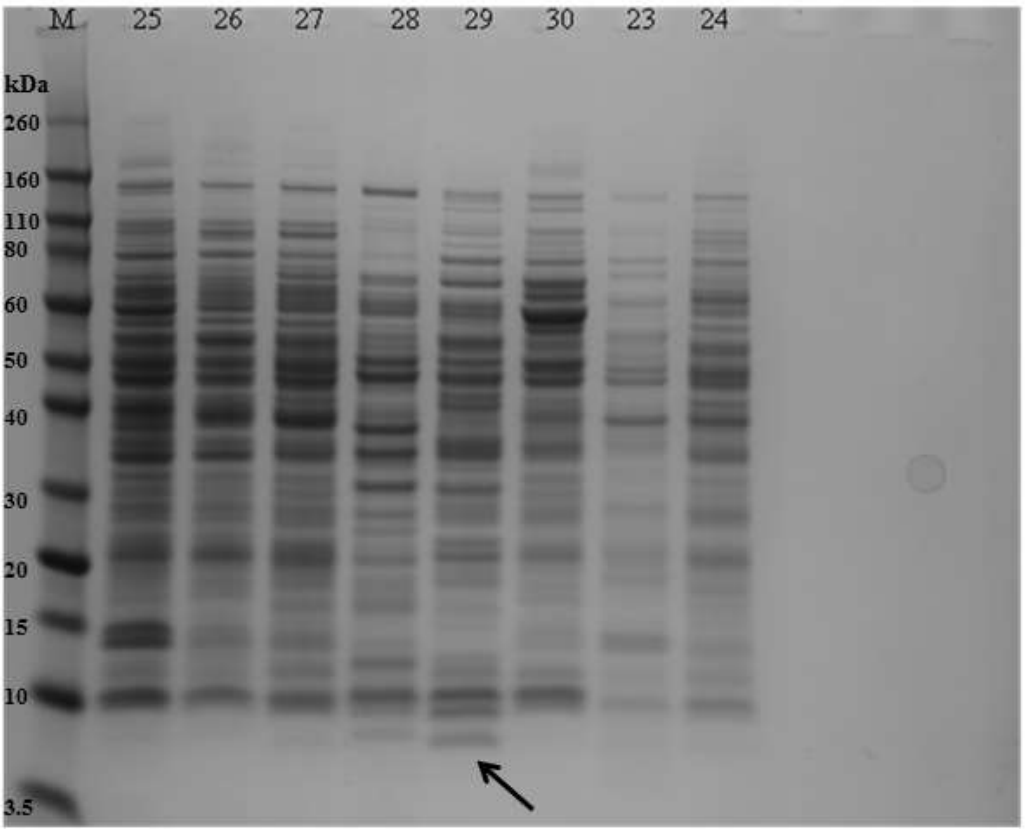

Figure 3.31. One-dimensional SDS PAGE analysis of 5 µg protein extracts of *Listeria* and *Brochothrix* species. Lane M shows the protein marker, Lane 25 - NCTC 11288 (*L. innocua*), 26 - NCTC 11846 (*L. ivanovii* subsp *ivanovii*), 27 - NCTC 11856 (*L. seeligeri*), 28 - NCTC 11857 (*L. welshimeri*), 29 - DSM 4712 (*B. campestris*), 30 - DSM 20171 (*B. thermosphacta*), 23 - NCTC 10890 (*L. monocytogenes*) and 24 - NCTC 10815 (*L. gray*i subsp *grayi*). The protein profiles show the diversity among the species as there were several bands which were present in some isolates and absent in others. An example is the protein band in the 3.5 - 10 kDa marker region which is present in lane 29 (indicated by black arrow) and absent in lanes 25, 26, 30 and 23.

It was considered that the quality of the remaining ProteinChip H50 arrays were poor as results from other in-house laboratory projects showed that the ProteinChip CM10 arrays produced good quality spectra. As a result of limited resources the ProteinChips H50 arrays were not replaced and analysis was continued using ProteinChips CM10 arrays and established in-house protocols. This involved manual spotting, using a smaller amount of protein (6 μg) which was harvested from isolates grown on BN agar, and a different buffer composition (25 mM ammonium acetate/0.01% Triton). In an initial test, extracts obtained from growth in BHI broth and BN agar produced good quality spectra with peak intensities up to 40 units (Figure 3.32). Comparison of peak intensities showed that ProteinChip CM10 arrays produced higher mass abundance intensities than ProteinChip H50 array results depicted in Figure 3.21 and Figure 3.25. Spectra corresponding to isolates grown on BN agar produced a mass spectrum ranging from approximately 15 - 17 kDa which were absent from spectra corresponding to isolates grown in BHI broth (indicated by green arrows on Figure 3.33). Based on these results the 30 isolates were retested using extracts obtained from BN plates. These spectra were of good quality, with the majority of peaks detected ranging from approximately 5 - 22 kDa (Figures 3.34 - 3.37). The results also showed that the data was reproducible as spectra corresponding to isolates H10 162 0552, NCTC 10357, *L. monocytogenes* F2365 and H10 146 0091 (Figure 3.33) were similar when re-analysed (Figures 3.34 - 3.37).

Evidence of experimental control is depicted in Figure 3.38. In this figure the negative control is the lower spectra. A solution containing matrix only was applied to this spot of the ProteinCip CM10 array. Due to the absence of protein in this sample the result was as expected and no ions were detected. On the other hand the upper spectra of Figure 3.38 showed that ions were detected using the molecular weight standard obtained from Bio-Rad which served as a positive control.

As reproducible data for all 30 isolates was satisfactorily produced and with evidence of successful controls, the subsequent stage of using the spectra to construct a dendrogram was carried out. This was achieved using the spectra in Figures 3.34 - 3.37.

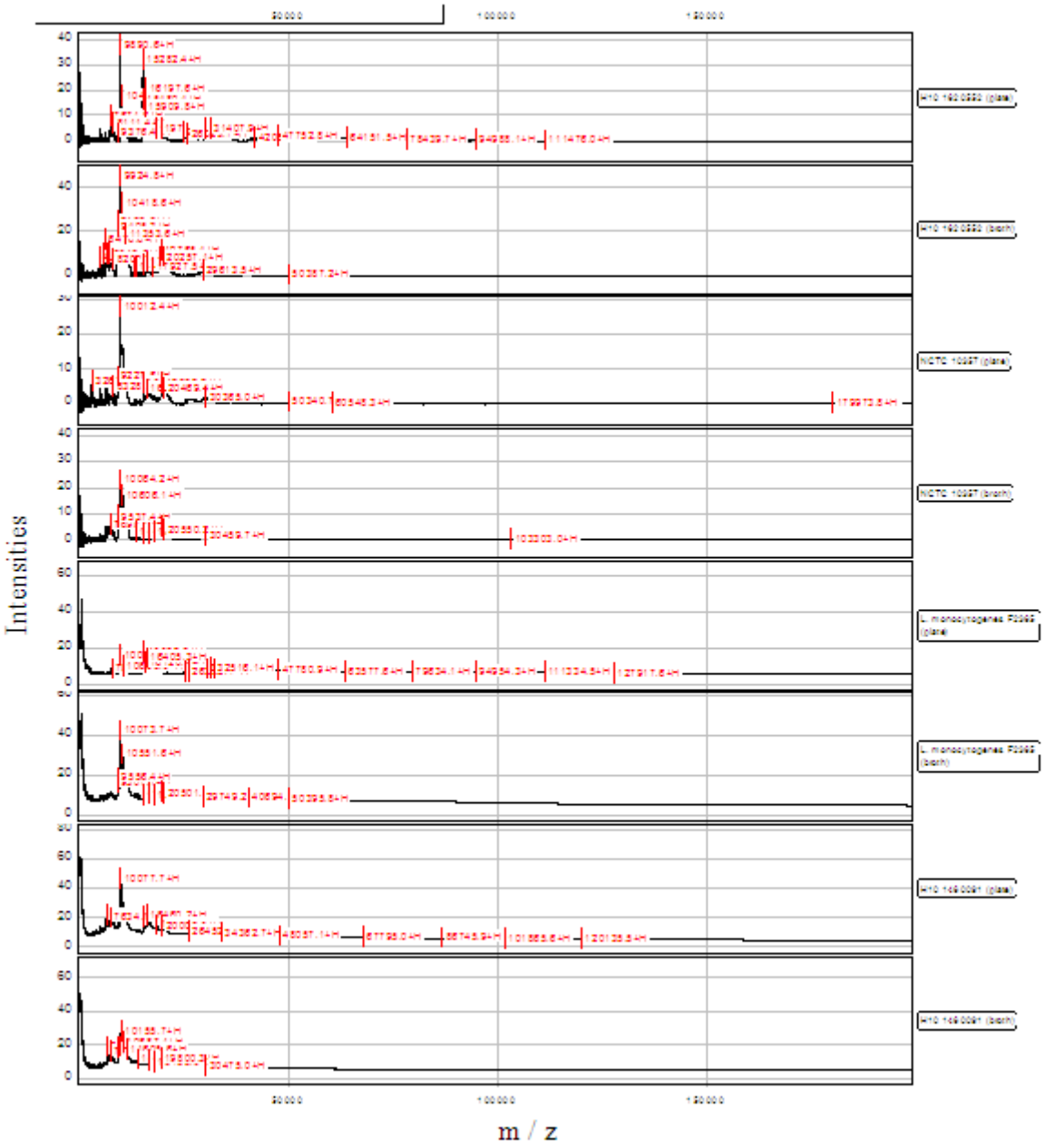

Figure 3.32. Ions detected on a ProteinChip CM10 array which was prepared by manual spotting using 6 µg of various *L. monocytogenes* protein extracts obtained from BHI broth and BN agar plate cultures. The chip allows simultaneous processing of 8 samples and the data are therefore presented as 8 stacked spectra. The identity of each sample is noted at the end of each spectra. From top to bottom they include isolates H10 162 0552 (from plate), H10 162 0552 (from broth), NCTC 10357 (from plate), NCTC 10357 (from broth), *L. monocytogenes* (from plate), *L. monocytogenes* (from broth), H10 146 0091 (from plate) and H10 146 0091 (from broth). The image shows peak intensity (y-axis) versus m/z (x-axis).

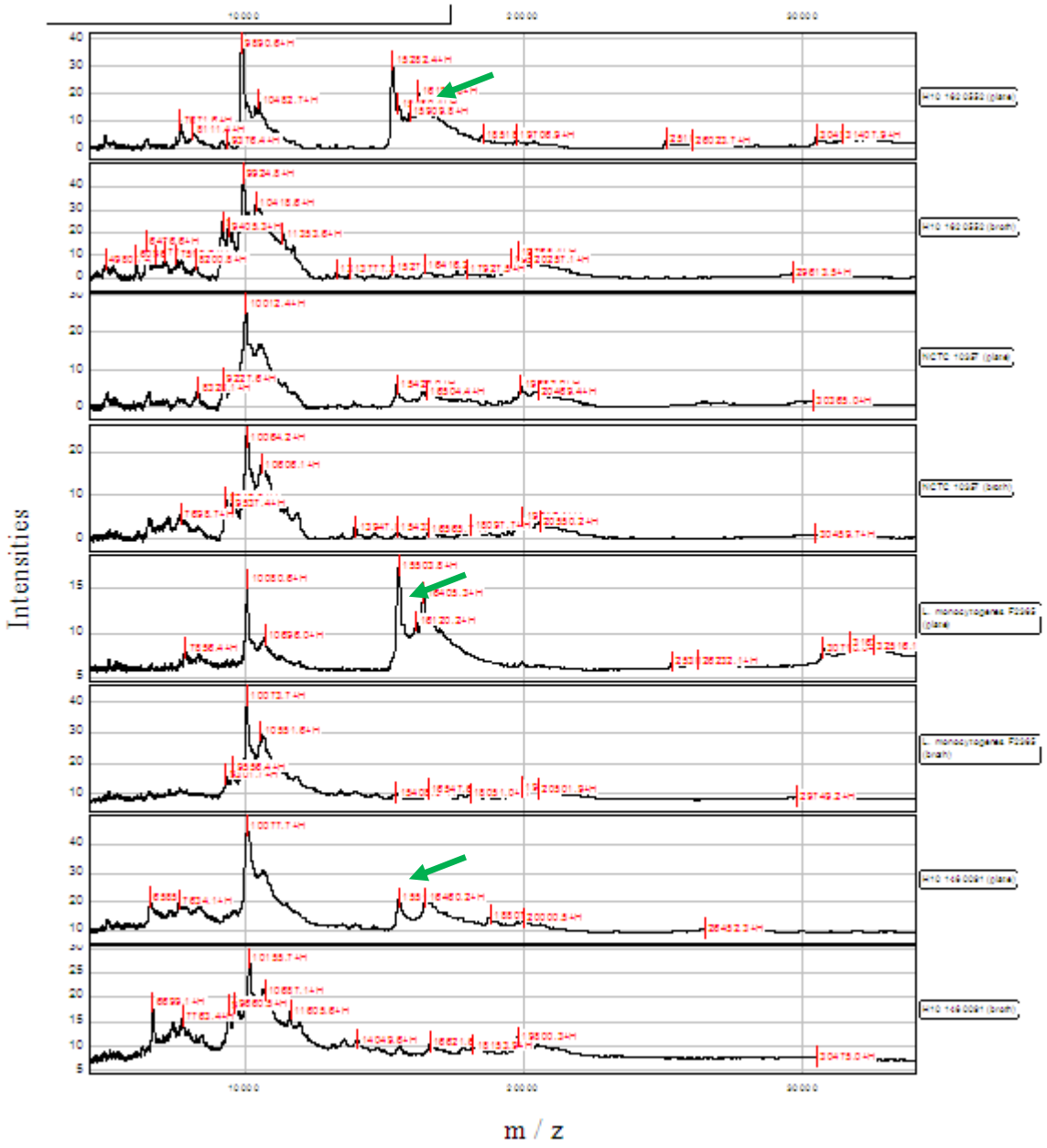

Figure 3.33. Ions detected on a ProteinChip CM10 array which was prepared by manual spotting using 6 µg of various *L. monocytogenes* protein extracts obtained from BHI broth and BN agar plate cultures. The chip allows simultaneous processing of 8 samples and the data are therefore presented as 8 stacked spectra. The identity of each sample is noted at the end of each spectra. From top to bottom they include isolates H10 162 0552 (from plate), H10 162 0552 (from broth), NCTC 10357 (from plate), NCTC 10357 (from broth), *L. monocytogenes* F2365 (from plate), *L. monocytogenes* F2365 (from broth), H10 146 0091 (from plate) and H10 146 0091 (from broth). The image is a zoomed version of Figure 3.32 between the 0-35000 Da region. The image shows peak intensity (y-axis) versus m/z (x-axis).

Green arrows indicate ions ranging from approximately 15 - 17 kDa which are present in samples obtained from growth on plate which are absent from samples derived from broth.

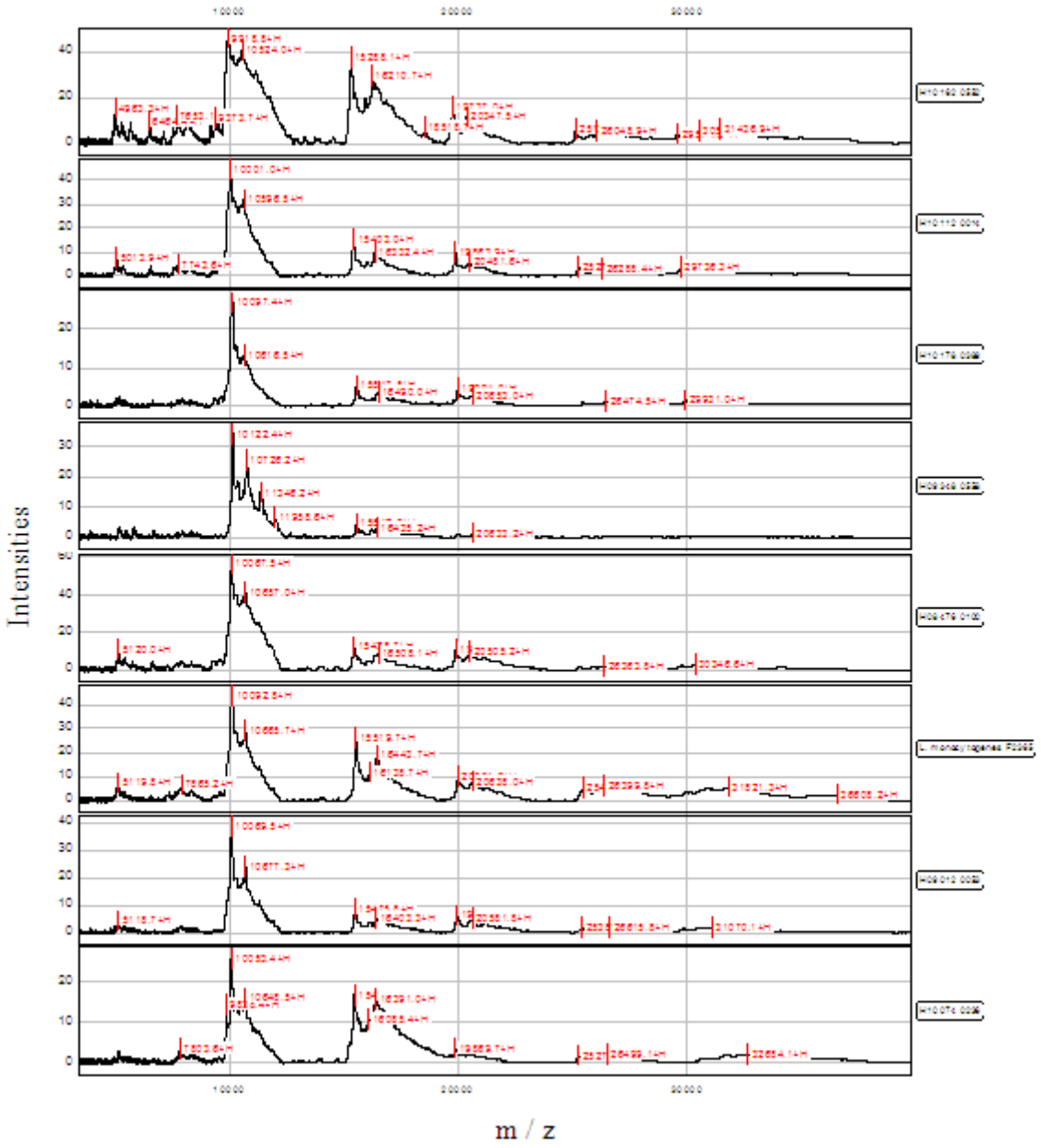

Figure 3.34. Ions detected on a ProteinChip CM10 array which was prepared by manual spotting using 6 µg of various *L. monocytogenes* protein extracts obtained from BN agar plate cultures. The chip allows simultaneous processing of 8 samples and the data are therefore presented as 8 stacked spectra. The identity of each sample is noted at the end of each spectra. From top to bottom they include isolates H10 162 0552, H10 112 0014, H10 178 0389, H09 348 0558, H08 476 0100, *L. monocytogenes* F2365, H09 012 0053, H10 074 0236. The image shows peak intensity (y-axis) versus m/z (x-axis).

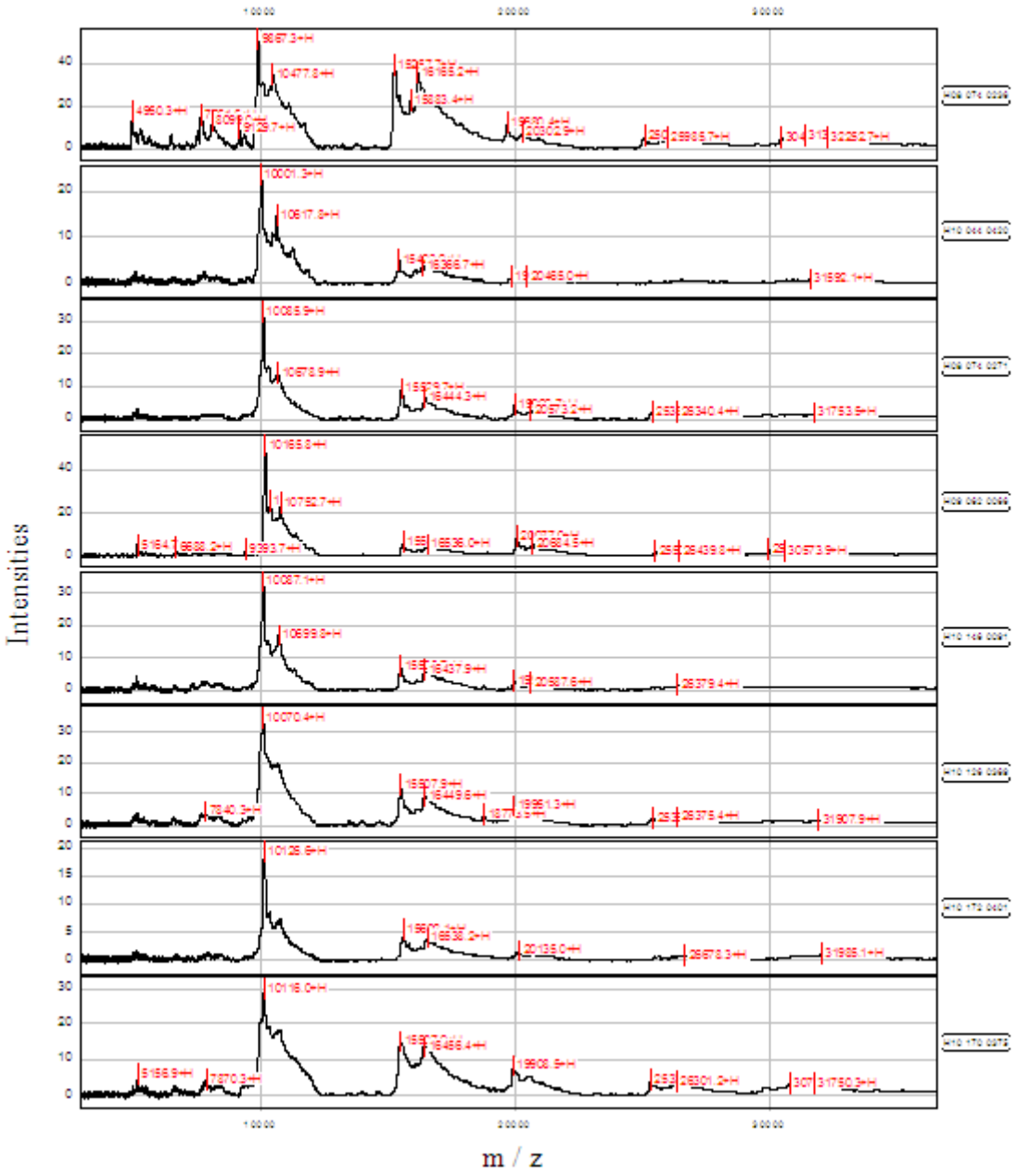

Figure 3.35. Ions detected on a ProteinChip CM10 array which was prepared by manual spotting using 6 µg of various *L. monocytogenes* protein extracts obtained from BN agar plate cultures. The chip allows simultaneous processing of 8 samples and the data are therefore presented as 8 stacked spectra. The identity of each sample is noted at the end of each spectra. From top to bottom they include isolates H08 074 0236, H10 044 0420, H08 074 0271, H09 062 0066, H10 146 0091, H10 126 0369, H10 172 0401 and H10 170 0375. The image shows peak intensity (y-axis) versus m/z (x-axis).

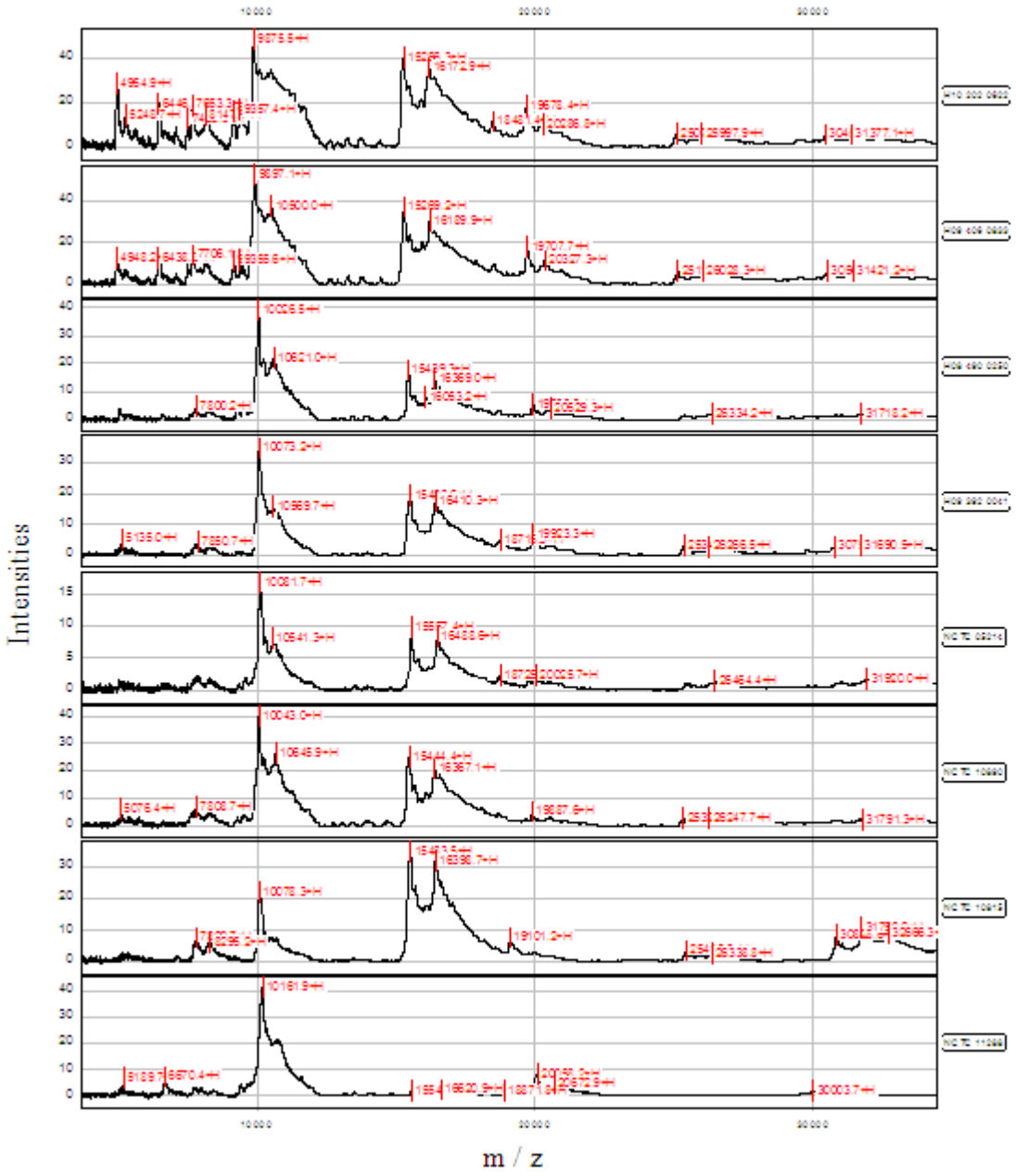

Figure 3.36. Ions detected on a ProteinChip CM10 array which was prepared by manual spotting using 6 µg of various *Listeria* species protein extracts obtained from BN agar plate cultures. The chip allows simultaneous processing of 8 samples and the data are therefore presented as 8 stacked spectra. The identity of each sample is noted at the end of each spectra. From top to bottom they include isolates H10 202 0622, H09 406 0833, H08 490 0250, H09 392 0041, NCTC 05214, NCTC 10890, NCTC 10815 and NCTC 11288. The image shows peak intensity (y-axis) versus m/z (x-axis).

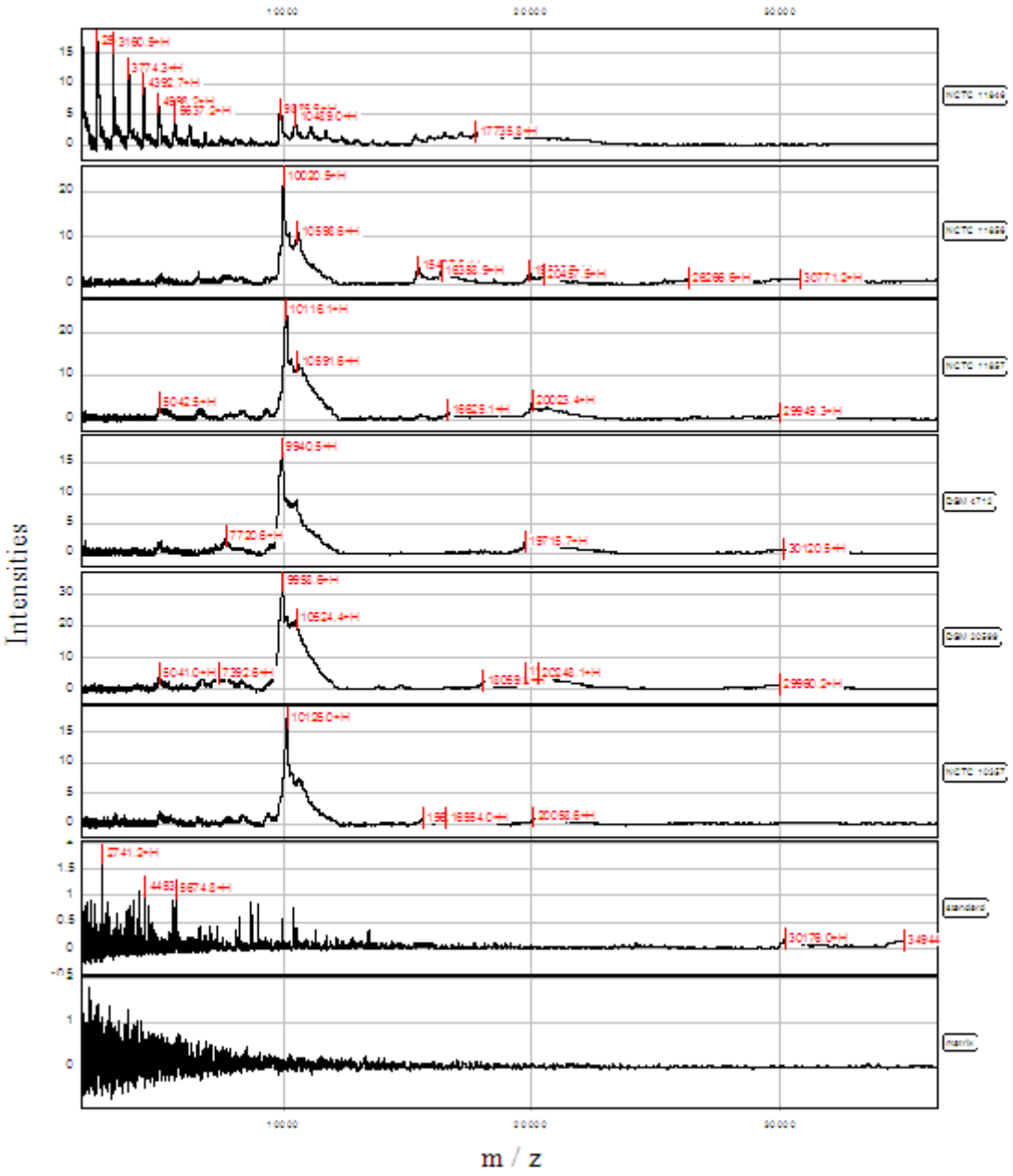

Figure 3.37. Ions detected on a ProteinChip CM10 array which was prepared by manual spotting using 6 µg of various *Listeria* and *Brochothrix* species protein extracts obtained from BN agar plate cultures. The chip allows simultaneous processing of 8 samples and the data are therefore presented as 8 stacked spectra. The identity of each sample is noted at the end of each spectra. From top to bottom they include isolates NCTC 11846, NCTC 11856, NCTC 11857, DSM 4712, DSM 20599, NCTC 10357, Bio-Rad standard and matrix. The image shows peak intensity (y-axis) versus m/z (x-axis).

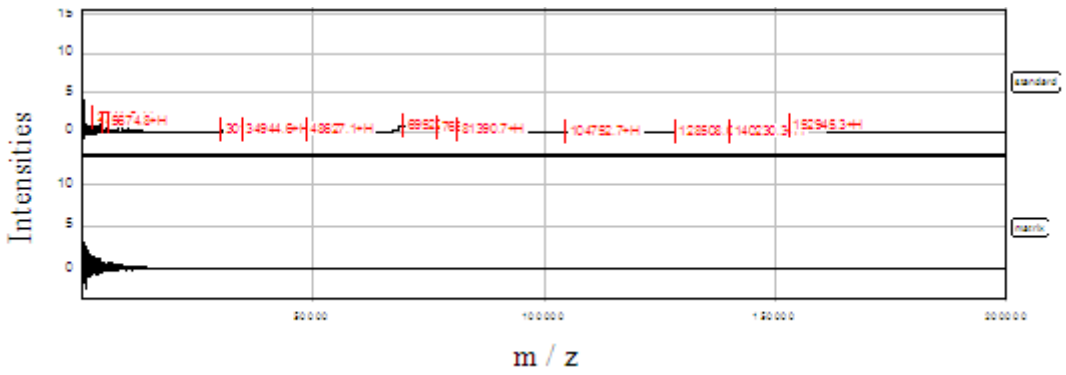

Figure 3.38. Ions detected on a ProteinChip CM10 array which was prepared by manual spotting using Bio-Rad standard (top) and matrix (bottom). The identity of each sample is noted at the end of each spectra. The image shows peak intensity (y-axis) versus m/z (y-axis).

Analysis of Figures 3.34 - Figure 3.37 using the Ciphergen ProteinChip software, lead to the creation of a heat map, from which a dendrogram was deduced (Figure 3.39). The heat map is a visual representation of proteins which were detected in each sample. In this representation all protein ions are assigned a red, green or black colour code. Ions depicted in red were up-regulated, ions depicted in green were down-regulated whilst those depicted in black were at the same expression level across all isolates. A visual inspection of the heat map showed dense patches of up-regulated and down regulated proteins. Furthur analysis of the heat map using the Ciphergen ProteinChip software produced the dendrogram illustrated at the top of Figure 3.39. The dendrogram showed that the isolates delineated into 5 clearly distinct clusters. Closer observation showed that the clusters did not correlate with molecular serotypes, or AFLP patterns. Each cluster contained a mixture of *Listeria* species whilst *Brochothrix* species did not cluster separately. In this study the result showed the close relationship amongst *Listeria* species and the close relationship between *Listeria* and *Brochothrix*.

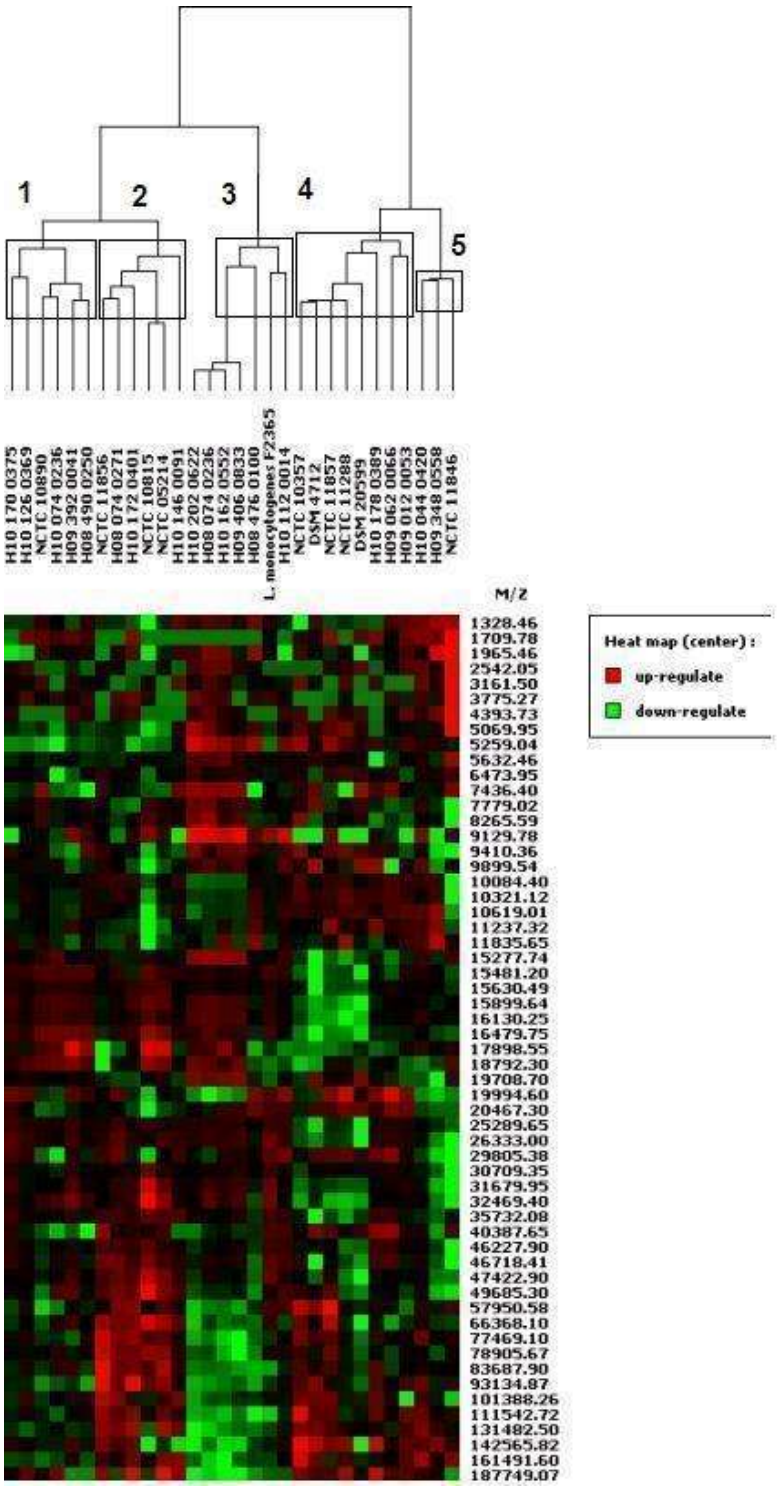

Figure 3.39. Dendrogram (top) and heat map (botton) generated by analysis of *Listeria* and *Brochothrix spp*. SELDI-TOF-MS spectra. The heat map was generated using software analysis through which each detected protein ion was assigned an m/z value. These are listed along the right border of the heat map which is a rectangular image composed of red, green and black coloured squares. Each ion is assigned a red, green or black colour which indicated

whether in that particular sample, the protein was up-regulated (red), down-regulated (green) or did not have a change in expression across all isolates. The isolates are listed above the heat map. A dendrogram is constructed basedon the relative amounts of protein ions detected.

3.4 Analysis of *L. monocytogenes* proteins differentially expressed at 4°C and 37°C

Prior to investigating proteins that are differentially expressed at 4°C and 37°C, it is necessary to determine a suitable time for harvesting *L. monocytogenes* cultures grown under each condition. Cultures harvested during mid to late exponential growth phase yielded sufficient protein for the study. For cultures grown at 4°C, it was necessary to allow sufficient time for cells to adapt to environmental conditions. Growth curves were established. A total of 7 *L. monocytogenes* isolates were used in this study, one of which was type strain NCTC 10357 and the remaining 6, H10 162 0552, H08 446 0286, H08 446 0286, H09 012 0053, H10 146 0091, H08 074 0271 were isolates obtained from FPRU. The growth curves of NCTC 10357 at 4°C and 37°C were pre-determined in this study (Figures 3.1 and 3.12 respectively). In order to determine whether similar results would be obtained for the other 6 isolates, clinical isolate H10 162 0552 was selected as a test isolate for growth curve comparison.

The growth curve of a *L. monocytogenes* clinical isolate H10 162 0552, was confirmed as being similar to the type strain at 4°C and 37°C (Figures 3.40 and 3.41 respectively). From this data, it was deduced that growth of all *L. monocytogenes* isolates selected for this study would have a similar growth curve; such isolates were therefore harvested at similar absorbance values, that is, between OD_{600} 0.5 and 0.7 and between OD_{600} 0.8 and 1.0 when grown at 4°C and 37°C respectively. This was carried out so that as previously discussed the majority of cells would be in exponential growth phase.

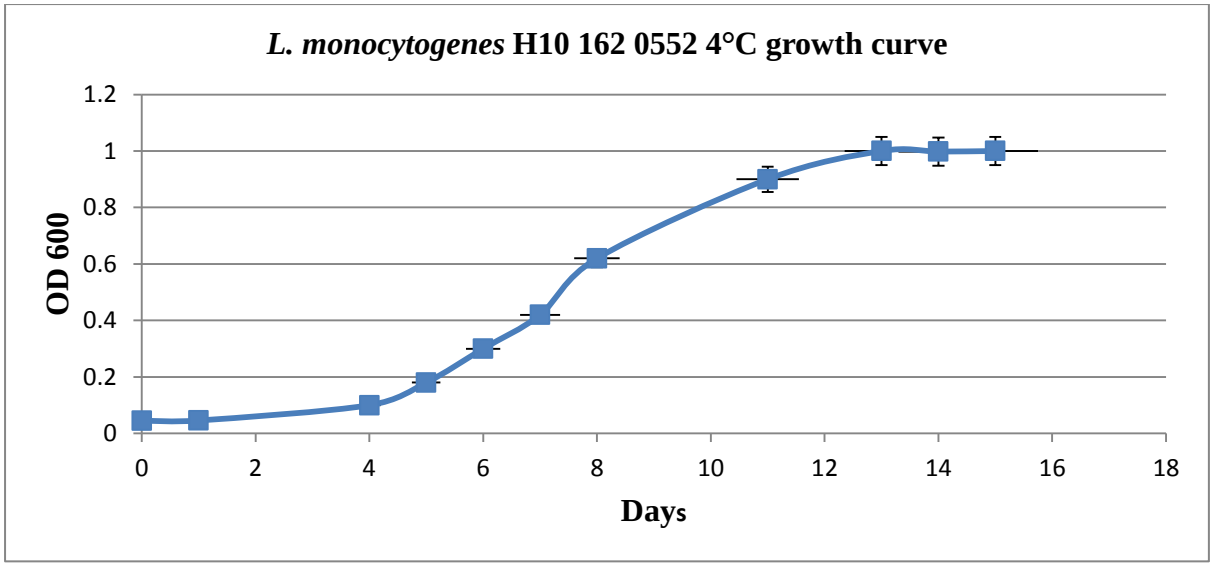

Figure 3.40. *L. monocytogenes* H1 0162 0552 growth curve at 4°C. Absorbance at OD_{600} (y-axis) versus days (x-axis). The curve shows that at an absorbance between OD_{600} 0.5 and 0.7 cells were in their exponential growth phase.

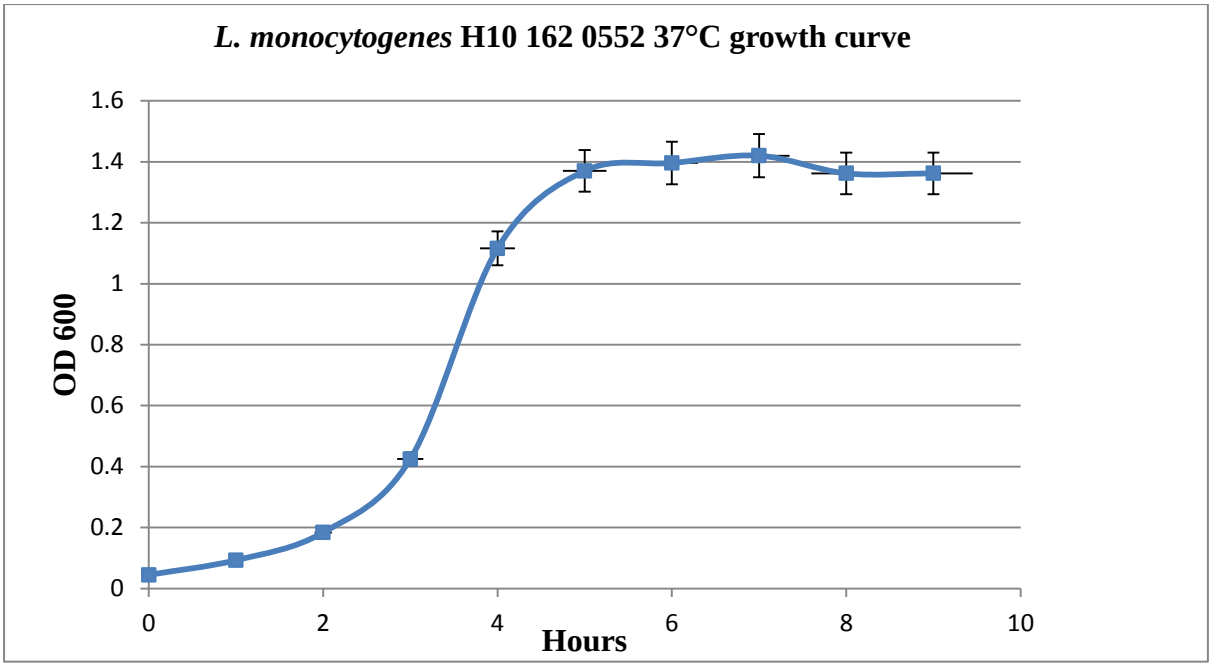

Figure 3.41. *L. monocytogenes* H1 0162 0552 growth curve at 37°C. Absorbance at OD_{600} (y-axis) versus days (x-axis). The curve shows that at an absorbance between OD_{600} 0.8 and 1.0 cells were in their exponential growth phase.

One-dimensional gel images of protein extracts obtained from the 7 *L. monocytogenes* isolates grown at 4°C and 37°C, showed that a number of bands had different intensities across all biological replicates. In all 7 isolates, it was consistently observed that a protein band corresponding to approximately 10 kDa in size was more intense at 4°C than 37°C. Also, consistently present in all isolates was a protein band corresponding to approximately 10 kDa which was present at 37°C and absent at 4°C (these bands are indicated on the gel images by black arrows) (Figures 3.42 and 3.43).

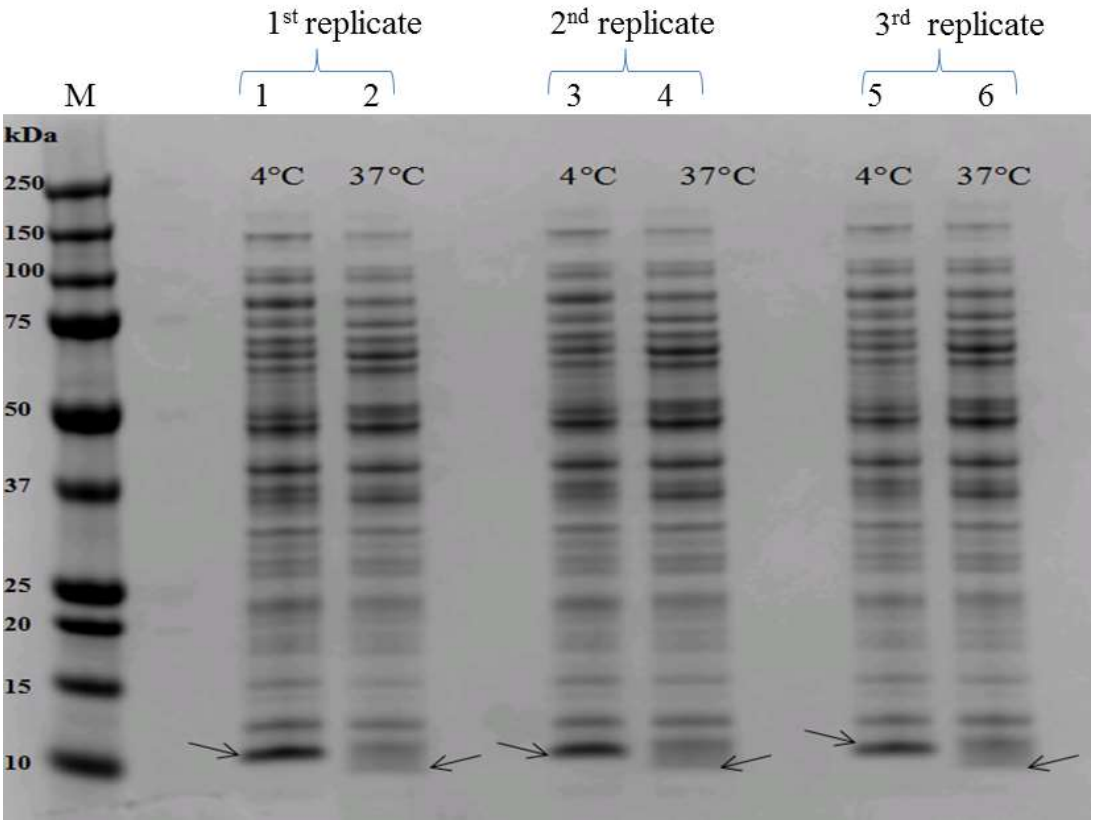

Figure 3.42. One-dimensional SDS PAGE analysis of proteins expressed in *L. monocytogenes* NCTC 10357 at 4°C and 37°C. Lanes: M-Marker; lanes 1 and 2 - 4°C and 37°C respectively (1st replicate); lanes 3 and 4 - 4°C and 37°C respectively (2nd replicate); and lanes 5 and 6 - 4°C and 37°C respectively (3rd replicate). A comparison of all three biological replicates showed that samples obtained from 4°C and 37°C cultured isolates both appear to have a unique protein band in the 10- 15 kDa marker range (indicated by black arrows).

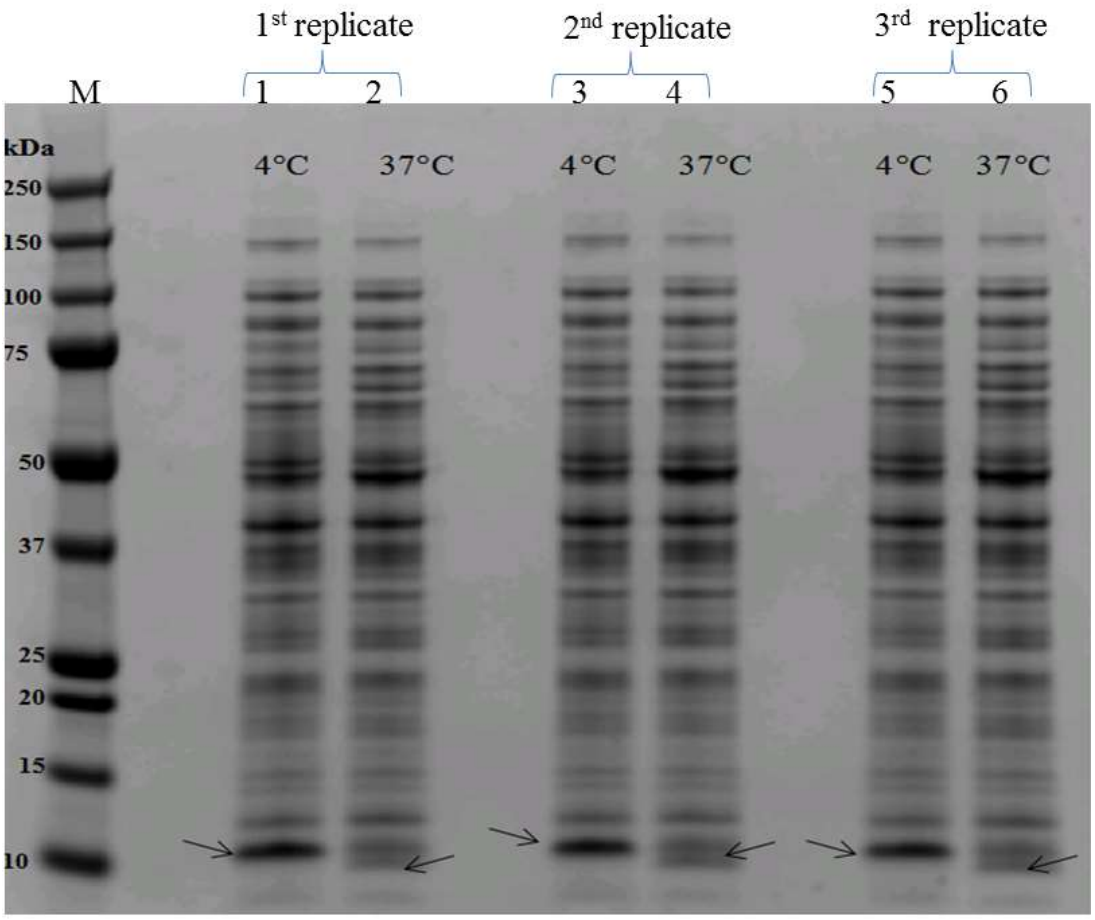

Figure 3.43. One-dimensional SDS PAGE analysis of proteins expressed in *L. monocytogenes* H10 162 0552 at 4°C and 37°C. Lanes: M-Marker; lanes 1 and 2 - 4°C and 37°C respectively (1st replicate); lanes 3 and 4 - 4°C and 37°C respectively (2nd replicate); and lanes 5 and 6 - 4°C and 37°C respectively (3rd replicate). A comparison of all three biological replicates showed that samples obtained from 4°C and 37°C cultured isolates both appear to have a unique protein band in the 10 - 15 kDa marker range (indicated by black arrows).

The observed differences in band intensities were confirmed using the Bio-Rad Image Lab 4.0 software which assigns an intensity value to each band. As 7 isolates were tested in this study, the small sample size means that the data cannot be statistically tested, however, compilation of the data on bar graphs showed that overall, the 10 kDa band was more intense at 4°C than 37°C (Figures 3.44). (One figure is shown, however, the same trend was observed for all isolates).

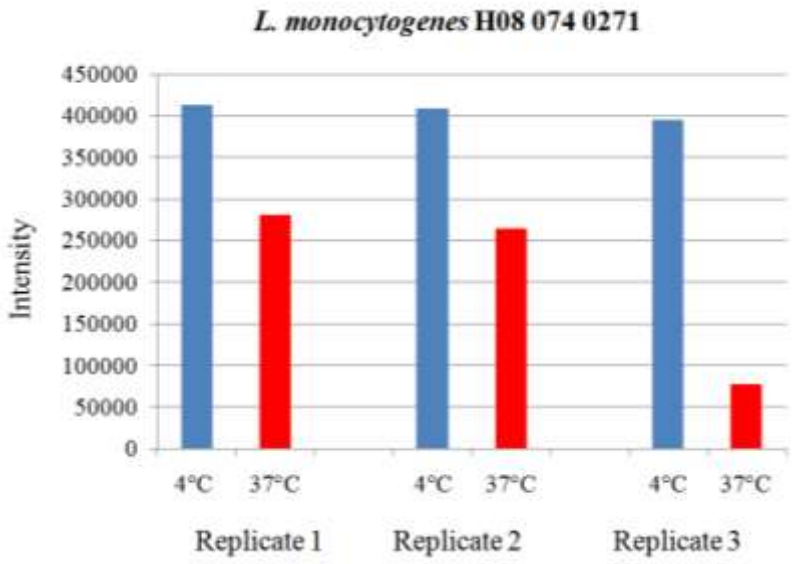

Figure 3.44. Intensity of the ~10 kDa protein band at 4°C and 37°C in biological replicates 1, 2 and 3 of *L. monocytogenes* isolate H08 074 0271. The intensity was 32%, 35% and 81% greater at 4°C (blue bars) than at 37°C (red bars) for replicates 1 and 2, and 3 respectively.

Protein bands which showed differential expression at approximately 10 kDa (Figures 3.42 and 3.43) were further analysed using LC-MS/MS followed by Scaffold software analysis and results indicated 9 that proteins were either up or down-regulated at either temperature (Figures 3.45 - 3.53 and Table 3.5). As expected changes in growth temperature affected protein expression. The most dramatic change can be seen in Figure 3.50. Here, at 4°C hypothetical protein lin2124 had a normalized spectrum count ranging between 1.0 and 3.5, whilst at 37°C the normalized spectrum count ranged between 25.0 and 67.5.

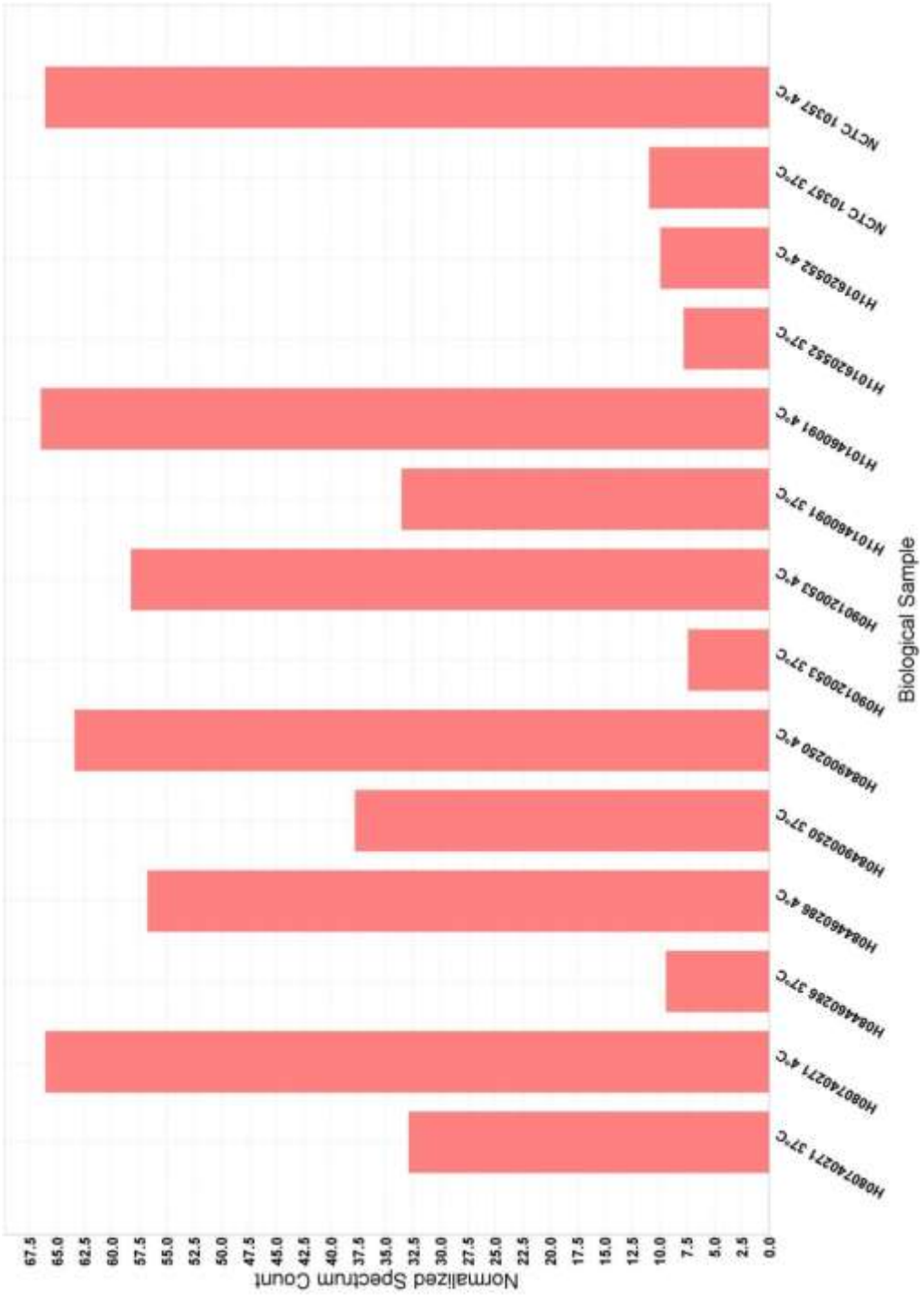

Figure 3.45. A bar graph showing the relative abundance of hypothetical protein lin1401 across different protein samples. Protein samples were obtained from seven *L. monocytogenes* isolates H080740271, H084460286, H084900250, H090120053, H101460091, H101620552 and NCTC 10357. Each isolate was cultured at 37°C and 4°C giving a total of 14 biological samples on the x-axis. The y-axis shows the normalized spectral count of the protein in each sample. The data indicates that overall hypothetical protein lin1401 was expressed at a higher level in isolates grown at 4°C.

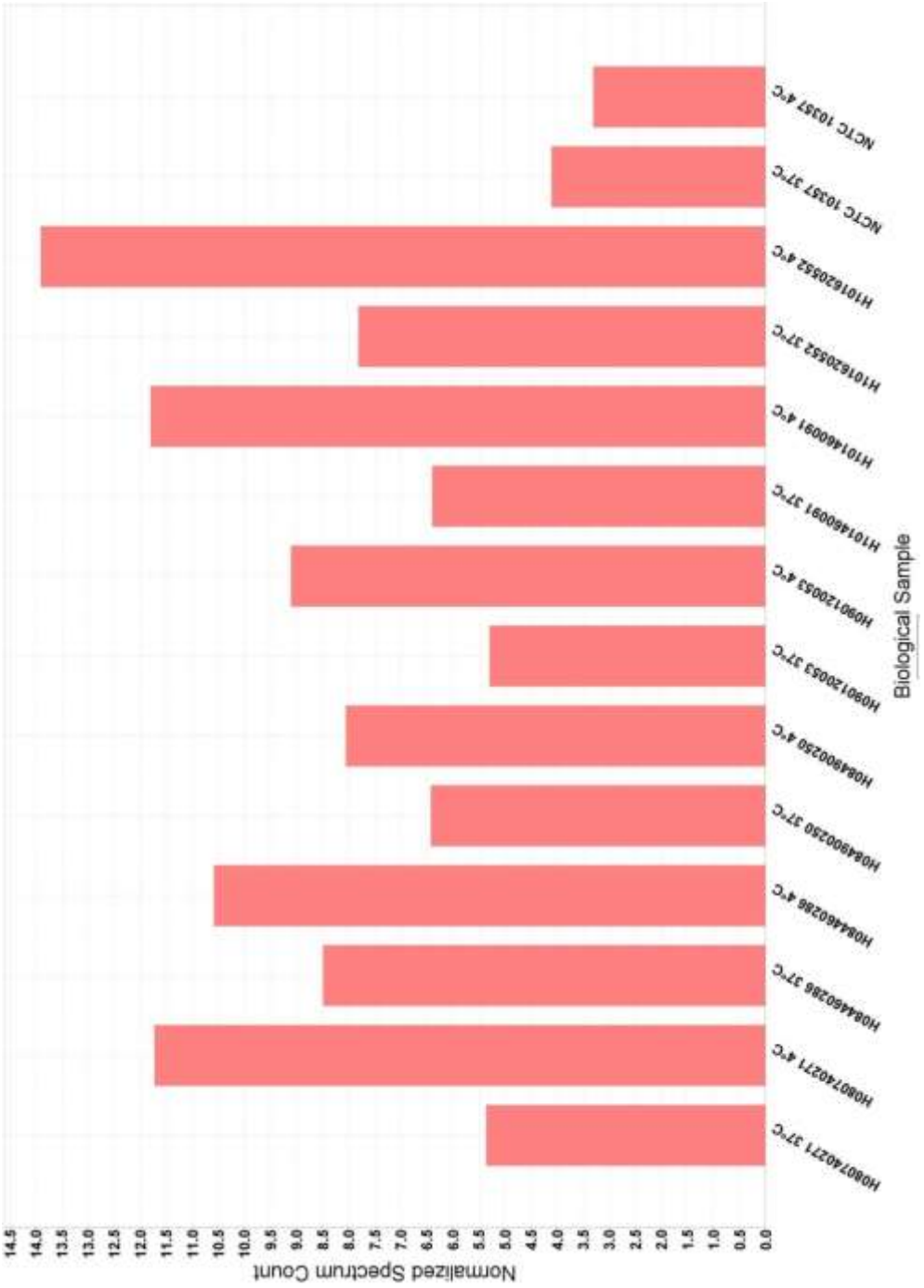

Figure 3.46. A bar graph showing the relative abundance of PTS system, cellobiose specific, IIB component protein across different protein samples. Protein samples were obtained from seven *L. monocytogenes* isolates H080740271, H084460286, H084900250, H090120053, H101460091, H101620552 and NCTC 10357. Each isolate was cultured at 37°C and 4°C giving a total of 14 biological samples on the x-axis. The y-axis shows the normalized spectral count of the protein in each sample.The data indicates that overall PTS system, cellobiose specific, IIB component protein was expressed at a higher level in isolates grown at 4°C.

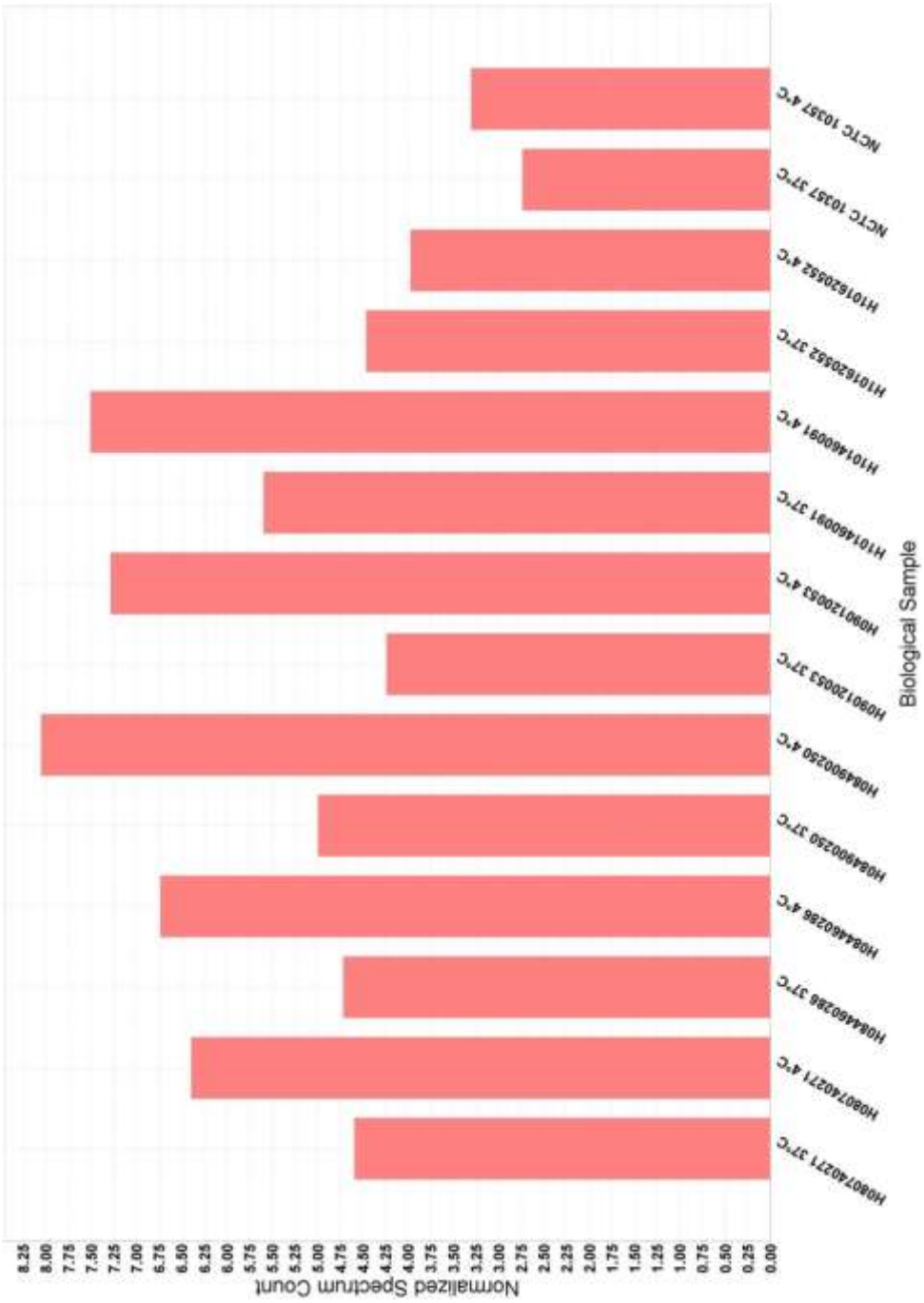

Figure 3.47. A bar graph showing the relative abundance of hypothetical protein lin1183 across different protein samples. Protein samples were obtained from seven *L. monocytogenes* isolates H080740271, H084460286, H084900250, H090120053, H101460091, H101620552 and NCTC 10357. Each isolate was cultured at 37°C and 4°C giving a total of 14 biological samples on the x-axis. The y-axis shows the normalized spectral count of the protein in each sample. The data indicates that overall hypothetical protein lin1183 was expressed at a higher level in isolates grown at 4°C.

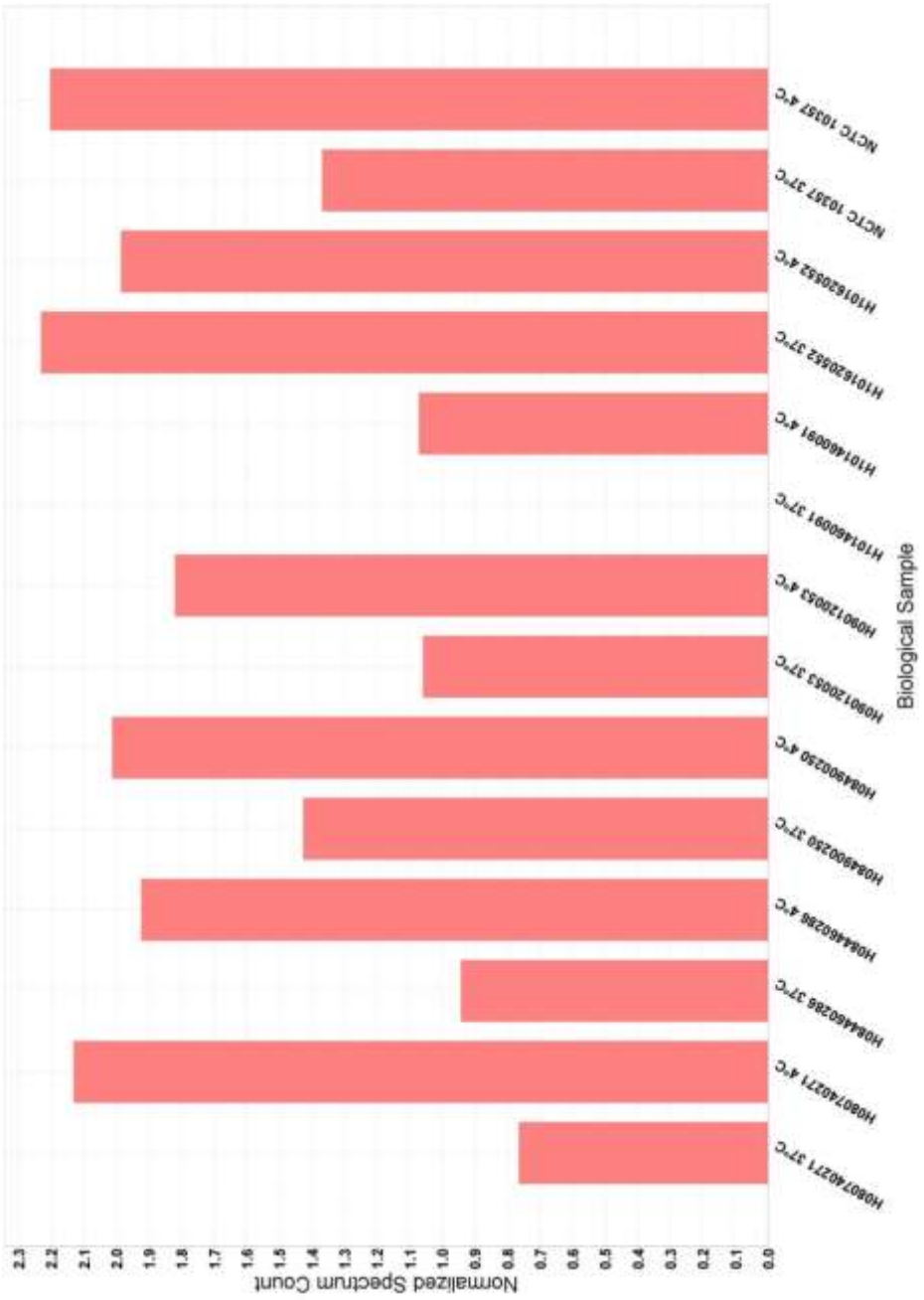

Figure 3.48. A bar graph showing the relative abundance of 50s ribosomal protein L29 across different protein samples. Protein samples were obtained from seven *L. monocytogenes* isolates H080740271, H084460286, H084900250, H090120053, H101460091, H101620552 and NCTC 10357. Each isolate was cultured at 37°C and 4°C giving a total of 14 biological samples on the x-axis. The y-axis shows the normalized spectral count of the protein in each sample. The data indicates that overall 50s ribosomal protein L29 was expressed at a higher level in isolates grown at 4°C.

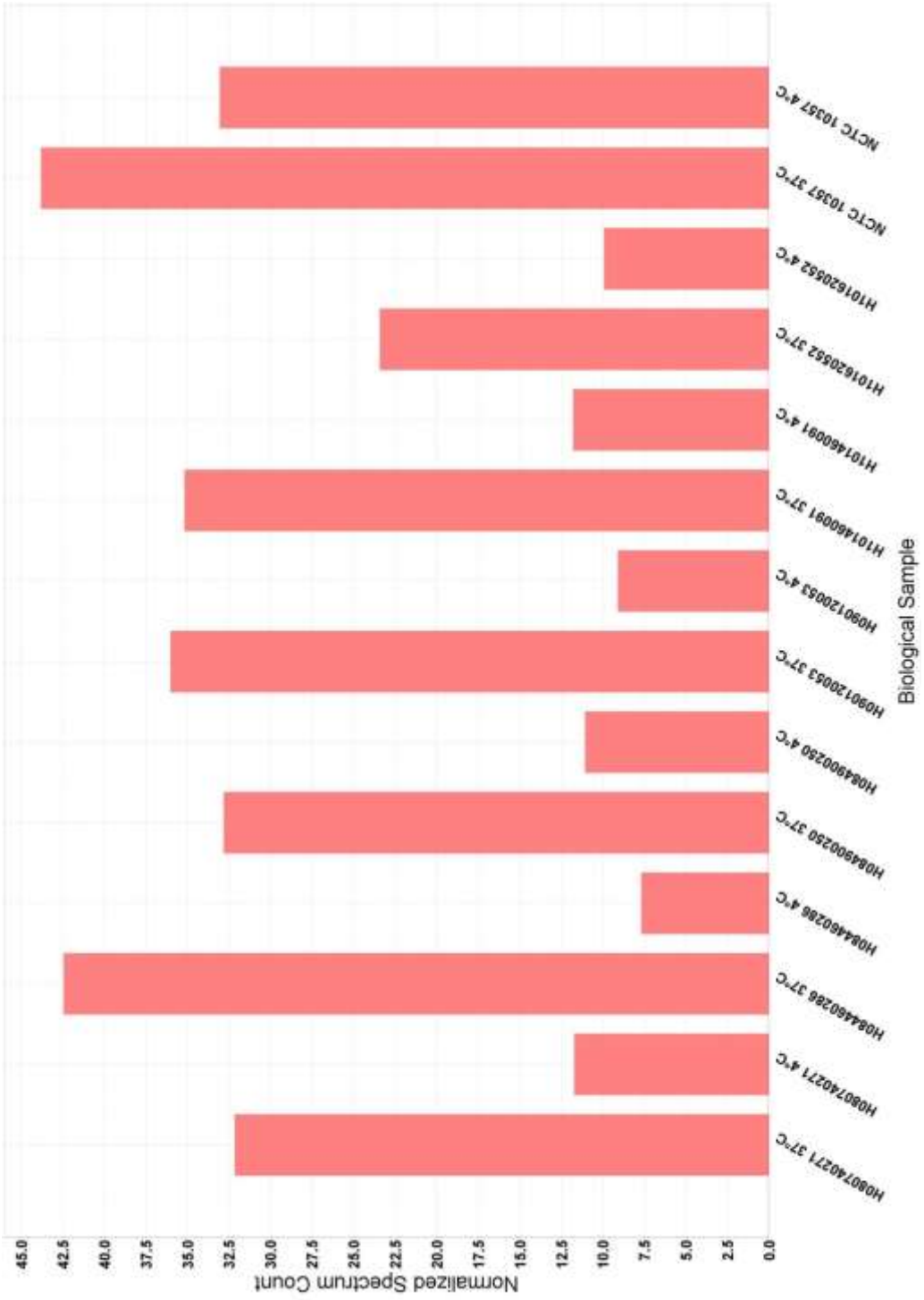

Figure 3.49. A bar graph showing the relative abundance of co-chaperonin GroES across different protein samples. Protein samples were obtained from seven *L. monocytogenes* isolates H080740271, H084460286, H084900250, H090120053, H101460091, H101620552 and NCTC 10357. Each isolate was cultured at 37°C and 4°C giving a total of 14 biological samples on the x-axis. The y-axis shows the normalized spectral count of the protein in each sample. The data indicates that overall co-chaperonin GroES was expressed at a higher level in isolates grown at 37°C.

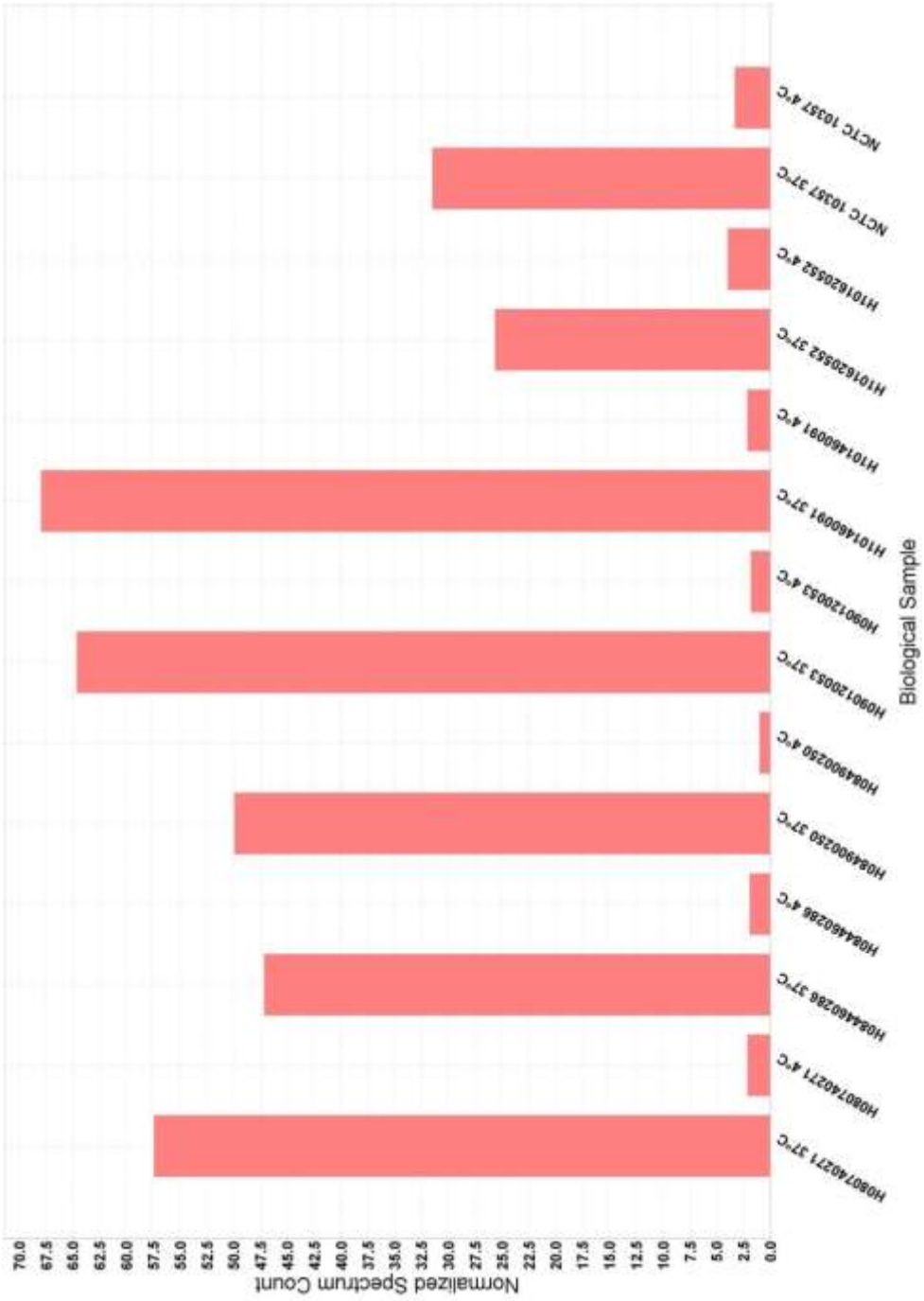

Figure 3.50. A bar graph showing the relative abundance of hypothetical protein lin2124 across different protein samples. Protein samples were obtained from seven *L. monocytogenes* isolates H080740271, H084460286, H084900250, H090120053, H101460091, H101620552 and NCTC 10357. Each isolate was cultured at 37°C and 4°C giving a total of 14 biological samples on the x-axis. The y-axis shows the normalized spectral count of the protein in each sample. The data indicates that overall hypothetical protein lin2124 was expressed at a higher level in isolates grown at 37°C.

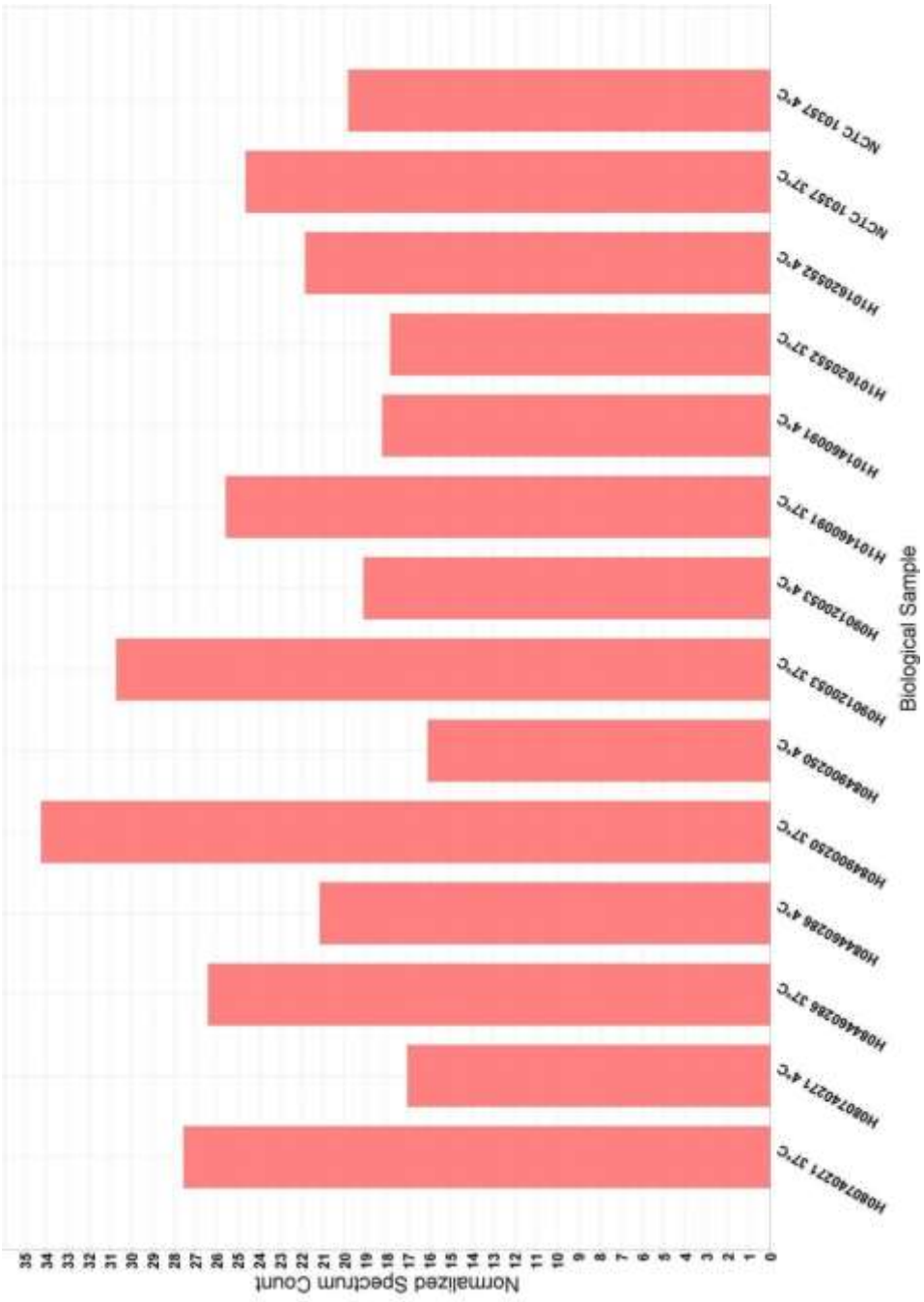

Figure 3.51. A bar graph showing the relative abundance of phosphocarrier protein HPr across different protein samples. Protein samples were obtained from seven *L. monocytogenes* isolates H080740271, H084460286, H084900250, H090120053, H101460091, H101620552 and NCTC 10357. Each isolate was cultured at 37°C and 4°C giving a total of 14 biological samples on the x-axis. The y-axis shows the normalized spectral count of the protein in each sample. The data indicates that overall phosphocarrier protein HPr was expressed at a higher level in isolates grown at 37°C.

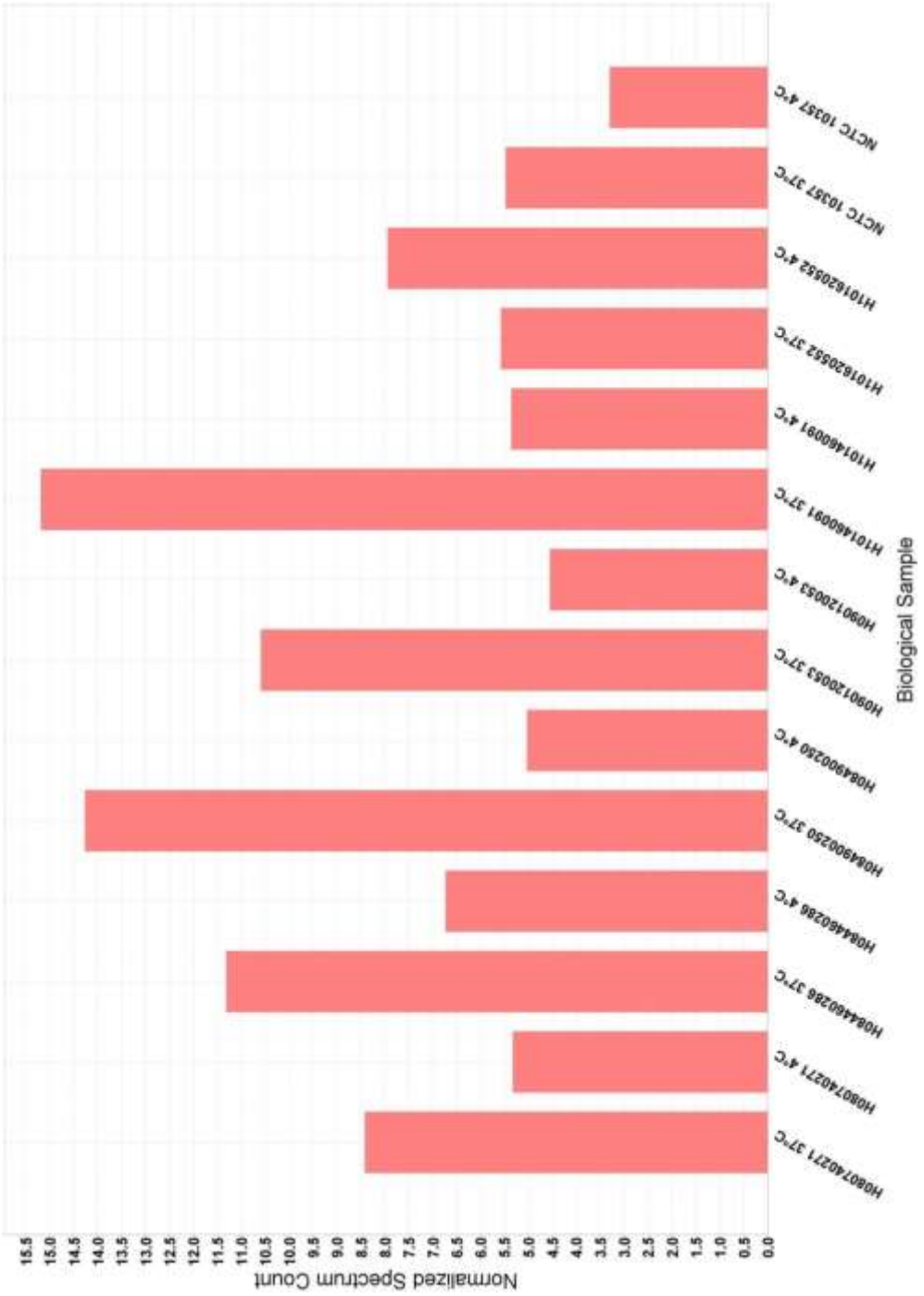

Figure 3.52. A bar graph showing the relative abundance of anti-anti-sigma factor across different protein samples.. Protein samples were obtained from seven *L. monocytogenes* isolates H080740271, H084460286, H084900250, H090120053, H101460091, H101620552 and NCTC 10357. Each isolate was cultured at 37°C and 4°C giving a total of 14 biological samples on the x-axis. The y-axis shows the normalized spectral count of the protein in each sample. The data indicates that overall anti-anti-sigma factor was expressed at a higher level in isolates grown at 37°C.

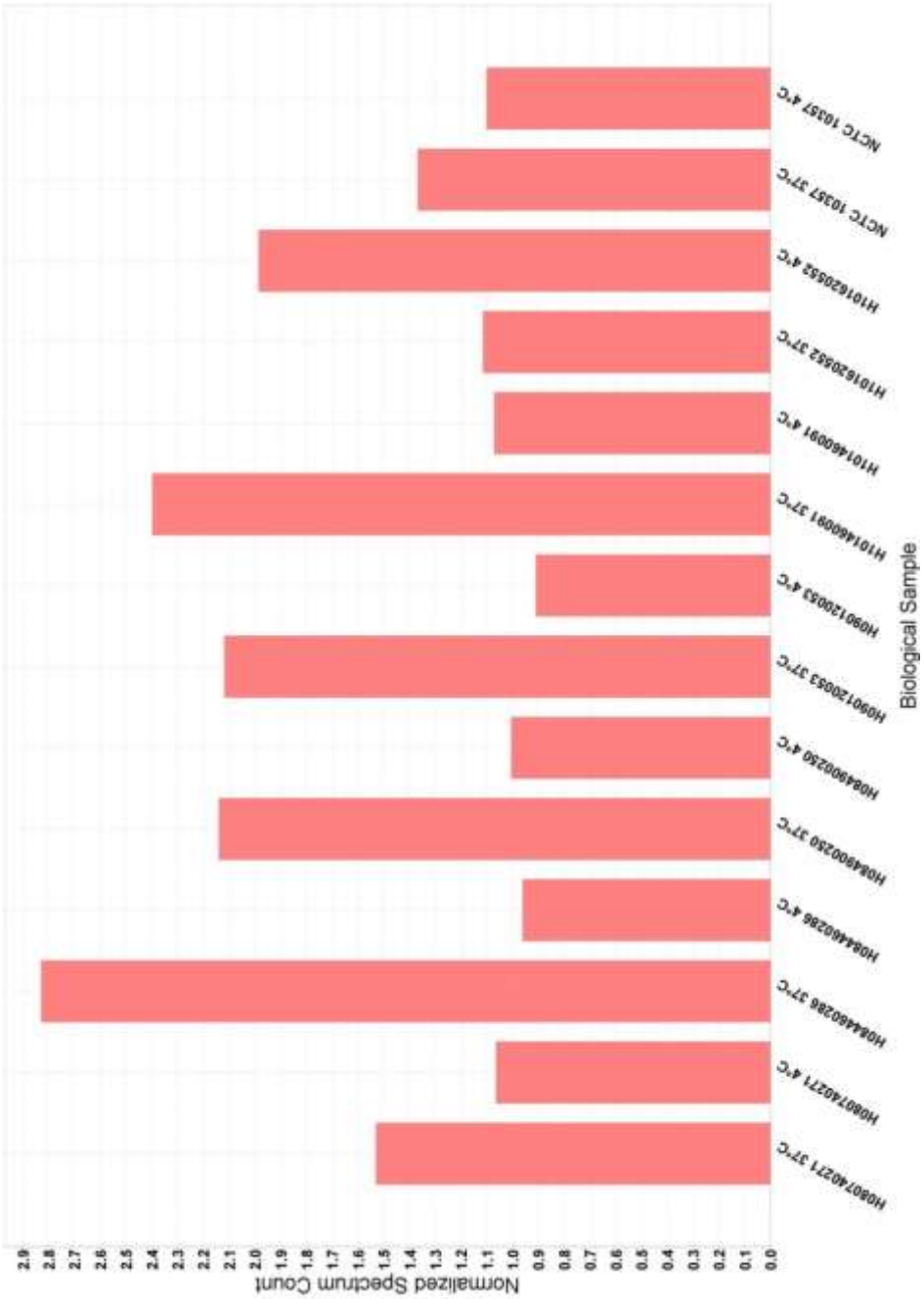

Figure 3.53. A bar graph showing the relative abundance of 30s ribosomal protein S16 factor across different protein samples. Protein samples were obtained from seven *L. monocytogenes* isolates H080740271, H084460286, H084900250, H090120053, H101460091, H101620552 and NCTC 10357. Each isolate was cultured at 37°C and 4°C giving a total of 14 biological samples on the x-axis. The y-axis shows the normalized spectral count of the protein in each sample. The data indicates that overall 30s ribosomal protein S16 was expressed at a higher level in isolates grown at 37°C.

Table 3.5 Proteins up regulated at 4°C and 37°C. Four proteins are upregulated at 4°C and down-regulated at 37°C, whilst 5 proteins are up-regulate at 37°C and down-regulated at 4°C. The table is a summary of Figures 3.45 - 3.53 which shows in more detailed the differences in expression levels.

Proteins up-regulated at 4°C (down-regulated at 37°C).	**Proteins up-regulated at 37°C (down-regulated at 4°C).**
Hypothetical protein lin1401 (7 kDa) (except H10 162 0552)	Co-chaperonin GroES (10 kDa)
Phosphotransferase system (PTS system), cellobiose specific, IIB component (11 kDa) (except NCTC 10357)	Hypothetical protein lin2124 (7 kDa) (except H10 162 0552)
Hypothetical protein lin1183 (12 kDa) (except H10 162 0552)	Histidine phosphocarrier protein (HPr) (9 kDa) (except H10 162 0552)
50s ribosomal protein L29 (7 kDa) (except H10 162 0552)	Anti-anti sigma factor (13 kDa) (except H10 162 0552)
	30s ribosomal protein S16 (10 kDa) (except H10 162 0552)

Analysis also indicated that 3 proteins were uniquely expressed at 4°C and 37°C. Hypothetical protein lwe06778, an 11 kDa protein, was present at 4°C and absent at 37°C in all isolates except the type strain where it was present at both temperatures (Figure 3.54). Phosphoribosyl-AMP cyclohydrolase , a 12 kDa protein, was also present at 4°C and absent at 37°C in all isolates except the type strain where it was absent at both temperatures (Figure 3.55). On the other hand, hypothetical protein lmo0056, an 11 kDa protein, was present at 37°C and absent at 4°C (Figure 3.56).

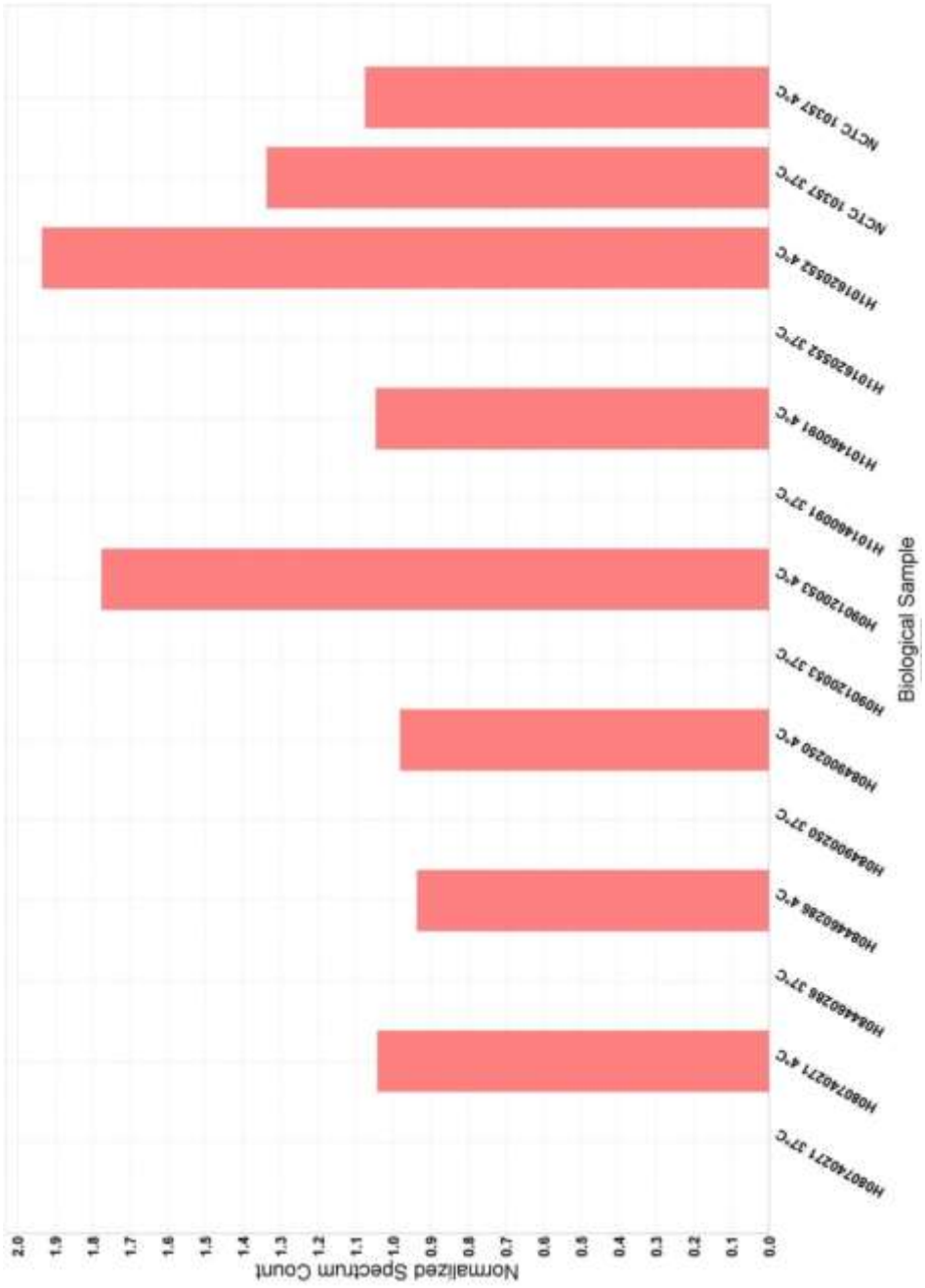

Figure 3.54. A bar graph showing the relative abundance of hypothetical protein lwe06778 across different protein samples. Protein samples were obtained from seven *L. monocytogenes* isolates H080740271, H084460286, H084900250, H090120053, H101460091, H101620552 and NCTC 10357. Each isolate was cultured at 37°C and 4°C giving a total of 14 biological samples on the x-axis. The y-axis shows the normalized spectral count of the protein in each sample. The data indicates that hypothetical protein lwe06778 was soley expressed at 4°C, with the exception of thype strain NCTC 10357 where the protein was also present at 37°C

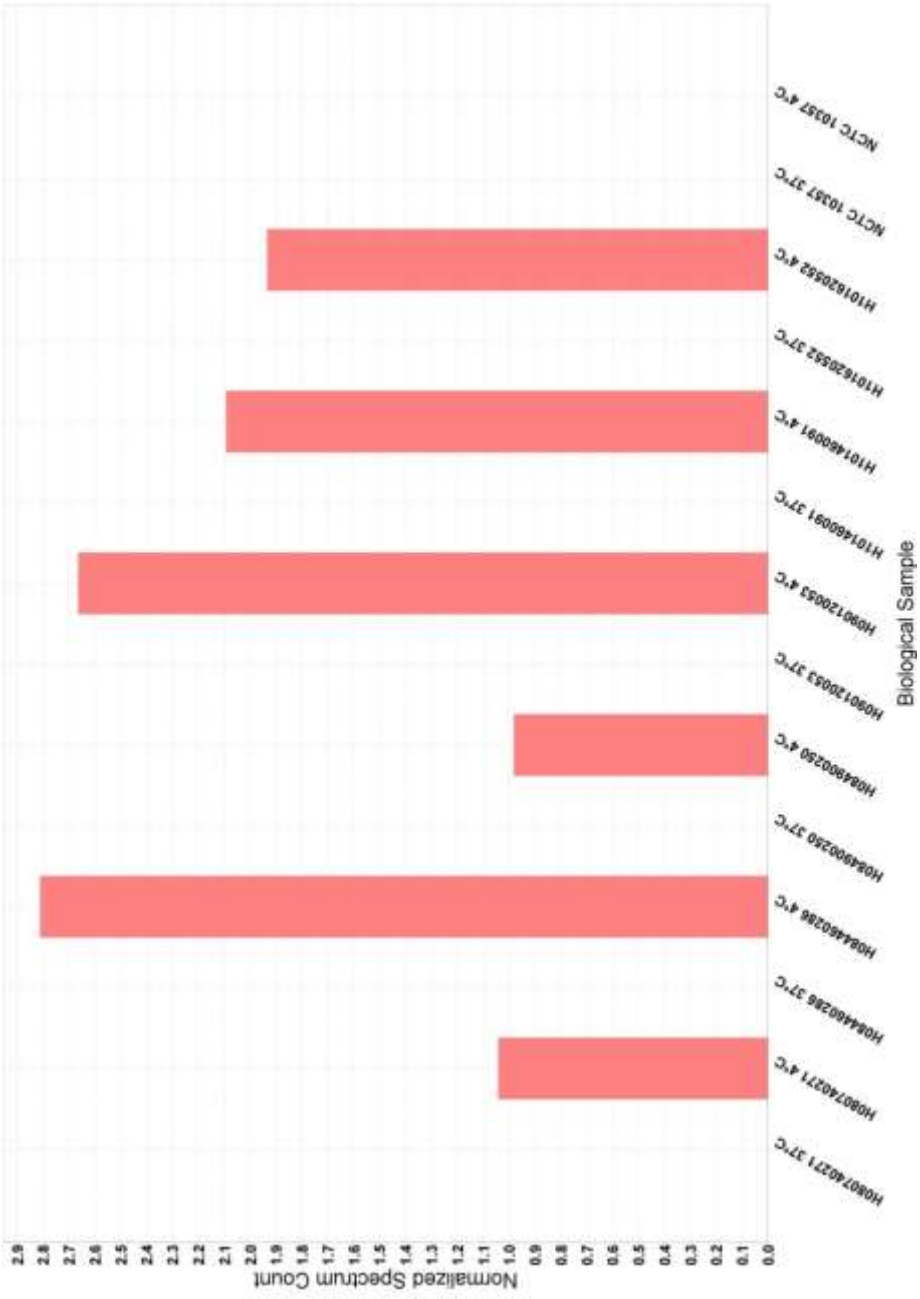

Figure 3.55. A bar graph showing the relative abundance of phosphoribosyl-AMP cyclohydrolase across different protein samples. Protein samples were obtained from seven *L. monocytogenes* isolates H080740271, H084460286, H084900250, H090120053, H101460091, H101620552 and NCTC 10357. Each isolate was cultured at 37°C and 4°C giving a total of 14 biological samples on the x-axis. The y-axis shows the normalized spectral count of the protein in each sample. The data indicates that, with the exception of NCTC 10357, phosphoribosyl-AMP cyclohydrolase was soley expressed at 4°C. The protein was not exptressed in the type strain at either temperature.

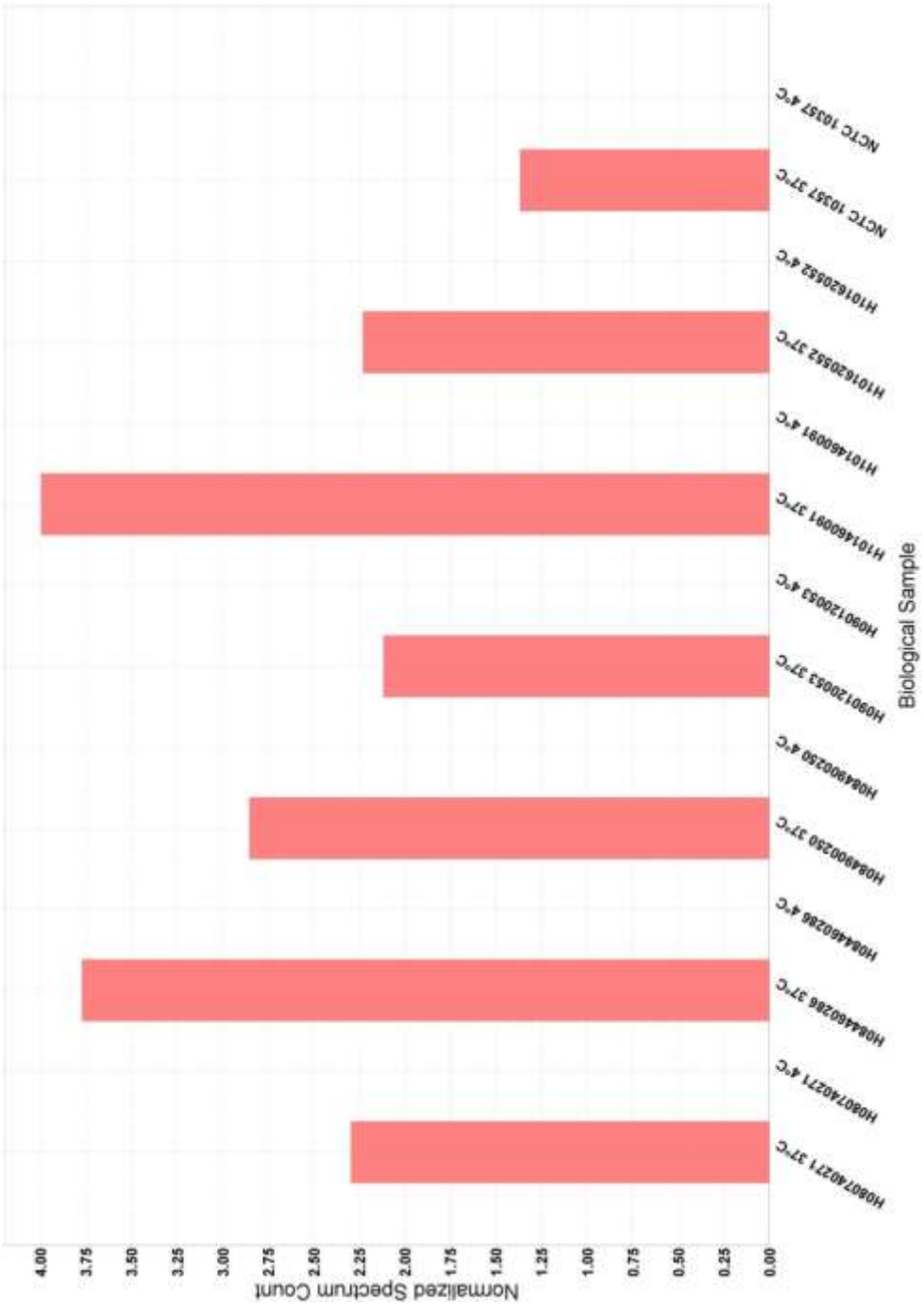

Figure 3.56. A bar graph showing the relative abundance of protein lmo0056 different protein samples. Protein samples were obtained from seven *L. monocytogenes* isolates H080740271, H084460286, H084900250, H090120053, H101460091, H101620552 and NCTC 10357. Each isolate was cultured at 37°C and 4°C giving a total of 14 biological samples on the x-axis. The y-axis shows the normalized spectral count of the protein in each sample. The data indicates that protein lmo0056 was soley expressed at 37°C.

Proteins extracts from H101620552 were analysed by high resolution capillary electrophoresis (deltaDOT) to further establish the presence of the unique ~10 kDa protein bands. SDS-PAGE gel analysis of the samples confirmed the presence of a more intense protein band at ~10 kDa (figure not shown). These were analysed against the protein ladder using the GST electropherogram and EVA (Figures 3.57 and 3.58) combining the information in a mass calibration tool to assign molecular weights for peaks of interest in the *L. monocytogenes* H101620552 lysate samples (Figures 3.59 and 3.60). Differences in peak area were calculated and showed that the area of peak A was decreased by 78% in the protein sample expressed at 37°C while the area of peak B was decreased by 54% in the sample expressed at 4°C.

The SDS-CGE analysis showed that the average molecular weight of the protein corresponding to peak A was 12.88 kDa while the average molecular weight of the protein corresponding to peak B was 40.65 kDa. There was a 78% decrease in peak A at 37°C and a 54% decrease in peak B at 4°C. High resolution capillary electrophoresis (deltaDOT) therefore unequivocally corroborated the findings of hypothetical protein lwe06778 and phosphoribosyl-AMP cyclohydrolase which were 11 kDa and 12 kDa respectively.

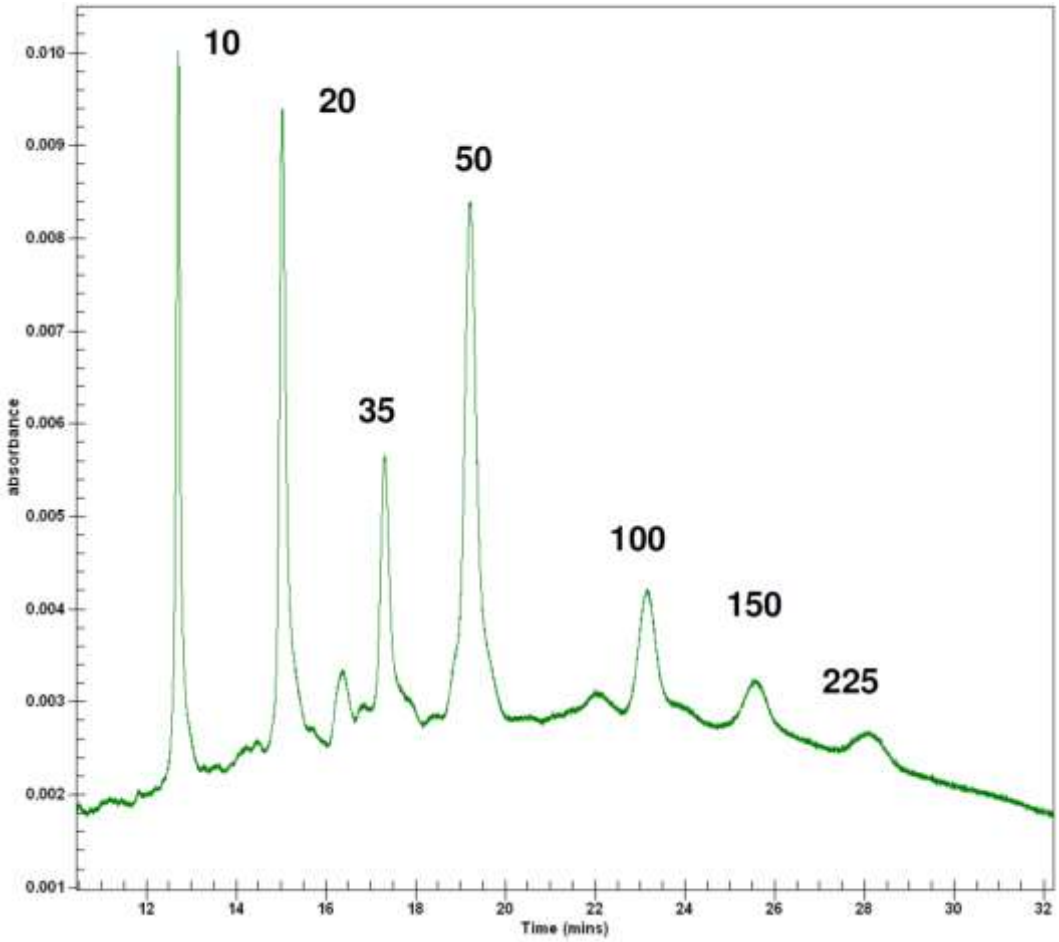

Figures 3.57. GST electropherogram depicting the separation of the molecular weight ladder. The plot of absorbance (y-axis) versus time in minutes (x-axis) shows the molecular weights of seven proteins present in the mixture: 10, 20, 35, 50, 100, 150 and 225 kDa. The ladder combined with the mass calibration tool built into the processing software were used to assign molecular weights for the peaks of interest in the lysate samples. (Image obtained from deltaDOT).

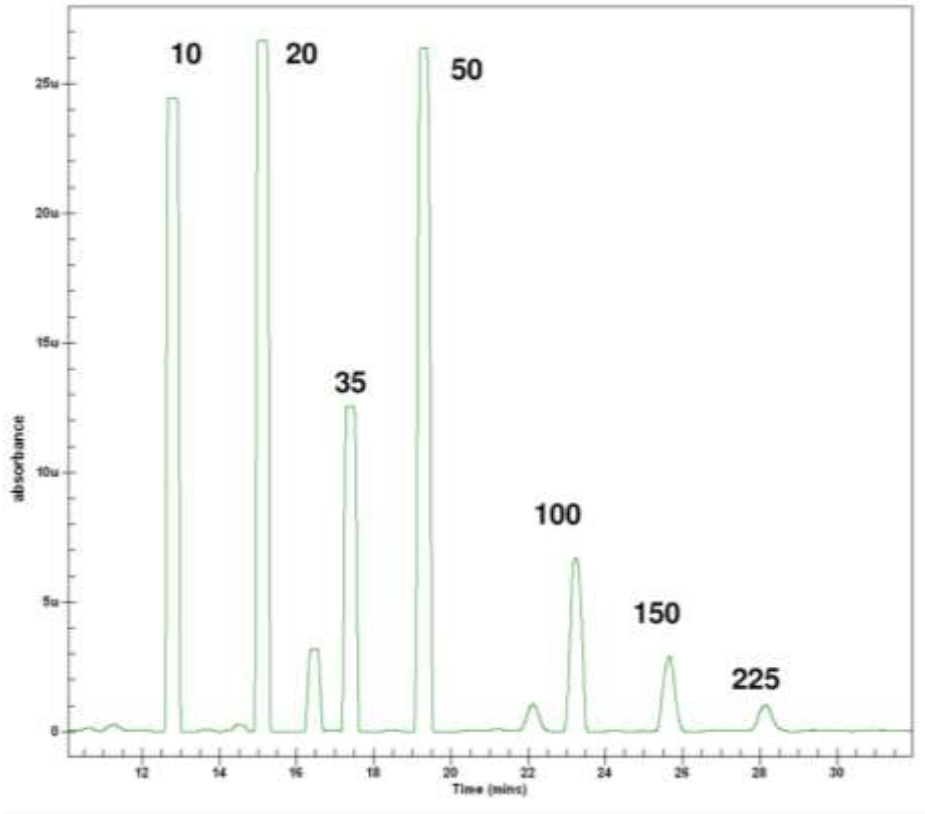

Figures 3.58. EVA trace depicting the separation of the molecular weight ladder. The plot of absorbance (y-axis) versus time in minutes (x-axis) shows the molecular weights of seven proteins present in the mixture: 10, 20, 35, 50, 100, 150 and 225 kDa. The ladder combined with the mass calibration tool built into the processing software were used to assign molecular weights for the peaks of interest in the lysate samples. (Image obtained from deltaDOT).

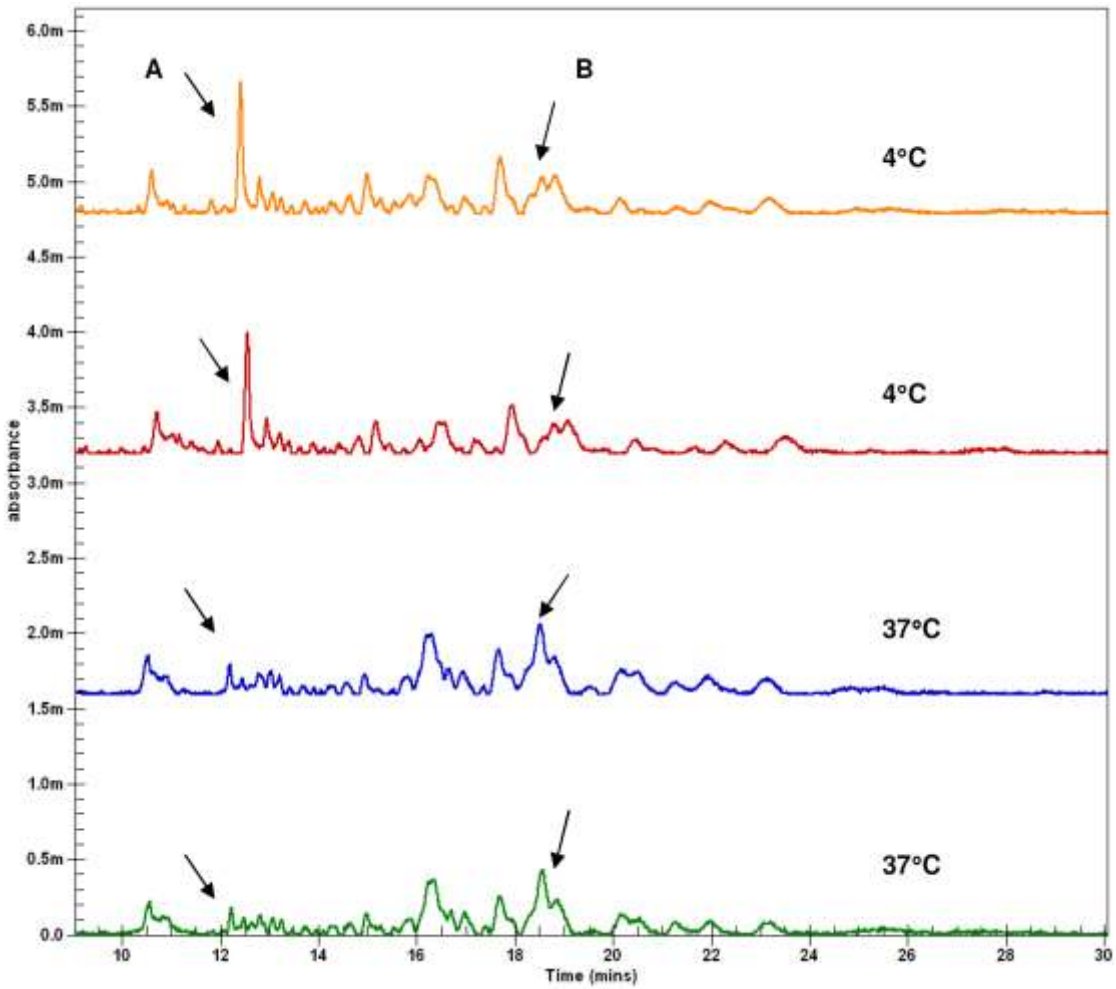

Figures 3.59. GST electropherogram depicting the separation of *L. monocytogenes* H101620552 protein extracts expressed at 4°C (orange and red traces) and 37°C (blue and green traces). Replicates of each sample were run. The plot shows absorbance (y-axis) versus time in minutes (x-axis). Clear differences are indicated by black arrows as peak A and peak B. Peak A is appears to exhibit greater expression at 4°C than at 37°C, while Peak B appears to exhibit greater expression at 37°C than at 4°C. (Image obtained from deltaDOT).

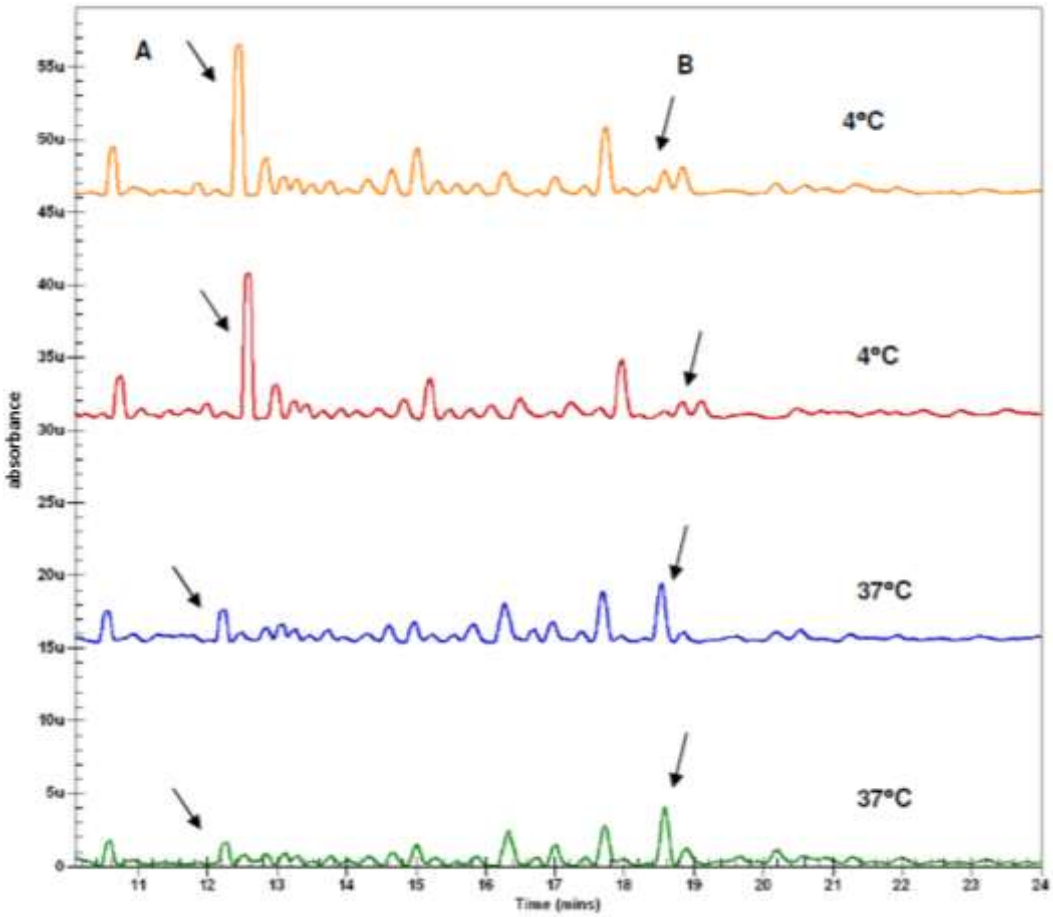

Figure 3.60. EVA trace depicting the separation of *L. monocytogenes* H101620552 protein extracts expressed at 4°C (orange and red traces) and 37°C (blue and green traces). Replicates of each sample were run. The plot shows absorbance (y-axis) versus time in minutes (x-axis). Clear differences are indicated by black arrows as peak A and peak B. Peak A is appears to exhibit greater expression at 4°C than at 37°C, while Peak B appears to exhibit greater expression at 37°C than at 4°C. (Image obtained from deltaDOT).

4: Discussion

The symptoms associated with listeriosis are severe (with 20-30% of cases resulting in mortality). It is therefore important to be able to rapidly identify *L. monocytogenes* as well as discriminate beyond the species level, as such information is valuable for outbreak investigations. Subtyping information ultimately contributes to implementation of control measures required to reduce the risk of infection to unexposed individuals. Currently subtyping methods (see Section 1.2.6.3) each have limitations, consequently more recent technologies such as MALDI-TOF-MS, SELDI-TOF-MS and LC-MS/MS were explored in this study.

Experiemental work particularly in proteomics is often subject to huge variables which may affect the validity of the data presented and subsequently result in incorrect or inconclusive findings. Consideration was therefore given to this fact before experimental work was carried out. Care was taken to implement appropriate negative and positive controls to reduce variables and to ensure that the resulting data was reproducible. This also ensured that all data was robust and that conclusions were derived confidently. The work began by devising a method for the effective lysis of various *Listeria* species. In this work, the negative controls were Gram stained images of unlysed cells with which the stained images of lysed cell debris could be compared. Reproducibility was confirmed when the same result was evident across all species. This will be discussed in detail later. The study then moved on to characterisation of *Listeria* using MALDI-TOF-MS and SELDI-TOF-MS derived dendrograms. In both instances the negative control was the matrix, in which, as expected no ions were detected. In the case of MALDI-TOF-MS the positive control was the BTS: a protein extract of *E. coli* supplied by Brucker. Identification of this organism was an indication that the instrument and identification procedure was in working condition, therefore giving credibility to the identity and characterisation of unknown samples. In the case of SELDI-TOF-MS the negative control was also the matrix. A separate positive control was not used as it was decided that the molecular weight standard supplied by Bio-Rad was sufficient. A heat map (which is a representation of up- and down-regulated protein) was generated from SELDI-TOF-MS generated spectra, care was also taken to ensure that the same amount of protein extracts (6µg) was used in each experiment, as this further reduces variability and provides a basis for comparative expression.

In some experimental designs, it is not always possible to introduce a positive and a negative control. In such instances, where appropriate the data are made robust by conducting experiments with a number of biological replicates. This was the case when invesitigating proteins differentially expressed at 4°C and 37°C. A total of 7 isolates were tested in biolological triplicates using two proteomics methods 1-D SDS PAGE followed by band intensity measurement and 1D SDS PAGE followed by LC-MS/MS analysis. The same amount of protein (5µg) was used in each experiment. The differences obsereved between the two conditions were consistently observed. This was the case for all biological replicates across all 7 isolates. This reproducibility lent additional support to findings and conclusions, which is discussed in further detail later.

As cited by Dare, the possibility of using MALDI-TOF-MS as a characterisation tool for microorganisms was first reported in three separate studies: Claydon et al. (1996), Holland et al. (1996), and Krishnamurthy et al. (1996) (Dare 2005). Claydon and colleagues, for example, clearly showed the difference that existed among the partial spectra of *Staphylococcus aureus* (SA), *Citrobacter freundi* (CF) and *Escherichia coli C*J532 NCTC 50167 (ECC2) (Figure 4.1). These differences allowed the three genera to be identified from a quick visual inspection. Currently, MALDI-TOF-MS is coupled with software analysis, negating the need for visual inspection.

Subsequently, Shah and colleagues used MALDI-TOF-MS to discriminate various pathogenic species (Shah et al. 2000). Since many of the pathogenic properties of a cell are surface-associated, they reasoned that such a targeted approach would simultaneously shed light on the pathpgenic potential of the strains. For Gram positive species, 5-chloro-2-mercaptobenzothiazole (CMBT) matrix, which enables profiling based on unique surface proteins, was used. However, they discovered that surface-associated proteins are markedly affected by environmental parameters such as growth media, pH and temperature such that a MALDI-TOF-MS spectrum of a strain grown on blood and nutrient agar are different (Shah et al. 2000). CMBT was subsequently superseded by DHB and HCCA, and lead to improvements in identification. These matrices permit detection of ribosomal proteins which are abundant in the cell, stable and unique for species regardless of culture conditions (Welker and Moore 2010). In this study the application of HCCA matrix to formic acid extracted proteins yielded greater amounts of protein ions (Figures 3.14a, 3.14b, 3.16a and

3.16b). This yielded more confidence in microbial identification to the species level (Table 3.4) (Culak et al. 2012).

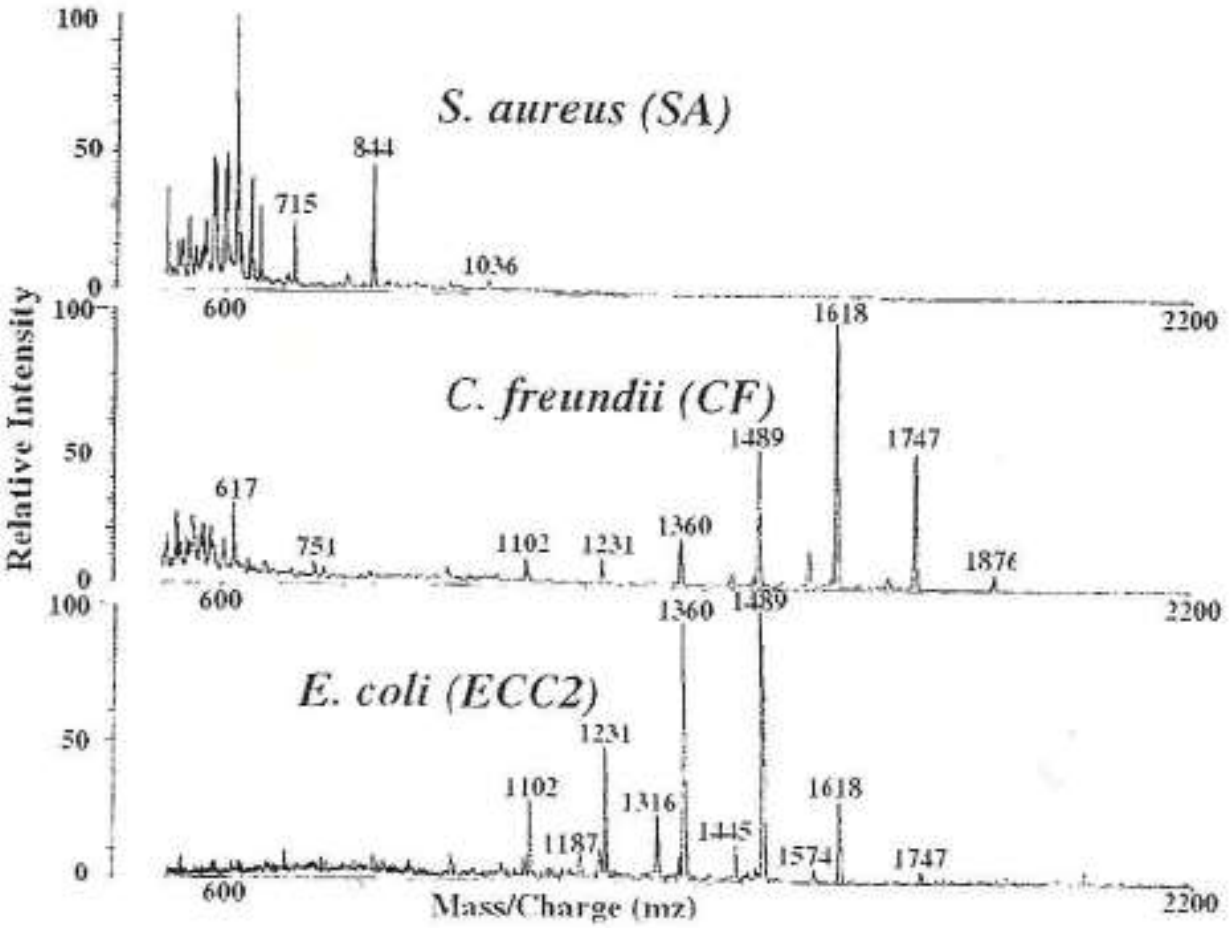

Figure 4.1. Partial, positive ion, mass spectra of SA, CF and ECC2. Relative peptide/protein ion intensity (y-axis) and mass/charge (m/z) (x-axis). SA peaks are in the lowest molecular weight range, whilst CF is distinguishable from ECC2 due to the difference in relative intensity of the 1618 Da. The spectra therefore show that each isolate has a set of ions that may serve as a unique fingerprint for identification amongst other bacteria (taken from Claydon et al., 1996).

In 2008, Barbuddhe and colleagues also reported the successful rapid identification of all species, (except newly discovered *L. marthii* and *L. roucourtiae*), and typing of *L. monocytogenes* using MALDI-TOF-MS (Barbuddhe et al. 2008). They reported that two different peak pairs 5,597/11,193 and 5,590/11,179 Da led to the separation of *L. monocytogenes* into lineages I and II respectively, and that a 7970 Da mass ion led to identification of *L. monocytogenes* lineage III isolates.

In this study, the MSP dendrogram showed that *L. grayi* distantly separated from other *Listeria* species (Figure 3.18). The topography of the tree is similar to that derived by 16S rRNA sequencing (Figure 4.2) and highlights congruency between methods.

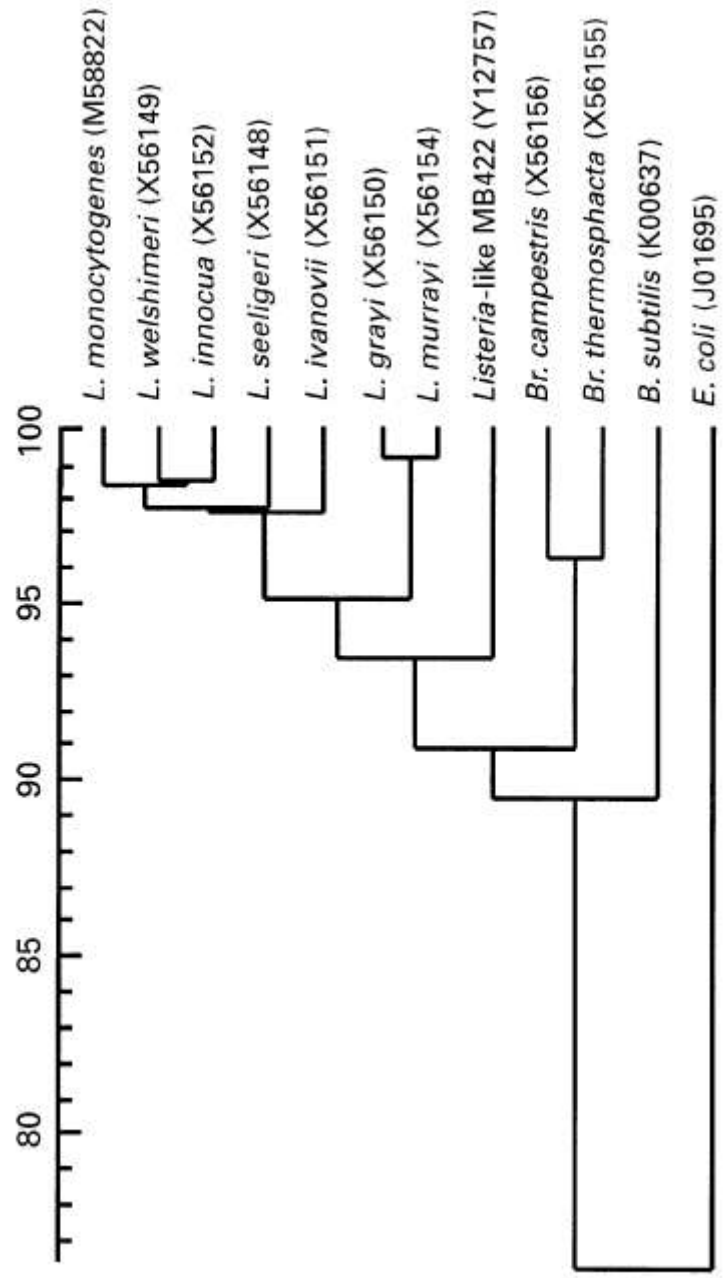

Figure 4.2. Phylogenetic tree of *Listeria* species, *Brochothrix* species, *Bacillus subtilis* and *E. coli* based on sequence analysis of 16S rRNA gene. Distance level (y-axis) species name (x-axis). The dendrogram shows the relationship between *Listeria* species, *Brochothrix* species, *B. subtilis* and *E.coli*. All *Listeria* species are closely related forming one cluster, with the exception of *L. grayi* which separates into a separate phena. *Brochothrix* is the only genus in the Listereacea family along with *Listeria* and clusters in separate phena as did *B. subtilis* and *E.coli* (taken from Rijpens et al. 1998).

The MSP dendrogram shows that the remaining species were clustered into 5 major phena, each with further subdivisions (Figure 3.19). The results also show that these phena are not clustered according to their serotypes. This is an expected result as serotypes are based on flagella and somatic proteins, while the HCCA matrix used for MALDI-TOF-MS spectra generation allows the analysis of ribosomal proteins. As a result, it would be more appropriate to view these results as an emergence of a new descriptive category, referred to as MALDI types.

Unlike sample preparation for MALDI-TOF-MS (which simply required a nominal formic acid extraction), a preamble to SELDI-TOF-MS analysis required selecting a suitable growth phase for harvesting cells from BHI broth, and devising a suitable extraction method which was reproducible. As previously mentioned the conserved size of the *Listeria* genome is 28 - 32 Mb. Therefore, theoretically it could be expected that a protein concentration of approximately 28 - 32 mg/ml would be harvested using an efficient lysis method. However, in reality this is not possible due to the factors previously mentioned (see section 1.3.5), as a result the focus was to devise a reproducible method which allowed extraction of as much protein as possible.

The first measure taken was to harvest cells from BHI broth which were in their exponential phase (see section 3.1.1). The impact of this would be the ability to obtain a larger quantity of viable and healthy cells from which a larger amount of protein may be harversted. The second measure taken was to investigate three cell lysis methods. Of the three lysis methods investigated in this study (pressure cycling, glass bead beating and enzymatic endolysin), results showed that lysis of *Listeria spp*. with endolysin was most efficient in terms of the amount of cells which were no longer visibly intact after incubation with the enzyme, and the amount of protein released. The former was evident upon examination of the cell debris, as generally intact cells appeared to be absent when 5 µg of endolysin was used to lyse a 100 mg cell pellet. By contrast, intact cells were visible following glass bead beating (Figure 3.5) or pressure cycling. This evidence concurs with research published by Lossner and colleagues, in which complete lysis of *L. monocytogenes* WSLC1001 cells was demonstrated by a plot of absorbance against time. They reported that the *L. monocytogenes* cell suspension was cleared after 8-10 minutes of endolysin treatment (Figure 1.15) (Loessner, Schneider, and Scherer 1995). The data from the current study suggests that the amount of protein

extracted from *L. monocytogenes* F2365 cells was higher when endolysin was used in conjunction with glass bead beating in comparison to lysis by pressure cycling and glass bead beating only. However, in comparison to lysis with glass beads beating only, lysis with endolysin consistently resulted in the identification of fewer proteins across all three biological replicates (Table 3.1). For this reason, lysis with glass beads was the preferred method for producing protein extracts for SELDI-TOF-MS analysis, and subsequently for investigating proteins that were differentially expressed at 4°C and 37°C.

In this study analysis of extracted proteins on a 1-D SDS gel (Figure 3.31) showed diversity between *Listeria* and *Brocothrix* species. The protein profiles show that several bands were consistently present amongst all the species. In addition, it was also evident that in *B. campestris* a protein band in the 3.5 - 10 kDa marker region was absent from *L. innocua*, *L ivanovii* subsp *ivanovii*, *L. monocytogenes* and *B. thermosphacta*. Here the huge diversity among the strains was also visualised through a heat map (Figure 3.39), supporting the view that analysis of SELDI-TOF-MS data would provide greater insight into *Listeria* species diversity. The heat map showed that a number of mass ions were differentially expressed, providing a visual image of areas of the mass spectrum that may be useful for biomarker discovery. The heat map resolved isolates into 5 phena. Members of the *Brochothrix* genus, (the only taxon belonging to the *Listeriaceae* family alongside the genus *Listeria*), did not cluster into a separate phenon, suggesting a large number of common cytosolic proteins among these genera despite their phylogenetic distance.

Unlike MALDI-TOF-MS where there has been considerable development in the technology, SELDI-TOF-MS has remained largely unchanged since its inception by the parent company, Ciphergen Biosystems, and its transfer to the new company, Bio-Rad, (Hercules, CA, USA). The instrument (PBS ll) was superseded by the Series 4000 instrument but changes were mostly in the introduction of new software and not technology. The data generated is often compared to an SDS-PAGE gel because the software presents the mass ions into a ‘Gel View’ image (Figure 1.14)

However, SELDI-TOF-MS is more complex than SDS-PAGE in terms of resolution (Figure 1.14) while the selective sample of the affinity chips makes it far more versatile. The SELDI technology was designed to perform MS analysis of protein mixtures retained on

chromatographic array surfaces which are made through chemical coupling affinity characteristics, such as ion-exchange, hydrophobicity, metal binding etc. Compounds dock onto the surface through the selected affinity interactions whilst non-binding "contaminants" are removed by washing. The captured molecules (which are non-covalently bound) are then analysed by MALDI-TOF-MS which provides molecular weight information. Once molecular-docking is achieved, the mass spectrum is usually obtained within minutes (Shah et al. 2005). It produces a spectrum of complex protein mixtures based on the mass-to-charge ratio of the proteins and on their binding affinity to the ProteinChip surface. Differentially expressed proteins may be determined from these protein profiles by comparing peak intensities, often represented as 'Heat Maps'. Comparison of the protein peak patterns obtained from isolates grown under similar conditions provides a unique protein fingerprint pattern between bacterial strains as seen here for various strains of *Listeria spp* (Figure 3.39).

Proteins, rather than DNA or RNA, carry out most of the cellular functions. Therefore, the direct measurement of protein levels and activity within the cell is the best determinant of overall cellular function. Moreover, since there is often a poor correlation between transcript and protein levels, an accurate conclusion regarding protein function based upon mRNA levels is currently difficult to attain. Proteomic analysis, however, is a valuable means of determining cellular function and can now be measured accurately. Furthermore, it can also play a pivotal role in mapping protein profiles in different sample groups, e.g. aggressive vs benign strains or the same strain grown at different temperatures to search for differential protein expression markers. The result of such an experiment is a list of proteins that are up- or down-regulated between both states. Currently, SELDI-TOF-MS can display differential patterns but not identify the proteins. For this, an LC-MS/MS based approach is required and has been used to map out differentially expressed proteins of *L. monocytogenes* grown at 4^{o}C and 37^{o}C.

The differential expression of *L. monocytogenes* proteins at 4°C and 37°C is of considerable interest. Cacacae and colleagues used type strain NCTC 10357 (also referred to as *L. monocytogenes* EGD-e) and found that higher amounts of enzymes which play a role in energy production were up-regulated at 4^{o}C (Cacace et al. 2010). The current study extended this work by the inclusion of clinical and food isolates which may be more appropriate. A survery of the literature shows that most studies investigating the molecular mechanisms of *L.*

monocytogenes are conducted using soley the type strain. As mentioned earlier (see section 1.1.1) the provenance of the type strain was a diseased rabbit (Gibbons 1972). During this study it was hypothesised that the molecular mechanisms involved in infection of other animals, including the diseased rabbit, may differ from those involved in infecting the human population. Provided that the hypothesis is correct, the implications would be observed differences in the expression level of induced genes and subsequently proteins. The type strain could therefore be atypical and possibly an unideal model for studying molecular mechanisms of strains that contaminate food and infect the human population. Routine tests already show that the type strain is atypical. It is non-hemolytic and lacks flagella, properties that are more compatible with *L. innocua*, therefore, in 1983, it was suggested that a more typical isolate NCTC 7973 should be declared the type strain (Jones and Seeliger 1983). For the above reasons differential expression at 4°C and 37°C was investigated using a variety of isolates which included the type strain, clinical isolates and food isolates. It was envisaged that the study may reveal further evidence of the atypical nature of the type strain. The organisms chosen belonged to serotypes 4b, 1/2b, 1/2c and 1/2a, (as these are implicated in 95% of hospitalisation cases (Nightingale 2010) and had AFLP patterns I, II, VII and IX respectively (the HPA's statistics show that these patterns occur most frequently in the respective serotypes (data not published)). A total of 7 isolates were tested; 3 clinical isolates and 3 food isolates, in addition to the type strain.

The 1-D gel analysis was carrried out on all isolates, two of which are illustrated (Figure 3.42 and 3.43). The results show the presence of an approximately 10 kDa protein band (indicated by black arrows) which was more intense at 4°C than at 37°C. The gel also shows the presence of a similar sized band (indicated by black arrows) which was more intense at 37°C than at 4°C. The Bio-Rad Image Lab 4.0 software analysis results (Figure 3.44) showed the presence of an approximately 10 kDa protein band which was more intense at 4°C than at 37°C. The same 1-D gels also showed the presence of an approximately 10 kDa band which was more intense at 37°C than at 4°C.

The differentially expressed proteins were analysed using LC-MS/MS. The Scaffold software which was used to sort the LC-MS/MS data, provided an output of quantification as a normalised spectrum count. Normalised spectrum counts refer to the number of spectra associated with all identified peptides that are representative of a protein. Subsequently,

spectrum counts are correlated with protein abundance. In this study, a number of the proteins identified were designated 'hypothetical', that is proteins which at present do not have a known function. Nevertheless, analysing their expression level at 4°C and 37°C has made it possible to putatively associate them with metabolic switches between these two phases. In this study 9 proteins were identified as either up- or down-regulated at 4°C and 37°C (Figures 3.45 - 3.62 and Table 3.5), and ranged from 7 - 13 kDa in size, and therefore showed that they may have contributed to the protein bands observed in the 10 kDa region of the 1-D gels. Two of the 4 proteins up-regulated at 4°C and down-regulated at 37°C, were 'hypothetical proteins'. The remaining 2 were phosphotransferase system (PTS) which plays a role in modulating the use of carbon sources in bacteria (Domenech et al. 2012) and 50S ribosomal protein L29 which plays a role in protein synthesis. Of the 5 proteins up-regulated at 37°C and down-regulated at 4°C, one was a 'hypothetical protein'. The remaining 4 were Co-chaperonin GroES and 30s ribosomal protein S16 which play a role in protein folding and synthesis respectively, an anti-anti sigma factor which participates in modulating gene expression in response to stress (Homerova et al. 2012) and histidine phosphocarrier protein (HPr) which forms part of PTS (Domenech et al. 2012).

In addition to these differentially expressed proteins, 3 were identified as uniquely expressed at either 4°C or 37°C. Hypothetical protein lmo0056 was uniquely expressed at 37°C in all isolates tested (Figure 3.56). Hypothetical protein lwe06778 was only expressed at 4°C in all isolates except NCTC 10357, in which it was present at both temperatures (Figure 3.54). Phosphoribosyl-AMP cyclohydrolase was expressed solely at 4°C in all isolates except NCTC 10357, in which it was absent at both temperatures (Figure 3.55). This data further supports the view that the type strain of *L. monocytogenes* is atypical. The data also strongly supports the decision made at the beginning of the study, not to base the entire investigation on the type strain as done in other studies designed to study this phenomenon. The fact that this type strain, NCTC 10357, which closely resembles *L. innocua* behaves so differently suggests that the mechanistic changes associated with growth at 4°C and 37°C may be restricted to *L. monocytogenes*.

The LC-MS/MS and Scaffold software analysis showed that the size of hypothetical protein lmo0056 was 11 kDa, hypothetical protein lwe06778 was 11 kDa and that phosphoribosyl-AMP cyclohydrolase was 12 kDa. The data obtained by high resolution capillary

electrophoresis (deltaDot) also supports the evidence of an increased abundance of small molecular weight proteins at 4°C as this data showed a 12 kDa protein peak at 4°C which was lower at 37°C (Figure 3.59 and 3.60).

As mentioned earlier, it is difficult to ascertain the role of hypothetical proteins lmo0056 and lwe06778. Further work, such as gene knockout studies would be necessary to elucidate their role, however, at present there is evidence from this study, that they may serve as possible biomarkers of the presence of *L. monocytogenes* in cold RTE foods. Hypothetical protein lwe06778 may serve as a cold storage biomarker, while lmo0056 may serve as a warm temperature indicator of the species.

Phosphoribosyl-AMP cyclohydrolase, (which was uniquely expressed at 4°C), is involved in the histidine biosynthesis pathway, an unbranched pathway with no route to bypass any of the 10 enzymes involved (Henriksen et al. 2010). In this pathway, ATP phosphoribosyltransferase (HisG) catalyses the first step resulting in the condensation of ATP and 5-phosphoribosyl 1-pyrophosphate (PRPP) to form phosphoribosyl-ATP. In the second step, the triphosphate of phosphoribosyl-ATP is then hydrolysed by phosphoribosyl-ATP pyrophosphohydrolase (HisE) to form phosphoribosyl-AMP. In the third step, the purine ring of phosphoribosyl-AMP is hydrolysed by phosphoribosyl-AMP cyclohydrolase (HisI) (the protein identified in this study), to form phosphoribosyl-formimino-5-aminoimidazole carboxamide ribonucleotide, which is denoted as phosphoribosyl-formimino-AICAR-P for short. In the fourth step, this product is converted to phosphoribulosyl formimino-5-amino imidazole carboxamide ribonucleotide denoted as phosphoribusyl-formimino-AICAR-P by the enzyme phospho-D-ribosyl formimino-5-amino-1-phosphoribosyl-4-imidazole carboxamide isomerase (His A) in a process called Amadori rearrangement. In the fifth step, this product is then cleaved by glutamine imidazole transferase (HisH) (which in the process converts a glutamine molecule to glutamate) to form 5-aminoimidazole-4-carboxamide 1-beta-D ribofuranosyl 5'-monophosphate (AICAR) which is used to synthesise purines and imidazole glycerol phosphate (referred to as imidazole acetol P or IGP). In the sixth step, IGP is dehydrated by imidazole glycerol phosphate dehydratase (IGPD) producing imidazole acetol phosphate (imidazole acetol-P), which is transaminated in the seventh step by histidinol phosphate amino transferase (HisC) to form L-histidinol-phosphate. In the eighth step, L-histidinol-phosphate is converted to L-histidinol by histidinol phosphatase (HisB). In

the ninth step L-histidinol-phosphate is converted to L-histidinal by histidinol dehydrogenase (HisD) and in the final step HisD is also responsible for converting L-histidinal to L-histidine (Figure 4.3) (Henriksen et al. 2010).

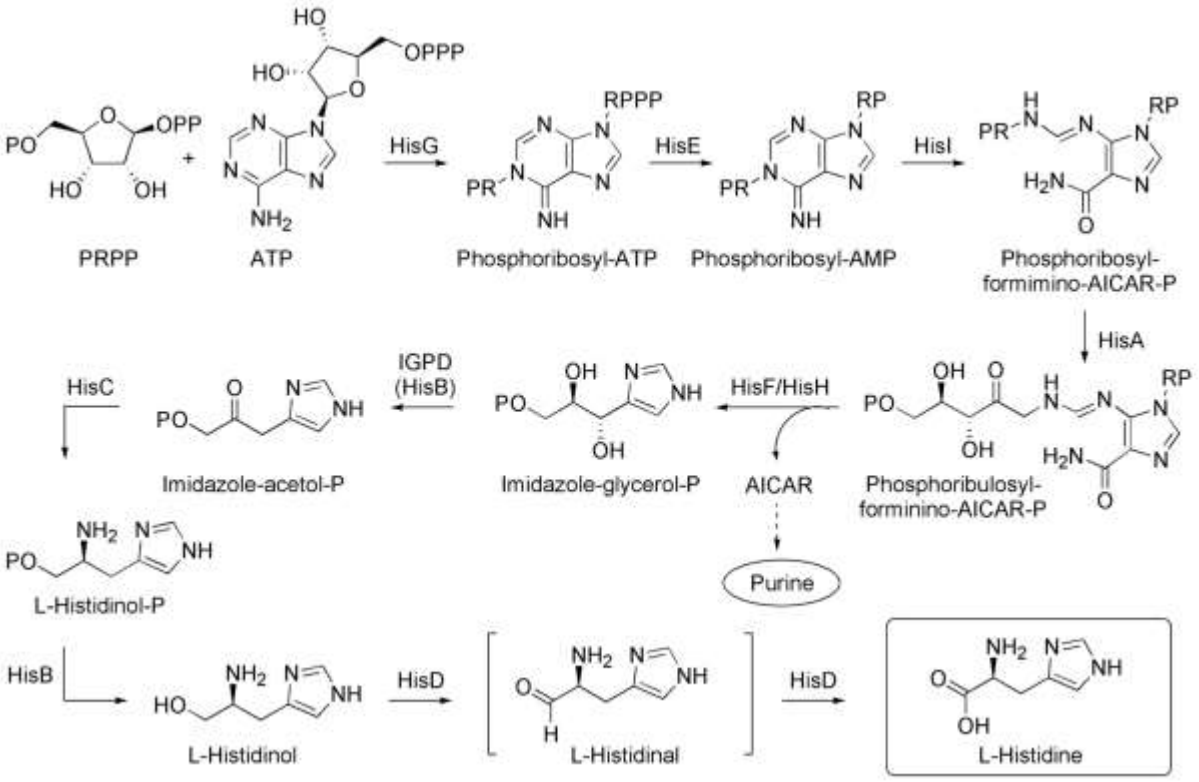

Figure 4.3. Histidine biosynthesis pathway The pathway is an unbranched with no route to bypass any of the 10 enzymes involved, the result of which is the synthesis of L-histidine (taken from Henriksen et al. 2010).

A survey of the literature did not offer an explanation for the up regulation of the histidine biosynthesis pathway at low temperatures in *L. monocytogenes*, however, a possible explanation may be as follows. Antarctic psychotropic bacteria are frequently used as models for studying cold adaptation, one of which is *Pseudomonas syringae*, which has the ability to grow below 0°C (Kannan et al. 1998; Regha, Satapathy, and Ray 2005). It was shown that *P. syringae* encodes *hut* genes that are involved in the histidine utilisation pathway at low temperatures (Kannan et al. 1998). Similar to antarctic psychotrophic bacteria, *L. monocytogenes* is capable of surviving below 0°C, it therefore seems plausible that *L. monocytogenes* may also have *hut* genes which are vital to the organism's survival at low temperatures. A survey of the literature showed that *Bacillus subtilis*, a close relative of *Listeria*, utilises L-histidine as a carbon and nitrogen source under nutrient limiting conditions. In *B. subtilis*, the genes responsible for L-histidine utilisation are within the hut operon, which consists of *hutP*, *hutH*, *hutU*, *hutI*, *hutG*, and *hutM* (Kumarevel, Mizuno, and Kumar 2005). By analogy, it seems plausible that at low temperatures *L. monocytogenes* switches on the expression of HisI in order to enable the biosynthesis of L-histidine, the utilisation of which is required as a carbon and nitrogen source under cold stress conditions. The ability to activate the histidine biosynthesis and histidine utilisation pathway may be vital to the organism's survival at low temperatures, as such temperatures may limit the activity of enzymes that would at ambient temperatures facilitate the uptake of environmental carbon and nitrogen sources. This hypothesis may form the basis for a future study to expand the present work.

The results shown here could have commercial implications, utilising the hypothetical protein lwe06778 and phosphoribosyl-AMP cyclohydrolase as biomarkers for the presence of the organism in foods being preserved at refrigeration temperatures. Alternatively, inhibitors of these proteins may be suitable candidates for preserving cold stored food against *L. monocytogenes*. This idea may be supported in a study by Henriksen and colleagues in which they used flux balance analysis to identify unconditionally essential *S. aureus* enzymes. One family of proteins identified in their study was those involved in histidine biosynthesis (Figure 4.3), and which included phosphoribosyl-AMP cyclohydrolase. Their aim was to screen various compounds in order to find an inhibitory candidate, and ultimately propose an antibacterial treatment alternative in an era where multiple drug resistant organisms pose a major healthcare challenge. They performed virtual screening to identify compounds which

docked into the active sites of all 9 enzymes involved in histidine biosynthesis (HisG, HisE, HisI, HisA, HisF, HisH, HisB (IGPD), HisC and HisD (Henriksen et al. 2010). They found that three enzymes HisI, IGPD and HisC had docking sites for 18 inhibitory compounds. Compounds HisI1, HisI2, HisI4, HisI8, HisI19 and HisI11 were selected inhibitors for HisI, compounds IGDP1, IGDP6, IGDP10, IGDP13, IGDP14, IGDP16 and IGDP17 were selected inhibitors for IGDP, and HisC5, HisC9, HisC11, HisC14, HisC16 and HisC19 were selected as inhibitors for HisC (Henriksen et al. 2010). Their disc inhibition assay studies showed that, relative to ampicillin, HisI2 showed weak inhibition, IDPG1 showed strong inhibition, followed by IGPD13, IGPD6 and HisC9 which showed weak inhibition (Figure 4.4).

Inhibitor of phosphoribosyl-AMP cyclohydrolase (HisI)

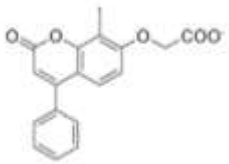

HisI2

Inhibitor of imidazole glycerol phosphate dehydratase (IGPD)

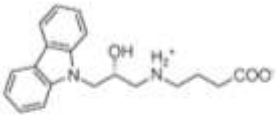

IGPD1

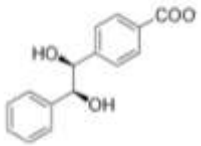

IGPD6

Inhibitor of histidinol phosphate amino transferase (HisC)

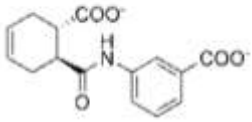

HisC9

Figure 4.4. Effective inhibitor molecules: HisI2, IGPD1, IGPD6 and HisC9 of enzymes phosphoribosyl-AMP cyclohydrolase (HisI), imidazole glycerol phosphate dehydratase (IGPD), and histidinol phosphate amino transferase (HisC) (taken from Henriksen et al. 2010).

Evolutionarily, the histidine biosynthesis pathway is highly conserved among different bacterial species (Henriksen et al. 2010), and in the case of *L. monocytogenes* the results presented in this study suggests that it is activated at 4°C. Based on the data generated by Henriksen and colleagues, and the findings presented in this thesis, it is suggested that HisI2, IDPG1, IDPG13, IDPG6 and HisC9 are likely to be inhibitors of *L. monocytogenes* when grown at 4°C.

IGPD has already been used as a target to design herbicides (Ohata, Mori, and Ward 1997) and Henriksen's findings indicate that the enzyme is a potential target for MRSA patient therapy. It therefore seems plausible that a similar approach may be undertaken for *L. monocytogenes* during cold storage of RTE products. The implication of these findings may be important to public health as this could contribute to the reduction in the number or listeriosis cases, which has recently seen a steady increase partly due to the consumption of contaminated cold stored RTE foods.

General Conclusion

This study has shown that MALDI-TOF-MS and SELDI-TOF-MS are potential tools for further discrimination of *L. monocytogenes* isolates with cluster analysis demonstrating clear distinction of isolates into separate phena. The data from MSP dendrogram derived from MALD-TOF-MS spectra strongly correlated with 16S rRNA dendrograms. Finally, the identification of hypothetical protein lwe06778 and phosphoribosyl-AMP cyclohydrolase which were both uniquely expressed at 4°C, suggest great potential as biomarkers for the presence of *L. monocytogenes* in cold stored RTE foods, with the possibility of phosphoribosyl-AMP cyclohydrolase being a target for arresting the growth of the organism in cold storage through the introduction of an inhibitor of the enzyme.

Future Work

The similarity between dendrograms produced by MALDI-TOF-MS and 16S rRNA is in accord with the view that MALDI-TOF spectra are derived from abundant ribosomal proteins. Currently, multilocus sequencing typing is now being carried out on ribosomal proteins encoding genes (rMLST). By sequential disruption of the gene of each ribosomal protein followed by comparative analysis of the MALDI-TOF data, it should be possible to begin assigning which ribosomal proteins contribute to the mass ions revelaed in the spectra of each species. It should therefore be possible in the near future to better define each species and then improve the resolution of MALDI-TOF-MS to the level of sub species and types.

At the commencement of this study, the goal was to develop MALDI-TOF-MS for use at the species level. Today that goal has been reached and MALDI is being used at the forefront of clinical diagnostics. Several laboratories aim to develop the system as a typing tool. The advantage this would bring food safety are immence in terms of speed, accuracy and cost.

The present study also focused on the differential expression of *L. monocytogenes* grown at 4°C and 37°C. This was done in order to simulate the two extremes where this species may reside and thrive in cold stored RTE food and in infect man, respectively. As expected there were changes in the protein expression associated with each growth temperature. However,

the type of protein analysis used (LC-MS/MS) relies on the analysis of trypsin digested peptides to reveal protein identity (bottom-up approach). This method, while quite comprehensive, misses a great deal of the post-translational modifications which are now readily mapped by new spectrometry methods, such as top-down proteomics. Future studies should therefore be based on a series of temperatures using new high resolution MS/MS methods to follow these translational changes. This would provide detailed insight into the mechanism associated with these changes and may reveal new approaches to stem the rise of this species as a human pathogen.

Relevance in Diagnostics

The discovery of proteins which are uniquely expressed at 37°C and 4°C may have diagnostic applications and could prove to be useful in the identification of *L. monocytogenes* in different environments. Since *L. monocytogenes* expresses hypothetical protein lwe06778 and phosphoribosyl-AMP cyclohydrolase uniquely at 4°C, it is envisaged that a biosensor could be used to detect the presence of the contaminant in cold stored RTE foods. Detection of the organism in this environment could be instrumental in ensuring safety against this foodborne pathogen. The same principle could also be applied for the detection of *L. monocytogenes* in clinical samples. In this case hypothetical protein lmo0056 which was uniquely expressed at 37°C would be suitable for patient diagnosis. Biosenors remain a viable diagnostic method. Recently Seung-Ho and Bhunia used a multiplex optic biosensor for the detection of *L. monocytogenes*, *E. coli* O157:H7 and *Salmonella enterica* in ready-to-eat meat samples (Sueng-Ho and Bhunia 2013). Briefly, they used specific antibody coated fibres to immobilse or trap the organisms, then added AF-reporter antibodies which are specific to the organisms. The fluorsence was then detected with a fluorometer which indicated the presence of the microbial contaminants. This multiplex biosensor technology could be developed for detection of *L. monocytogenes* at 4°C and 37°C.

References

Allberger, F. and Wagner, M. (2010) Listeriosis: a resurgent foodborne pathogen. *Clin Microbiol Infect*, **16** 16-23.

Barbuddhe, S.B., Maier, T., Schwarz, G., Kostrzewa, M., Hof, H., Domann, E., Chakraborty, T., and Hain, T. (2008) Rapid identification and typing of listeria species by matrix-assisted laser desorption ionization-time of flight mass spectrometry. *Appl Environ Microbiol* **74**, 5402-5407.

Begley, M., Hill, C., and Gahan, C.G. (2006) Bile salt hydrolase activity in probiotics. *Appl Environ Microbiol* **72**, 1729-1738.

Bergey, D.H. (1934) *Bergey's Manual of Determinative Bacteriology*, 4th ed. London, Baillière, Tindall and Cox.

Bergey, D.H., Breed, R.S., Murray, E.G.D., and Hitchens, A.P. (1939) *Bergey's Manual of Determinative Bacteriology*, 5th ed. London, Baillière, Tindall and Cox.

Bille, J., Catimel, B., Bannerman, E., Jacquet, C., Yersin, M.N., Caniaux, I., Monget, D., and Rocourt, J. (1992) API Listeria, a new and promising one-day system to identify Listeria isolates. *Appl Environ Microbiol* **58**, 1857-1860.

Bompard, G. and Caron, E. (2004) Regulation of WASP/WAVE proteins: making a long story short. *J Cell Biol* **166**, 957-962.

Bortollussi, R. (2008) Listeriosis: a primer. *CMAJ* **179**, 795-797.

Breed, R.S., Murray, E.G.D., and Hitchens, A.P. (1948) *Bergey's Manual of Determinative Bacteriology*, 6th ed. London, Baillière, Tindall and Cox.

Buchanan, R. E. and Gibbons, N. E. *Bergey's Manual of Determinative Bacteriology*. 8th, 593-596. (1974) Baltimore, The Williams and Wilkins Company.

Bucknall M., Fung K.Y., and Duncan M.W. (2002) Practical quantitative biomedical applications of MALDI-TOF mass spectrometry. *J Am Soc Mass Spectrom* **13**, 1015-27.

Cacace, G., Mazzeo, M.F., Sorrentino, A., Spada, V., Malorni, A., and Siciliano, R.A. (2010) Proteomics for the elucidation of cold adaptation mechanisms in *Listeria monocytogenes*. *J Proteomics* **73**, 2021-2030.

Cervantes, J., Nagata, T., Uchijima, M., Shibata, K., and Koide, Y. (2008) Intracytosolic *Listeria monocytogenes* induces cell death through caspase-1 activation in murine macrophages. *Cell Microbiol* **10**, 41-52.

Chan, Y.C., Hu, Y., Chaturongakul, S., Files, K.D., Bowen, B.M., Boor, K.J., and Wiedmann, M. (2008) Contributions of two-component regulatory systems, alternative sigma factors, and negative regulators to *Listeria monocytogenes* cold adaptation and cold growth. *J Food Prot* **71**, 420-425.

Chassaing, D. and Auvray, F. (2007) The lmo1078 gene encoding a putative UDP-glucose pyrophosphorylase is involved in growth of *Listeria monocytogenes* at low temperature. *FEMS Microbiol Lett* **275**, 31-37.

Chen, S., Li, J., Saleh-Lakha, S., Allen, V., and Odumeru, J. (2011) Multiple-locus variable number of tandem repeat analysis (MLVA) of *Listeria monocytogenes* directly in food samples. *Int J Food Microbiol* **148**, 8-14.

Chico-Calero, I., Suarez, M., Gonzalez-Zorn, B., Scortti, M., Slaghuis, J., Goebel, W., and Vazquez-Boland, J.A. (2002) Hpt, a bacterial homolog of the microsomal glucose- 6-phosphate translocase, mediates rapid intracellular proliferation in *Listeria*. *Proc Natl Acad Sci U S A* **99**, 431-436.

Corcoran, D., Clancy, D., O'Mahony, M., Grant, K., Hyland, E., Shanaghy, N., Whyte, P., McLauchlin, J., Moloney, A., and Fanning, S. (2006) Comparison of *Listeria monocytogenes* strain types in Irish smoked salmon and other foods. *Int J Hyg Environ Health* **209**, 527-534.

Culak, R., Fang. M., Bishop Simon, S., Dekio, I., Rajakaruna, L., Shah, H. (2012) Changes in the Matrix Markedly Enhance the Resolution and Accurate Identification of Human

Pathogens by MALDI-TOF MS. *J. Anal. Bioanl. Techniques* S2:002. doi:10.4172/2155-9872.S2-002.

Dare, D. (2005) "Microbial Identification Using MALDI-TOF-MS," *In Encyclopedia of Rapid Microbiological Methods*, M. J. Miller, ed., Baltimore: Davis Healthcare International Publishing, pp. 19-56.

De Vos, P., Garrity, G. M., Jones, D., Krieg, N. R., Ludwig, W., Rainey, F. A., Schleifer, K., and Whitman, W. *Bergey's Manual of Systematic Bacteriology*. 2[3], 244-257. (2009) , Springer Science+Business Media.

den Bakker, H., Cummings C. A., Ferreira1, V., Vatta, P., Orsi1, R. H., Degoricija, L., Barker, M., Petrauskene, O., Furtado, M., and Wiedmann, M. 2010 Comparative genomics of the bacterial genus Listeria: Genome evolution is characterized by limited gene acquisition and limited gene loss. *BMC Genomics* **11**, 688.

Denny, J. and McLauchlin, J. (2008) Human *Listeria monocytogenes* infections in Europe--an opportunity for improved European surveillance. *Euro Surveill* **13**, 8082.

Di, P.A., Novello, L., Montemurro, F., Bonerba, E., and Tantillo, G. (2010) Occurrence of *Listeria monocytogenes* in ready-to-eat foods from supermarkets in Southern Italy. *New Microbiol* **33**, 249-252.

Di Domenico M., Scumaci D., Grasso S., Gaspari M., Curcio A., Oliva A., Ausania F., Di Nunzio C., Ricciardi C., Santini A.C., Rizzo F.A., Romano Carratelli C., Lamberti M., Conti D., La Montagna R., Tomei V., Malafoglia V., Pascali V.L., Ricci P., Indolfi C., Costanzo F. and Cuda G. (2013) Biomarker discovery by plasma proteomics in familial Brugada Syndrome. *Front Biosci* **18**, 564-71.

Domenech, R., Martinez-Gomez, A.I., Aguado-Llera, D., Martinez-Rodriguez, S., Clemente-Jimenez, J.M., Velazquez-Campoy, A., and Neira, J.L. (2012) Stability and binding of the phosphorylated species of the N-terminal domain of enzyme I and the histidine phosphocarrier protein from the *Streptomyces coelicolor* phosphoenolpyruvate:sugar phosphotransferase system. *Arch Biochem Biophys* **526**, 44-53.

Doumith, M., Buchrieser, C., Glaser, P., Jacquet, C., and Martin, P. (2004) Differentiation of the major *Listeria monocytogenes* serovars by multiplex PCR. *J Clin Microbiol* **42**, 3819-3822.

Emonet S, Shah HN, Cherkaoui A, Schrenzel J. (2010) Application and use of various mass spectrometry methods in clinical microbiology. *Clin Microbiol Infect* **16**,1604-13.

Fiedler F. (1988) Biochemistry of the cell surface of Listeria strains: a locating general view. *Infection* **16 Suppl**, S92-7.

Ferreira L., Sanchez-Juanes F., Munoz-Bellido J.L. and Gonzalez-Buitrago J.M. (2010) Rapid method for direct identification of bacteria in urine and blood culture samples by matrix-assisted laser desorption ionization time-of-flight mass spectrometry: intact cell vs. extraction method. *Clin Microbiol Infect* **17**,1007-1012.

Fliss I., Emond E., Simard R.E., and Pandian S. (1991) A rapid and efficient method of lysis of *Listeria* and other gram-positive bacteria using mutanolysin. *Biotechniques* **11**, 453, 456-457.

Forster, B.M., Bitar, A.P., Slepkov, E.R., Kota, K.J., Sondermann, H., and Marquis, H. (2011) The metalloprotease of *Listeria monocytogenes* is regulated by pH. *J Bacteriol* **193**, 5090-5097.

Furrer, B., Candrian, U., Hoefelein, C., and Luethy, J. (1991) Detection and identification of Listeria monocytogenes in cooked sausage products and in milk by in vitro amplification of haemolysin gene fragments. *J Appl Bacteriol* **70**, 372-379.

Gasanov, U., Hughes, D., and Hansbro, P.M. (2005) Methods for the isolation and identification of *Listeria spp*. and *Listeria monocytogenes*: a review. *FEMS Microbiol Rev* **29**, 851-875.

Gekara, N.O., Zietara, N., Geffers, R., and Weiss, S. (2010) *Listeria monocytogenes* induces T cell receptor unresponsiveness through pore-forming toxin listeriolysin O. *J Infect Dis* **202**, 1698-1707.

Gibbons, N.E. (1972) *Listeria* Pirie - Whom does it honour? *Int J Syst Bacteriol* **22**, 1-3.

Gillespie, I.A., McLauchlin, J., Grant, K.A., Little, C.L., Mithani, V., Penman, C., Lane, C., and Regan, M. (2006) Changing pattern of human listeriosis, England and Wales, 2001-2004. *Emerg Infect Dis* **12**, 1361-1366.

Gillespie, I.A., McLauchlin, J., Little, C.L., Penman, C., Mook, P., Grant, K., and O'Brien, S.J. (2009) Disease presentation in relation to infection foci for non-pregnancy-associated human listeriosis in England and Wales, 2001 to 2007. *J Clin Microbiol* **47**, 3301-3307.

Gorski, L. (2008) "Phenotypic Identification," *In Handbook of Listeria monocytogenes*, D. Liu, ed., Boca Raton: CRC Press, pp. 139-168.

Goulet, V., Hedberg, C., Le, M.A., and de, V.H. (2008) Increasing incidence of listeriosis in France and other European countries. *Emerg Infect Dis* **14**, 734-740.

Graves, L.M., Helsel, L.O., Steigerwalt, A.G., Morey, R.E., Daneshvar, M.I., Roof, S.E., Orsi, R.H., Fortes, E.D., Milillo, S.R., den Bakker, H.C., Wiedmann, M., Swaminathan, B., and Sauders, B.D. (2010) *Listeria marthii* sp. nov., isolated from the natural environment, Finger Lakes National Forest. *Int J Syst Evol Microbiol* **60**, 1280-1288.

Gray, M.J., Freitag, N.E., and Boor, K.J. (2006) How the bacterial pathogen *Listeria monocytogenes* mediates the switch from environmental Dr. Jekyll to pathogenic Mr. Hyde. *Infect Immun* **74**, 2505-2512.

Greginat, G. and Grauling-Halama, S. (2008) "Innate Immunity," *In Handbook of Listeria monocytogenes*, D. Liu, ed., Boca Raton: CRC Press, pp. 397-426.

Guerra, M.M., Bernardo, F., and McLauchlin, J. (2002) Amplified fragment length polymorphism (AFLP) analysis of *Listeria monocytogenes*. *Syst Appl Microbiol* **25**, 456-461.

Henriksen, S.T., Liu, J., Estiu, G., Oltvai, Z.N., and Wiest, O. (2010) Identification of novel bacterial histidine biosynthesis inhibitors using docking, ensemble rescoring, and whole-cell assays. *Bioorg Med Chem* **18**, 5148-5156.

Holt, J.G., Krieg, N.R., Sneath, P.H.A., Staley, J.T., and Williams, S.T. (1994) *Bergey's Manaul of Determinative Bacteriology*, 9 ed. Williams and Wilkins.

Homerova, D., Sevcikova, B., Rezuchova, B., and Kormanec, J. (2012) Regulation of an alternative sigma factor sigmaI by a partner switching mechanism with an anti-sigma factor PrsI and an anti-anti-sigma factor ArsI in *Streptomyces coelicolor* A3(2). *Gene* **492**, 71-80.

Jones, D. and Seeliger, H.P.R. (1983) Designation of a New Type Strain for *Listeria monocytogenes* Request for an Opinion. *Int J Syst Bacteriol* **33**, 429.

Julotok, M., Singh, A.K., Gatto, C., and Wilkinson, B.J. (2010) Influence of fatty acid precursors, including food preservatives, on the growth and fatty acid composition of *Listeria monocytogenes* at 37 and 10°C. *Appl Environ Microbiol* **76**, 1423-1432.

Kannan, K., Janiyani, K.L., Shivaji, S., and Ray, M.K. (1998) Histidine utilisation operon (hut) is upregulated at low temperature in the antarctic psychrotrophic bacterium *Pseudomonas syringae*. *FEMS Microbiol Lett* **161**, 7-14.

Kerouanton, A., Marault, M., Petit, L., Grout, J., Dao, T.T., and Brisabois, A. (2010) Evaluation of a multiplex PCR assay as an alternative method for *Listeria monocytogenes* serotyping. *J Microbiol Methods* **80**, 134-137.

Kiehntopf, M., Melcher, F., Hanel, I., Eladawy, H., and Tomaso, H. (2011) Differentiation of Campylobacter species by surface-enhanced laser desorption/ionization-time-of-flight mass spectrometry. *Foodborne Pathog Dis* **8**, 875-885.

Köhling H.L., Bittner A., Müller K.D., Buer J., Becker M., Rübben H., Rettenmeier A.W., Mosel F. (2012) Direct identification of bacteria in urine samples by matrix-assisted laser desorption/ionization time-of-flight mass spectrometry and relevance of defensins as interfering factors. *J Med Microbiol* **61**, 339-344.

Korndörfer, I.P., Danzer, J., Schmelcher, M., Zimmer, M., Skerra, A., Loessner, M.J. (2006) The crystal structure of the bacteriophage PSA endolysin reveals a unique fold responsible for specific recognition of *Listeria* cell walls. *J Mol Biol* **364**, 678-689.

Kuhn, M., Scortti, M., and Vazquez-Boland, J. A. (2008) "Pathogenesis," *In Handbook of Listeria monocytogenes*, D. Liu, ed., Boca Raton: CRC Press, pp. 97-136.

Kumarevel, T., Mizuno, H., and Kumar, P.K. (2005) Characterization of the metal ion binding site in the anti-terminator protein, HutP, of Bacillus subtilis. *Nucleic Acids Res* **33**, 5494-5502.

Lambrechts, A., Gevaert, K., Cossart, P., Vandekerckhove, J., and Van, T.M. (2008) *Listeria* comet tails: the actin-based motility machinery at work. *Trends Cell Biol* **18**, 220-227.

Lamont, R.F., Sobel, J., Mazaki-Tovi, S., Kusanovic, J.P., Vaisbuch, E., Kim, S.K., Uldbjerg, N., and Romero, R. (2011) Listeriosis in human pregnancy: a systematic review. *J Perinat Med* **39**, 227-236.

Leclercq, A., Clermont, D., Bizet, C., Grimont, P.A., Le Fleche-Mateos, A., Roche, S.M., Buchrieser, C., Cadet-Daniel, V., Le, M.A., Lecuit, M., and Allerberger, F. (2010) *Listeria rocourtiae* sp. nov. *Int J Syst Evol Microbiol* **60**, 2210-2214.

Leli C., Cenci E., Cardaccia A., Moretti A., D'Alò F., Pagliochini R., Barcaccia M., Farinelli S., Vento S., Bistoni, F. and Mencacci A. (2013). Rapid Identification of bacterial aand fungal pathogens from positive blood cultures by MALDI-TOF-MS. *Int J Med Microbiol* **13** doi: 10.1016/j.ijmm.2013.03.002.

Little, C.L., Sagoo, S.K., Gillespie, I.A., Grant, K., and McLauchlin, J. (2009) Prevalence and level of *Listeria monocytogenes* and other *Listeria* species in selected retail ready-to-eat foods in the United Kingdom. *J Food Prot* **72**, 1869-1877.

Liu, D. (2006) Identification, subtyping and virulence determination of *Listeria monocytogenes*, an important foodborne pathogen. *J Med Microbiol* **55**, 645-659.

Liu, D. Handbook of *Listeria monocytogenes*. 99-101. (2008) New York, CRC Press.

Liu, D., Lawrence, M. L., Ainsworth, A. J., and Austin, F. W. (2008) "Genotypic Identificatiom," *In Handbook of Listeria monocytogenes*, D. Liu, ed., Boca Raton: CRC Press, pp. 169-202.

Loessner, M. (2005) Bacteriophage endolysins –current state of research and applications. *Curr Opin Microbiol* **8,** 480-487.

Loessner, M.J., Schneider, A., and Scherer, S. (1995) A new procedure for efficient recovery of DNA, RNA, and proteins from *Listeria* cells by rapid lysis with a recombinant bacteriophage endolysin. *Appl Environ Microbiol* **61**, 1150-1152.

McKellar, R.C. (1994) Use of the CAMP test for identification of *Listeria monocytogenes*. *Appl Environ Microbiol* **60**, 4219-4225.

McLauchlin, J. (1997) The identification of *Listeria* species. *Int J Food Microbiol* **38**, 77-81.

Mercanoglu, B., Aykut, S., Ergun, M.A., and Tan, E. (2003) Isolation of *Listeria monocytogenes* by immunomagnetic separation and atomic force microscopy. *Journal of Microbiology* **41**, 144-147.

Mitsuyama, M. (2008) "Adaptive Immunity," *In Handbook of Listeria monocytogenes*, D. Liu, ed., Boca Raton: CRC Press, pp. 427-448.

Moser, J., Gerstel, B., Meyer, J.E., Chakraborty, T., Wehland, J., and Heinz, D.W. (1997) Crystal structure of the phosphatidylinositol-specific phospholipase C from the human pathogen *Listeria monocytogenes*. *J Mol Biol* **273**, 269-282.

Newell, D.G., Koopmans, M., Verhoef, L., Duizer, E., Aidara-Kane, A., Sprong, H., Opsteegh, M., Langelaar, M., Threfall, J., Scheutz, F., van der Giessen, J., and Kruse, H. (2010) Food-borne diseases - the challenges of 20 years ago still persist while new ones continue to emerge. *Int J Food Microbiol* **139**, S3-15.

Nightingale, K. (2010) *Listeria monocytogenes*: knowledge gained through DNA sequence-based subtyping, implications, and future considerations. *J AOAC Int* **93**, 1275-1286.

Ohata, D., Mori, I., and Ward, E. (1997) Inhibitors of imidazoleglycerolphosphate dehydratase as herbicides. *Weed Science* **45**, 610-620.

Olier, M., Garmyn, D., Rousseaux, S., Lemaitre, J.P., Piveteau, P., and Guzzo, J. (2005) Truncated internalin A and asymptomatic *Listeria monocytogenes* carriage: in vivo investigation by allelic exchange. *Infect Immun* **73**, 644-648.

Parisi, A., Latorre, L., Normanno, G., Miccolupo, A., Fraccalvieri, R., Lorusso, V., and Santagada, G. (2010) Amplified Fragment Length Polymorphism and Multi-Locus Sequence Typing for high-resolution genotyping of *Listeria monocytogenes* from foods and the

environment. *Food Microbiol* **27**, 101-108. Proteomic analysis of the response of Listeria monocytogenes to bile salts under anaerobic conditions

Payne A, Schmidt, T.B., Nanduri, B., Pendarvis, K., Pittman, J.R, Thornton, J.A., Grissett, J., Donaldson, J.R. (2013) Proteomic analysis of the response of Listeria monocytogenes to bile salts under anaerobic conditions. *J Med Microbiol* **62,** 25-35.

Paul D, Kumar A, Gajbhiye A, Santra MK, Srikanth R. (2013) Mass spectrometry-based proteomics in molecular diagnostics: discovery of cancer biomarkers using tissue culture. *Biomed Res Int*. doi: 10.1155/2013/783131.

Ragon, M., Wirth, T., Hollandt, F., Lavenir, R., Lecuit, M., Le, M.A., and Brisse, S. (2008) A new perspective on *Listeria monocytogenes* evolution. *PLoS Pathog* **4**, e1000146.

Ramaswamy, V., Cresence, V.M., Rejitha, J.S., Lekshmi, M.U., Dharsana, K.S., Prasad, S.P., and Vijila, H.M. (2007) Listeria--review of epidemiology and pathogenesis. *J Microbiol Immunol Infect* **40**, 4-13.

Regha, K., Satapathy, A.K., and Ray, M.K. (2005) RecD plays an essential function during growth at low temperature in the antarctic bacterium *Pseudomonas syringae* Lz4W. *Genetics* **170**, 1473-1484.

Rijpens, N., Vlaemynck, G., Rossau, R., Herman, L., and Jannes, G. (1998) Unidentified Listeria-like bacteria isolated from cheese. *Lett Appl Microbiol* **27**, 198-202.

Rocourt, J., Hof, H., Schrettenbrunner, A., Malinverni, R., and Bille, J. (1986) Acute purulent *Listeria seeligeri* meningitis in an immunocompetent adult. *Schweiz Med Wochenschr* **116**, 248-251.

Rowan, N.J. and Anderson, J.G. (1998) Effects of above-optimum growth temperature and cell morphology on thermotolerance of *Listeria monocytogenes* cells suspended in bovine milk. *Appl Environ Microbiol* **64**, 2065-2071.

Schnupf, P. and Portnoy, D.A. (2007) Listeriolysin O: a phagosome-specific lysin. *Microbes Infect* **9**, 1176-1187.

Schuerch, D.W., Wilson-Kubalek, E.M., and Tweten, R.K. (2005) Molecular basis of listeriolysin O pH dependence. *Proc Natl Acad Sci U S A* **102**, 12537-12542.

Schuppler, M. and Loessner, M.J. (2010) The Opportunistic Pathogen *Listeria monocytogenes*: Pathogenicity and Interaction with the Mucosal Immune System. *Int J Inflam* **2010:**704321.

Scortti, M., Monzo, H.J., Lacharme-Lora, L., Lewis, D.A., and Vazquez-Boland, J.A. (2007) The PrfA virulence regulon. *Microbes Infect* **9**, 1196-1207.

Seveau, S., Pizarro-Cerda, J., and Cossart, P. (2007) Molecular mechanisms exploited by *Listeria monocytogenes* during host cell invasion. *Microbes Infect* **9**, 1167-1175.

Shah, H.N., Rajakaruna, L., Ball, G., Misra, R., Al-Shahib, A., Fang, M., and Gharbia, S.E. (2011) Tracing the transition of methicillin resistance in sub-populations of *Staphylococcus aureus*, using SELDI-TOF Mass Spectrometry and Artificial Neural Network Analysis. *Syst Appl Microbiol* **34**, 81-86.

Shah, H.N., V. Encheva, and O. Schmi (2005). Surface Enhanced Laser Desorption/Ionization Time of Flight Mass Spectrometry (SELDI-TOF-MS): A Potentially Powerful Tool for Rapid Characterisation of Microorganisms. In *"Encyclopedia of Rapid Microbiological Methods.*Vol.3. Ed. M.J. Miller; DHI Publishing, LLC, River Grove, IL, USA. pp. 57 – 96.

Shah, H. N., Keys, C., Gharbia, S.E., Ralphson, K., Trundle, F., Brookhouse, I. and Claydon, M. (2000) The application of MALDI-TOF Mass Spectrometry to profile the surface of intact bacterial cells. *Microb Ecol in Health Dis* **12**, 241-246.

Sneath, P. H. A. *Bergey's Manual of Systematic Bacteriology*. 1st[2], 1235-1245. (1986) , Williams and Wilkins.

Songer, J.G. (1997) Bacterial phospholipases and their role in virulence. *Trends Microbiol* **5**, 156-161.

Sonia, K. A., Nannapaneni, R. and Hagens, S. (2010) Reduction of Listeria monocytogenes on the surface of fresh channel catfish fillets by bacteriophage Listex P100. Foodborne Pathog disease **9**, 427-434.

Sueng-Ho O. and Bhunia A. (2013) Multiplex fiber optic biosensor for detection of *Listeria monocytogenes*, *Eschericia coli* O157:H7 and *Salmonella enterica* from ready-to-eat meat samples. *Food Microbiol* **33**, 166-171.

Thomas, E.J., King, R.K., Burchak, J., and Gannon, V.P. (1991) Sensitive and specific detection of *Listeria monocytogenes* in milk and ground beef with the polymerase chain reaction. *Appl Environ Microbiol* **57**, 2576-2580.

Torres, D., Barrier, M., Bihl, F., Quesniaux, V.J., Maillet, I., Akira, S., Ryffel, B., and Erard, F. (2004) Toll-like receptor 2 is required for optimal control of *Listeria monocytogenes* infection. *Infect Immun* **72**, 2131-2139.

Vazquez-Boland, J.A., Dominguez-Bernal, G., Gonzalez-Zorn, B., Kreft, J., and Goebel, W. (2001a) Pathogenicity islands and virulence evolution in Listeria. *Microbes Infect* **3**, 571-584.

Vazquez-Boland, J.A., Kuhn, M., Berche, P., Chakraborty, T., Dominguez-Bernal, G., Goebel, W., Gonzalez-Zorn, B., Wehland, J., and Kreft, J. (2001b) Listeria pathogenesis and molecular virulence determinants. *Clin Microbiol Rev* **14**, 584-640.

Walker, J.K., Morgan, J.H., McLauchlin, J., Grant, K.A. and Shallcross, J.A. (1994) *Listeria innocua* isolated from a case of ovine meningoencephalitis. *Vet Microbiol* **42,** 245-253.

Walsh, J.G., Logue, S.E., Luthi, A.U., and Martin, S.J. (2011) Caspase-1 promiscuity is counterbalanced by rapid inactivation of the processed enzyme. *J Biol Chem*, **286**, 32513-14.

Way, S.S., Thompson, L.J., Lopes, J.E., Hajjar, A.M., Kollmann, T.R., Freitag, N.E., and Wilson, C.B. (2004) Characterization of flagellin expression and its role in *Listeria monocytogenes* infection and immunity. *Cell Microbiol* **6**, 235-242.

Welker, M. and Moore, R.B. (2011) Applications of whole-cell matrix-assisted laser-desorption/ionization time-of-flight mass spectrometry in systematic microbioology. *Syst Appl Microbiol* **34,** 2-11.

Yeung, P.S., Na, Y., Kreuder, A.J., and Marquis, H. (2007) Compartmentalization of the broad-range phospholipase C activity to the spreading vacuole is critical for *Listeria monocytogenes* virulence. *Infect Immun* **75**, 44-51.

Yeung, P.S., Zagorski, N., and Marquis, H. (2005) The metalloprotease of *Listeria monocytogenes* controls cell wall translocation of the broad-range phospholipase C. *J Bacteriol* **187**, 2601-2608.

Yoshikawa, Y., Ogawa, M., Hain, T., Chakraborty, T., and Sasakawa, C. (2009) *Listeria monocytogenes* ActA is a key player in evading autophagic recognition. *Autophagy* **5**, 1220-1221.

Zhang, Q., Feng, Y., Deng, L., Feng, F., Wang, L., Zhou, Q., and Luo, Q. (2011) SigB plays a major role in *Listeria monocytogenes* tolerance to bile stress. *Int J Food Microbiol* **145**, 238-243.

http://www.ppdictionary.com/bacteria/gnbac/enterocolitica.htm (2011)

Appendix

Table A1. List of proteins identified in *L. monocytogenes* F2365 cell extracts produced using glass bead beating and endolysin, their corresponding accession number and number of unique peptides in each biological replicate.

Protein Number	**Identified Proteins (434)**	**Accession Number**	**Number of Unique Peptides Samples:**					
			A	B	C	D	E	F
1	bifunctional acetaldehyde-CoA/alcohol dehydrogenase	gi|16800743	16	17	12	14	16	11
2	phosphopyruvate hydratase	gi|16801611	16	16	15	16	17	14
3	elongation factor Tu	gi|16804690	14	13	13	12	12	12
4	glyceraldehyde-3-phosphate dehydrogenase	gi|16801615	11	11	9	9	9	7
5	formate acetyltransferase	gi|46907634	18	18	16	16	17	14
6	hypothetical protein lin2048	gi|16801114	4	4	3	3	4	2
7	chaperonin GroEL	gi|116873505	14	18	9	15	13	9
8	50S ribosomal protein L7/L12	gi|116871634	4	4	3	4	4	2
9	hypothetical protein lmo2556	gi|16804594	4	4	6	5	4	5
10	DNA-directed RNA polymerase subunit beta	gi|46906496	22	18	12	17	22	11
11	chaperone protein DnaK	gi|46907701	11	13	13	10	11	10
12	elongation factor Ts	gi|46907886	11	13	8	10	11	9
13	phosphocarrier protein HPr	gi|168000	4	5	3	4	4	5

		70						
14	50S ribosomal protein L17	gi|116873971	4	3	3	3	3	4
15	fumarate reductase flavoprotein subunit	gi|16802400	8	10	9	8	8	7
16	elongation factor G	gi|116874019	9	10	10	8	9	9
17	pyruvate carboxylase	gi|254823658	16	15	11	13	16	11
18	DNA-directed RNA polymerase subunit beta	gi|116871647	14	13	9	9	10	9
19	30S ribosomal protein S8	gi|16801828	3	3	2	3	3	2
20	pyruvate kinase	gi|47093107	4	8	10	7	5	6
21	phosphotransferase system enzyme I	gi|16803043	6	10	7	10	9	7
22	50S ribosomal protein L4	gi|16801841	4	5	3	3	4	3
23	phosphoglyceromutase	gi|16804494	7	8	6	7	6	6
24	triosephosphate isomerase	gi|16801613	5	5	4	5	5	3
25	50S ribosomal protein L5	gi|16801830	4	5	5	4	4	4
26	co-chaperonin GroES	gi|116873506	2	3	2	4	4	2
27	50S ribosomal protein L23	gi|16804668	3	6	4	4	5	3
28	50S ribosomal protein L29	gi|16801834	2	2	2	2	2	2
29	50S ribosomal protein L21	gi|16803582	4	4	2	3	4	2
30	acetolactate synthase	gi|254825504	6	8	6	6	6	4
31	hypothetical protein lin2463	gi|16801525	7	6	10	5	5	7
32	30S ribosomal protein S2	gi|16800835	5	6	6	3	4	5

33	50S ribosomal protein L3	gi|16804670	4	4	4	3	3	2
34	6-phosphofructokinase	gi|16803611	5	6	5	5	5	2
35	L-lactate dehydrogenase	gi|116871592	2	5	4	3	1	4
36	30S ribosomal protein S5	gi|16801825	3	3	3	4	4	3
37	CD4+ T cell-stimulating antigen, lipoprotein	gi|16803428	6	8	7	10	9	7
38	50S ribosomal protein L1	gi|16799358	4	4	3	4	3	3
39	50S ribosomal protein L15	gi|16804651	2	3	2	3	2	3
40	phosphoglycerate kinase	gi|116873822	4	4	5	5	7	5
41	ATP-dependent Clp protease proteolytic subunit	gi|254823607	3	3	2	3	4	2
42	30S ribosomal protein S10	gi|16801843	2	3	2	2	2	2
43	30S ribosomal protein S1	gi|254993213	7	7	4	6	7	4
44	hypothetical protein lin2128	gi|16801194	4	3	2	3	3	2
45	30S ribosomal protein S7	gi|16801865	4	3	2	4	3	1
46	aspartyl-tRNA synthetase	gi|46907747	8	9	8	5	7	6
47	acetate kinase	gi|116873010	8	10	5	8	8	7
48	adenylate kinase	gi|217966190	2	3	3	3	2	3
49	hypothetical protein lin0859	gi|16799933	9	12	6	8	8	6
50	30S ribosomal protein S11	gi|16801817	3	3	2	3	3	2
51	trigger factor	gi|16800374	5	7	4	7	6	4
52	polynucleotide	gi|254829	5	8	6	8	5	4

	phosphorylase/polyadenylase	912						
53	transketolase	gi|226223907	7	7	7	7	7	5
54	hypothetical protein lin2786	gi|16801847	3	4	2	2	2	2
55	hypothetical protein LMOf2365_0621	gi|46906837	2	3	2	2	2	2
56	30S ribosomal protein S4	gi|116873025	4	3	3	4	4	1
57	valyl-tRNA synthetase	gi|254993780	9	10	3	7	5	3
58	dihydrolipoamide acetyltransferase	gi|46907286	3	3	4	2	4	2
59	hypothetical protein lin0145	gi|16799222	3	3	5	3	3	5
60	alanyl-tRNA synthetase	gi|217964349	9	6	3	8	5	2
61	50S ribosomal protein L6	gi|16804655	5	5	5	4	4	3
62	pyruvate dehydrogenase beta subunit	gi|116872447	1	3	6	4	3	5
63	dipeptidase	gi|217964227	8	6	9	5	7	8
64	isoleucyl-tRNA synthetase	gi|217963834	7	8	5	6	3	2
65	hypothetical protein lmo2638	gi|16804676	3	3	5	4	4	2
66	glutamyl-tRNA(Gln) amidotransferase	gi|254826001	6	7	4	4	6	5
67	hypothetical protein lmo0219	gi|16802265	2	1	3	1	3	1
68	uracil phosphoribosyltransferase	gi|16804576	3	3	3	2	2	3
69	hypothetical protein lse_0235	gi|289433604	3	2	3	2	2	3
70	6-phosphogluconate dehydrogenase	gi|16800481	6	7	4	4	5	2
71	enoyl-(acyl carrier protein) reductase	gi|16803010	5	5	5	6	5	3

72	universal stress protein	gi|116873009	6	5	4	4	6	2
73	DNA-directed RNA polymerase subunit alpha	gi|16801816	4	5	4	5	5	3
74	hypothetical protein lmo0223	gi|16802269	3	3	5	3	4	3
75	30S ribosomal protein S6	gi|16799116	3	3	1	3	3	1
76	glutamate dehydrogenase	gi|16802603	3	3	6	5	6	2
77	ATP synthase F1, beta subunit	gi|315283679	5	5	6	4	5	6
78	D-amino acid aminotransferase	gi|46907849	4	5	5	4	3	3
79	hypothetical protein lin2901	gi|16801960	7	5	3	5	4	3
80	prolyl-tRNA synthetase	gi|226223920	7	6	6	6	5	4
81	superoxide dismutase, Mn	gi|46907667	4	4	3	5	5	3
82	50S ribosomal protein L19	gi|116873225	2	2	1	2	2	1
83	epitope LemA	gi|254993263	2	3	2	3	2	2
84	lysyl-tRNA synthetase	gi|16802274	3	5	4	4	4	5
85	glutamyl-tRNA amidotransferase subunit A	gi|217964097	5	5	5	2	4	4
86	hypothetical protein lmo2223	gi|16804262	2	2	2	2	2	3
87	L-glutamine-D-fructose-6-phosphate amidotransferase	gi|226223357	5	7	5	4	7	4
88	DNA polymerase III (alpha subunit)	gi|226223921	2	5	1	4	7	2
89	hypothetical protein lmo1603	gi|16803643	8	6	3	6	4	3
90	hypothetical protein lin1027	gi|16800096	3	3	2	3	2	1
91	preprotein translocase	gi|168045	7	6	3	7	5	4

	subunit SecA	48						
92	clpB protein	gi|254931681	9	6	1	6	4	3
93	hypothetical protein lin2510	gi|16801572	6	4	1	2	2	1
94	50S ribosomal protein L14	gi|16801832	3	3	2	3	3	3
95	putative manganese-dependent inorganic pyrophosphatase	gi|16803488	3	7	5	6	4	5
96	F0F1 ATP synthase subunit alpha	gi|16801736	4	5	4	4	3	4
97	glutamyl-tRNA synthetase	gi|16802283	4	5	3	2	4	3
98	hypothetical protein lin0410	gi|16799487	5	10	7	4	5	3
99	glucose-6-phosphate isomerase	gi|16801528	3	2	2	3	3	2
100	non-heme iron-binding ferritin	gi|16802983	3	4	2	4	3	2
101	(3R)-hydroxymyristoyl-ACP dehydratase	gi|16801729	3	3	1	3	3	1
102	30S ribosomal protein S13	gi|16801818	2	1	1	1	3	1
103	arginyl-tRNA synthetase	gi|217963335	3	4	1	5	5	2
104	50S ribosomal protein L11	gi|16799357	2	3	2	2	2	2
105	hypothetical protein lin0182	gi|16799259	4	5	2	4	5	2
106	hypothetical protein lmo0096	gi|16802144	2	2	1	2	2	1
107	hypothetical protein lmo0891	gi|16802932	4	5	4	5	5	4
108	pyruvate-formate lyase activating enzyme	gi|16800512	3	4	1	3	2	1
109	catalase	gi|47092675	2	3	2	3	3	2
110	50S ribosomal protein L16	gi|168018	2	2	2	1	2	2

		35						
111	DNA gyrase subunit A	gi|16799086	9	5	2	8	3	1
112	tyrosyl-tRNA synthetase	gi|226224199	5	3	3	3	5	2
113	50S ribosomal protein L13	gi|16804635	2	2	2	2	2	1
114	hypothetical protein LMOf2365_0340	gi|46906560	4	5	4	5	3	3
115	cell division protein FtsZ	gi|116873462	6	5	3	2	3	3
116	translation initiation factor IF-3	gi|16800963	4	4	2	2	4	2
117	30S ribosomal protein S3	gi|16801836	1	2	2	2	1	2
118	D-alanine-D-alanyl carrier protein ligase	gi|47093668	2	5	3	0	3	2
119	rod shape-determining protein MreB	gi|16803588	5	5	1	2	3	1
120	ATP-dependent Clp protease proteolytic subunit	gi|16804506	3	2	1	2	2	1
121	hypothetical protein lmo1807	gi|16803847	4	2	3	2	2	3
122	hypothetical protein lin2350	gi|16801413	4	4	3	1	4	2
123	ABC transporter, ATP-binding protein	gi|46908350	5	3	3	4	3	4
124	threonyl-tRNA synthetase	gi|16803599	4	5	2	4	5	0
125	CTP synthetase	gi|46908730	3	6	3	3	4	0
126	50S ribosomal protein L9	gi|16802101	3	2	2	3	2	2
127	translation initiation factor IF-2	gi|16800430	3	3	3	4	4	2
128	aconitate hydratase 1	gi|217964207	4	2	2	3	3	2
129	rod shape-determining protein MreB	gi|16804563	5	6	2	4	5	3

130	transcriptional repressor CodY	gi|16800387	4	5	1	4	5	1
131	hypothetical protein lin1642	gi|16800710	3	4	2	3	3	2
132	naphthoate synthase	gi|16803713	4	4	3	3	4	2
133	azo-dye reductase 2	gi|254828869	2	3	4	3	2	2
134	ribonucleotide-diphosphate reductase subunit alpha	gi|16804194	5	4	3	4	4	1
135	thioredoxin reductase	gi|16804516	5	7	3	6	7	1
136	catabolite control protein A	gi|16803639	6	8	2	2	6	1
137	hypothetical protein lin1044	gi|16800113	1	1	2	1	1	1
138	recombinase A	gi|116872830	3	4	3	3	2	2
139	hypothetical protein lin0250	gi|16799327	2	2	1	1	2	2
140	serS	gi|307572335	5	4	3	4	4	3
141	transcription elongation factor GreA	gi|16800599	2	3	2	3	1	3
142	phosphomethylpyrimidine kinase	gi|116872050	3	1	1	2	2	1
143	hypothetical protein lmo1299	gi|16803339	3	5	4	2	3	2
144	DNA topoisomerase IV subunit A	gi|16803327	3	5	3	2	3	3
145	asparaginyl-tRNA synthetase	gi|16803935	4	2	1	4	4	3
146	Smc protein	gi|226224407	7	3	1	1	4	1
147	DAK2 domain protein	gi|47093051	1	5	4	1	3	4
148	leucyl-tRNA synthetase	gi|300766055	3	3	2	4	3	1
149	positive regulator of sigma-B	gi|255026	1	2	4	2	2	2

	activity	473						
150	malonyl CoA-acyl carrier protein transacylase	gi|217964039	4	5	2	4	3	0
151	50S ribosomal protein L2	gi|116873995	3	5	3	1	3	3
152	hypothetical protein lmo1888	gi|16803927	2	3	1	2	2	1
153	ribose-phosphate pyrophosphokinase	gi|16799315	3	3	3	2	2	2
154	hypothetical protein lmo1067	gi|16803107	4	2	1	1	3	3
155	inorganic polyphosphate/ATP-NAD kinaseLCC5334]	gi|116873015	3	1	2	1	1	3
156	phosphoglucomutase	gi|226224475	2	3	2	2	2	2
157	thymidylate kinase	gi|16804730	4	2	1	6	5	1
158	peptidase	gi|254824448	4	5	3	5	3	1
159	hypothetical protein lmo1339	gi|16803379	3	4	3	4	3	3
160	hypothetical protein LmonocFSL_04711	gi|255520525	3	3	3	3	3	2
161	hypothetical protein lmo1544	gi|16803584	4	3	2	2	3	2
162	glucosamine-6-phosphate deaminase	gi|217963543	4	3	3	1	3	2
163	phenylalanyl-tRNA synthetase	gi|254823524	3	2	2	3	3	1
164	glutamate synthase (large subunit)	gi|226224337	3	3	0	3	4	0
165	formate--tetrahydrofolate ligase	gi|16801056	4	5	4	6	5	2
166	glucose-specific phosphotransferase enzyme iia component	gi|217964883	1	1	1	2	1	2
167	ribosome recycling factor	gi|16800419	2	2	2	1	1	1

168	MTA/SAH nucleosidase	gi|254828272	4	3	1	4	2	1
169	GMP synthase	gi|16803136	1	3	2	2	1	1
170	FeS assembly protein SufD	gi|217963486	2	1	5	2	2	2
171	redox-sensing transcriptional repressor Rex	gi|16801243	1	2	1	2	2	1
172	UDP-N-acetylmuramoyl-L-alanyl-D-glutamate synthetase	gi|46908272	5	4	1	1	3	0
173	transcription-repair coupling factor	gi|217965700	5	2	0	0	3	0
174	DNA-binding protein	gi|254851904	2	3	2	2	2	1
175	phosphoglucomutase/phosphomannomutase family protein	gi|224499832	4	5	3	1	3	2
176	ABC transporter, substrate-binding protein	gi|47094438	2	2	3	2	2	2
177	serine-protein kinase RsbW	gi|46907126	5	4	2	3	3	1
178	phosphoglucosamine mutase	gi|217963721	2	2	1	4	2	1
179	beta-ketoacyl-acyl-carrier-protein synthase II	gi|315304368	3	4	3	3	4	2
180	post-translocation molecular chaperone	gi|226224827	4	4	3	4	3	3
181	glycerol-3-phosphate dehydrogenase, NAD-dependent	gi|46908169	5	5	3	5	4	1
182	ribosomal subunit interface protein	gi|116873875	3	2	0	2	2	1
183	DNA mismatch repair protein MutS	gi|16803443	4	3	0	2	1	0
184	Tetrahydrofolate dehydrogenase/cyclohydrolase	gi|226223961	2	3	4	2	2	2
185	hypothetical protein lin2434	gi|168014	3	4	2	3	3	2

		96						
186	hypothetical protein LmonocyFSL_13924	gi|255024248	1	2	0	1	1	0
187	hypothetical protein lin1645	gi|16800713	2	1	2	2	2	1
188	GTP-binding protein LepA	gi|116872908	3	4	1	2	3	3
189	dihydrolipoamide dehydrogenase	gi|16800116	2	3	3	1	3	2
190	dihydrodipicolinate synthase	gi|116872868	2	2	2	2	2	2
191	hypothetical protein lin1010	gi|16800079	2	2	1	3	2	1
192	ClpC ATPase	gi|1314297	6	7	3	2	3	0
193	IspC	gi|126143318	5	7	5	0	0	0
194	glycyl-tRNA synthetase beta subunit	gi|254932643	1	3	0	3	3	2
195	pyridoxal biosynthesis lyase PdxS	gi|16804140	4	3	2	3	3	1
196	hypothetical protein lin2475	gi|16801537	1	0	2	2	1	2
197	adenine phosphoribosyltransferase	gi|289434804	0	1	2	2	2	1
198	hypothetical protein lin1776	gi|16800844	1	1	2	1	1	1
199	hypothetical protein lin1007	gi|16800076	1	3	1	0	2	1
200	metallo-beta-lactamase family protein	gi|46907808	3	3	1	2	2	2
201	hypothetical protein lmo2033	gi|16804072	3	3	1	3	3	0
202	hypothetical protein lin1536	gi|16800604	2	2	1	1	2	1
203	alkylphosphonate utilization operon protein PhnA	gi|46906605	1	0	2	2	3	1
204	phosphopentomutase	gi|46908188	2	3	2	4	3	1

205	transcription elongation factor NusA	gi|116872753	0	3	0	3	1	1
206	thioredoxin	gi|16800265	1	2	1	1	1	2
207	F0F1 ATP synthase subunit delta	gi|116873896	2	3	0	2	2	2
208	50S ribosomal protein L30	gi|16801824	1	2	0	1	1	0
209	UTP-glucose-1-phosphate uridylyltransferase	gi|46907310	3	2	2	1	2	2
210	30S ribosomal protein S17	gi|16801833	2	2	0	2	2	0
211	methionyl-tRNA synthetase	gi|226222806	2	2	2	2	3	1
212	putative glycerol-3-phosphate acyltransferase PlsX	gi|16803849	4	4	1	1	4	1
213	hypothetical protein lwe0170	gi|116871590	2	1	1	2	2	1
214	50S ribosomal protein L25/general stress protein Ctc	gi|116871593	1	2	2	0	1	0
215	DNA polymerase I	gi|16803605	3	2	1	3	1	1
216	protein-export membrane protein SecDF	gi|47094198	2	4	2	0	4	3
217	ATP-dependent DNA helicase	gi|16803799	5	6	0	2	4	0
218	cytidylate kinase	gi|46908172	2	2	3	1	2	2
219	tellurite resistance protein, putative	gi|116873409	2	2	2	1	3	1
220	LuxR family DNA-binding response regulator	gi|116872424	2	2	2	3	3	2
221	purine nucleoside phosphorylase	gi|16801036	2	2	2	3	3	2
222	anaerobic ribonucleoside-triphosphate reductase	gi|217965627	3	5	1	4	2	1
223	hypothetical protein lin1505	gi|168005	3	2	2	1	2	1

		73						
224	partition protein ParB homolg	gi|16801981	2	3	0	2	2	0
225	50S ribosomal protein L31 type B	gi|116873913	2	2	0	0	2	0
226	aminopeptidase	gi|116873147	3	3	2	3	2	1
227	cysteinyl-tRNA synthetase	gi|315274656	2	1	1	2	3	1
228	aspartate aminotransferase	gi|16803936	2	4	1	2	2	1
229	PTS system, beta-glucoside-specific, IIA component	gi|46907950	2	2	0	1	2	0
230	thermostable carboxypeptidase	gi|226224489	4	4	2	3	3	0
231	hypothetical protein lmo0814	gi|16802856	2	2	2	2	2	1
232	3-oxoacyl-(acyl carrier protein) synthase III	gi|16804241	2	3	1	2	3	2
233	3-dehydroquinate dehydratase	gi|255522128	3	3	1	2	2	0
234	ribonucleotide-diphosphate reductase subunit beta	gi|16804193	3	2	0	2	2	1
235	co-chaperone GrpE	gi|217964380	1	2	1	1	2	0
236	hypothetical protein lin0373	gi|16799450	1	2	1	1	2	2
237	Rrf2 family protein	gi|46907743	2	2	1	3	2	0
238	putative secreted protein	gi|116873080	1	2	1	2	2	0
239	anti-anti-sigma factor (antagonist of RsbW)	gi|16799965	1	2	1	1	1	1
240	peptide deformylase	gi|46907283	1	2	0	2	0	1
241	hypothetical protein lmo0558	gi|16802601	1	1	0	2	1	1
242	hypothetical protein lmo2700	gi|16804737	2	2	0	2	2	1

243	threonine synthase	gi|16801751	2	2	1	1	1	2
244	hypothetical protein lmo1236	gi|16803276	2	1	2	1	1	2
245	hypothetical protein LMOf2365_1263	gi|46907472	2	2	1	2	2	1
246	flavodoxin family protein	gi|116873146	1	2	1	2	2	1
247	PTS system, cellobiose-specific, IIB component	gi|116873738	1	2	1	2	2	1
248	DHH subfamily 1 protein	gi|46907806	1	4	3	3	1	1
249	hypothetical protein LMHCC_1728	gi|217965005	1	2	1	1	0	0
250	excinuclease ABC, A subunit	gi|217963410	6	2	0	0	4	0
251	hypothetical protein LMOf2365_1769	gi|46907974	1	3	0	1	2	1
252	hypothetical protein LMOf2365_1664	gi|46907872	1	2	1	2	2	1
253	ATP-dependent protease ATP-binding subunitCC5334]	gi|116872712	4	4	1	1	4	0
254	chorismate mutase	gi|16803640	1	2	2	2	0	0
255	glucose-6-phosphate 1-dehydrogenase	gi|16801151	3	1	0	1	2	0
256	hypothetical protein lmo2692	gi|16804729	1	1	3	1	1	0
257	NAD-dependent DNA ligase LigA	gi|46907988	1	1	0	0	0	2
258	peptide chain release factor 1	gi|16801748	2	3	1	4	3	0
259	transcriptional regulator, Fur family	gi|47093385	2	1	2	1	2	2
260	hypothetical protein lmo1283	gi|16803323	1	3	0	3	2	1
261	putative lipid kinase	gi|16803793	3	3	2	3	0	0

262	MEP cytidylyltransferase 2	gi|217964827	1	1	2	1	1	2
263	DNA polymerase III subunit beta	gi|16802050	1	3	0	2	0	1
264	DNA gyrase subunit B	gi|16802054	3	1	2	1	2	1
265	cell division ATP-dependent metalloprotease	gi|116871603	2	5	0	0	2	0
266	phenylalanyl-tRNA synthetase, alpha subunit	gi|217964713	2	4	0	3	2	0
267	nitroreductase family protein	gi|116874175	2	2	2	2	1	2
268	oligoendopeptidase F	gi|217963650	1	1	2	1	2	1
269	tRNA-binding domain protein	gi|47094077	3	2	1	3	3	1
270	hypothetical protein lin1391	gi|16800459	2	2	2	2	2	2
271	glutamate racemase	gi|116872608	2	2	2	1	2	1
272	CBS domain-containing protein	gi|313624857	1	1	2	1	1	1
273	conserved hypothetical protein	gi|254853053	2	2	0	1	2	2
274	glyoxalase family protein	gi|46907332	2	2	0	2	1	0
275	GTPase ObgE	gi|16803577	2	1	2	2	1	1
276	chorismate synthase	gi|46908161	3	2	2	3	2	1
277	hypothetical protein lmo0487	gi|16802530	1	1	1	2	1	0
278	phosphoglycerate mutase	gi|226223186	3	4	0	2	3	0
279	phosphoglycerate dehydrogenase	gi|226222719	3	2	1	3	3	2
280	DNA-directed RNA polymerase subunit delta	gi|116873926	1	1	1	1	1	2
281	UDP-N-acetylglucosamine	gi|226222	2	2	0	3	2	1

	pyrophosphorylase	827						
282	lipoyltransferase and lipoate-protein ligase family protein	gi|46907165	1	3	1	1	2	1
283	branched-chain amino acid aminotransferase	gi|46907211	2	4	0	1	2	0
284	acetyl-CoA carboxylase, biotin carboxylase	gi|217964497	3	3	2	3	3	0
285	hypothetical protein lin1225	gi|16800294	2	1	0	1	1	0
286	putative lipoprotein	gi|116872665	2	3	3	2	1	0
287	CBS domain-containing protein	gi|116873005	3	2	0	1	2	1
288	hypothetical protein lmo1463	gi|16803503	0	0	0	2	0	0
289	purine nucleoside phosphorylase	gi|116873395	1	1	2	1	1	1
290	hypothetical protein lmo1738	gi|16803778	3	1	0	3	3	0
291	ribulose-phosphate 3-epimerase	gi|116873253	1	2	1	1	0	0
292	hypothetical protein lin1772	gi|16800840	2	1	2	0	0	0
293	GTP-binding protein EngA	gi|116873379	1	2	0	2	2	1
294	hypothetical protein lmo0797	gi|16802839	1	2	1	2	1	1
295	putative heme peroxidase	gi|16801283	1	2	0	2	0	0
296	DNA topoisomerase 3 (DNA topoisomerase III)	gi|217966040	4	3	1	0	2	1
297	hydroxy-3-methylglutaryl coenzyme A synthase	gi|226224016	1	1	0	2	1	1
298	hypothetical protein lmo1434	gi|16803474	2	2	0	2	2	0
299	RNA methyltransferase	gi|116871624	1	1	2	0	0	0
300	hypothetical protein lmo2754	gi|16804791	1	2	0	2	1	0

301	hypothetical protein lmo1579	gi|16803619	3	3	2	3	2	1
302	ATP-dependent protease ATP-binding subunit ClpX	gi|16803308	1	2	0	2	1	2
303	Rel [Listeria monocytogenes]	gi|14325225	2	3	1	2	2	1
304	dihydrolipamide acetyltransferase	gi|46907600	2	1	1	2	1	1
305	dUTPase family protein	gi|46907922	2	1	2	1	1	1
306	hypothetical protein lmo1745	gi|16803785	3	3	1	1	1	0
307	protein kinase, putative	gi|47093057	0	2	1	1	1	1
308	hypothetical protein lmo0152	gi|16802200	2	2	0	1	2	0
309	UDP-N-acetylmuramoylalanyl-D-glutamate--2,6-diaminopimelate ligase	gi|255520496	1	1	1	2	2	1
310	aspartate aminotransferase	gi|16804291	2	5	1	4	1	1
311	hypothetical protein lin2650	gi|16801712	1	1	1	0	2	1
312	hypothetical protein lmo1334	gi|16803374	2	1	1	1	1	1
313	conserved hypothetical protein	gi|254931550	1	3	0	2	0	1
314	hypothetical protein LmonocFSL_03787	gi|255520343	0	0	0	3	0	0
315	hypothetical protein lmo0796	gi|16802838	2	3	1	0	1	0
316	hypothetical protein lmo1621	gi|16803661	0	2	1	0	0	2
317	metallo-beta-lactamase family protein	gi|116872429	2	3	1	3	0	0
318	menaquinone biosynthesis protein menD	gi|254829597	1	2	0	0	3	0
319	thiamine biosynthesis	gi|217966	2	2	0	2	1	0

	membrane-associated lipoprotein	165						
320	putaive secreted, lysin rich protein	gi|16802349	1	2	0	2	2	0
321	hypothetical protein lin1218	gi|16800287	2	1	0	1	1	1
322	hypothetical protein lin1180	gi|16800249	1	2	1	1	1	1
323	conserved hypothetical protein	gi|254823789	1	1	1	2	3	0
324	hypothetical protein lmo1868	gi|16803908	1	2	0	2	0	0
325	alcohol dehydrogenase	gi|254824114	2	2	0	1	1	1
326	ArsC family protein	gi|116873789	1	1	0	1	2	0
327	acetyltransferase	gi|46906914	1	0	2	0	2	1
328	hypothetical protein LMHCC_0113	gi|217963411	1	0	1	2	2	1
329	hypothetical protein lmo0292	gi|16802338	2	2	1	2	2	2
330	hypothetical protein lmo0534	gi|16802577	1	2	0	0	2	0
331	conserved hypothetical protein	gi|254853667	1	2	0	2	1	0
332	Xaa-Pro dipeptidase	gi|217964274	0	2	0	1	1	0
333	nucleoside diphosphate kinase	gi|16803968	1	1	0	2	1	0
334	dihydrodipicolinate reductase	gi|16803946	2	2	1	1	1	1
335	hypothetical protein lmo0443	gi|16802487	1	2	2	1	1	1
336	D-alanine--D-alanine ligase	gi|217965050	1	1	1	2	1	0
337	lipase/acylhydrolase family protein	gi|46906740	1	1	1	1	1	2
338	hypothetical protein lmo0955	gi|168029	2	3	1	1	3	0

		95						
339	hypothetical protein lin2851	gi|16801911	1	1	0	1	2	1
340	DNA-binding response regulator	gi|116873879	1	2	0	1	2	0
341	hypothetical protein lin2544	gi|16801606	1	1	3	1	2	1
342	hypothetical protein lmo2216	gi|16804255	1	1	1	1	2	0
343	FeS assembly protein SufB	gi|116873774	2	1	0	2	0	0
344	tryptophan--tRNA ligase	gi|313622777	1	2	0	1	0	3
345	branched-chain alpha-keto acid dehydrogenase E1 subunit	gi|116872804	1	1	2	2	2	0
346	chaperone protein DnaJ	gi|46907700	1	2	0	2	2	0
347	hypothetical protein lmo1850	gi|16803890	1	1	1	2	1	0
348	UDP-N-acetylmuramate--alanine ligase	gi|217964242	3	2	1	1	1	0
349	transcription antitermination protein NusB	gi|116872790	1	1	0	1	3	0
350	thymidylate synthase	gi|217963973	0	1	0	0	2	0
351	amino acid (glutamine) ABC transporter (ATP-binding protein)	gi|255520513	2	1	1	0	1	0
352	acetyl-CoA acetyltransferase	gi|254824526	1	2	0	2	1	0
353	peptide chain release factor 3	gi|116872389	1	1	2	0	0	1
354	DNA topoisomerase IV subunit B	gi|16803326	1	0	2	0	0	1
355	hypothetical protein lin0344	gi|16799421	0	1	0	2	0	0
356	hypothetical protein lmo0788	gi|16802830	2	2	0	0	2	0

357	glycine cleavage system protein H	gi|16804463	2	1	0	1	1	0
358	Ami 4b protein	gi|12054956	0	2	0	0	0	0
359	PfpI family intracellular peptidase	gi|116873688	2	1	0	1	1	0
360	ribonuclease PH	gi|16803278	1	2	0	2	1	0
361	N-acetylglucosaminyl transferase	gi|254854028	3	3	1	1	2	0
362	hypothetical protein lmo2506	gi|16804544	2	1	1	0	0	1
363	pyrophosphatase PpaX	gi|46908653	2	0	1	0	2	0
364	Gfo/Idh/MocA family oxidoreductase	gi|46907956	0	3	0	1	1	0
365	histidyl-tRNA synthetase	gi|226224121	2	1	0	1	2	0
366	lactate/malate dehydrogenase family protein	gi|46907898	2	1	0	0	1	1
367	aspartate kinase	gi|254932887	0	0	1	0	2	1
368	ribosome-binding factor A	gi|116872758	1	2	0	2	2	0
369	nicotinate phosphoribosyltransferase	gi|16800146	2	4	0	3	0	0
370	hypothetical protein lmo0509	gi|16802552	1	3	1	1	0	0
371	cell-shape determining protein MreC	gi|116872976	2	3	0	2	2	0
372	2-amino-4-hydroxy-6-hydroxymethyldihydropteridine pyrophosphokinase	gi|217965687	1	0	2	2	2	2
373	hypothetical protein lmo0047	gi|16802095	1	2	0	1	1	0
374	UDP-glucose 4-epimerase	gi|217963421	2	1	0	0	1	0
375	fructose-1-phosphate kinase	gi|16804374	0	1	2	0	0	2

376	phosphotransbutyrylase	gi|217964485	1	2	0	1	1	1
377	hypothetical protein lmo0620	gi|16802662	1	0	0	1	1	2
378	guanylate kinase	gi|116873262	1	2	1	1	1	0
379	conserved hypothetical protein	gi|258611892	2	1	0	0	1	0
380	hypothetical protein lmo2168	gi|16804207	2	0	0	0	0	0
381	hypothetical protein lmo2196	gi|16804235	0	2	1	3	1	0
382	hypothetical protein lin0315	gi|16799392	1	1	2	0	1	2
383	glycosyl transferase, group 2 family protein	gi|46907306	2	1	1	1	1	1
384	S-adenosylmethionine synthetase	gi|47094312	1	1	1	1	2	0
385	hypothetical protein lin2297	gi|16801361	1	3	1	1	1	0
386	transcriptional regulator LytR	gi|254993053	1	4	0	0	1	0
387	peptide chain release factor 2	gi|46908681	2	0	0	1	2	1
388	ribosomal RNA small subunit methyltransferase B	gi|217964025	2	2	0	1	1	0
389	aminodeoxychorismate lyase	gi|217964354	2	1	0	0	1	0
390	alcohol dehydrogenase, iron-dependent	gi|217964116	2	1	0	0	1	0
391	cell division ABC transporter, substrate-binding protein FtsY	gi|46908034	2	1	0	0	2	1
392	serine/threonine protein phosphatase family protein	gi|46908053	2	1	0	2	2	0
393	phosphodiesterase	gi|116872831	1	3	0	1	2	0
394	aspartate kinase I	gi|16803476	1	2	0	1	1	2

395	glutathione peroxidase	gi|290893460	1	1	0	1	3	1
396	hypothetical protein LMOf2365_0451	gi|46906669	0	2	0	0	0	0
397	hypothetical protein lin0297	gi|16799374	2	0	0	0	0	0
398	septation ring formation regulator EzrA	gi|16803634	0	1	0	2	1	1
399	putative metalloprotease	gi|16803505	2	1	0	2	2	0
400	TPR domain-containing protein	gi|116872939	1	2	0	1	2	0
401	thiol peroxidase	gi|46907814	2	1	0	0	2	0
402	conserved hypothetical protein	gi|254826165	2	1	0	2	1	0
403	S-adenosyl-methyltransferase MraW	gi|116873471	2	1	1	1	1	0
404	exoribonuclease RNase-R	gi|226224997	3	1	0	1	0	0
405	histidine kinase domain protein	gi|217964958	0	1	1	1	2	0
406	hypothetical protein lin1643	gi|16800711	1	2	0	1	0	1
407	hypothetical protein lin1494	gi|16800562	1	0	1	0	2	0
408	prephenate dehydratase (PDT)	gi|217964317	0	2	1	1	0	1
409	recombination and DNA strand exchange inhibitor protein	gi|16803272	3	1	0	0	1	0
410	peptidase, M20/M25/M40 family	gi|217964888	1	2	0	0	0	0
411	hypothetical protein lwe0905	gi|116872323	1	2	0	1	1	1
412	sugar ABC transporter ATP-binding protein	gi|116872821	0	3	0	0	0	0
413	hypothetical protein LMOf2365_2003	gi|46908207	1	1	0	1	2	1

414	DNA replication intiation control protein YabA	gi|16802212	1	0	1	2	1	0
415	acetyl-CoA carboxylase, carboxyl transferase, alpha subunit	gi|217964280	2	2	0	2	1	0
416	hypothetical protein lmo1487	gi|16803527	2	1	0	2	1	0
417	hypothetical protein Lm4b_01084	gi|226223682	1	2	0	0	0	1
418	hypothetical protein Lm4b_01462	gi|226224053	0	2	0	1	1	0
419	GntR family transcriptional regulator	gi|46907005	2	3	0	0	1	0
420	hypothetical protein lin2554	gi|16801616	0	2	1	1	0	1
421	pyridine nucleotide-disulfide oxidoreductase family protein	gi|116873753	3	2	0	0	1	0
422	O-methyltransferase family protein	gi|217964355	0	0	0	0	1	2
423	hypothetical protein lmo1873	gi|16803913	0	1	0	2	1	0
424	diaminopimelate epimerase	gi|224498531	1	0	0	1	2	0
425	malate dehydrogenase	gi|224500265	0	2	0	0	0	0
426	pyrroline-5-carboxylate reductase	gi|254825797	1	0	2	0	0	0
427	general stress protein 13	gi|16804407	2	0	0	0	0	0
428	bifunctional glutamate--cysteine ligase/glutathione synthetase	gi|116874133	2	0	0	0	0	0
429	Peptidoglycan linked protein (atypical IPALG motif)	gi|226224269	1	2	0	0	0	0
430	DNA polymerase III subunit delta	gi|16803521	1	2	0	0	0	0
431	hypothetical protein lwe1906	gi|116873322	1	2	0	0	0	0

432	DNA topoisomerase I	gi|116872708	0	0	2	0	0	0
433	NADPH dehydrogenase NamA	gi|16804509	0	2	0	0	0	0
434	tRNA pseudouridine synthase A	gi|16804636	0	2	0	0	0	0

Where:

A = Endolysin Replicate 1

B = Endolysin Replicate 2

C = Endolysin Replicate 3

D = Glass Bead Beating Replicate 1

E = Glass Bead Beating Replicate 2

F = Glass Bead Beating Replicate 3

Reprint of Publication